EPA-600/2-76-038
February 1976

Environmental Protection Technology Series

RESIDENTIAL OIL FURNACE SYSTEM OPTIMIZATION
Phase I

Industrial Environmental Research Laboratory
Office of Research and Development
U.S. Environmental Protection Agency
Research Triangle Park, North Carolina 27711

RESEARCH REPORTING SERIES

Research reports of the Office of Research and Development, U.S. Environmental Protection Agency, have been grouped into five series. These five broad categories were established to facilitate further development and application of environmental technology. Elimination of traditional grouping was consciously planned to foster technology transfer and a maximum interface in related fields. The five series are:

1. Environmental Health Effects Research
2. Environmental Protection Technology
3. Ecological Research
4. Environmental Monitoring
5. Socioeconomic Environmental Studies

This report has been assigned to the ENVIRONMENTAL PROTECTION TECHNOLOGY series. This series describes research performed to develop and demonstrate instrumentation, equipment, and methodology to repair or prevent environmental degradation from point and non-point sources of pollution. This work provides the new or improved technology required for the control and treatment of pollution sources to meet environmental quality standards.

EPA REVIEW NOTICE

This report has been reviewed by the U.S. Environmental Protection Agency, and approved for publication. Approval does not signify that the contents necessarily reflect the views and policy of the Agency, nor does mention of trade names or commercial products constitute endorsement or recommendation for use.

This document is available to the public through the National Technical Information Service, Springfield, Virginia 22161.

EPA-600/2-76-038
February 1976

RESIDENTIAL OIL FURNACE SYSTEM OPTIMIZATION--PHASE I

by

L. P. Combs and A. S. Okuda

Rocketdyne Division
Rockwell International
6633 Canoga Avenue
Canoga Park, California 91304

Contract No. 68-02-1819
ROAP No. 21BCC-27
Program Element No. 1AB014

EPA Project Officer: G. Blair Martin

Industrial Environmental Research Laboratory
Office of Energy, Minerals, and Industry
Research Triangle Park, NC 27711

Prepared for

U.S. ENVIRONMENTAL PROTECTION AGENCY
Office of Research and Development
Washington, DC 20460

CONTENTS

Section I: Conclusions 1
Thermal Efficiency 1
Pollutant Emissions 3
Section II: Recommendations 5
Section III: Introduction 7
Objectives 8
Approach 8
Section IV: Analytical Investigation 11
Current Commercial Practices 11
Furnace Systems Performance Analysis 19
Section V: Experimental Investigation 55
Optimized Conventional Burner Study 55
Combustion Gas Recirculation (CGR) Burner Study 89
Flue Gas Recirculation (FGR) Burner Study 97
Section VI: Prototype System Design Investigation 109
Preliminary Designs: Areas of Commonality 109
Conceptual Design Study: Warm-Air Furnace 118
Conceptual Design Study: Hydronic Boiler 131
Section VII: References 141
Appendix A
Warm Air Oil Furnace Computer Model A-1
Appendix B
Flue Gas Compositional Analysis B-1
Appendix C
Data Tabulation: Optimum Burner Experiments C-1
Appendix D
Data Tabulation: CGR Burner Experiments D-1
Appendix E
Data Tabulation: FGR Burner Experiments E-1
Appendix F
Pre-Prototype Air-Cooled Finned Combustor Tests F-1

ILLUSTRATIONS

1. Furnace Floor Area and Volume vs Output Capacity for High-Boy Installations 17
2. Occupied Floor Space and Volume vs Output Capacity for Commercially Available, Warm-Air, Low-Boy Oil Furnaces 18
3. Calculated Steady-State Thermal Efficiency Superimposed on Experimental Una*Spray Furnace Efficiency Curves 24
4. Calculated Effects of Flue Gas Temperature and Stoichiometric Ratio on Oil Furnace Steady-State Thermal Efficiency 25
5. Calculated Effects of Furnace Cabinet Heat Losses to the Surroundings and of Stoichiometric Ratio on Oil Furnace Steady-State Thermal Efficiency 26
6. Calculated Effects of Ambient-Temperature Changes on Oil Furnace Steady-State Thermal Efficiency 27
7. Calculated Effect of Air Humidity on Oil Furnace Steady-State Thermal Efficiency 28
8. Calculated Effect of Emulsifying Oil With Water on Oil Furnace Steady-State Thermal Efficiency 29
9. Calculated Cycle Thermal Efficiency Compared With Measured Overall Heating Efficiencies of Combustion Improving Devices . . . 34
10. Calculated Effect on Oil Furnace Cycle Thermal Efficiency of Continuing to Circulate Warm Air Furnace Coolant After Burner Cutoff 36
11. Calculated Effect of Ambient-Temperature Changes on Oil Furnace Cycle Thermal Efficiency 37
12. Calculated Effects on Oil Furnace Cycle Thermal Efficiency of Varying Cycle Timing at Constant Thermal Demand 39
13. WAFURN-Calculated Overall Cycle Thermal Efficiency Compared With Measured Efficiencies 42
14. Calculated Effects on Oil Furnace Cycle Thermal Efficiency of Varying Cycle Timing at Constant Thermal Demand 45
15. Calculated Thermal Efficiencies for Lennox OF7 Furnace for Some Dual-Firing-Level Situations 48

16. Calculated Effects of External Flue Gas Recirculation (FGR) on Warm-Air Oil-Fired Furnace Efficiency and Flue Gas Temperature . . 51
17. Optimum 1 ml/s (gph) Oil Burner 56
18. Experimental Combustion Chamber and Heat Exchanger Arrangement 59
19. Heat Exchanger for Variable Combustion Chamber Configuration Tests 62
20. Schematic of Oil Burner and Research Combustion Chamber Test Installation 64
21. Effect of Combustion Chamber Length Upon Flue Gas Emissions as Functions of Stoichiometric Ratio in a 0.222 m (8.75 inches) Diameter, Air-Cooled, Tunnel-Fired Combustor 68
22. Cycle-Averaged Flue Gas Emission, 1.0 ml/s Optimum Oil Burner in 0.279 m Diameter, Air-Cooled, Tunnel-Fired Combustor at Various Heat Exchanger Positions 70
23. Cycle-Averaged Flue Gas Emission, 1.0 ml/s Optimum Oil Burner in a 0.22 m Diameter, Partially Insulated, Tunnel-Fired Combustor at a 0.40 m Heat Exchanger Position 72
24. Cycle-Averaged Flue Gas Emissions, 1.0 ml/s (gph) Optimum Oil Burner in a 0.175 m (6.89 inches) Diameter, Insulated, Tunnel-Fired Combustor at Various Heat Exchanger Positions 74
25. Cycle-Averaged Flue Gas Emissions, 1.0 ml/s Optimum Oil Burner in a 0.222 m Diameter, Insulated, Tunnel-Fired Combustor at Various Heat Exchanger Positions 75
26. Cycle-Averaged Flue Gas Emissions, 1.0 ml/s (gph) Optimum Oil Burner in a 0.222 m (8.75 inches) Diameter, Water-Cooled, Tunnel-Fired Combustor at Various Heat Exchanger Positions . . . 77
27. Cycle-Averaged Flue Gas Emissions, 1.0 ml/s (gph) Optimum Oil Burner in a 0.279 m (11 inches) Diameter, Air-Cooled, Side-Fired Combustor at Various Heat Exchanger Positions 79
28. Cycle-Averaged Flue Gas Emissions, 1.0 ml/s (gph) Optimum Oil Burner in a 0.222 m (8.75 inches) Diameter, Air-Cooled, Side-Fired Combustor at Various Heat Exchanger Positions 80

29. Cycle-Averaged Flue Gas Emissions, 1.0 ml/s Optimum Oil Burner in a 0.222 m (8.75 inches) Diameter, Partially Insulated, Side-Fired Combustor at a 0.40 m (16 inches) Heat Exchanger Position . . 82
30. Cycle-Averaged Flue Gas Emissions, 1.0 ml/s Optimum Oil Burner in a 0.222 m Diameter, Insulated, Side-Fired Combustor at Various Heat Exchanger Positions 83
31. Burner/Chamber Configuration for Combustion Gas Recirculation (CGR) Tests 91
32. Photograph of Combustion Gas Recirculation Burner 92
33. Photograph of the Flue Gas Recirculation Research Burner 99
34. Schematic of the Residential-Size Optimized Burner With Positive-Pressure Air Flow/Draft Loss Control Device 111
35. Conventional and Sealed-Air Furnace Installations 115
36. Preliminary Layout Drawing of the Air-Cooled-Combustor, Warm-Air Furnace 119
37. Layout Drawing of the Finned-Combustion, Prototype Warm-Air-Furnace Unit With a Sealed Air System 123
38. Layout Drawing of the Horizontal-Pass, Prototype Hydronic-Furnace With a Sealed Air System 132

TABLES

1. Summary Assessment of Commercial Practices: Oil Burners 13
2. Summary Assessment of Commercial Practices: Fireboxes 14
3. Summary Assessment of Commercial Practices: Forced Air Heat Exchange 14
4. Summary Assessment of Commercial Practices: Hydronic Heat Exchange 15
5. Summary Assessment of Commercial Practices: Support Systems . . . 15
6. Summary Assessment of Commercial Practices: Operating Mode, Safety, and Control 16
7. Optimum Burner/Chamber Matching Test Matrix 65
8. Summary of Results From 1 ml/s (GPH) Optimum Burner/Combustion Chamber Matching Experiments 86
9. Combustion Gas Recirculation Burner Test Matrix 94
10. Summary of Combustion Gas Recirculation Burner, Hot Fire Experiments 95
11. Composition and Properties of Fuel Oils Used in Oil Burner Experiments 106
12. Summary of Finned Combustor/Heat Exchanger Operating Conditions Heat Transfer Analysis 121

ABBREVIATIONS AND SYMBOLS

A		Area, m^2
A_b		Area, burner combustion air inlet, m^2
B	=	Exponential decay coefficient
c_p	=	Heat capacity, constant pressure, J/kg-K
CGR	=	Combustion gas recirculation
D	=	Diameter, m
FGR	-	Flue gas recirculation
H_f		Effective flue height, m
ΔH_c	=	Heat of combustion, J/kg
NOFI	-	National Oil Fuel Institute
$\dot{Q}$	=	Heat exchange rate, J/s
$\dot{Q}_{fan}$		Volumetric output of fan, m^3/s
SR	=	Stoichiometric ratio, (actual air/fuel ratio)/(stoichiometric air/fuel ratio)
T		Temperature, K
t	=	Time, s or min
UHC	=	Unburned hydrocarbons
$\dot{V}$	=	Volumetric flowrate, m^3/s
W	=	Mass, kg
$\dot{w}$	=	Mass flowrate, kg/s
x	=	Mass fraction
η	=	Efficiency
$\bar{(\ )}$	=	Average value of a parameter

Subscripts

air	Pertains to air supply
amb	Pertains to ambient atmospheric conditions
b	Pertains to burner
cyc	Pertains to furnace firing cycle
elec	Pertains to furnace electrical power consumption
emul	Pertains to water emulsified in fuel oil
f	Pertains to fuel
fan	Pertains to warm air furnace coolant fan
fb	Pertains to firebox
fg	Pertains to flue gases
fuel	Pertains to fuel oil
furn	Pertains to furnace
he	Pertains to furnace heat exchanger
hum	Pertains to humidity in combustion air
$H_2O(\ell)$	Pertains to liquid water
$H_2O(v)$	Pertains to water vapor
losses	Pertains to furnace thermal losses
net	Pertains to lower heating value of fuel
n.d. air	Pertains to natural draft air flow through furnace
off	Pertains to burner cut-off time or off-period
on	Pertains to burner start-up time or on-period
react	Pertains to reactants (fuel and air)
surr	Pertains to furnace surroundings
ss	Pertains to steady state
th	Pertains to thermal conditions

SECTION I

CONCLUSIONS

Conclusions from the research reported herein may be separated conveniently into those related to fuel utilization efficiency and those related to emission of air pollutants.

THERMAL EFFICIENCY

Residential space heating equipment - warm-air furnaces and hydronic boilers - typically have net thermal efficiencies (based on the fuel's lower heating value) on the order of 70 to 80 percent during steady-state operation, with season averages of perhaps 60 to 75 percent. Gross efficiencies (based on the fuel's higher heating value) are about 5 to 7 percent lower than net efficiencies. Potentially, then, fuel utilization efficiencies might be increased by as much as 35 to 40 percent. Achieving such large gains, however, would entail very significant departures from current design concepts, and manufacturing, marketing, and utilization practices. To maximize efficiency, considerably larger heat exchangers would be needed to cool flue gases to near room temperature and condense their combustion-generated water vapor. A number of problems would arise immediately, e.g., inadequate firebox draft, need for corrosion-resistant furnace and flue construction materials, condensate disposal, and noncompetitive initial costs. For these reasons, it was concluded that the current research should be addressed to defining efficiency gains achievable by less drastic modifications of existing commercial technology, i.e., improvements which can be achieved in a relatively near-term period of time and remain cost-competitive in the market place.

The greatest source of thermal inefficiency in residential space heating equipment is the convection of heat up the flue. When the burner is being fired, exhausted product gases carry off substantial sensible heat and the heat of vaporization of combustion-generated water vapor. Flue gas sensible heat losses

may be reduced by lowering either excess air or flue gas temperatures. Steady-state net thermal efficiencies might thus be increased by 5 to 10 percent before furnace operation is constrained by pollutant formation, low draft, and condensation problems. During this same time, most installations use heated, humidified living-space air for burner combustion air and for barometric draft control air. Although the resultant heat losses are not charged against furnace thermal efficiency, fuel utilization efficiency can be raised by 10 percent or more by using a sealed air system to bring in outdoor ambient air for these uses.

When the burner is not being fired, a natural draft flow of air through the burner, firebox, etc., cools furnace components and continues to convect heat up the flue. This loss can reduce net thermal efficiency by as much as 5 percent and is a major fraction of the transient heat losses which cause cycle-averaged efficiencies to be lower than steady state. The lower the draft air loss is, the less sensitive is cycle-averaged efficiency to variations of cycle duration and of fractional burner-on time. Draft air loss can be eliminated by providing a positive shutoff device in the combustion air supply. It can also be reduced or eliminated by having the burner fire more nearly continuous, e.g., by using modulated flow or high/low/off burner control. No real thermal efficiency advantage can be realized with such control schemes, however, because the flue gas temperature varies enough to offset the reduction or elimination of draft air heat losses.

Heat conducted to the furnace's exterior cabinet is radiated and convected to the surroundings. Although treated as a furnace loss, this heat in some installations may contribute directly to heating the residence and not be a true heat loss. These furnace setting losses average about 1-1/2 to 2 percent for warm-air furnaces. They are higher (3 to 3-1/2 percent) for hydronic boilers because component temperatures are more nearly constant during standby than are those in warm-air furnaces. Reduction of these losses nominally depends upon a straightforward economic tradeoff of fuel economy versus more expensive insulation, although manufacturers must also be concerned about first-cost competition.

The electrical energy expended in operating furnaces amounts to no more than 2 to 3 percent of the fuel's net heat of combustion. Nevertheless, minimizing electric power consumption is a worthwhile goal because of its greater cost to the homeowner than fuel oil and because of the factor of 2-1/2 to 3 on total energy savings when the electric generating plant's inefficiency is considered.

POLLUTANT EMISSIONS

Goals were established for flue gas pollutant emissions as follows: CO $\leq$ 1.0 g/kg fuel burned, UHC $\leq$ 0.1 g/kg fuel burned, NO $\leq$ 0.5 g/kg fuel burned, and smoke $\leq$ Bacharach No. 1. It was found experimentally that these goals could be satisfied by an optimized low-emission conventional burner fired into a properly matched firebox. At a 1-ml/s (gph)* firing rate, the optimized firebox was found to require: (1) A somewhat larger diameter ($\geq$0.28 m (11 inches)) than is conventional practice, (2) uniform extraction of 20 to 25 percent of the heat through the firebox walls over approximately 0.5 m (20 inches) of firebox length, and (3) retention of heat in the firebox during the burner-off or standby time. It was concluded that the burner/firebox combination could be either water-cooled or air-cooled, either side-fired or tunnel-fired, and designed for nominal operation at a relatively-efficient 15-percent excess air (13-percent CO_2 in dry flue gases).

A similar experimental effort to determine firebox matching criteria for a 1-ml/s (gph) combustion gas recirculation (CGR) burner was frustrated by an inability to simultaneously satisfy the NO, CO, and UHC emission goals. Because of these problems and the inherent potential problems of passing moderately high-temperature mixed gases through the combustion air fan, it was concluded that further work with this burner concept was not warranted.

*1.00 ml/s = 0.951 gph. The 5-percent difference is neglected in this report when referring to burner firing rates.

Tests of a 1-ml/s (gph) flue gas recirculation (FGR) burner were more successful, and showed good potential for satisfying the emission goals under efficient operating conditions. However, actually achieving all of the emission goals probably would be contingent upon using a more complicated burner start sequence to eliminate start-spike emissions of CO, smoke, and UHC experienced under conditions with acceptably low NO. Again, it was concluded that the optimized conventional burner in cooled combustion chambers is a preferred choice over the FGR burner.

SECTION II

RECOMMENDATIONS

Recommendations derived from the Phase I research are concerned with incorporating the results into a prototype furnace capable of satisfying the pollutant emission and performance goals, while remaining cost-competitive, and evaluating its behavior experimentally. In essence, this constitutes a go-ahead recommendation for the Phase II activities as planned.

SECTION III

INTRODUCTION

The Environmental Protection Agency has sponsored studies over the past few years to document the emission of air pollutants from existing residential and commercial oil-fired space heating equipment (Ref. 1 and 2). Concurrently, the EPA has also supported applied research programs to determine the effects of design and operating parameters on exhaust gas emission levels and to devise strategies for minimizing pollutant emissions (e.g., Ref. 3 through 5). These and related studies have shown that substantial reductions in total emissions from furnaces can be realized by applying combustion control technology, such as flue gas recirculation, two-stage combustion, and advanced burner designs. As a portion of those EPA activities, Rocketdyne performed an intensive investigation of residential and commercial oil burners (Ref. 5) which led to criteria for optimizing conventional burner designs with respect to emissions. The optimized burners were shown to be capable of reducing NO_x emissions to below 1 g NO/kg fuel, in contrast to typical manufactured residential burners which operate at about 1-1/2 to 3 g NO/kg fuel or higher. During that same program, some variations in the combustion chamber construction (adiabatic refractory walls versus metal heat-sink or water-cooled walls) and design (relative orientation of the burner and chamber axes and relative burner and chamber diameters) were studied. The results clearly demonstrated that the total emissions are sensitive to the design of each component comprising a residential heating system and to design interactions among the components. It became obvious, therefore, that minimum emissions could be achieved only by systematically optimizing the burner in conjunction with the combustion chamber and furnace as well as operating mode. The research described and discussed in this report was undertaken to investigate such optimization and to delineate furnace design requirements for commercializing the optimum furnace technology.

In view of uncertainties in fossil fuel supplies and prices and of the national emphasis on striving toward energy independence, an optimized furnace should, in addition to providing low levels of pollutant emissions, also provide some substantial increase in overall thermal efficiency. Further, for the developed

technology to be adopted commercially, the optimized design must be cost competitive. In this regard, significantly increased fuel economy will be important in allowing consumer recovery, within a reasonable number of heating seasons, of any increased capital costs which might result from modifications required for system optimization. Establishing the technological requirements for optimizing residential heat systems is important, therefore, because it addresses both improvement of air quality and better utilization of our dwindling energy resources.

OBJECTIVES

The principal objective of this research program is to establish the technology required for engineering optimization of residential heating furnace systems combining minimum pollutant emissions with maximum system efficiency. Primary emphasis will be given to systems fueled with No. 2 distillate fuel oil; however, the impact on performance and emissions of substituting gaseous fuels for oil also will be assessed. General overall goals are to reduce emissions of oxides of nitrogen to less than 0.5 g NO/kg fuel burned, while maintaining minimum emissions of CO, UHC, and smoke, and to increase overall season-averaged furnace energy efficiencies 10 percent or more above those achieved by current conventional systems.

APPROACH

The research program undertaken to accomplish these objectives is divided into two phases, each of which is further subdivided into several tasks. The first phase, Systems Analysis and Experimental Research, has been performed in the first year of the program and is the subject of this interim report. It comprised tasks as follows:

1. Systems Analysis, in which current commercial designs were reviewed and analyzed to identify potential areas for improvement
2. Conventional Burner/Combustor Matching Experiments, in which the 1.0 ml/s (gph) optimum burner was tested in research combustors having a variety of sizes, configurations, and constructions to further the optimization

3. Experimental Definition of Requirements for an Integrated Furnace System, in which burner/combustor matching tests were conducted with burners employing forced combustion gas recirculation (CGR) and flue gas recirculation (FGR)

4. Data Evaulation and Systems Analysis, in which the results of prior tasks were synthesized to support preliminary conceptual designs for two prototype, low-emission, improved-efficiency furnace units. One preliminary design is for a warm-air furnace and the other is for a hydronic boiler. Each design was submitted to a leading manufacturer of its particular type of residential heating system for review and assessment by knowledgeable engineering personnel. Cognizance was taken of their comments and recommendations in selecting design features for candidate prototype residential furnace systems. These were then discussed with the EPA Project Officer, and the warm-air system was selected as the more promising of the two; therefore a prototype warm-air unit will be built for further study in the continuing work.

The second phase of the program will involve the construction and experimental evaluation of a prototype optimized warm-air furnace unit. The data and experiences gained will be applied to the final design of a cost-competitive, commercially producible warm-air furnace which embodies the derived low-emission, improved-efficiency technology. This phase will be documented in a final report upon completion of the research.

SECTION IV

ANALYTICAL INVESTIGATION

An analytical investigation of conventional residential oil heating equipment was conducted to identify areas where improvements might be made and to quantify the potential gains. Although both pollutant emission reduction and thermal efficiency enhancement were of interest, the emissions are more amenable to experimental than to analytical characterization, so efficiency aspects were emphasized in this effort.

As a preface to numerical analysis, a brief survey was conducted of current and alternate practices in the design of components for residential heating systems. Thereafter, two thermal analysis models for furnaces were formulated and programmed for computer solution. The first model (FURNAC) treated furnace design and operational aspects strictly parametrically (and largely empirically) to screen and isolate those aspects requiring more vigorous analytical examination. The second model (WAFURN) accounted in a simplified manner for transient firebox and heat exchanger heating and cooling phenomena in a rather generalized warm-air furnace.

CURRENT COMMERCIAL PRACTICES

A brief informal survey was conducted to gather and systematize information regarding predominant current commercial practices, alternate approaches, trends foreseen for the near future, and areas for potential improvement in residential oil furnace systems. Sources of information included:

1. Previous work performed at Rocketdyne
   a. EPA Contract 68-02-0017 (Ref. 5)
   b. NOFI contract for development of Una*Spray Integrated Furnace
2. EPA-R2-73-084a, "Field Investigation of Emissions from Combustion Equipment for Space Heating" (Battelle)

3. Manufacturers' brochures on currently available burners and furnaces in the 0.5- to 1.5-ml/s (1/2 to 1-1/2 gph) size range
4. Published results from NAPCA/EPA in-house studies
5. Applicable codes and standards
6. Proceedings of API and NOFI Workshops
7. Personal contacts with furnace manufacturers, NOFI, Battelle, etc.

Qualitative information obtained was systematized into a number of summary assessment tables, categorized by subsystems, components, and functions. These assessments are given in Tables 1 through 6, which are essentially self-explanatory.

Current catalogs describing warm-air and hydronic residential oil furnaces were requested from approximately 30 U.S. manufacturers. They were studied to discern design trends and practices and to collate data on burner types, furnace weights and volumes, floor space requirements, etc., as functions of system type and structural configuration (high-boy, low-boy, horizontal). While there are substantial differences among the various manufacturers' products, there are also some distinct similarities. For example, the floor areas and volumes of high-boy oil furnaces increase approximately linearly with firing rate, and exhibit only about a ±25 percent scatter about mean values (Fig. 1). The moderately small scatter probably reflects the constraint imposed by closet-type installation. Low-boy furnaces are more often installed in basements, and are not so spatially confined as are high-boys; similar floor area and volume plots for low-boys (Fig. 2) show a substantially greater scatter (about ±35 percent).

Comparing current data with results from earlier surveys revealed that oil furnaces have experienced little change since the Rocketdyne survey conducted for NOFI (Ref. 6) and the Battelle survey for the U.S. EPA (Ref. 4). Since those surveys were both broader and more detailed than the informal investigation conducted here, the interested reader is referred to those documents.

TABLE 1. SUMMARY ASSESSMENT OF COMMERCIAL PRACTICES: OIL BURNERS

SUBSYSTEM OR COMPONENT	PREDOMINANT CURRENT PRACTICES	ALTERNATE CURRENT PRACTICES	FUTURE DIRECTIONS: DESIGN TRENDS	POTENTIAL IMPROVEMENT		
				AREA	METHODS TO USE	CONSTRAINTS
Burner head	Conventional head • Small peripheral swirl • Some choke	Low-press air-atomizing Rotary atomizing Pre-vaporizing burners • Old techniques Avg ages ~15-18 yrs • Usage declining	Conventional head still numerically dominant	Lower NO_x emissions	Optimized conventional head • Higher swirl • Greater choke Further optimize burner/chamber • Improve stability	
	Flame retention head • Low-vel turbulent-wake devices • Moderate-high swirl		Increasing usage of flame-retention heads • Adaptable to a variety of furnaces • Smaller dia blast tubes • Lower smoke	Retention-head designs for lower NO_x	Non-adiabatic combustion techniques • Flue gas recircul. • Flame cooling	
	Shell head • Inner mixing chamber (shell) • Shell-by-pass air		Decreasing usage of shell heads	Shell head designs for lower NO_x	Design favorable for pseudo-staged-combustion • Needs heat removal from flame ahead of by-pass air	
Oil nozzle	Hi-pressure, self-atomizing, Simplex	As above	Produce finer sprays • Higher oil press. • Multiple nozzles • Smaller orifices	Match fine spray distribution to combustion air		Cost, plugging
Igniter	Continuous spark electrodes • 10-12,000 V transformer • Draws~250W power	Interrupted spark	Lower power consumption Solid-state devices	Reduce power consumption	Interrupted spark • Smaller, pulse-duty transformer Piezoelectric/solenoid capacitive discharge	Codes & Stds
Fuel pump	Positive displacement • 100 psig output press • By-pass pressure regulation	300 psig output press. for larger burners	Increasing usage of 100 psig pumps	Reduce power consumption	Reduce by-pass/firing rate ratio Use a smaller pump	Cost
Combustion air fan	Centrifugal, squirrel cage • 3450 RPM •~50-150 Pa (0.2-0.6 in. H_2O) output pressure	Squirrel cage at 1725 RPM Radial-flow fans • Higher output press. • Rotary burners	Squirrel cage at 3450 RPM • Smaller fan • Steadier flow	Reduce fan noise		Cost, power
Motor	115 VAC • Single phase, constant speed • Drives both fuel pump & combustion air fan				Multi-speed drives for throttling applications	Cost, matching stoich-ratio
Fuel cut-off	Small burners - none Large burners - solenoid valve • Req'd at ≥6 GPH	Solenoid valve Centrifugal clutch Combine cut-off with press. regulator in fuel pump	Decreasing application to small burners			Cost, safety

TABLE 2. SUMMARY ASSESSMENT OF COMMERCIAL PRACTICES: FIREBOXES

SUBSYSTEM OR COMPONENT	PREDOMINANT CURRENT PRACTICES	ALTERNATE CURRENT PRACTICES	FUTURE DIRECTIONS: DESIGN TRENDS	POTENTIAL IMPROVEMENT		
				AREA	METHODS TO USE	CONSTRAINTS
Configuration	Right circul. cylinder	Rectangular box	Increasing use of cyl. combustors			
Size	Volume matched to nominal firing rate ● ~1.8 x 10^6 J/S-m^3 (1.74x10^5 Btu/hr-ft^3) All dimensions ≥ 0.2 m (8-in.)		Increasing use of shorter chambers	Chamber/burner matching		Smoke prod'n
Construction materials	Refractories ● Uncooled, adiabatic ● Firebrick • High heat capacity • Slow thermal resp. ● Insulating brick • Low heat capacity • Fast thermal resp.	Ceramic fiber ● Similar to insulating brick ● Shape flexibility Steel ● Temp limitations ● Rad'n or convection cooling	Increasing uses of ceramic fiber & steel ● Prefabricate ● Design flexibility ● Lower weight			
Firebox/burner orientation	Side-fired (Perpendicular port) ● Vertical firebox ● Horizontal burner	Tunnel-fired (Coaxial) ● Horizontal axes	Static	Develop vertical coaxial ● Minimize floor space	Vertical burner axis	

TABLE 3. SUMMARY ASSESSMENT OF COMMERCIAL PRACTICES: FORCED AIR HEAT EXCHANGE

SUBSYSTEM OR COMPONENT	PREDOMINANT CURRENT PRACTICES	ALTERNATE CURRENT PRACTICES	FUTURE DIRECTIONS: DESIGN TRENDS	POTENTIAL IMPROVEMENT		
				AREA	METHODS TO USE	CONSTRAINTS
Air supply	Return duct from heated space ● Low velocity ● Low ΔP ● Uninsulated ● Fiberglass filter ● 50 in.^{2}/gph		Static	None		
Air blower	Centrifugal squirrel-cage fan ● 7 or 3 speed ● 1200-1400 fm/gph ● Low pressure (1-2" H_2O)	Higher capacity if unit includes air conditioning	Static	Reduce noise More efficient rotors		Cost
Heat exchanger	Formed, welded carbon steel plate ● 10-12 ft^2/100,000 Btu/hr ● ~80% thermal effic. ● ~500 F gas temp. discharge			Compact design concepts Higher effic.		Cost, cleaning
Distribution	Insulated, galvanized sheet steel ducts ● Flow control dampers	Fiber ducts		Integral humidifier		

TABLE 4. SUMMARY ASSESSMENT OF COMMERCIAL PRACTICES: HYDRONIC HEAT EXCHANGE

SUBSYSTEM OR COMPONENT	PREDOMINANT CURRENT PRACTICES	ALTERNATE CURRENT PRACTICES	FUTURE DIRECTIONS: DESIGN TRENDS	POTENTIAL IMPROVEMENT		
				AREA	METHODS TO USE	CONSTRAINTS
System type	Closed, forced circulation water circuit • Low-temp, ≤ 250 F • Working press ≤ 30 psig • Low pumping heads • Low water temp. changes (~11K) (~20°F)	Gravity circulation water circuit Steam heating system	Steam & gravity circ. systems supplanted by forced-circ. water Dual-temperature water systems • Hot in winter • Cold in summer Higher water ΔT's • Better control • Smaller equipment • Lower flows, costs			
Heat exchanger	Cast-iron boiler type	Formed, welded carbon steel plate & tubes ASME fired-boiler code Fire-tube or water tube Finned water tube type	-			
Pump	Centrifugal	Positive displacement				

TABLE 5. SUMMARY ASSESSMENT OF COMMERCIAL PRACTICES: SUPPORT SYSTEMS

SUBSYSTEM OR COMPONENT	PREDOMINANT CURRENT PRACTICES	ALTERNATE CURRENT PRACTICES	FUTURE DIRECTIONS DESIGN TRENDS	POTENTIAL IMPROVEMENT		
				AREA	METHODS TO USE	CONSTRAINTS
Fuel supply system	Single pipe system Zero-press ± gravity head	Two-pipe system (large by-pass)	Single pipe			Furnace-to-oil distance safety code?
Atomization air	10-50 psig	Self-atomizing (no air)	Self-atomizing	• Small, low cost air pump • Quiet air pump		
Filters • Furnace • Fuel Nozzle • Fuel line • Burner air	 Glass wool Sintered metal In-line cut (metal or paper) None	 • Screen or permanent cleanable filter Fine mesh screen No filter	 Glass wool Sintered metal			
Flue System	Draft (neg. press.)	Sealed, pressurized	Draft	Draft system requires low ΔP system	Draft - no leak hazard	Cost (fab.)

TABLE 6. SUMMARY ASSESSMENT OF COMMERCIAL PRACTICES: OPERATING MODE, SAFETY, AND CONTROL

SUBSYSTEM OR COMPONENT	PREDOMINANT CURRENT PRACTICES	ALTERNATE CURRENT PRACTICES	FUTURE DIRECTIONS: DESIGN TRENDS	POTENTIAL IMPROVEMENT		
				AREA	METHODS TO USE	CONSTRAINTS
Operating mode	On-Off	Hi-Lo Fire, (req'd ≥ 12 GPH), Lo-fire: start, Hi-fire: run		Throttling	Lo-fire continuous, Hi-fire On-Off or Modulated flow	Cost (control circuit & equip. wear)
Safety/Control						
• Ignition	Continuous on	Interrupted (On for start)				U.L.
• Flame detection	Cad-sulfide cell	UV cell	Detect/shut-down time varies with firing rate			U.L.
• Electrical fail-safe						U.L.
• Toxicity	No monitoring • Fire box press <forced air press.					
• Operating mode	Flame detect	≥6 GPH - add fuel cut-off ≥10 GPH - add lo-fire start - Add pre-ign purge	Solid state electronic control circuit	Reduce size & cost of circuitry (IC's)		Standardize firing cycle

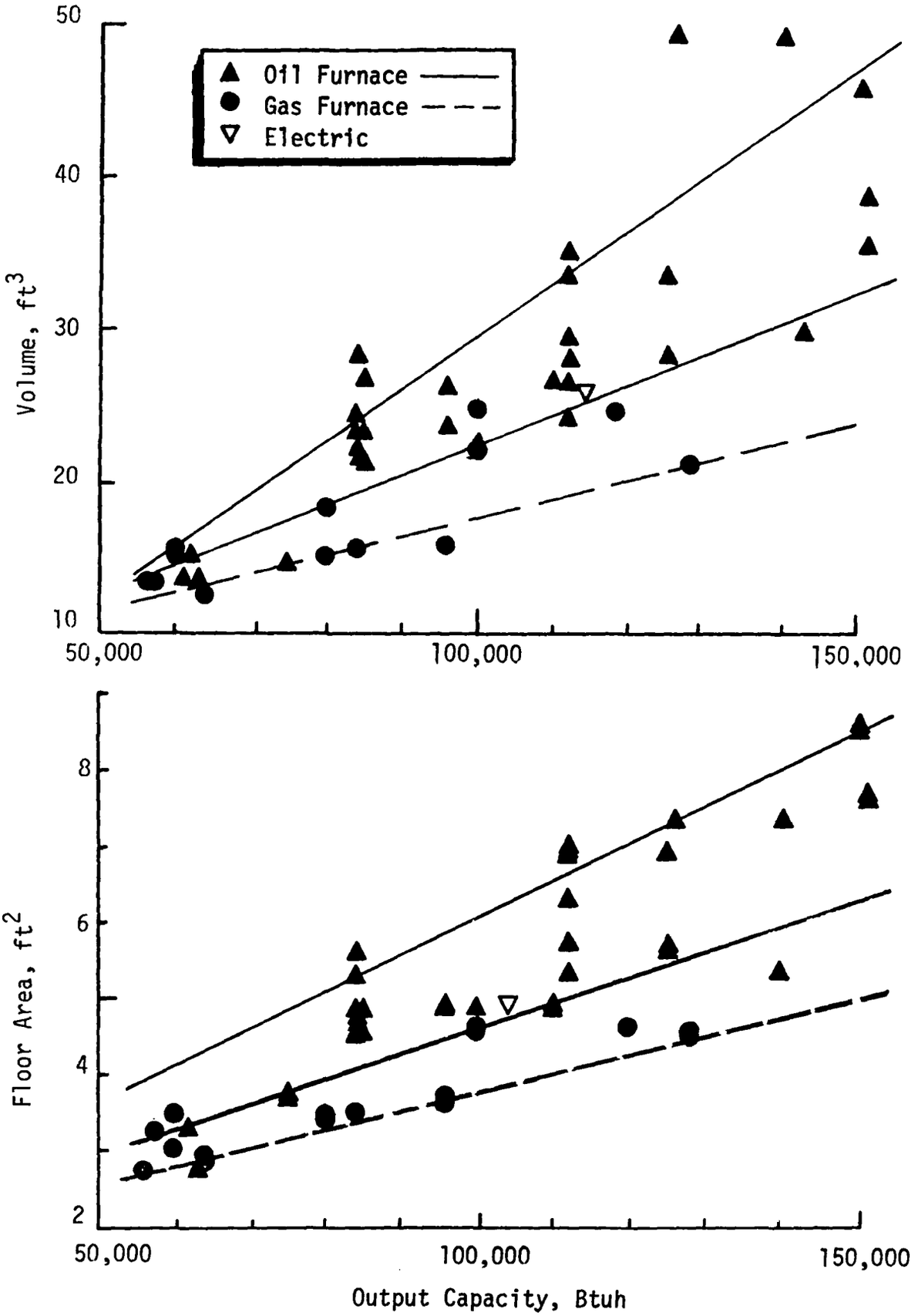

Figure 1. Furnace Floor Area and Volume vs Output Capacity for High-Boy Installations

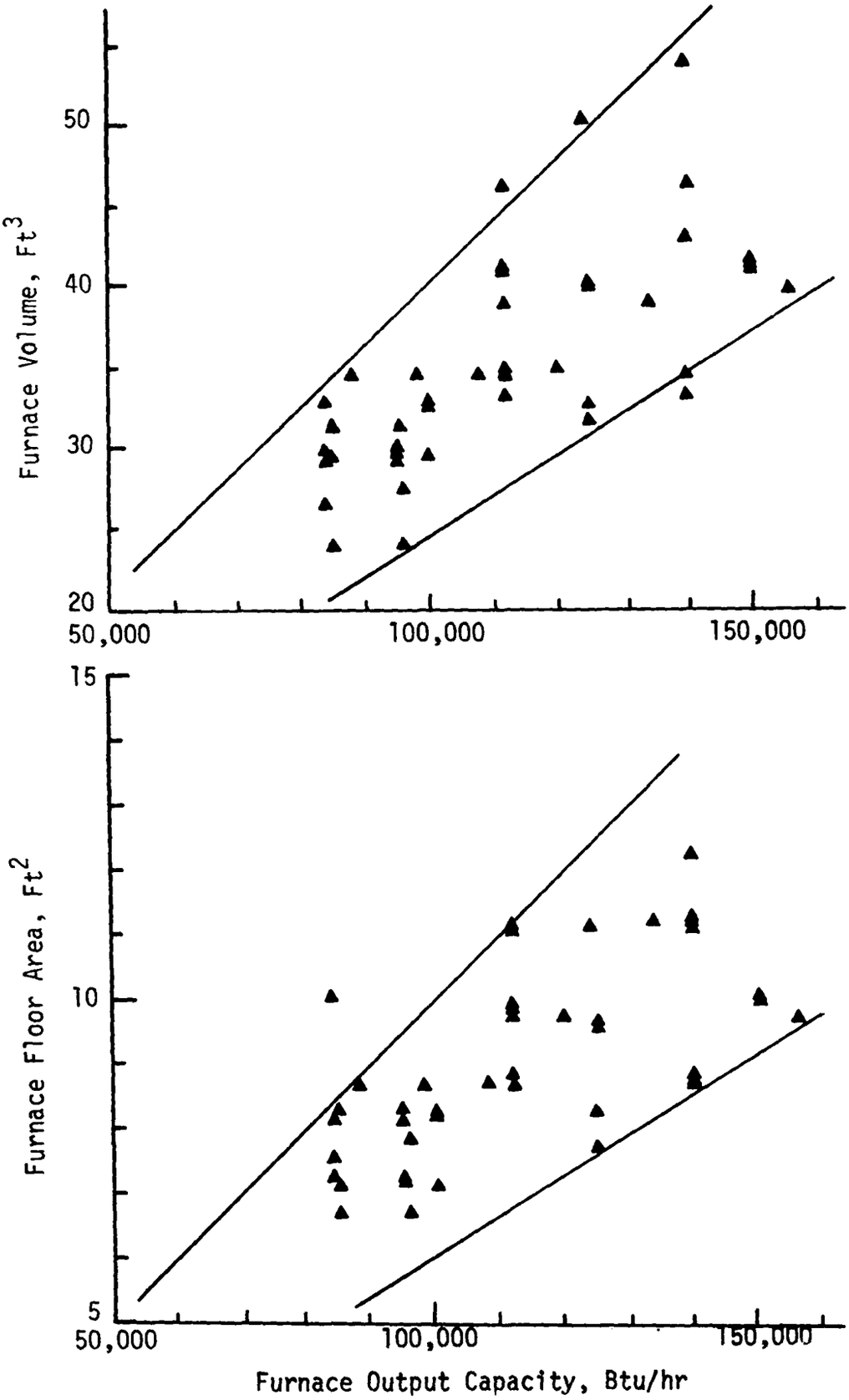

Figure 2. Occupied Floor Space and Volume vs Output Capacity for Commercially Available, Warm-Air, Low-Boy Oil Furnaces

In the process of examining oil furnace manufacturers' specification sheets, three companies were selected as being approximately representative of the industry, and arrangements were made for technical visits to their plants. Two of the three companies make warm-air furnaces; the other builds hydronic boilers. One-day visits were made to each of the three plants by Rocketdyne personnel. The principal objective of the visits was to engage in informal technical discussions to enhance our understanding of current design practices, how they are constrained by fabrication, installation, and cost considerations, and trends foreseen for the near future.

FURNACE SYSTEMS PERFORMANCE ANALYSIS

Numerical analyses of furnaces' thermal performance was undertaken to help quantify the importance of various design and operating parameters on overall efficiency. Two separate computer models were developed to perform the numerical analysis. Consider a usual definition of thermal efficiency:

$$\eta_{th} = \frac{\text{useful heat delivered}}{\text{heat input}} \tag{1}$$

The two models differed in their methods of calculating the "useful heat delivered" in the numerator of Eq. 1. The first, and simpler, model attempted to quantify the known thermal losses and subtracted them from the heat input to obtain an estimate of the useful heat output. This model was used, principally, to examine the potential and relative impacts on thermal efficiency of individually varying a number of parameters. It was also instrumental in determining which parameters should be modeled accurately, which could be treated with simplified approximations and which could be omitted in formulating the second furnace thermal analysis model.

The second model's approach to obtaining a value for the useful heat delivered was to solve for the heat transferred to the furnace cooling medium. With this approach, loss quantification is necessary only for those losses which interact with the heat transmission rates (and, secondarily, so that they can be understood well enough to design ways for reducing them).

Thermal Loss Deduction Method

The "heat input" denominator of Eq. 1 should include all of the energy supplied to the oil furnace. This is sometimes assumed to consist solely of the fuel oil's heat of combustion. While that is unquestionably the largest energy source, there are other sources, e.g., the sensible heat (which may be negative) associated with reactant supply at nonstandard conditions, and electricity to drive the fuel pump and air blowers and to power the ignition circuit and basic furnace controls. For simplicity, the energy inputs may be categorized as reactant thermal energy, $\dot{Q}_{react}$, and electric power, $\dot{Q}_{elec}$.

Heat transferred to the furnace cooling medium constitutes the useful heat output and is designated as $\dot{Q}_{he}$. Its value may be calculated by subtracting thermal losses from the total energy inputs:

$$\dot{Q}_{he} = \dot{Q}_{react} + \dot{Q}_{elec} \quad \dot{Q}_{losses} \tag{2}$$

The last term must include all energy losses from the furnace, viz, the sensible heat of combustion gases convected up the flue, the latent heat of water vapor in the flue gases formed by fuel combustion, fresh air induced into the flue for furnace barometric pressure control, and all heat dissipated from the furnace to the surroundings by radiation and convection. Several assumptions were made concerning the losses in formulating a model for computer solution. First, it was assumed that none of the water formed by fuel combustion would condense within the flue. As a result, the input reactant thermal energy was based upon the fuel's lower or net heating value, $(\Delta H_c)_{net}$, obtained by adjusting the measured value at 21 C (70 F) for water emulsified in the fuel, humidity in the air, and reactant supply temperature deviations from that reference temperature:

$$(\Delta H_c)_{net} = (\Delta H_c)_{net}^{21\ C} - (21-T_{fuel})\left[(1-x_{emul})\ c_{p,fuel} + x_{emul}\ c_{p,H_2O(\ell)}\right] -$$

$$(21-T_{air})\left[(1-x_{hum})\ c_{p,air} + x_{hum}\ c_{p,H_2O(v)}\right] \tag{3}$$

Second, it was assumed that the heat dissipated from the outside of the furnace is completely lost, even though it does actually contribute to satisfying the residential demand heat load in many installations. Similarly, the furnace's electrical power consumption was assumed to be entirely lost, even though much of it is deposited in the reactants and combustion gases as kinetic and thermal energy, which may be recovered in the heat exchanger, and the remainder is dissipated in the furnace surroundings. With these assumptions, $\dot{Q}_{elec}$ can be dropped from Eq. 2 and the remaining losses categorized as flue gas losses, $\dot{Q}_{fg}$, and losses to the surroundings, $\dot{Q}_{surr}$. Both of these are time-varying quantities which take place over an entire firing cycle. The terms $\dot{Q}_{he}$ and $\dot{Q}_{react}$ in Eq. 2, however, may be applicable only during some discreet portion of a cycle, such as the burner firing time, Δt_{on}. To perform energy balances and efficiency calculations, mean effective rate terms may be defined by

$$\bar{\dot{Q}} = \frac{1}{\Delta t_{on}} \int_{cycle} \dot{Q} dt \tag{4}$$

with all of the various heat rates normalized to the burner firing time. Then Eq. 2 becomes

$$\bar{\dot{Q}}_{he} = \dot{Q}_{react} - \bar{\dot{Q}}_{fg} \quad \bar{\dot{Q}}_{surr} \tag{5}$$

The overall cycle-averaged furnace thermal efficiency is

$$\bar{\eta}_{furn} = \frac{\bar{\dot{Q}}_{he}}{\dot{Q}_{react} + \bar{\dot{Q}}_{elec}} \tag{6}$$

In this form, it is possible to separate the electrical power consumption from the fuel usage by defining a cycle-averaged reactant thermal efficiency

$$\bar{\eta}_{react} = \frac{\bar{\dot{Q}}_{he}}{\dot{Q}_{react}} \tag{7}$$

Combining Eq. 6 and 7 gives

$$\bar{\eta}_{furn} = \bar{\eta}_{react} \frac{\dot{Q}_{react}}{\dot{Q}_{react} + \bar{\dot{Q}}_{elec}} \tag{8}$$

from which an approach was derived first for studying reactant thermal efficiency and, subsequently, for those situations still of interest, studying overall efficiency by assessing their electrical power requirements.

The foregoing concepts were formulated as a system of equations requiring input values for a number of reactant and furnace operational parameters, and programmed for solution on a Honeywell Timeshare computer. Entitled FURNAC, the program is designed to calculate $\bar{\eta}_{react}$ and $\bar{\eta}_{furn}$ iteratively for several values of stoichiometric ratio* (SR).

Although the FURNAC program is not restricted basically to a particular cooling medium, it has been used primarily to evaluate warm-air furnace behavior. Except where specifically denoted as applying to a hydronic unit, the following discussion concerns its application to warm-air systems.

Steady-State Operation. Quantitative analysis of cyclical heat loss effects requires that $\dot{Q}_{fg}$, $\dot{Q}_{surr}$, and $\dot{Q}_{elec}$ be defined as functions of time throughout the cycle. Before attempting that, however, they can be treated as simple numerical parameters to gain some insight to their relative importance or, alternatively, to examine steady-state operation. This approach was used in running a number of exploratory cases to aid in selecting appropriate nominal parametric values for subsequent use in sensitivity analyses. Computed thermal efficiencies were compared with some available steady-state furnace efficiency data as indicated

*The definition of stoichiometric ratio permits ready identification of the excess air level. For example, SR = 1.50 is equivalent to 150 percent of stoichiometric air, which is 50 percent excess air. The relationships between SR and flue gas concentrations of CO_2 and O_2 are illustrated for No. 2 fuel oil in Fig. B-2, page B-11.

in Fig. 3. Thereupon, the following nominal values were chosen for steady-state input parameters:

$\dot{w}_{fuel}$ = 0.885×10^{-4} kg/s (corresponds to 1.00 gph dry oil)

x_{emul} = 0.0025 kg $H_2O(\ell)$/kg oil (tank moisture)

x_{hum} = 30 percent of saturation, kg $H_2O(v)$/kg dry air

T_{fuel} T_{air} = 10 C (50 F)

T_{fg} = 325 C (617 F)

$\dot{Q}_{surr}$ = 1580 J/s (5400 Btu/hr)

$\dot{Q}_{elec}$ = 500 J/s (watts)

$1 \leq SR \leq 3$

The FURNAC computer program was structured to compute points across the stoichiometric ratio range for each selected set of parametric values. Computed overall steady-state thermal efficiencies from computer runs using the nominal values and using one-parameter deviations from nominal are plotted in Fig. 4 through 8.

Figure 4 shows that flue gas exhaust temperature has a strong effect on achievable furnace efficiency. The effect is accentuated by increasing the stoichiometric ratio because, if flue gas temperature remains constant, increasing the excess air simply increases the sensible heat swept up the flue.

The effects on thermal efficiency of varying furnace cabinet heat losses (other than flue losses) are shown in Fig. 5. Efficiency decreases linearly with increasing losses; the nominal value of 1580 J/s (1.5 Btu/sec) corresponds to 4.2 percent of No. 2 fuel oil's lower heating value of 4.273×10^7 J/kg (18,370 Btu/lbm) at the designated firing rate.

Ambient-temperature variations were found to exert very little influence on furnace thermal efficiency if other parameters remain fixed (Fig. 6). (This result is seen later <u>not</u> to apply to cyclical furnace operations.)

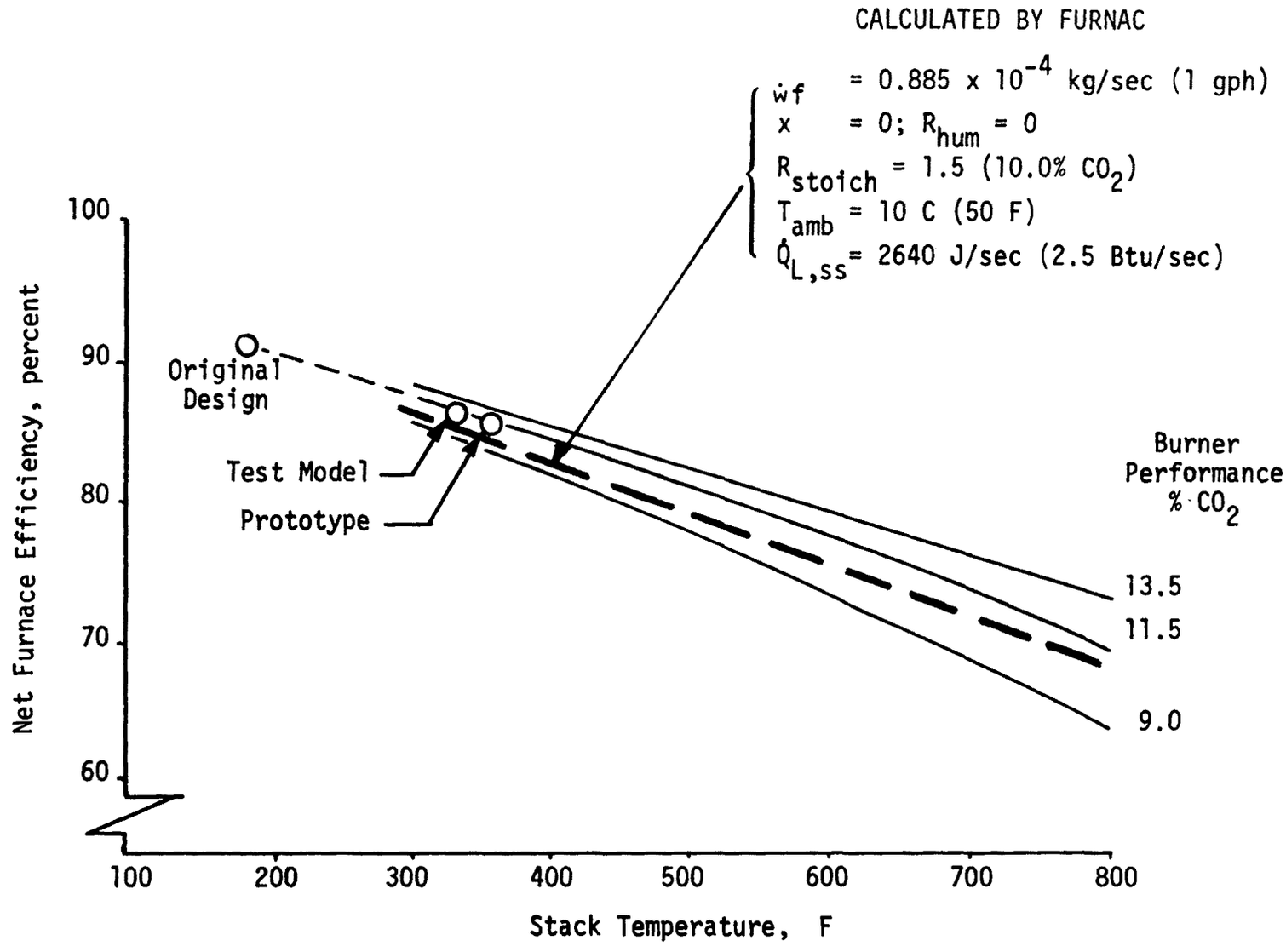

Figure 3. Calculated Steady-State Thermal Efficiency Superimposed on Experimental Una*Spray Furnace Efficiency Curves (Ref. 6)

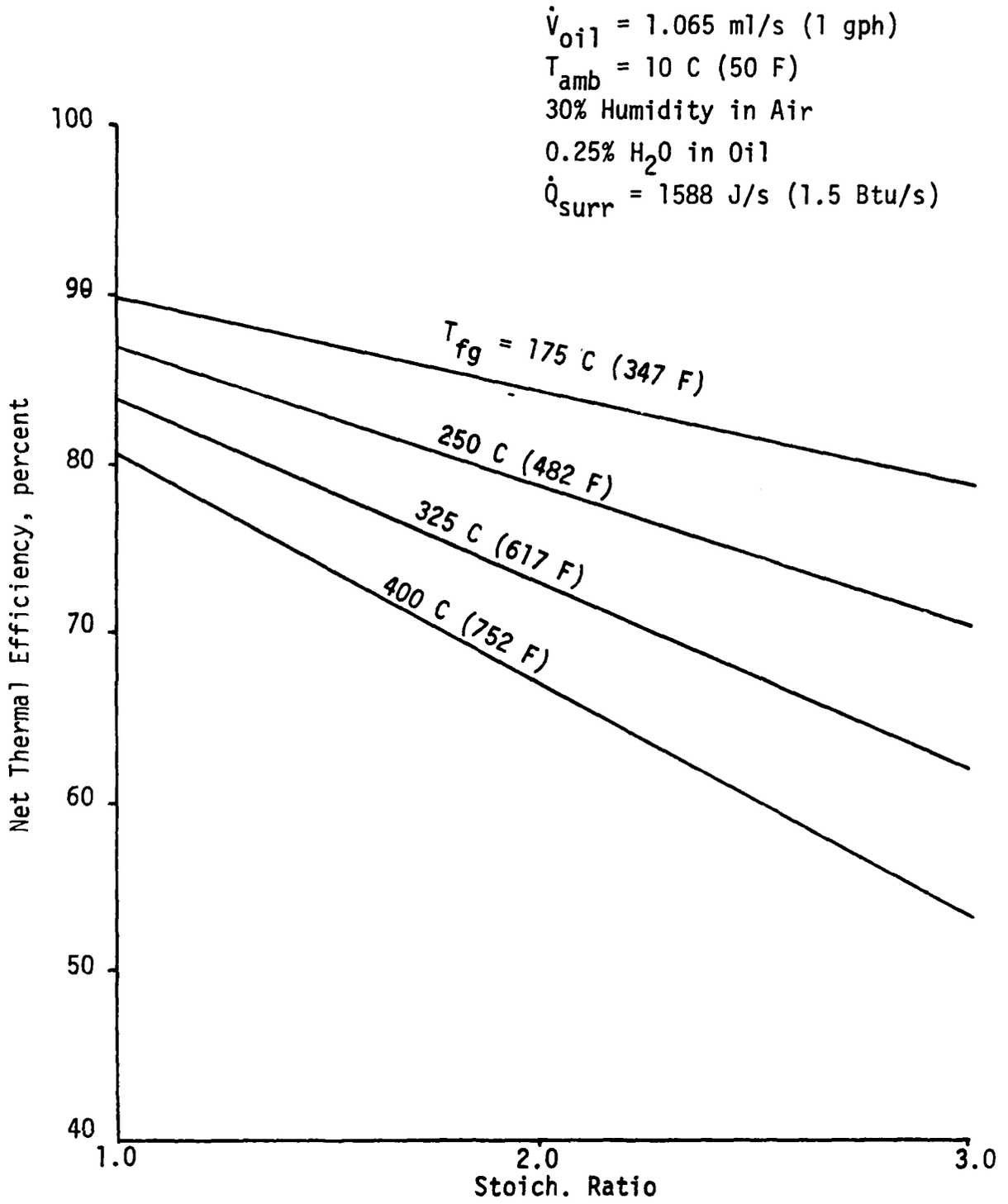

Figure 4. Calculated Effects of Flue Gas Temperature and Stoichiometric Ratio on Oil Furnace Steady-State Thermal Efficiency

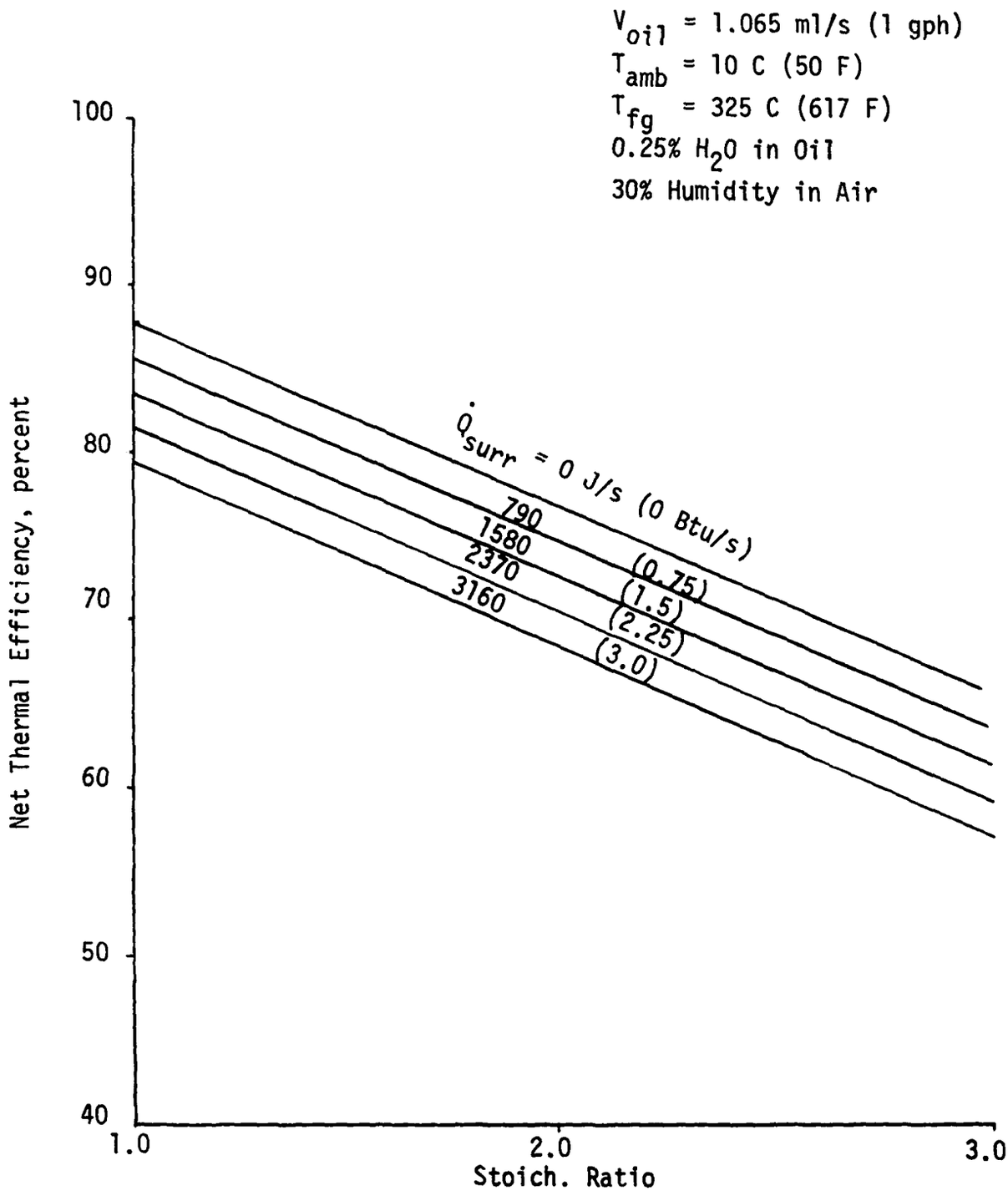

Figure 5. Calculated Effects of Furnace Cabinet Heat Losses to the Surroundings and of Stoichiometric Ratio on Oil Furnace Steady-State Thermal Efficiency

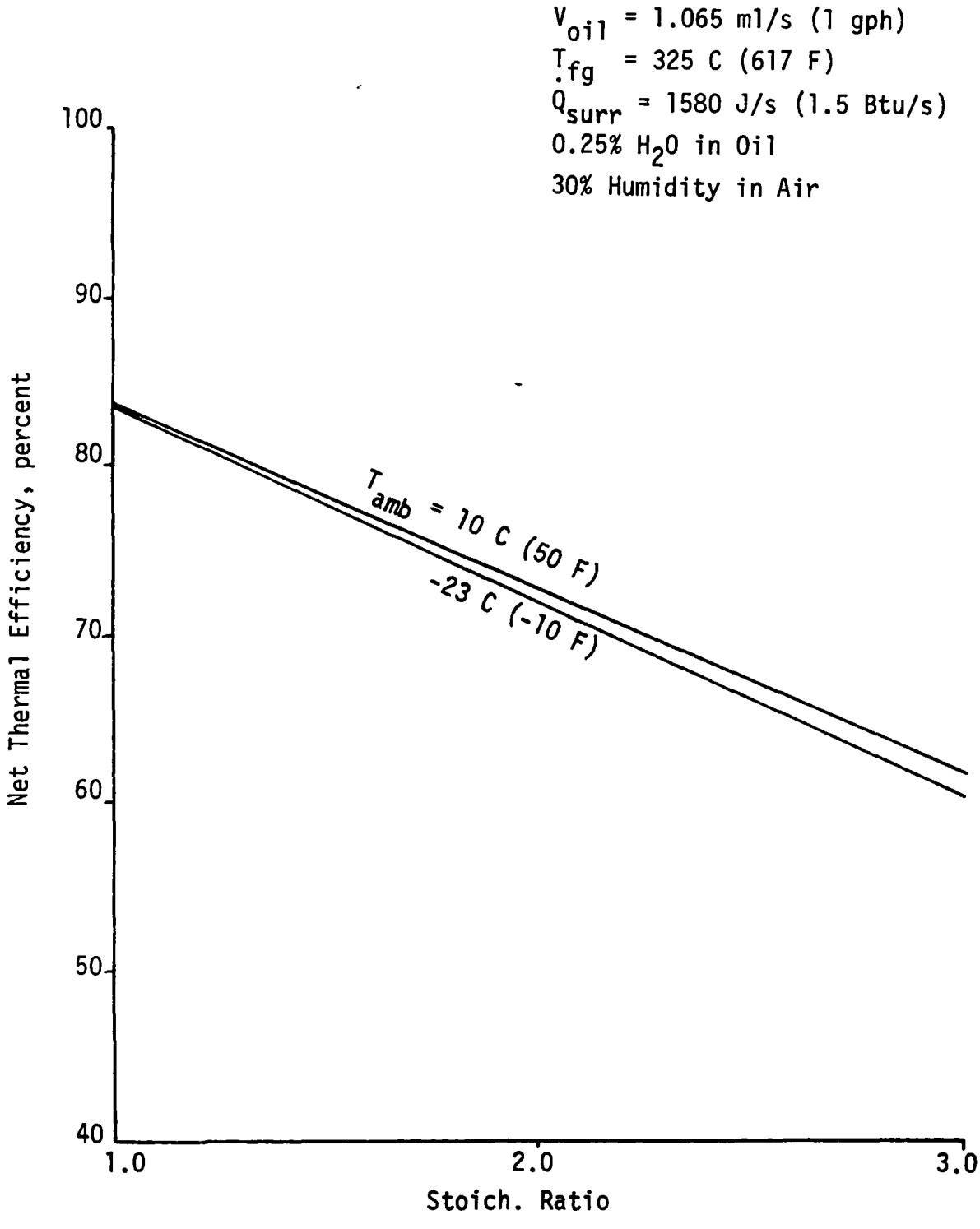

Figure 6. Calculated Effects of Ambient-Temperature Changes on Oil Furnace Steady-State Thermal Efficiency

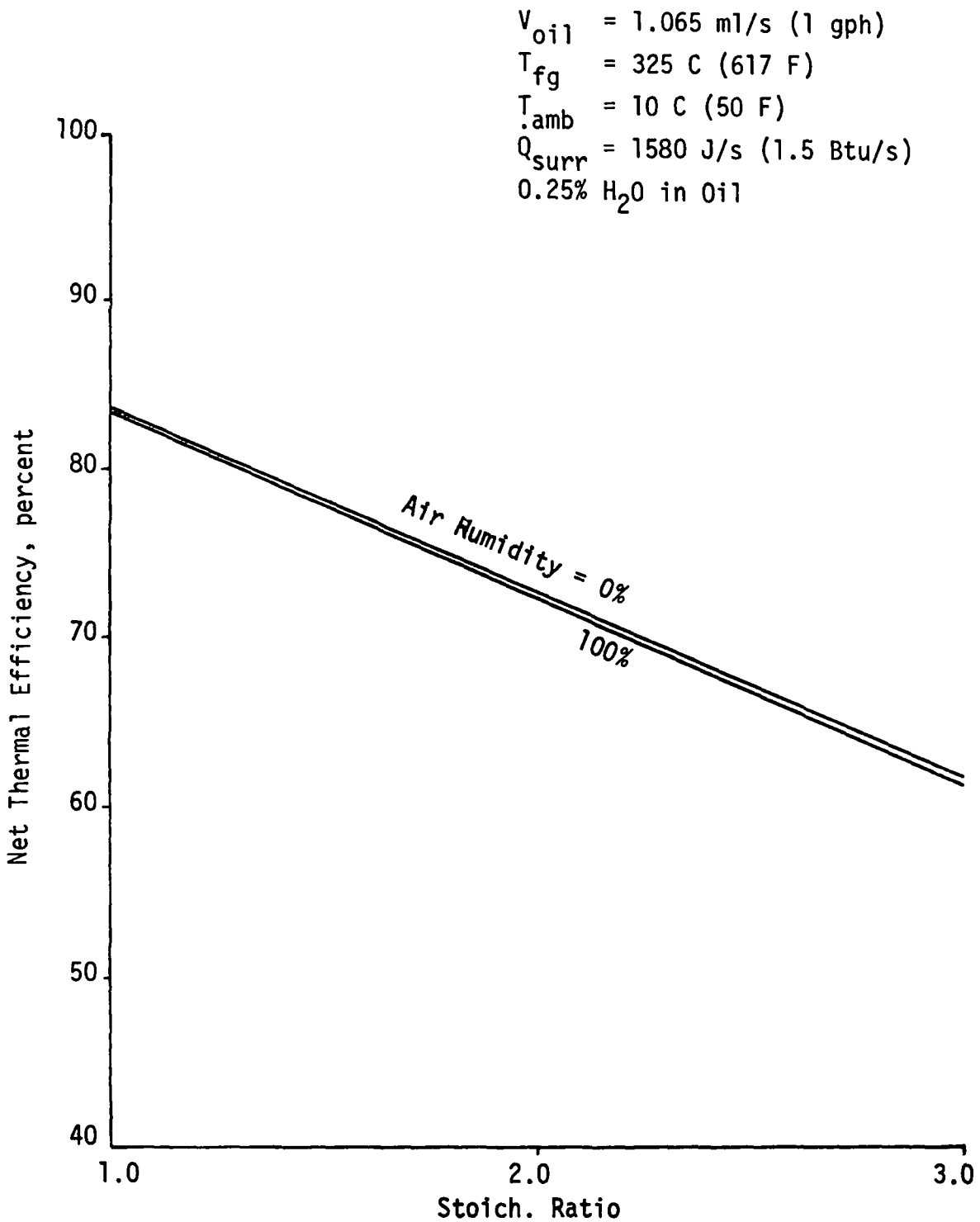

Figure 7. Calculated Effect of Air Humidity on Oil Furnace Steady-State Thermal Efficiency

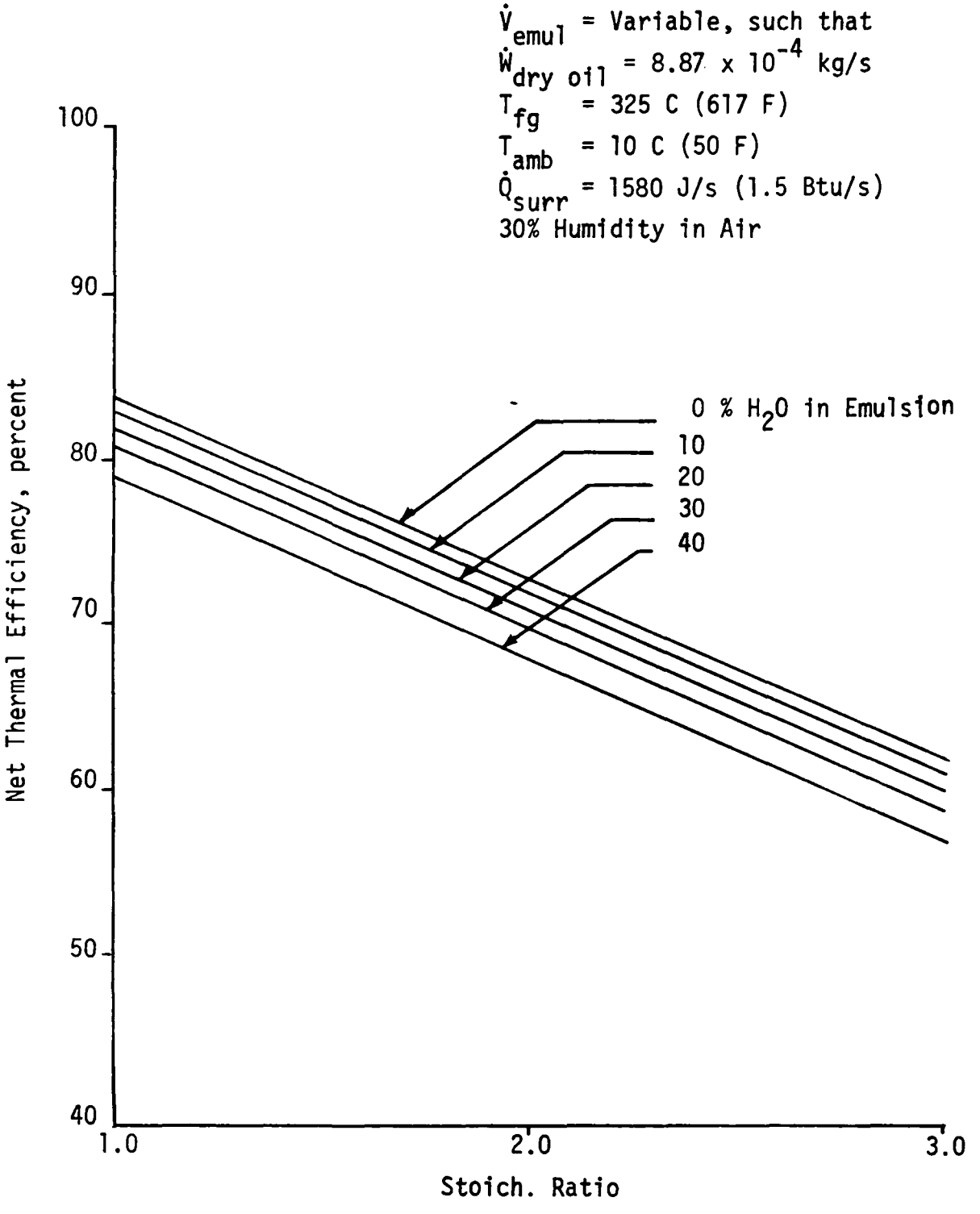

Figure 8. Calculated Effect of Emulsifying Oil With Water on Oil Furnace Steady-State Thermal Efficiency

Data plotted in Fig. 7 show that variations in air humidity have an almost negligible effect on furnace thermal efficiency when the ambient temperature is 10 C (50 F). An even less significant effect would be expected at lower ambient temperatures, because absolute saturation humidity falls sharply with decreasing ambient-air temperature.

Emulsifying fuel oil with increasing quantities of water is seen to degrade overall steady-state efficiency by about 1 percent $\Delta\eta_{react}$ per 10 percent water increase, Fig. 8.

At a nominal oil flowrate of 1 ml/s (gph), the oil heat production rate is 38,000 J/s (129,700 Btu/hr). The relationship between overall efficiency and reactant efficiency (Eq. 8) becomes

$$\eta_{furn} = \eta_{react} \frac{38,000}{38,000 + \dot{Q}_{elec}}$$

which for various values of Q_{elec}, gives

$\dot{Q}_{elec}$ (watts) = 0; 250; 500; 750; 1000

η_{furn}/η_{react} = 1.000; 0.993; 0.987; 0.981; 0.974

Typical steady-state power consumption for warm-air furnaces in this size range is on the order of 880 W (500 W blower motor, 250 W burner motor, 100 W ignition transformer, and 30 W control circuit). Thus, the overall steady-state efficiency is typically on the order of 97 to 98 percent of reactant thermal efficiency. This result immediately suggests that efforts to reduce power consumption can yield only relatively small gains in overall system efficiency. However, because electrical power costs are substantially higher than fuel oil prices (for an equivalent energy level), a 1-percent increase in system efficiency achieved by reducing power consumption may represent a significant decrease in annual operating cost. Therefore, continuing attention should be given to finding reasonable ways of reducing power consumption consistent with safety, reliability, and initial cost considerations.

Cyclical Operation. There are two types of flue gas heat losses during cyclic furnace operation, one associated with the combustion gases during the burner firing time and another associated with a natural draft flow of air through the burner, firebox, etc., during the standby period when the burner is off. These two components were treated separately in FURNAC. The steady-state calculation of $\dot{Q}_{fg}$ described above was applied directly during Δt_{on} to evaluate heat convected up the flue with the combustion gases. Natural draft heat losses during Δt_{off} were evaluated as follows.

All of the hot furnace components were lumped into one mass having a given mean heat capacity and initial mean temperature at the burner cutoff time. This mass was cooled by transfer of heat to the furnace coolant air flow, as long as it continued, and to the natural draft air flow. The latter flowrate was calculated as a function of the mean furnace temperature, ambient outdoor temperature, flue height, and effective combustion air inlet area* of the burner's adjustable air louvers:

$$\dot{w}_{n.d.air} = \frac{782.1\ A_b\ R_{stoich}\ \sqrt{H_f}}{T_{amb}} \left[\frac{T_{fb} - T_{amb}}{T_{fb} + T_{amb}}\right]^{1/2} \qquad (9)$$

wherein an effective area flow coefficient of 0.60 was included and it was assumed that this air flow has negligible effect on the flue's draft effect. The draft air flow was assumed to be heated to the mean temperature of the lumped "firebox" mass.

Rather than try to calculate the external losses to the surroundings, they were represented heuristically as a time-varying fraction of a steady-state loss rate (which represents the maximum loss rate during a cycle). The assumed behavior of loss rate versus time is sketched below for one cycle of furnace operation.

*The read-in value of A_b, the effective combustion inlet area, corresponded to a burner air setting yielding SR = 1. That value was multiplied by SR to account approximately for the changing air louvers' setting as stoichiometric ratio was increased.

The burner is started at t_{on1} to start this cycle, turned off at t_{off}, and restarted at t_{on2} to end the cycle. The warm-air (furnace coolant) fan is assumed to run for a few minutes after burner cutoff, and is stopped at t_{fan}. As a result of furnace cooling during the standby period, the losses will be at their lowest value at the end of the cycle (and the beginning of the next cycle). In the computer program, they were taken to increase linearly from that low magnitude to ($\dot{Q}_{surr,ss}$) after 1/3 of Δt_{on}, to be equal to $\dot{Q}_{surr,ss}$ for the remaining 2/3 of Δt_{on} and to drop linearly over the time, $t_{off} < t \leq t_{fan}$.

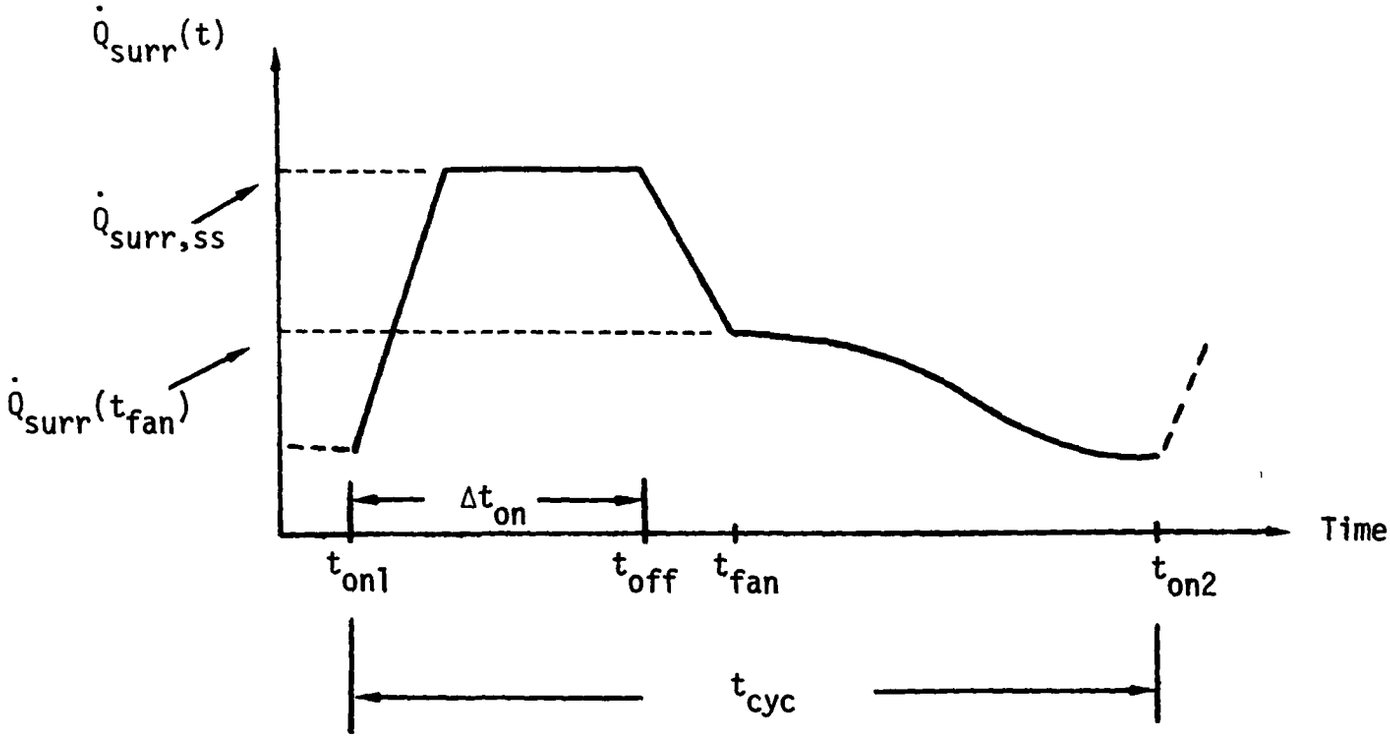

The level to which the losses fall during this latter time period was determined by the cooling effect of that continuing air flow. The heat content of the furnace's firebox and heat exchanger was estimated at t_{off} and again at t_{fan}; the fractional value of the loss at time t_{fan} was assumed to be proportional to the ratio of those two estimated furnace heat contents.

During the period between t_{fan} and t_{on2}, a Gaussian decay of the heat losses was assumed:

$$\dot{Q}_{surr}(t) = \dot{Q}_{surr}(t_{fan}) \quad \exp\left[-B(t \quad t_{fan})^2\right] \tag{10}$$

(Here, the value of B controls the rate of decay of the furnace heat losses. B = 0.004 gives $\dot{Q}_{surr}(t_{on})/\dot{Q}_{surr}(t_{fan})$ = 0.407 for $t_{on2} - t_{fan}$ = 15 minutes, and gives 0.202 for 20 minutes.) Total furnace setting heat loss is the integral over the cycle time of the time-varying losses.

Nominal values of the several adjustable parameters in the computer model were selected by running exploratory cases and comparing calculated efficiencies with cycle efficiency data obtained by Howekamp and Hooper (Ref. 7). A graph of their results is reproduced from Ref. 2 in Fig. 9. Those data were obtained by cyclical testing (10 minutes on, 20 minutes off) of a reference ABC burner fired in a Williamson Low-Boy furnace with several alternate burner heads. Superimposed on their data is a bold-face dashed line calculated by running the FURNAC computer model with the following nominal parametric values:

$\dot{V}_f$	= 1.0 ml/s (gph)	W_{fb}	53.1 kg (117 pounds)
T_{amb}	-7 C (20 F)	$\bar{c}_{pfb}$	= 500 J/kg-K (0.12 Btu/lb-R)
T_{fg}	325 C (617 F)	$\bar{T}_{fb}(t_{fan})$	= 355 C (670 F)
x_{hum}	0	t_{fan}	= t_{off} + 5 minutes
x_{emul}	= 0	A_b	= 1.12 x 10^{-3} m^2 ($1.2x10^{-2}$ ft^2)
Δt_{on}	= 10 minutes	H_f	= 6.10 m (20 feet)
Δt_{off}	= 20 minutes	$\dot{Q}_{fan}$	= 0.472 m^3/s (1000 cfm)
$\dot{Q}_{surr,ss}$	= 527 J/s (0.5 Btu/sec)	B	= 0.004

This set of values was neither unique nor particularly thought to be the "best" set for matching the Howekamp and Hooper data, but represented a reasonable compromise among the efficiency level and the slope with stoichiometric ratio as

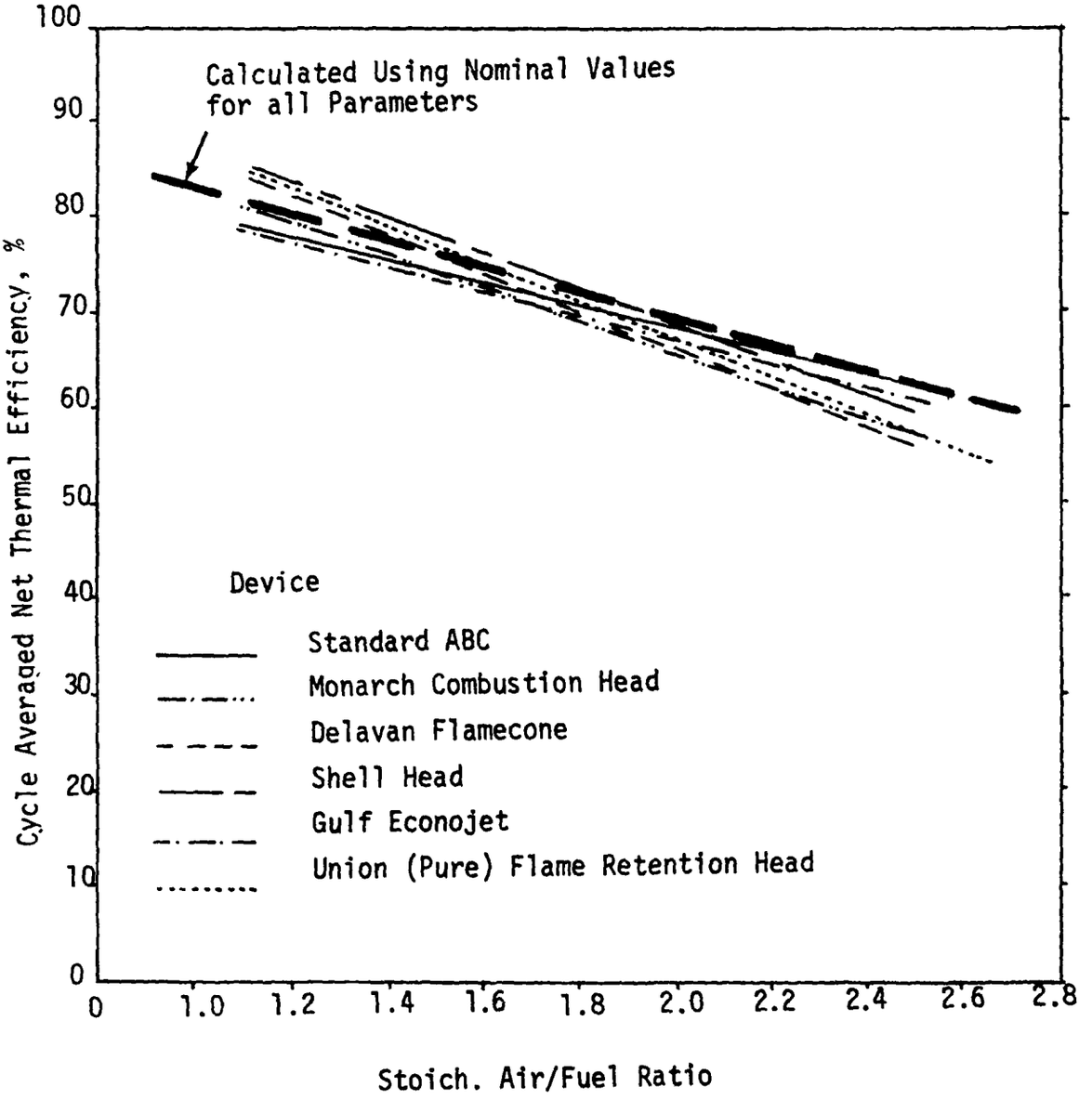

Figure 9. Calculated Cycle Thermal Efficiency Compared with Measured Overall Heating Efficiencies of Combustion Improving Devices (Ref. 7)

influenced by flue gas temperature, steady-state heat loss level, warm-air cooling effect, and natural draft losses. There are probably significant deviations from reality in the assumption of constant flue gas temperature, in the use of a rather small value for $\dot{Q}_{surr,ss}$ and in the calculation of draft air heat losses. In spite of such shortcomings, it is highly instructive to examine the variation of cycle thermal efficiency with variations of certain parameters.

The nominal value of $\dot{Q}_{surr,ss}$ corresponded to about 1.4 percent of the oil heating value. For the nominal 10 minutes on/20 minutes off cycle, losses to the surroundings rose to about 2.3 percent of the oil burned, essentially irrespective of the stoichiometric ratio. Calculated draft air heat losses, however, were a strong function of stoichiometric ratio, increasing from 2.9 percent at R_{stoich} = 1 to 6.9 percent at R_{stoich} = 3.

Continuing to circulate the warm air furnace coolant for several minutes after burner cutoff can contribute significantly to reducing the cycle losses in thermal efficiency. This is illustrated graphically in Fig. 10. Five minutes of fan operation after burner cutoff apparently can recover approximately 70 percent of the hardware-stored heat which would otherwise be lost. Even so, the cycle efficiencies are about 5 percent lower than the steady-state values. Even longer fan operation would help recover some of that loss, but not all of it is available because losses to the surroundings continue while it is being recovered.

The natural draft air flow, and therefore the standby flue gas heat losses, are dependent upon ambient outdoor temperature. As a result, cycle thermal efficiency is somewhat more dependent upon ambient temperature (Fig. 11) than is the steady state (Fig. 6).

Cyclical heat losses can be reduced, conceptually, in a number of ways. If the firing rate, average cycle time, and ratio of on-time to cycle-time are fixed, one must consider: better external insulation (lower $\dot{Q}_{surr}$); lighter weight, more compact firebox and heat exchanger components; and, possibly, a method to eliminate natural draft air flow (i.e., mechanical solutions). If the firing

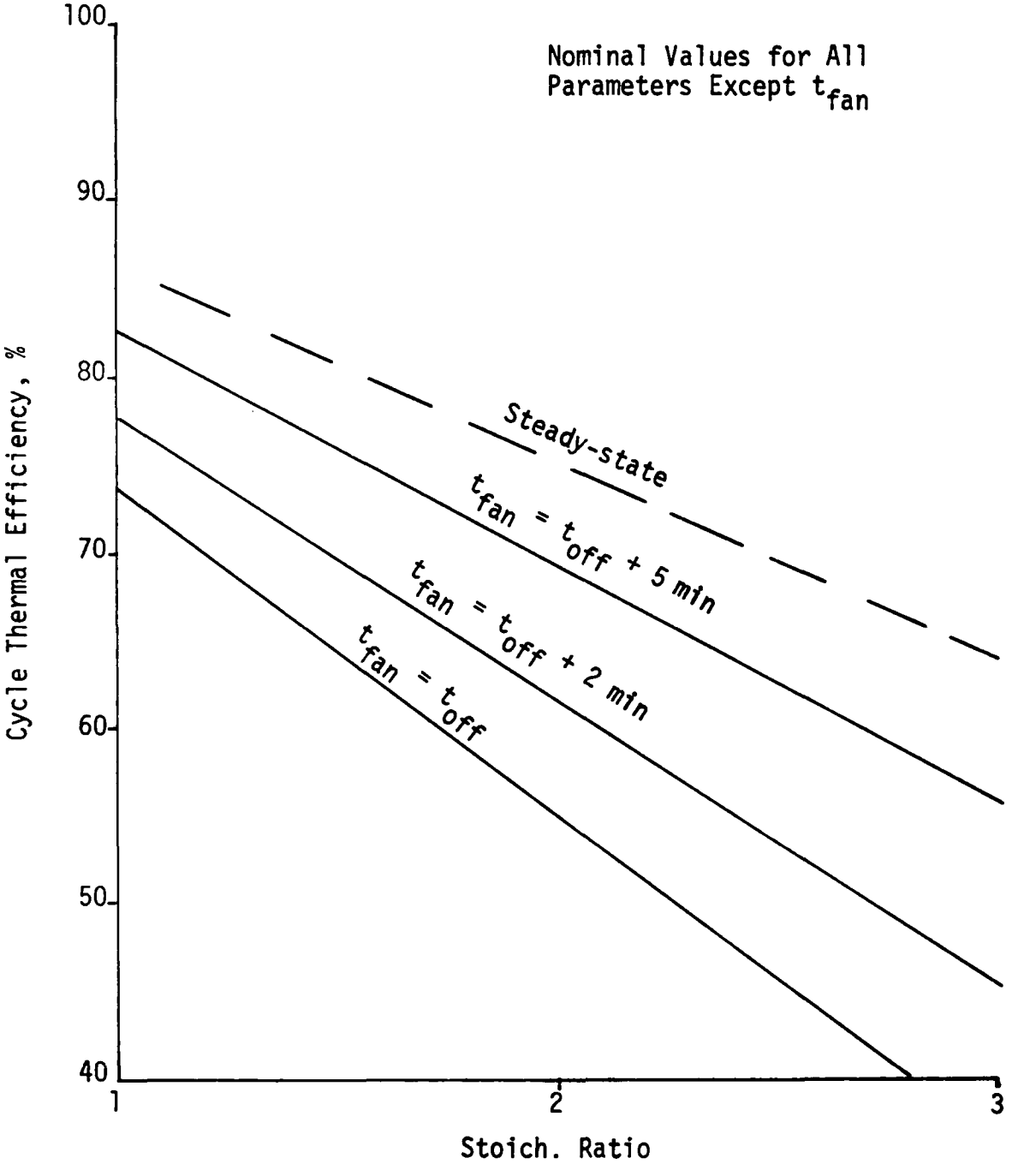

Figure 10. Calculated Effect on Oil Furnace Cycle Thermal Efficiency of Continuing to Circulate Warm Air Furnace Coolant After Burner Cutoff

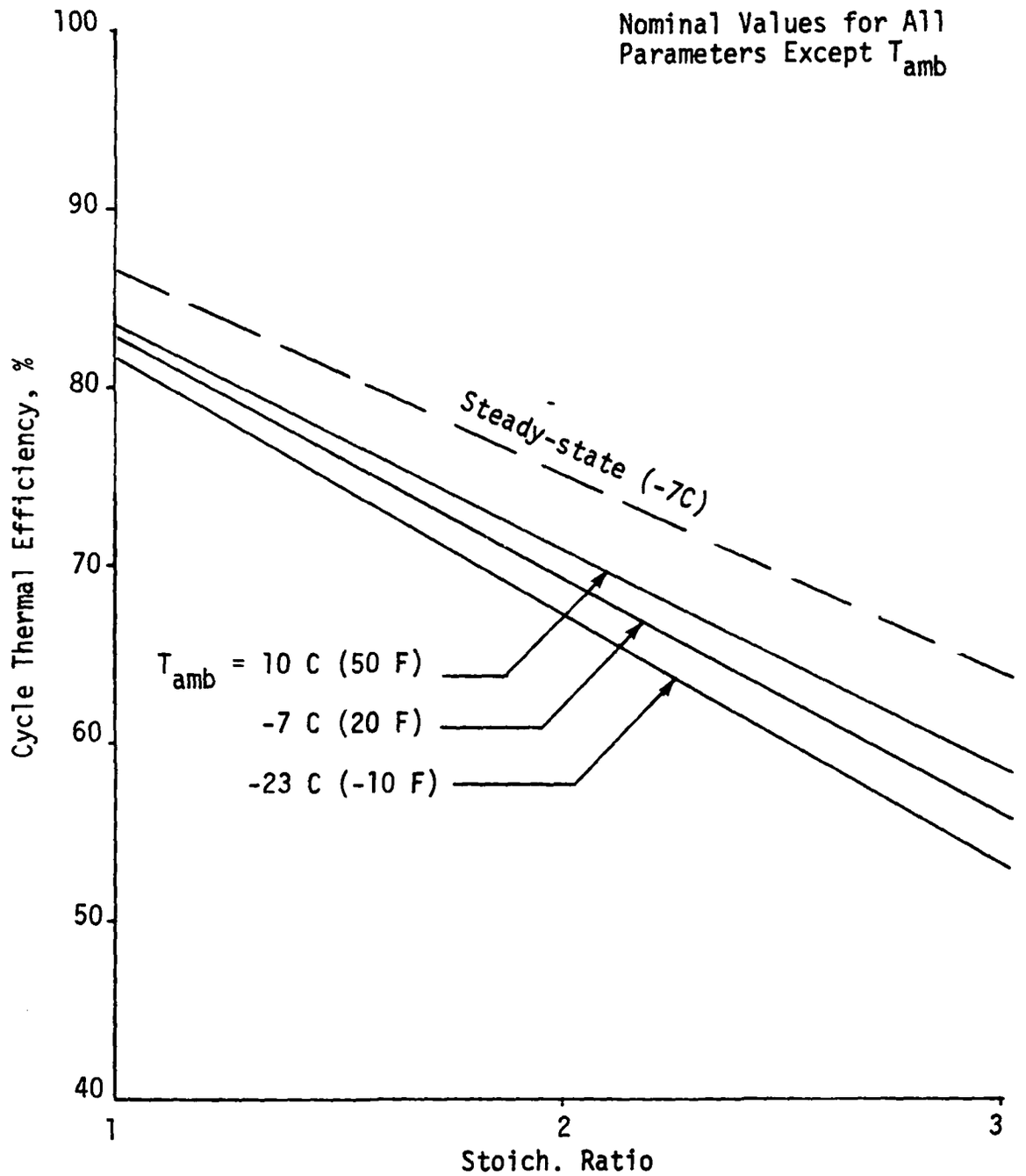

Figure 11. Calculated Effect of Ambient-Temperature Changes on Oil Furnace Cycle Thermal Efficiency

rate and cycle parameters can be varied, it might be possible to reduce losses by tailoring the cycle to the heating demand load. For a fixed heating demand, the firing rate would be invariant with cycle time *per se*, but would vary inversely with the ratio t_{on}/t_{cyc}. Analyses were made with values of fractional burner on time of 1/5, 1/3, and 1/2. Under the assumption of constant thermal demand, the corresponding firing rates were 1-2/3, 1, and 2/3 ml/s (gph), respectively. Calculated cycle thermal efficiency results are plotted in Fig. 12 for a constant stoichiometric ratio of 1.5 and for $t_{fan} = t_{on} + 5$. Plotted as the zero-cycle-time intercepts are the calculated steady-state efficiencies for the various firing rates. The dashed lines extend through a region where the warm-air furnace coolant must be circulated continuously (i.e., $\Delta t_{off} \leq 5$ min).

Examination of Fig. 12 shows that there is very little influence of cycle time *per se*, on cycle efficiency but that significant gains result from approaching continuous firing. If more nearly continuous firing were achieved by throttling the oil flow, and flue gas temperature were to remain constant as in Fig. 12, on the order of 5 to 10 percent higher thermal efficiency would be expected. With a fixed heat exchanger however, substantially lower flue gas temperatures should be experienced during throttling, resulting in even higher efficiency gains. However, if the furnace system has been designed to give high steady-state thermal efficiencies by producing low flue gas temperatures, throttling or modulating the oil flowrate could easily drive the flue gas temperature into the neighborhood of the dew-point with concomitant corrosion problems.

Hydronic Boiler Performance. Several FURNAC cases were run with appropriate input parameters modified to approximate a hydronic boiler. Specifically, the "lumped parameter" firebox and heat exchanger weight and mean temperature were altered to include approximately 110 kg of water at about 75 C as a heat sink rather than as a circulating coolant.

Calculated thermal efficiencies for hydronic cases were compared (at corresponding cycle and firing rates, stoichiometric ratios, and ambient and flue gas temperatures) with warm-air cases in which the warm-air fan ran for 5 minutes after

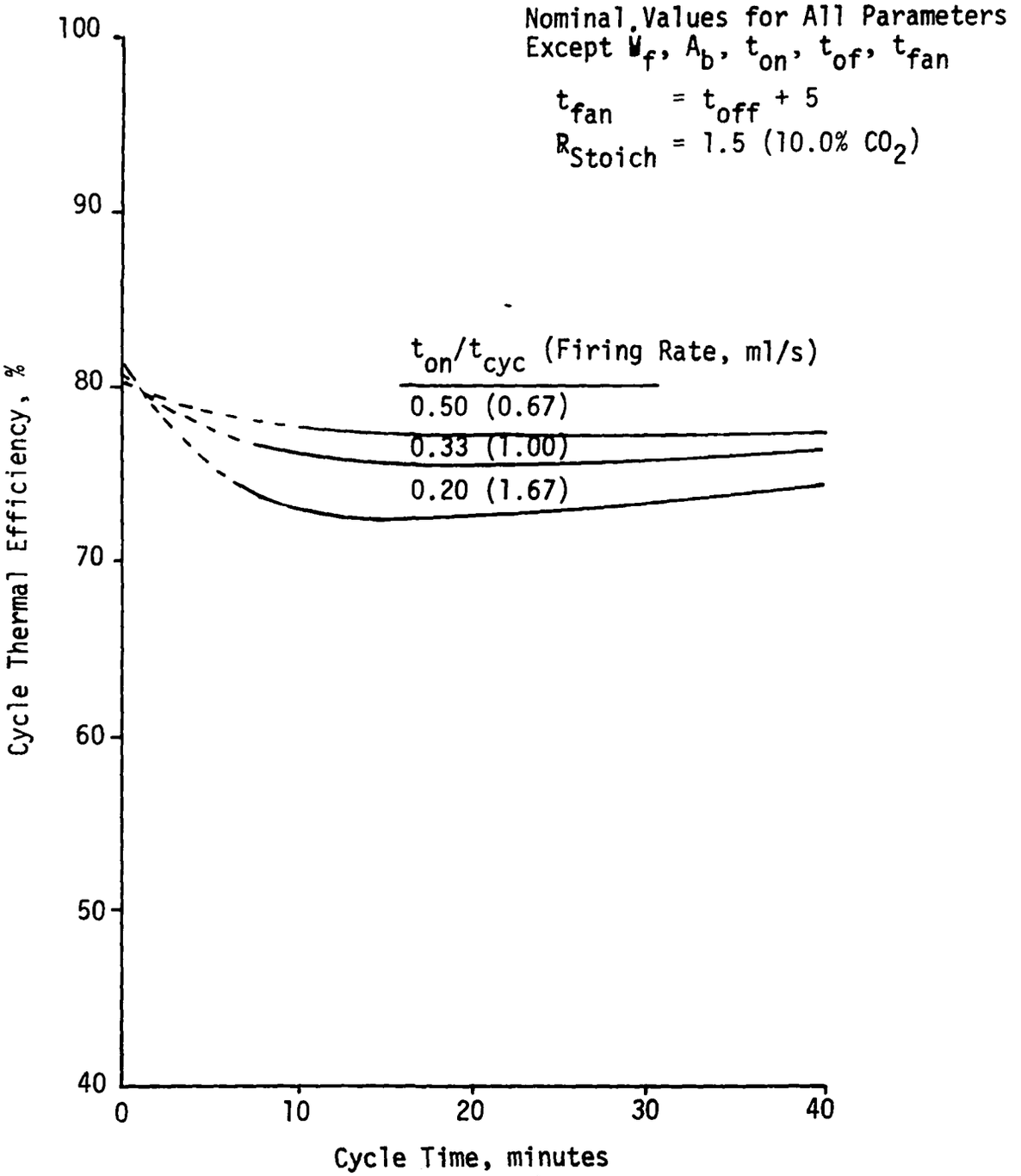

Figure 12. Calculated Effects on Oil Furnace Cycle Thermal Efficiency of Varying Cycle Timing at Constant Thermal Demand

burner cutoff. Generally, the hydronic efficiencies were within about 1 to 2 percent of those for the corresponding warm-air cases. Although the draft air losses were initially substantially lower for the hydronic unit than for warm-air, they continued essentially unabated for the entire burner offtime; their persistence appeared to effectively counterbalance their lower level.

Heat Transfer Analysis Method

The foregoing oil furnace thermal analyses were performed by treating flue gas and furnace coolant outlet temperatures as known, constant-valued parameters. Optimizing efficiency requires careful selection of a nominal design point and more detailed analysis of furnace behavior under a variety of ambient and demand conditions. Analyses of that type would best be done with a furnace performance analysis model which includes a treatment of the dynamics of furnace heat exchange so that furnace coolant and flue gas temperatures can vary dynamically. Such a capability is also needed for analyzing effects on efficiency of flue gas recirculation.

To facilitate more realistic analyses of design aspects (such as firebox and heat exchanger size and construction), operational aspects (such as firing level, cycle timing, and climatic conditions) and pollutant reduction concepts (such as flue gas recirculation and water-emulsified fuel), an expanded-capability computer model for a warm-air oil furnace was formulated using a rather general, physically simplified, lumped-parameter approach. The resultant formulation was programmed as a warm-air oil-furnace model which marches in time through an operating cycle and calculates combustion gas, draft air, warm air, firebox (lined or unlined), and heat exchanger cooling and heating as functions of time. Entitled WAFURN, that computer program is described and listed in Appendix A.

Furnace Cyclical Operation Analysis. The WAFURN computer program was run with a variety of inputs to: (1) assess briefly its ability to simulate furnace behavior and (2) re-examine the influence on cycle thermal efficiency of some parameters previously indicated as being important.

For comparison with the overall cycle thermal efficiency data of Howekamp and Hooper (Ref. 7), WAFURN input parameters corresponding to a Lennox 0F7-105M furnace were used. (The construction and size of this Lennox furnace are quite similar to the Williamson furnace used by Howekamp and Hooper.) Calculated overall cycle thermal efficiency* data at four stoichiometric ratios are plotted as black triangles superimposed upon Howekamp and Hooper's curves in Fig. 13. The calculated results are seen to be in quite good agreement with the experimental data. There is, however, an apparent curvature in the calculated results not indicated by the straight line representations of the experimental data. A simple explanation of the curvature comes from examination of the calculated flue gas temperatures, which tend to increase with increasing stoichiometric ratio but approach an asymptotic value at about a stoichiometric ratio of 1.8:

Stoichiometric Ratio		1.2	1.5	1.8	2.1
T_{fg}(10 minutes),	K	= 600	638	653	653
	(F)	= (620)	(689)	(715)	(715)

However, two additional factors may contribute to the differences between the calculated and experimental results. These are that WAFURN assumes 100 percent combustion efficiency in the firebox; whereas, there is evidence of significant heat losses due to incomplete combustion in the Williamson furnace at low stoichiometric ratios (Ref. 2). The other factor is the loss of heat due to draft air flowing through the furnace and up the flue during the burner off time. This amounted to less than 1/2 percent in the WAFURN calculated cases, limited by having a barometric control damper 2 m above the center of the firebox. Had these losses been calculated as being higher, they would have reduced the curvature of the calculated efficiency plot, because the draft air flowrate is approximately proportional to stoichiometric ratio (Eq. 9).

*Thermal efficiency was defined by Howekamp and Hooper as the total heat transferred to the warm-air stream divided by the total net heating value of oil burned in a cycle. This is completely consistent with the definition in WAFURN.

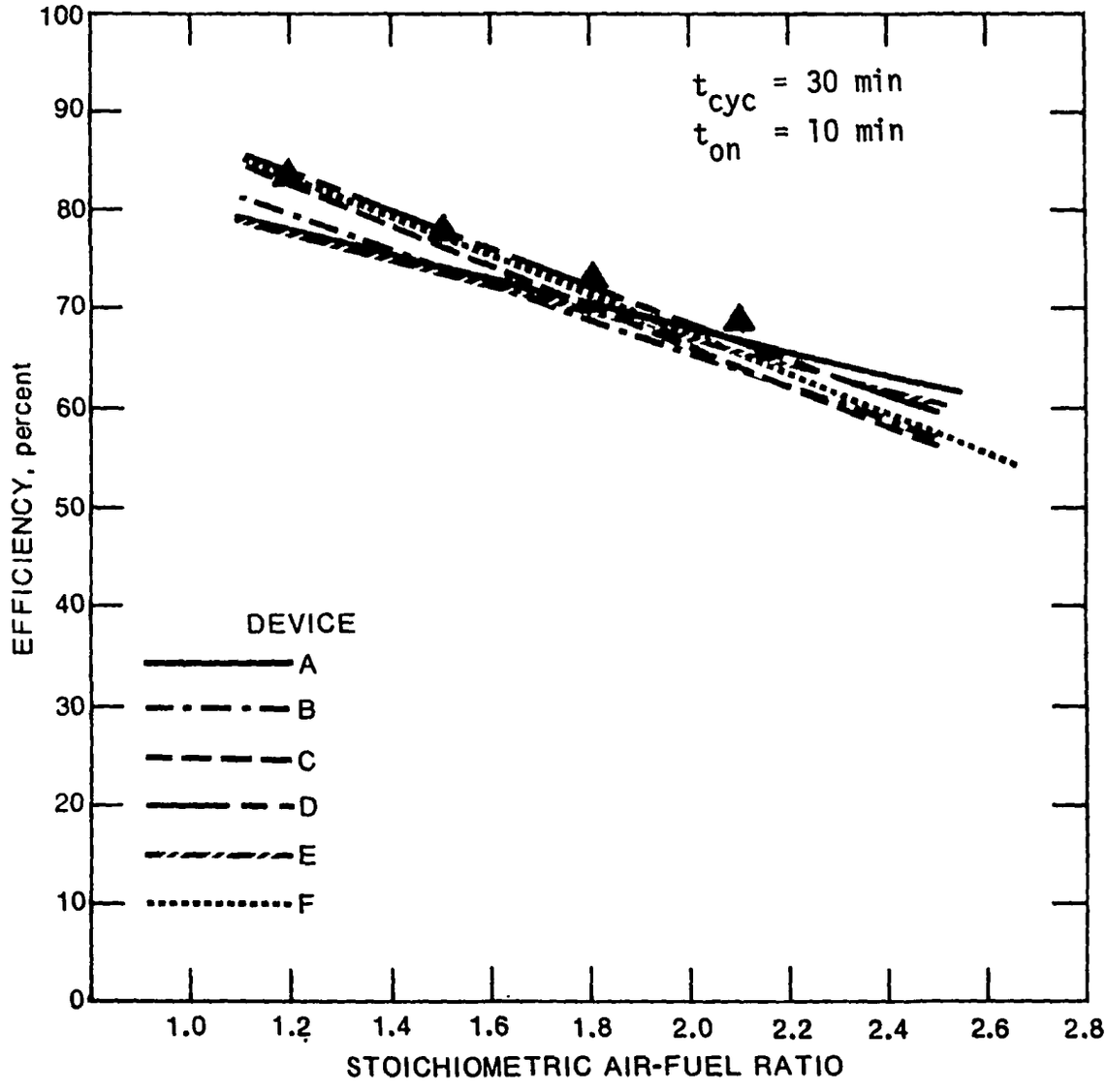

Figure 13. WAFURN-Calculated Overall Cycle Thermal Efficiency Compared With Measured Efficiencies (Ref. 7)

For further assessment of the WAFURN computations, the firing rate was reduced from 1.00 ml/s (0.95 gph) to 0.75 ml/s (0.71 gph) and the calculated flue gas temperatures were compared with experimental temperatures measured during steady-state operation of the OF7 furnace with a Union AFC burner (Ref. 5). Over the 1.2 to 2.1 stoichiometric range, the measured temperatures ranged from 528 to 579 K (490 to 582 F). Tenth-minute WAFURN-calculated flue gas temperatures for the same stoichiometric range fell between 528 and 605 K (490 to 630 F). Although the calculated temperatures differ significantly from those measured, it was believed that the correspondence was good enough, particularly in the 1.2 to 1.5 stoichiometric range, to support immediate application of the computer model without further empirical "tuning up" of the heat exchanger film coefficient expressions.

Calculated net cycle thermal efficiencies were approximately 5 percent higher at the 0.75 ml/s (0.71 gph) firing rate than at the 1.00 ml/s (0.95 gph) rate, predominantly as a result of the lower flue gas heat losses attending reduced flue gas temperatures. Another way of reducing flue gas temperatures is to utilize a more effective heat exchanger. Increased heat exchanger effectiveness might be achieved in several ways; the simplest way is to increase the heat transfer area. To illustrate the potential performance improvement, WAFURN was run with Lennox OF7 inputs, except for a 1/3 greater heat exchanger area.* Computed 4th minute flue gas temperatures and cycle efficiencies for a 12-minute cycle and a 4-minute burner operation at the 1-ml/s firing rate were as follows:

Stoich. Ratio	Heat Exchanger Area, m^2	Flue Gas Temperature		Cycle Thermal Efficiency, %
		K	(F)	
1.2	2.25	599	618	82.25
	3.00	455	359	89.39
1.5	2.25	637	686	76.72
	3.00	495	432	85.25

*Although the mass of the heat exchanger was left invariant for these computer program runs, it was varied parametrically in other runs by ±25 percent and found to influence flue gas temperature by less than 1 K, and cycle efficiency by less than 0.5 percent.

Cycle Timing Effects. In view of the calculated variability of cycle thermal efficiency with firing rate, cases were run to examine the dependence of efficiency on cycle timing. A situation in which thermal demand and flue gas temperature are both constant was considered previously using the FURNAC computer model; the results are reproduced from Fig. 12 as dotted curves in Fig. 14. WAFURN-calculated results for the fixed heat exchanger of the Lennox 0F7 are the solid curves in this figure. It is seen that there is only a small predicted effect of cycle time *per se* on furnace efficiency, but that a substantial efficiency penalty can be expected if a given thermal load is satisfied by brief firings at elevated firing rates. Reduced efficiencies at higher firing rates are caused primarily by increases in flue gas temperature.

It is constructive at this point to examine the effects of cycle timing in satisfying a variable thermal load with a constant firing rate. For the Lennox 0F7 fired at 1.00 ml/s (0.95 gph) and 1.5 stoichiometric ratio, the following results were calculated by WAFURN:

t_{cycle}, minutes	t_{on}/t_{cycle}	T_{fg} at t_{off}, K	(F)	$\eta_{thermal}$, %
12	0.20	647	704	76.01
	0.333	637	686	76.72
	0.50	638	689	77.72
20	0.333	637	686	76.78
30	0.20	636	685	76.99
	0.333	638	689	77.79
	0.50	638	689	78.05

Comparison of these efficiency values with those plotted in Fig. 14 reveals that flow modulation is almost wholly responsible for the wide range of efficiency variation in Fig. 14. Apparently, at a constant firing rate, quite wide excursions of cycle time and burner-on time can be experienced without incurring

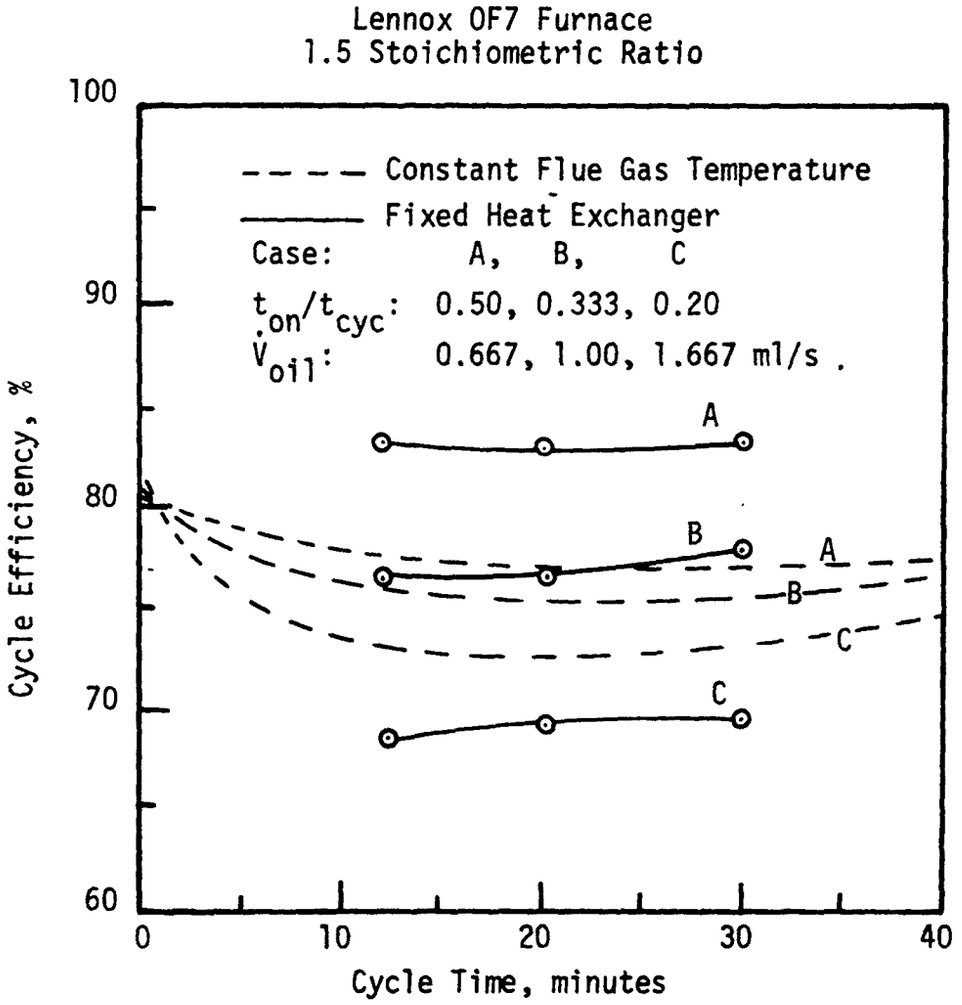

Figure 14. Calculated Effects on Oil Furnace Cycle Thermal Efficiency of Varying Cycle Timing at Constant Thermal Demand

substantial deviations from steady-state thermal efficiency.* If that constant firing rate is the design rate, the flue gas temperature approaches its design value closely in all but the very shortest firings. Higher firing rates lead to reduced efficiency primarily because the flue gas temperature increases. Conversely, firing rates lower than the design value result in increased thermal efficiency by decreasing the flue gas temperature. Assuming that the design value of flue gas temperature was selected to avoid condensation in and corrosion of the heat exchanger and flue, the lower temperatures attained by lowering the firing rate should be unacceptable. Thus, the two constraints of maintaining high efficiency and maintaining some minimum level of flue gas temperature provide persuasive arguments against designing for reactant flow modulation in residential furnaces having fixed heat exchangers.

High/Low/Off Burner Operation. There appears to be a modest efficiency advantage in designing for high ratios of burner firing time to cycle time. This suggests that high/low/off burner control might provide significant fuel savings over an entire heating season. The furnace would be designed with a two-firing level capability. Continuous firing at the lower level would meet or exceed the residential thermal demand for some large fraction of the demand time. Conventional on-off control would be used at this firing level, which would be selected to give maximized efficiency and operation - on the average - much closer to steady-state than is conventional practice. The higher firing level would be called upon when the demand exceeds the continuous-firing capability of the lower firing level, and on-off control would be supplanted by high-low control. The idea is to accept brief periods of reduced efficiency at the high level to permit operating at enhanced efficiencies for long periods.

*This observation is applicable to well-designed and well-insulated furnaces which have low external convective and radiant heat losses to the surroundings and low draft air losses during the burner-off time.

This concept was evaluated breifly by providing a high-low optional analysis path in WAFURN and calculating what might happen if the Lennox OF7 furnace were modified for low fire at 0.75 ml/s (0.71 gph) and high fire at 1.125 ml/s (1.07 gph). WAFURN-calculated cycle efficiencies for 12 minute cycles are plotted in Fig. 15. High/low/off operation at two stoichiometric ratios is shown as solid curves. The 100 percent point on the abscissa represents steady-state low-fire, and the 150 percent point represents steady-state high fire. Slightly decreasing efficiency with decreasing demand is caused by starting transient losses and by draft air losses during the burner off times. The more abrupt efficiency decline as demand exceeds 100 percent is the result of increased flue gas temperatures during high-fire times.

To assess the impact of such operation on overall season-averaged efficiency, it was assumed, for simplicity, that the time distribution of firing levels during some hypothetical heating season has a normal distribution about the 75 percent firing level point. The calculated firing-level-weighted and firing-time-weighted overall seasonal average efficiency was 87.05 percent at 1.2 stoichiometric ratio. If the high-fire capability were deactivated, the demand would exceed the low-fire heat supply about 15 percent of the time and the average efficiency would rise to 87.47 percent. Thus, an almost negligible efficiency penalty might be paid for the extra high-fire capability.

There are, of course, other ways to provide the thermal demand. One way is to simply use on-off control at the high-fire level. Peak (steady-state) efficiency is represented by the 150 percent point, and that is seen to be about 5 percent below the on-off/high-low seasonal average. A more meaningful comparison is to increase the heat exchanger area so that steady-state high-fire flue gas temperatures would be comparable to those for steady-state low fire. Calculated results for on-off control of the high-fire level using a 20.4 percent greater heat exchange area are plotted as dashed curves in Fig. 15. To match the seasonal heating demands, shorter burner on times/cycle are needed for this situation. The seasonal average efficiency was calculated to be 86.75 percent or only 0.3 percent below that for the more complicated--and more costly--on-off/high-low operation.

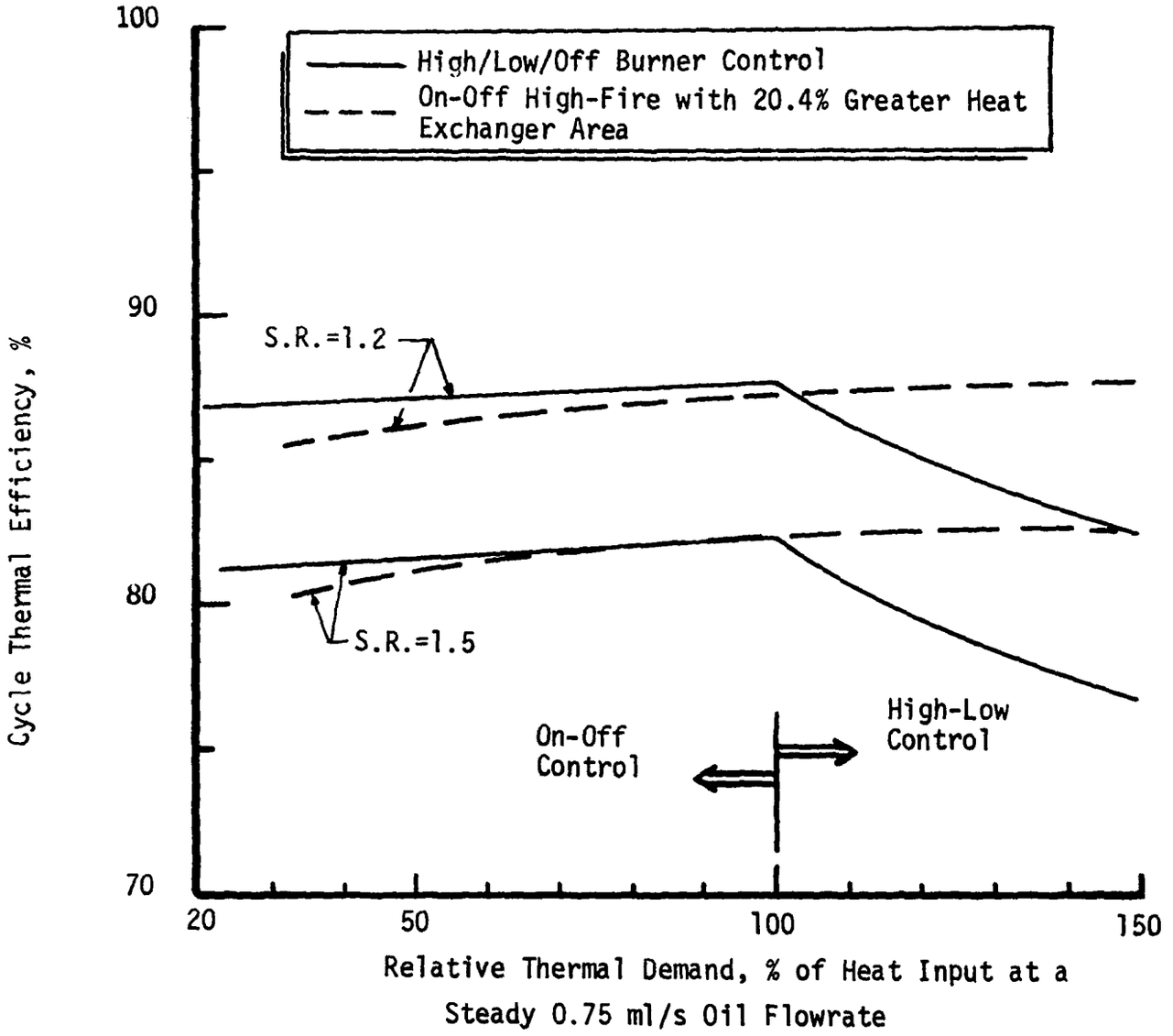

Figure 15. Calculated Thermal Efficiencies for Lennox OF7 Furnace for Some Dual-Firing-Level Situations

An efficiency difference of 0.3 percent is equivalent to that which would be gained by providing a 1 to 2 percent greater heat exchange area or by operating at a stoichiometric ratio that's smaller by about 0.01 to 0.02. Further, the furnace's electrical components would be required to run nearly 45 percent longer for the high-low operation than for the simpler on-off at high fire. The additional electric power consumption undoubtedly would cost considerably more than the small quantity of fuel saved and, in addition, more frequent maintenance and earlier equipment replacement should be anticipated. Thus, this kind of modulated-flow furnace control does not appear to be worthy of further consideration.

Water-Emulsified Fuel Oil. Emulsifying fuel oil with water, under the FURNAC assumption of invariant flue gas temperature, was found to effect an appreciable decrease in thermal efficiency which depended only upon the mass fraction of water in the fuel (Fig. 8). For example, 40 percent water in No. 2 fuel oil lowered the calculated thermal efficiency by about 5 percent over the stiochiometric range from 1.0 to 3.0. However, because the composition, temperature and mass flux of combustion product gases all change with varying fuel water content, a fixed heat exchanger should not be expected to produce a constant flue gas temperature. To get a more realistic preliminary indication of this effect, WAFURN was run with a 40 percent water emulsion supplied to the Lennox OF7 furnace at a dry oil flow-rate of 1.00 ml/s, several stoichiometric ratios and a 4-minute firing in a 12-minute cycle. The following tabulation characterizes the results.

Stoichiometric Ratio	% H_2O in Oil	Combustion Temperature, K	Combustion Temperature, F	Fourth-Minute Flue Gas Temperature, K	Fourth-Minute Flue Gas Temperature, F	Cycle-Averaged Thermal Efficiency, %
1.2	0	2081	3285	599	618	82.25
	40	1929	3011	613	643	77.41
1.5	0	1810	2729	637	686	76.72
	40	1690	2583	640	693	72.09
1.8	0	1605	2430	651	712	71.96
	40	1509	2255	648	707	67.47

It is seen that, although the combustion zone temperature is lowered by 100 C or more by diluting the fuel with water, the flue gas temperature is changed only slightly. Thus, the emulsion's impact on furnace cycle-averaged efficiency is quite comparable to that shown in Fig. 8.

Three ways in which emulsified oil could conceivably be beneficial (Ref. 8) were not included in the WAFURN calculations. First, if the oil spray nozzle were producing a coarse spray, leading to substantial combustion inefficiencies, emulsified fuel would tend to correct this poor operation by steam generation within heating droplets, causing them to disintegrate and burn more rapidly. It might then be possible to operate smoke-free with significantly less excess air and thus gain slightly in efficiency, rather than losing. Second, if the emulsified fuel flowrate were held constant (rather than dry oil flowrate, as above), the fractional burner-on-time would be increased and standby losses reduced proportionately. As indicated by the slopes of the curves on Fig.15 at demands below 100 percent, the potential gain from this effect would normally be only a small fraction of the loss caused by adding water to the fuel. Finally, if the heat exchange surfaces were sooted up, the extra water vapor in the combustion gases could conceivably aid in its oxidation and removal. However, combustion gases from burning dry oil contain about 63 percent as much water vapor as those produced by burning a 40 percent water-oil emulsion. Thus, dramatic efficiency increases, as a result of emulsifying the fuel with water, appear to be highly unlikely.

Flue Gas Recirculation. The WAFURN computer program was used to analyze some effects of recirculating flue gases and mixing them with the combustion air supplied to the burner. Calculations were made for the Lennox OF7 furnace fired for 1/3 of a 12-minute cycle. Flue gas recirculation (FGR) effects on cycle thermal efficiency and flue gas temperature are shown graphically in Fig. 16. At near-stoichiometric conditions, imposition of FGR causes the calculated flue gas temperature to increase substantially. As the excess air is increased, however, this effect becomes decidedly less pronounced until, at a stoichiometric ratio of about 2, the flue gas temperature and thermal efficiency apparently are little influenced by the presence or level of FGR*.

*Essentially identical trends were observed in comparable calculations for a 10-minute firing, 30-minute cycle condition.

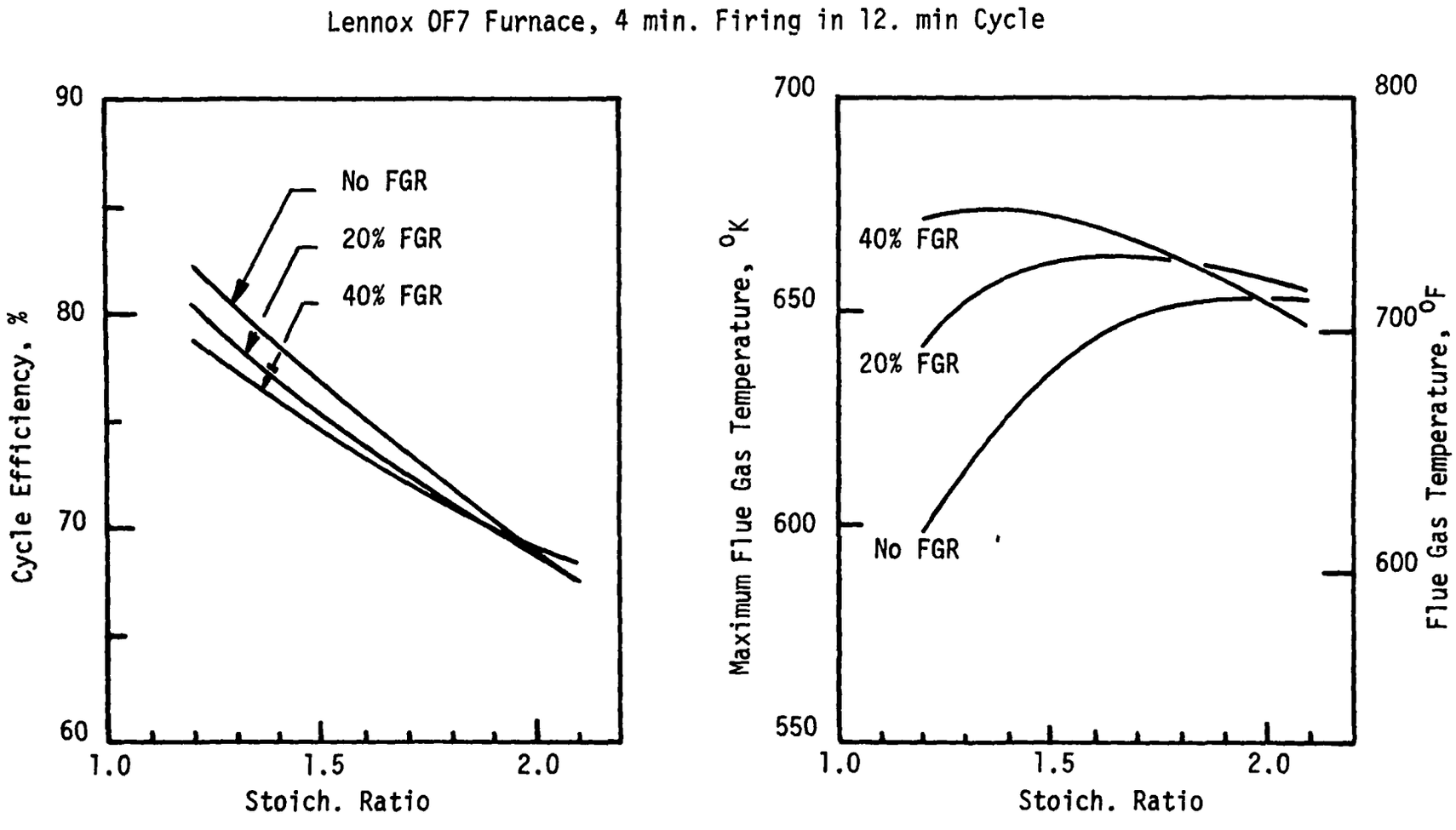

Figure 16. Calculated Effects of External Flue Gas Recirculation (FGR) on Warm-Air Oil-Fired Furnace Efficiency and Flue Gas Temperature

The adiabatic flame temperatures for conditions represented on Fig. 16 decrease monotonically with both increasing stoichiometric ratio and increasing FGR:

% FGR	Adiabatic Flame Temperatures, K (F)			
	R_{Stoich} = 1.2	1.5	1.8	2.1
0	2081 (3285)	1810 (2797)	1605 (2430)	1444 (2139)
20	1747 (2685)	1546 (2322)	1340 (2043)	1265 (1817)
40	1549 (2528)	1345 (1961)	1242 (1776)	1118 (1552)

Therefore, the calculated reduced effects of FGR on flue gas temperature as stoichiometric ratio is increased cannot be explained by reactant/diluent thermochemical phenomena. Rather, they must result from the dynamic interaction of flowrate and supply temperature in altering the heat transfer behavior of the furnace's heat exchanger.

Refractory-lined versus Unlined Fireboxes. As a final example of the WAFURN computer model's analysis capabilities, the 0.019 m (0.75-inch) thick refractory-lining in the Lennox OF7's firebox was assumed to be made 1/3 as thick in one case and removed altogether in another. Calculated results for a 4-minute firing at 1.00 ml/s (0.95 gph) oil in a 12-minute cycle were as follows:

Stoich. Ratio	Refractory Thickness, m (inch)	Refractory Surface Temperature, K (F)	Gas Temperature, K (F)		Thermal Efficiency, %
			Firebox Exit	Flue	
1.2	0.019 (0.75)	1796 (2773)	1984 (3111)	599 (618)	82.25
	0.0063 (0.375)	1541 (2314)	1878 (2920)	599 (618)	83.31
	0.0	(527)*(489)	1700 (2600)	596 (613)	83.75
1.5	0.019 (0.75)	1532 (2298)	1741 (2674)	637 (687)	76.72
	0.0063 (0.375)	1296 (1873)	1669 (2544)	634 (681)	77.80
	0.0	(475)*(395)	1562 (2352)	626 (667)	78.44
1.8	0.019 (0.75)	1335 (1943)	1556 (2340)	651 (712)	71.96
	0.0063 (0.375)	1117 (1551)	1504 (2247)	647 (705)	72.92
	0.0	(440)*(332)	1434 (2121)	638 (688)	73.80

*( ) represents uninsulated metal temperatures

It is seen that the computer model predicts that approximately 1-1/2 to 2 percent higher thermal efficiencies can be achieved by designing an air-cooled firebox without a refractory lining. The temperatures at burner cutoff tabulated above do not particularly indicate such an appreciable difference, but examination of the complete cycle printouts revealed that the flue gas temperatures early in the burner-on times were substantially lower for the unlined case, which accounts for the higher efficiency.

SECTION V

EXPERIMENTAL INVESTIGATION

An experimental investigation was conducted in which pollutant emissions and combustion performance were characterized as functions of burner and combustion chamber design and operating conditions. The objective was to define, in conjunction with the analytical investigation, the design requirements for an integrated furnace system capable of meeting the emission and efficiency goals stated in the Introduction.

The experimental investigation, which utilized research combustion chambers rather than typical furnaces, consisted of three separate, but related parts. One part dealt exclusively with the 1 ml/s (gph) conventional burner, optimized to produce low emissions, as described in Ref. 5. This effort sought to optimize the matching of the firebox (combustion chamber) to that fixed-burner design. The other two parts extended to burners having, in one case, forced flue gas recirculation (FGR) to the burner air intake and, in the other case, forced combustion gas recirculation (CGR) from the combustion chamber to the burner air intake. These efforts were directed toward optimizing the burner/firebox combination for low emissions. The three segments of the experimental investigation are described, and the results obtained are presented and discussed in the following subsections.

OPTIMIZED CONVENTIONAL BURNER STUDY

A previous intensive Rocketdyne investigation of residential and commercial oil burners (Ref. 5) led to criteria for optimizing conventional burner designs with respect to pollutant emissons. For high-pressure, atomizing, luminous-flame burners fired into refractory-lined combustion chambers, minimum pollutant emissions were obtained with burners having (1) no flame-retention device, (2) choke diameter related quantitatively to the firing rate, and (3) large peripheral swirl vanes oriented at 25 degrees relative to the blast tube axis. This swirl vane angle gave the best comprimise between smoke emissions and nitric oxide emissions. An optimum burner having a 1 ml/s (gph) firing rate is illustrated in Fig. 17.

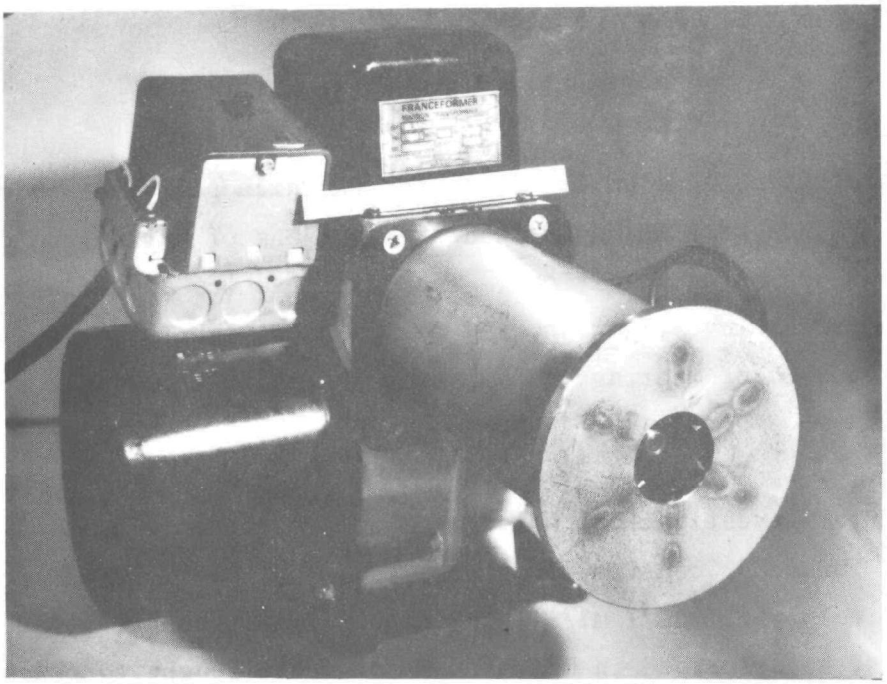

(a) External View 5DZ21-8/6/73-S1

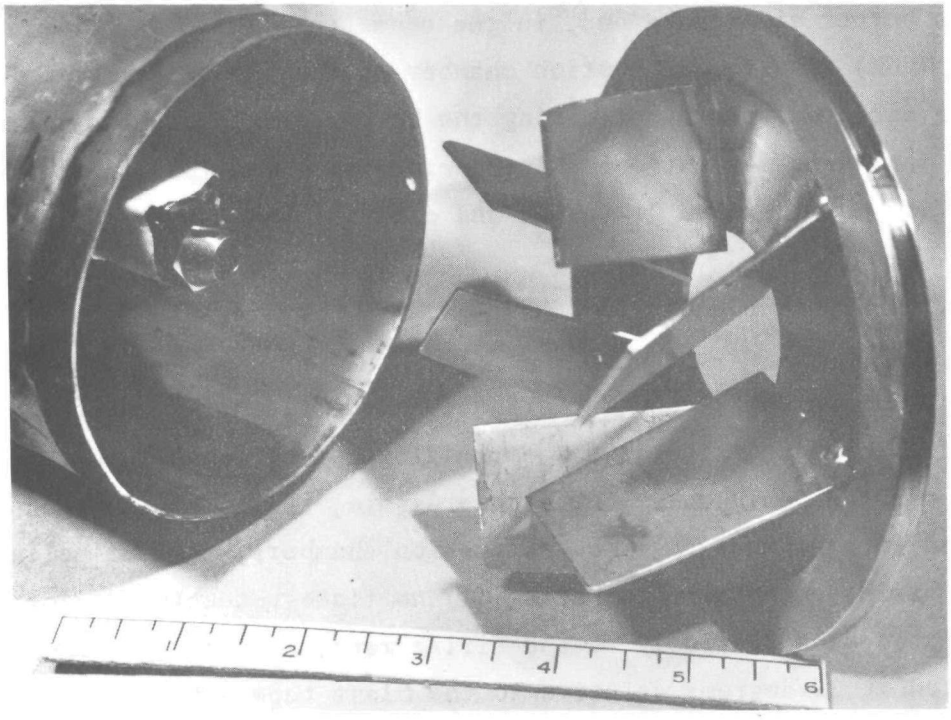

(b) Optimum 1 ml/s Burner Head 5DZ21-8/6/73-S1A

Figure 17. Optimum 1 ml/s (gph) Oil Burner

In addition to minimizing nitric oxide formation, the optimum burners were capable of operating with substantially less excess air than is used in conventional practice, without producing unacceptable levels of carbonaceous pollutants (CO, UHC, and smoke). As discussed in Section IV, such operation is beneficial in that it enhances overall furnace thermal efficiency.

Nitric oxide emissions were lower when the optimum burners were tunnel-fired into refractory-lined fireboxes than when the burners were side-fired. The explanation offered in Ref. 5 for this result was the same as that for obtaining lower NO emissions with nonretention burners than with those having flame retention heads. That is, at low excess air levels, formation of NO is minimized by the absence in the combustion zone of recirculation eddies, steep concentration gradients, and strong mixing. A uniform dispersion of fuel spray in an air stream that flows and reacts smoothly along the combustion chamber (i.e., in the manner of a plug flow reactor) produces the least nitric oxide, while vigorous intermixing of incoming fresh air with combustion products (as a result of adiabatic internal recirculation or steep gradients in the combustion field) tends to promote production of NO.

Combustion chamber design features other than burner orientation were varied in the Ref. 5 studies, but not sufficiently to delineate clear trends or to derive optimization criteria. However, there appeared to be significant effects on pollutant formation and emission concentrations of varying chamber diameter and length, at a given firing rate, and of providing nonadiabatic combustion zone conditions by cooling the combustion chamber walls. It was noted that recirculation of combustion gases within cooled (or partially cooled) combustors, was not necessarily detrimental and could even be beneficial with respect to reducing smoke and NO emissions.

This current experimental effort was undertaken to examine more thoroughly the matching of fireboxes to the optimum burner. The objective was to derive design criteria for further minimization of pollutant emissions and for acceptable operability (e.g., ignition, flame stability, and component temperature).

Experimental Apparatus

Optimum Burner. The 1 ml/s (gph) optimum oil burner illustrated in Fig. 17 was used. This burner consisted of a conventional burner (Beckett Model AF) body fitted with an optimized nonretention burner head at the discharge end of its 0.10 m (4-inches) diameter blast tube. The optimum head conformed to the design criteria given in Ref. 5. In the 1 ml/s (gph) size, the choke diameter was 0.042 m (1.65 inches), and the swirl vanes were relatively large, being approximately 0.05 m (2 inches) long and extending from about 0.03 m (1.2-inches) diameter out to the inside diameter (ID) of the blast tube. As noted earlier, the vanes were canted at 25 degrees from the blast tube centerline, cut from 0.0016 m (1/16-inch) Type 321 stainless sheet, and welded to the machined choke plate of the same material.

Most other burner components, viz, the housing, blast tube, fuel pump, combustion air fan, drive motor, ignition transformer, CdS flame-sensing cell, and burner control circuitry, were stock equipment supplied with the burner. The stock ignition electrodes were replaced by a smaller-diameter pair compatible with the more restricted space imposed by the swirl vanes. Use of a 1.0-60°-A Delavan spray nozzle provided good mixing between the fuel spray and air while minimizing spray impingement on combustion chamber walls.

As the testing progressed, some alterations of the optimum burner were made in order to satisfy specific test needs that arose. These alterations are later described and discussed in context with the experimental reasons for making them and the results achieved. Pertinent information appears on page 69, et seq., and page 71, et seq.

Research Combustion Chambers. Three combustion chambers were built to provide a matched set with considerable dimensional, structural and coolant variabilities. The basic approach is illustrated in Fig. 18 for one of the chambers. Each chamber was a 1.52 m (5-foot) long, flanged section of steel pipe with a stubby, flanged side-arm section of the same size of pipe attached near one end. The tunnel-fired

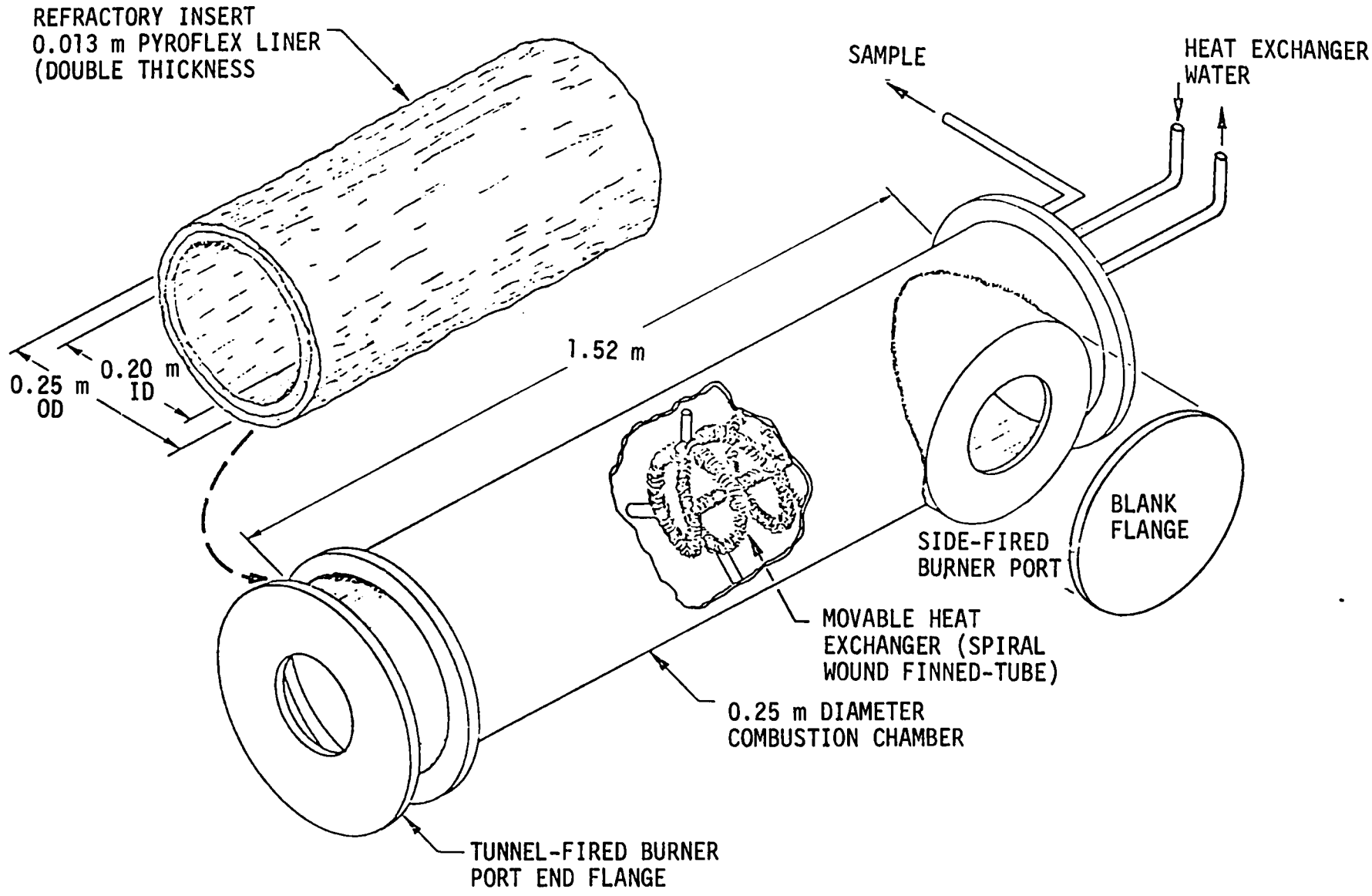

Figure 18. Experimental Combustion Chamber and Heat Exchanger Arrangement

orientation is illustrated in Fig. 18, in which the oil burner fits into the annular flange depicted at the left end of the chamber. In this orientation, the side-arm was redundant and so was positioned at the opposite end from the burner and simply blanked off. To achieve the side-fired configuration, the combustion chamber was simply turned end-for-end, with the blank and burner port flanges relocated as appropriate. The steel chamber could either be lined with a refractory fiber insert to form an adiabatic combustion zone or remain unlined and in some way be cooled. A movable, spiral-wound, finned-tube heat exchanger, shown inserted in the opposite end of the combustion chamber from the burner, provided effective variation of the combustion zone length.

Three chamber diameters were selected such that addition of refractory linings to the larger two would produce lined chambers having inside diameters comparable with the smaller two unlined chambers, viz.:

Steel Pipe ID, m (inches)	Nominal Combustion Chamber ID, m (inches)	Nominal Thickness of Pyroflex, m (inches)
0.162 (6.36)	0.162 (6.36)	--
0.222 (8.75)	0.222 (8.75)	--
0.222 (lined)	0.175 (6.89)	0.024 (0.93)
0.279 (11.0)	0.279 (11.0)	--
0.279 (lined)	0.22 (8.7)	0.030 (1.18)

In use, the major axes of the chambers were vertical, with the burner firing vertically upward when tunnel-fired and horizontally when side-fired. There were several reasons for selecting this arrangement: (1) it provided simulation of firebox draft and combustion-gas flow patterns present in a majority of furnace designs, (2) the spiral-wound heat exchanger could be simply suspended in the combustion chamber without having to provide lateral support, (3) natural convection air cooling would be more uniform than it would be with a horizontal axis, and (4) water-cooling could be effected with a fairly simple cylindrical housing around the chamber, open to the atmosphere at the top of the housing.

Combustion-Gas Heat Exchanger. A water-cooled heat exchanger was used to accomplish rapid cooling of the combustion gases as they flowed out of the primary "firebox" portion of any of the combustion chambers. The intention was for the gas temperature to be quenched rather rapidly so that changes in heat exchanger position (e.g., firebox length) could be readily correlated with variations in pollutant emissions.

As noted earlier, the heat exchanger was a spiral-wound, finned-tube assembly designed to fit inside all three combustors and to be positioned anywhere along the length of a chamber. Detailed dimensional data for the coil are given in Fig. 19; this coil was designed to cool the oil burner exhaust gases down to about 200 C to 350 C (390 F to 660 F) at a maximum water coolant flowrate of 3.8×10^{-4} m^3/s (6 gal/min). The 0.025 m (1-inch) outside diameter (OD) finned tubing used, has a 0.013 m OD by 0.0012 m wall (1/2-by 0.049-inch) stainless steel tubing with helically wound 0.00051 m (0.020-inch) thick carbon steel fins with nickel-chrome clad plating, 394 fins/m (10 fins/inch). The carbon steel fin material was selected over stainless steel because such material has better thermal conductivity properties, and the nickel-chrome clad plating provides resistance to corrosive exhaust products. Approximately 4.1 m (13-1/2 feet) of finned tubing was required in the construction of the heat exchanger, resulting in a total heat transfer surface area of about 1.4 m^2 (15 ft^2).

Several semicircular baffle plates were cut from a 21-gage stainless steel sheet, slipped between coils of the heat exchanger and wired in place. Cut so their outside diameters would just fit comfortably in a chamber's inside diameter, the baffles ensured that the gases passed repetitively over the heat exchanger coils and prevented them from bypassing around the outside of the coils.

Midway through the experimental studies, the cooling water was inadvertently shut off and, after a few minutes of burner firing in an insulated, adiabatic combustion chamber, the heat exchanger was destroyed by massive melting of both the fins and coiled core tubing. Upon finding that a replacement finned-coil could not be delivered in fewer than 6 weeks, a substitute heat exchanger was fabricated by coiling about 15 m (49 feet) of 0.001 m (3/8-inch) copper tubing into two nested,

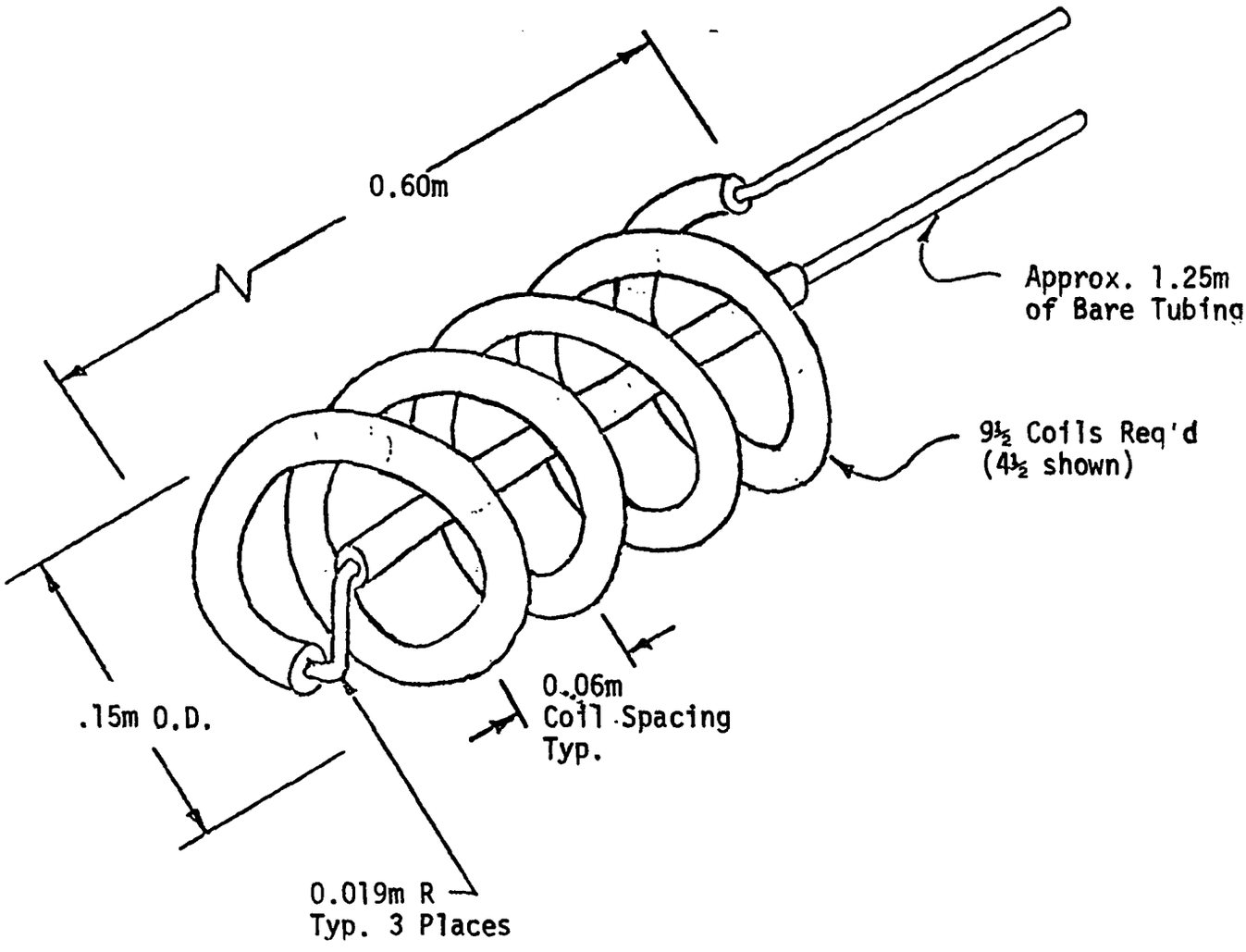

0.025 m (1.0-inch) OD Helically-Wound Finned Tube (Approximately 4.1 m (13.5 feet) Finned Length)

Core Tube: 0.013 by 0.0012 m (1/2-inch by 0.049-inch) Stainless Steel

Fins: 0.006 by 0.0005 m (1/4-inch by 0.020-inch) Carbon Steel - Nickel/ Chrome Clad 297 Fins/Meter (10 Fins/Inch)

Figure 19. Heat Exchanger for Variable Combustion Chamber Configuration Tests

parallel-plumbed coils. This device was checked out and found to be entirely satisfactory, and so was used for the remainder of the Phase I experimental work.

Test Facility. The optimum burner was fired in the various research combustion chambers at an outdoor test facility illustrated schematically in Fig. 20. The principal components were attached to a waist-high steel table as shown. Not shown is a Unistrut superstructure at the right-hand end of that table to support the vertically mounted combustion chamber and to suspend the spiral-wound heat exchanger within it. The facility was organized for rapid and easy changing of combustion chambers, burner orientation, and heat exchanger position. Minimum protection from inclement weather was provided by a simple sheet metal roof over the test apparatus.

Experimental data requirements were primarily concerned with flue gas pollutant concentrations. Concentrations of most pollutant species were measured by conducting a continuous flue gas sample to a train of analysis instruments located indoors in a nearby laboratory. Flue gas smoke content was measured intermittently at the flue with a manual smoke meter. The instruments used, analyses performed, and types of data obtained are described and discussed in Appendix B. In addition, the firing rate was monitored regularly by measuring the fuel oil flowrate, the flue gas temperature was indicated by immersing a thermocouple downstream of the heat exchanger, and the temperature rise of the heat exchanger coolant water was measured. Miscellaneous data taken less regularly, were firebox draft conditions, firebox shell metal temperatuares, and combustion air fan characteristics.

Experimental Test Matrices

Two matrices of 80 tests each were planned for experimentally matching combustor designs to the optimum oil burner. One matrix was for a tunnel-fired burner orientation and the second was for a side-fired burner arrangement. The planned distribution of tests was the same for both matrices and is denoted in Table 7. Variations of chamber wall construction of cooling medium, chamber inside diameter and length preceding the heat exchanger, and excess air level (stoichiometric ratio) were included. All tests were planned as transient (cyclical) tests, with the burner fired for 10 minutes of a 30-minute cycle.

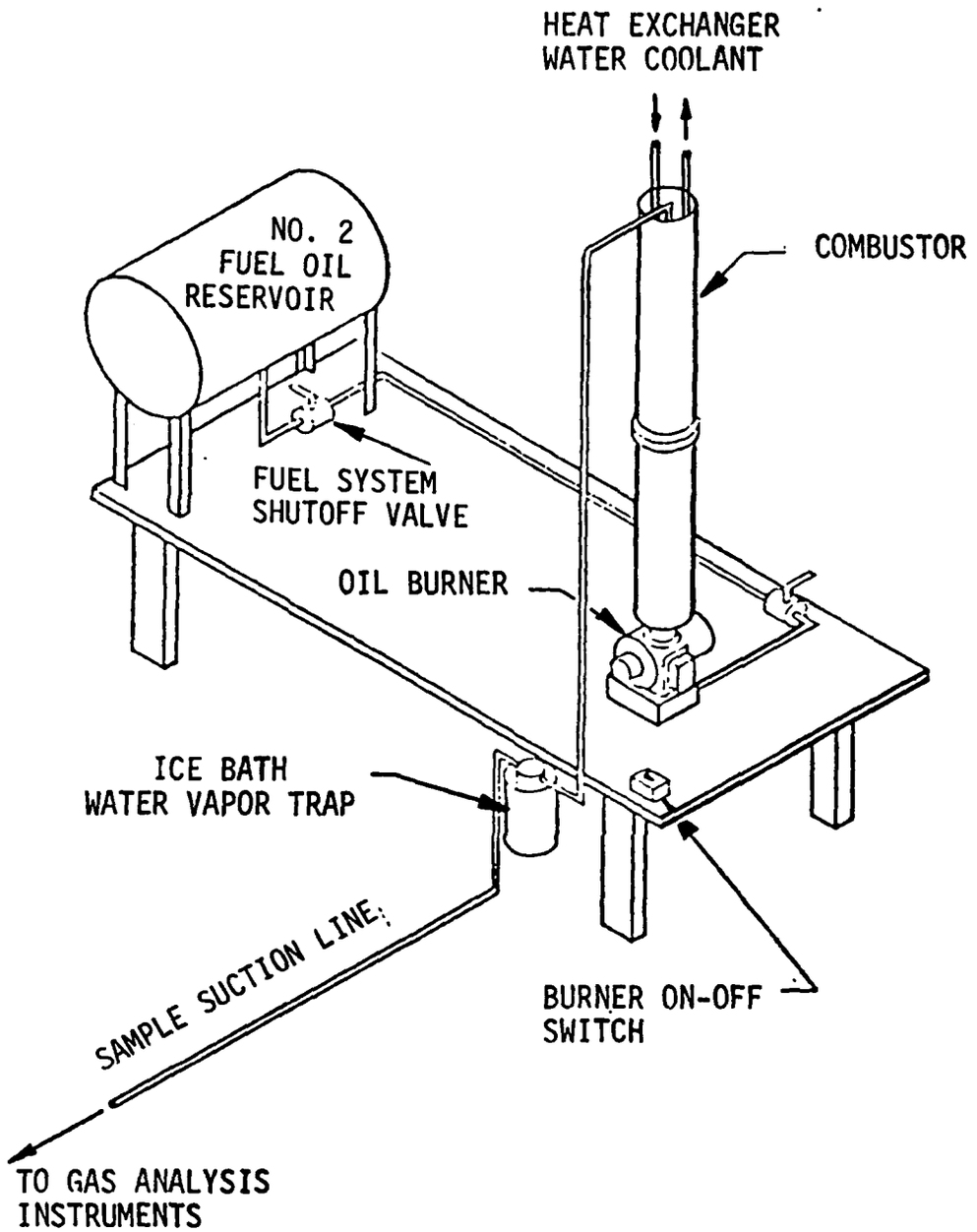

Figure 20. Schematic of Oil Burner and Research Combustion Chamber Test Installation

TABLE 7. OPTIMUM BURNER/CHAMBER MATCHING TEST MATRIX

Chamber Wall	Chamber Diameter, metre (inch)	Chamber Length, metre (inch)	No. of Excess Air Levels
Air-cooled	0.162 (6.36)	0.30 (12) 0.40 (16) 0.50 (20) 0.75 (30)	3
	0.222 (8.75)	0.30 (12) 0.40 (16) 0.50 (20) 0.75 (30)	3
	0.279 (11.0)	0.30 (12) 0.40 (16) 0.50 (20) 0.75 (30)	3
Fractional Air-cooled	1/4 1/2 3/4 0.222 (8.75)	0.40 (16)	3
Refractory-lined	0.221 (8.70)	0.30 (12) 0.40 (16) 0.50 (20) 0.75 (30)	3
	0.175 (6.89)	0.30 (12) 0.40 (16) 0.50 (20) 0.75 (30)	3
Water-cooled	0.222 (8.75)	0.30 (12) 0.40 (16) 0.50 (20) 0.75 (30)	3 1 1 3

"Air-cooled" chambers consisted of the uninsulated steel combustion chambers simply mounted vertically in the open air. As a result, the cooling was a combination of radiant heat transfer to the surroundings and natural convection heat transfer to ambient air. For the "fractional air-cooled" chamber configuration, the 0.222 m (8.75-inches) diameter chamber was blanketed externally with an approximately 0.013 m (1/2-inch) thick layer of Pyroflex refractory insulation. With the heat exchanger set to form a 0.40 m (16-inches) long firebox, that blanket was positioned initially such that the first 0.1 m (4 inches) of the firebox, near the burner, was uninsulated and, thus, was 1/4 air-cooled. It was then moved further downstream in two successive 0.1 m (4-inches) steps to provide 1/2 and 3/4 air-cooled conditions. Attaching the insulation to the outside allowed the steel shell of the chamber to be overheated, but the risk of damaging it was accepted rather than having step diameter changes placed inside the combustor by the use of partial-length internal liners.

Pyroflex linings were placed inside the "refractory-lined" combustors, as described earlier.

"Water-cooled" chambers were formed by placing an open-topped sheet metal "bucket" around the firebox end of the combustion chamber and filling the box with water. Openings in the water-jacket were provided as required for mounting the burner to the chamber, and a RTV silicone-type, low-pressure, moderate-temperature sealant was used to prevent water leaks. A flow of fresh water was admitted to the bottom of the jacket, and a hot-water overflow near the top controlled the water level.

The chamber inside diameters in Table 7 conform to those listed earlier. Variation of combustion chamber length, achieved by moving the water-cooled heat exchanger coil as previously described, was intended to cover the range of practicality exhibited by current commercial practice.

Testing at only three excess air levels was recognized as being quite limited. To avoid operating at leaner conditions, and because operation as close to stoichiometric conditions as possible promotes the desired higher thermal efficiency, testing was planned at stoichiometric ratios of approximately 1.10, 1.15, and 1.20.

Experimental Results

The methodology used in the experimental testing was to proceed, more or less sequentially, through the foregoing test matrices, first with the tunnel-fired, then with the side-fired orientations. Data were recorded for 160 runs (sets of different apparatus or different test conditions), although exploratory firings were made at a substantial number of other conditions for which test data were not recorded for one reason or another. A complete tabulation of the data obtained is given in Appendix C, listed sequentially by run number.

Tunnel-Fired Orientation Results. The tunnel-fired (coaxial) burner orientation was tested first (Run 1 through 81).

Air-Cooled Combustion Chambers. The recorded tests were preceded by experiments with the 0.162 m (6.38-inches) diameter, air-cooled combustor, which was found to be impractical for use with the 1 ml/s (gph) optimum burner. No operating conditions could be found to eliminate very rough combustion, characterized by loud, low-frequency rumbling and very high smoke levels. No valid reportable data were obtained.

With the 0.222 m (8.75-inches) diameter air-cooled chamber, combustion was significantly better, although some audible roughness was present in all tests. Start-up problems were experienced on cycle testing at stoichiometric ratios much removed from unity. The flue gas pollutant species data are plotted in Fig. 21. The various line segments on these plots represent the entire operable stoichiometric range; these segments are generally quite constricted between excessive smoke on the left and unreliable ignition on the right.

The relative carbon monoxide and unburned hydrocarbon levels suggest that chamber lengths of about 0.5 m (20 inches) or greater may be needed in order to avoid premature quenching of the combustion process. Even for the longer chambers, the quantities of CO and UHC produced were substantially higher than those typically experienced in conventional residential furnaces (Ref. 4). It was thought that the rough combustion may have caused these pollutant levels to be high.

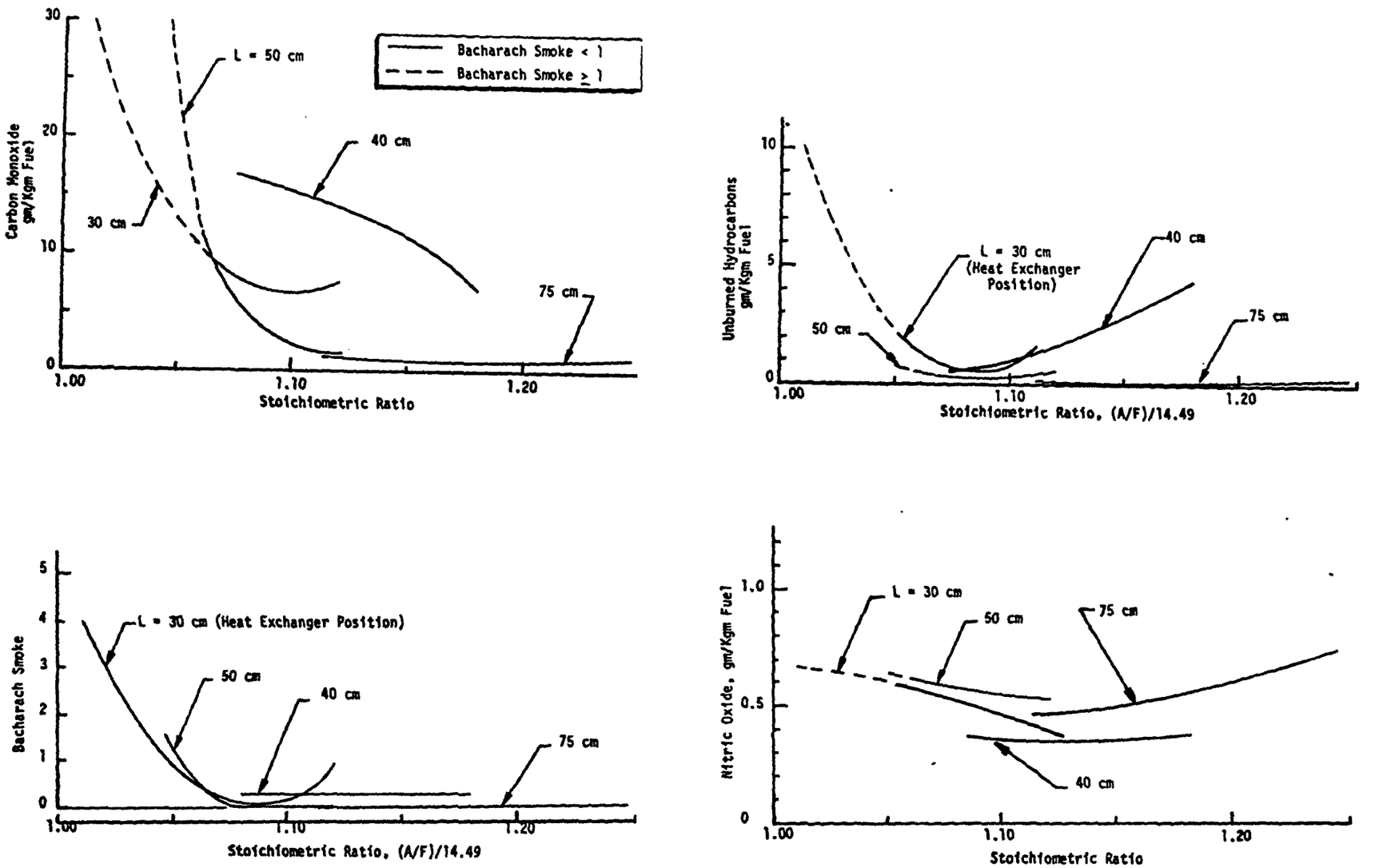

Figure 21. Effect of Combustion Chamber Length Upon Flue Gas Emissions as Functions of Stoichiometric Ratio in a 0.222 m (8.75 inches) Diameter, Air-Cooled, Tunnel-Fired Combustor

The NO concentrations measured in the flue gas were substantially lower than the steady-state levels reported in Ref. 5 for this burner. While this may be attributable to the difference between cycle-averaged and steady-state values, it may also reflect effects of air-cooling the combustor walls and of radiation from the flame zone to the water-cooled heat exchanger, both of which could produce moderately lower flame zone temperatures.

Emissions from the 0.279 m (11-inches) diameter air-cooled combustor are plotted in Fig. 22. The upper stoichiometric ratio limit for these tests was also limited by conditions where ignition of the air/oil mixture in the cooled combustor became marginal. This larger combustor produced slightly higher emissions of CO and UHC than did the 0.222 m (8.75-inches) chamber, and slightly lower NO emissions. Interestingly, among the four tested heat exchanger positions, emission data taken at 0.4 m showed distinctly different characteristics in both the 0.222 (8.75-inches) and 0.279 m (11-inches) chambers. The reason for this peculiarity was not explained. (It will be seen later that neither the water-cooled nor insulated chamber data exhibited a similar peculiarity.)

At this point in the testing, in response to a question as to whether the optimum oil burner head could be used effectively with burners having smaller blast tubes, a smaller 0.075 m (3-inches) diameter version of the 1 ml/s optimum head was made and fired on the same burner body fitted with a 0.075 m (3-inches) blast tube. Cyclic firings in the 0.222 m (8.75-inches) diameter insulated combustor gave results directly comparable with those reported in Ref. 5, showing that the more compact optimum head may be applied satisfactorily. That smaller head was retained thereafter for the rest of the 1 ml/s optimum burner testing.

The fractional air-cooled combustor test sereis was conducted with the 0.222 m (8.75-inches) diameter combustor wrapped externally with a movable 0.30 m (12-inches) long section of insulation and with the heat exchanger (i.e., chamber length) set at 0.40 m (16 inches). External rather than internal insulation was chosen to eliminate the effect of geometric changes that would be introduced by a movable internal liner. The objective of this test series was to study the effect

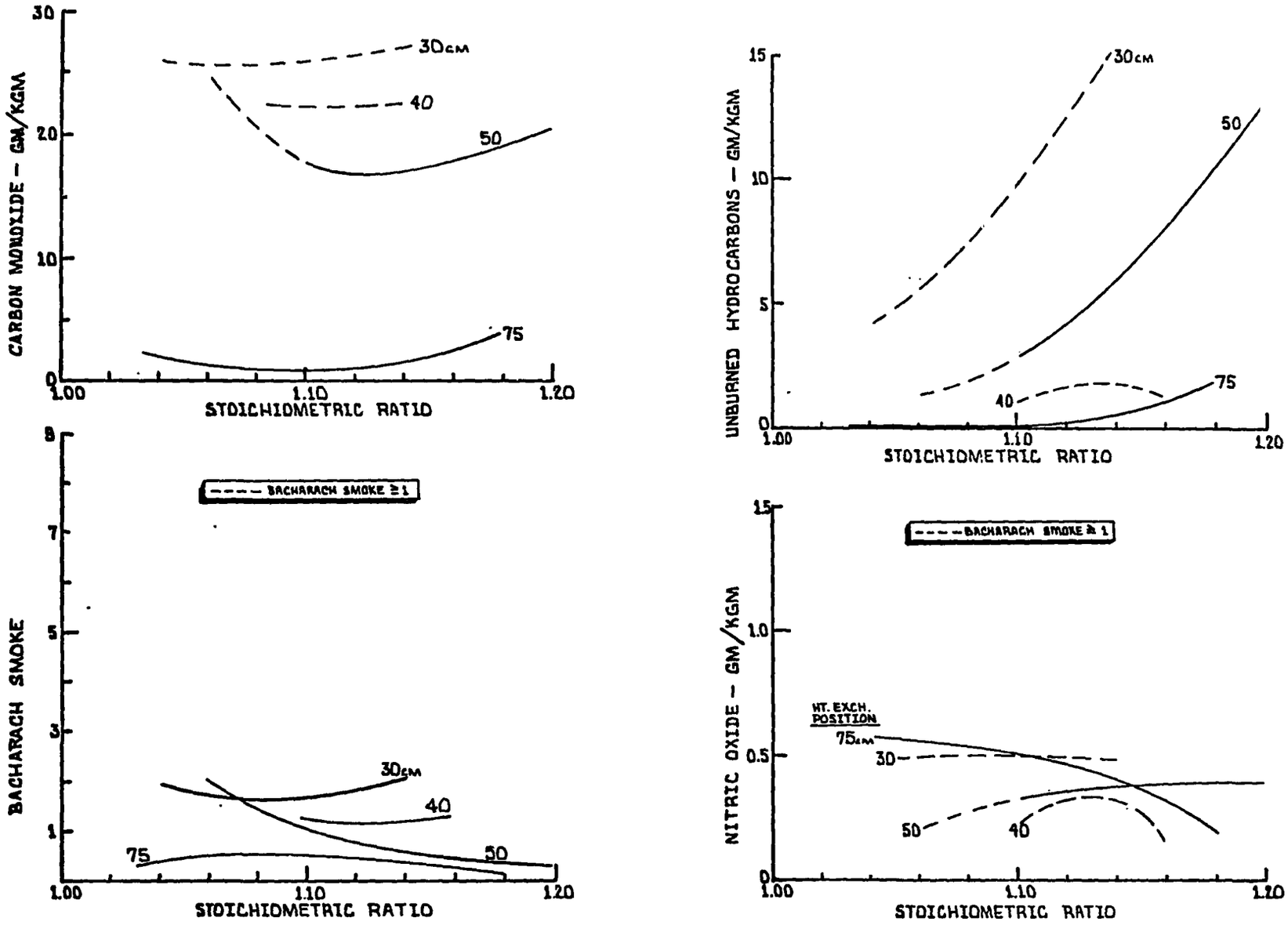

Figure 22. Cycle-Averaged Flue Gas Emission, 1.0 ml/s Optimum Oil Burner in 0.279 m Diameter, Air-Cooled, Tunnel-Fired Combustor at Various Heat Exchanger Positions

of changes in the location of heat extraction from the combustion zone on flue gas composition. The resulting flue gas composition data are plotted in Fig. 23. The numerical labels on the plotted curves indicate the uninsulated (i.e., air-cooled) fraction of the combustion chamber, measured from the burner-end.

Few differences exist among the curves for the various locations, a result that had not been anticipated. Two quite different inferences may be drawn from this result. One is that the combustion gas recirculation eddy, which surrounds the primary flame zone and supplies it with partially cooled diluent gases, must be so short that heat removed from the wall further than 0.1 m (4 inches) downstream does not cool the eddy. The other is that the water-cooled heat exchanger was cold enough and close enough to the main flame zone to extract sufficient radiant heat to overshadow the contribution of convective wall cooling to the reduction of flame zone temperatures. A decision was made not to conduct further exploratory tests until after the insulated and partially insulated side-fired test results were considered as contributions to the understanding of this result.

During much of the testing of the air-cooled chambers, the tunnel-fired 1 ml/s (gph) optimum burner flame would become very rough and unstable soon after ignition, especially at 20- to 25-percent excess air conditions. Burners with narrow ranges of operable conditions have restricted adaptability to field conditions and so would experience limited industry acceptance. Therefore, some peripheral tests were run to determine a method for alleviating this problem. Much of the past thinking about combustion roughness and its associated noise has been biased in the direction of flame front instability and the resulting need for flame retention devices on oil burners. The 1 ml/s (gph) optimum burner has a nonflame, retention-type head and that fact has an important bearing on its low emission characteristics. While in the rough combustion mode, increasing the air inlet to full-open would produce no increase in stoichiometric ratio, indicating that the air fan operation was limited by other influences.

A two-fans-in-series burner configuration was set up to create a supercharged burner capability, which sould seriously aggravate a flame-front-detachment-type instability. However, the supercharged burner was found to be far more stable

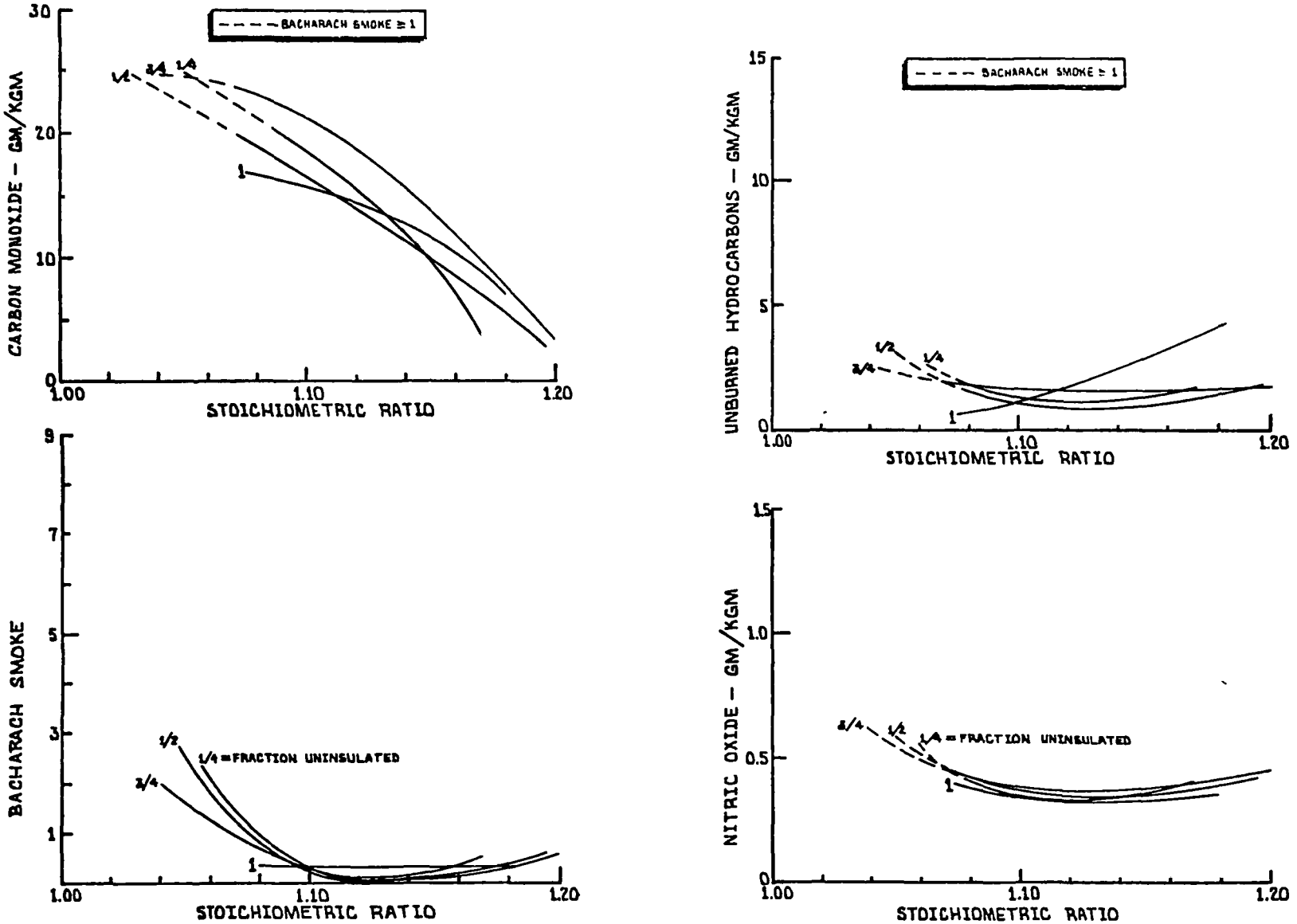

Figure 23. Cycle-Averaged Flue Gas Emission, 1.0 ml/s Optimum Oil Burner in a 0.22 m Diameter, Partially Insulated, Tunnel-Fired Combustor at a 0.40 m Heat Exchanger Position

than the single-fan burner. The combustion roughness is apparently a coupling between the combustion air fan and the combustion process where fan stall, caused by flame perturbations, becomes a contributing factor to further perturbations. The squirrel-cage fans used in most oil burners are characteristically low-pressure, high-volume devices subject to stalling from slight back-pressure perturbations. Fan stall may be aggravated further by the inlet-choke air flow control, used on most burners, which reduces the static pressure in the fan inlet and makes conditions more favorable for fan stall. Air flow control on the discharge (i.e., high pressure) side of the fan may alleviate a lot of flame instability problems. The two-fan burner set-up was initially fired during the insulated chamber experiments (Run 42, et seq.) and, to allow greater flexibility, this supercharged burner configuration was maintained for the rest of the optimum burner/chamber matching tests.

Insulated Combustion Chambers. The insulated chamber experiments involved adding Pyroflex refractory fiber linings [L = 0.75 m (30 inches) to two 0.222 m (8.75 inches) and 0.279 m (11 inches)] of the air-cooled chambers to produce 0.175 m (6.89 inches) and 0.222 m (8.75 inches) ID insulated chambers (inside wall temperatures = 1500 to 1600 C). Additional baffles were added to the finned-tube heat exchanger to maintain flue gas temperature within the 200 through 300 C (~390 through 570 F) range. Flue gas composition data for the insulated 0.175 m (6.89 inches) and 0.222 m (8.75 inches) diameter combustors are plotted in Fig. 24 and 25, respectively. The data plotted are very smooth and sequentially ordered with no peculiarities. The unburned hydrocarbon emissions for these insulated combustors are much improved over the air-cooled combustor results and do not appear to be much of a problem for refractory-lines combustion chambers. The emission improvement caused by adding insulation does not apply to the nitric oxide emissions where the higher temperatures increased the flue gas concentrations by a factor of 2 to 3. A quick tradeoff evaluation of best-operating-conditions in the 0.40 m (16 inches) length insulated combustor suggested a 50-percent excess air setting for the 0.175 m (6.89 inches) diameter combustor and a 25-percent excess air setting for the larger, 0.222 m (8.75 inches) diameter combustor. This corresponds to a a 2.5- to 3-percent furnace net efficiency advantage for the larger-diameter chamber.

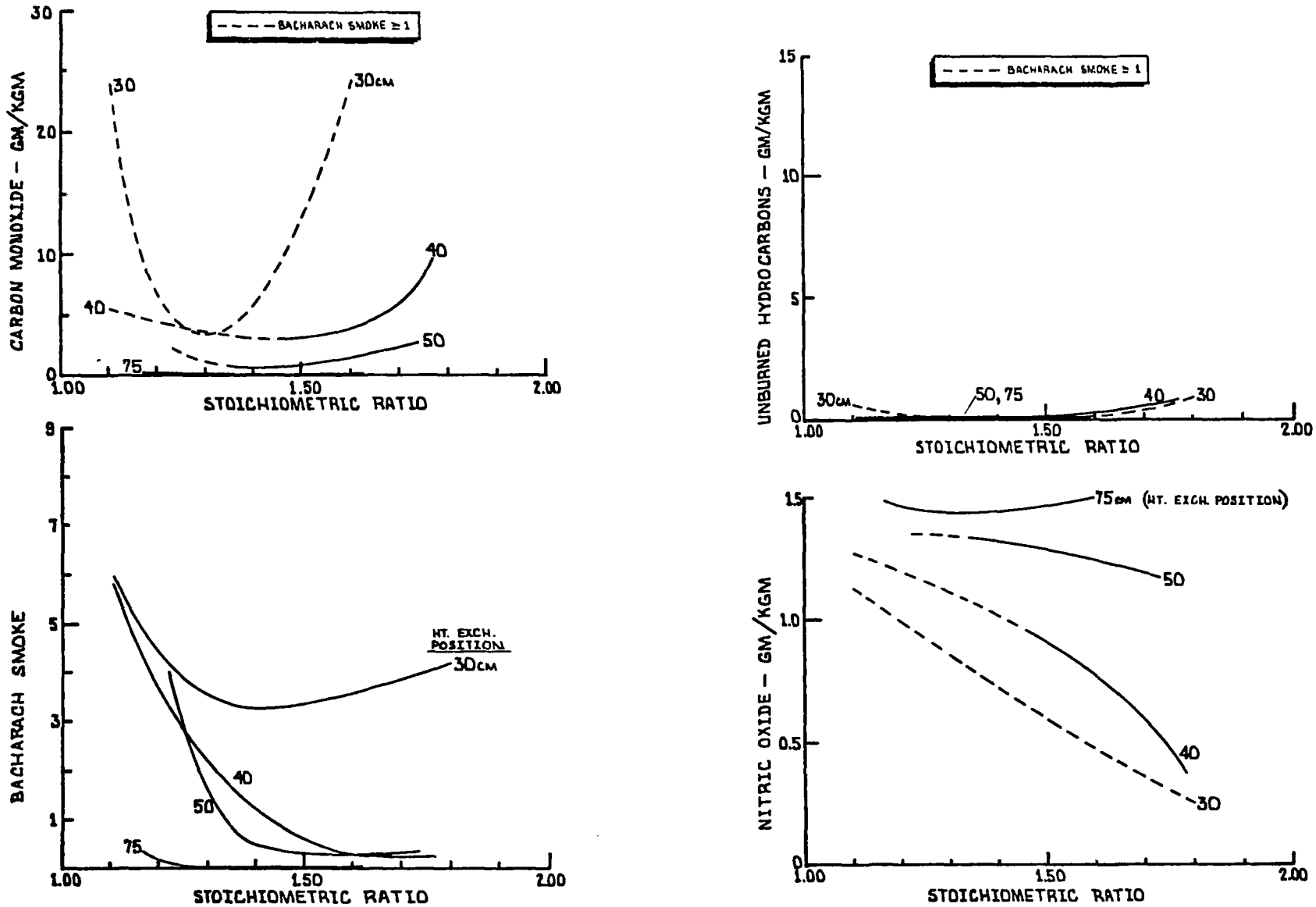

Figure 24. Cycle-Averaged Flue Gas Emissions, 1.0 ml/s (gph) Optimum Oil Burner in a 0.175 m (6.89 inches) Diameter, Insulated, Tunnel-Fired Combustor at Various Heat Exchanger Positions

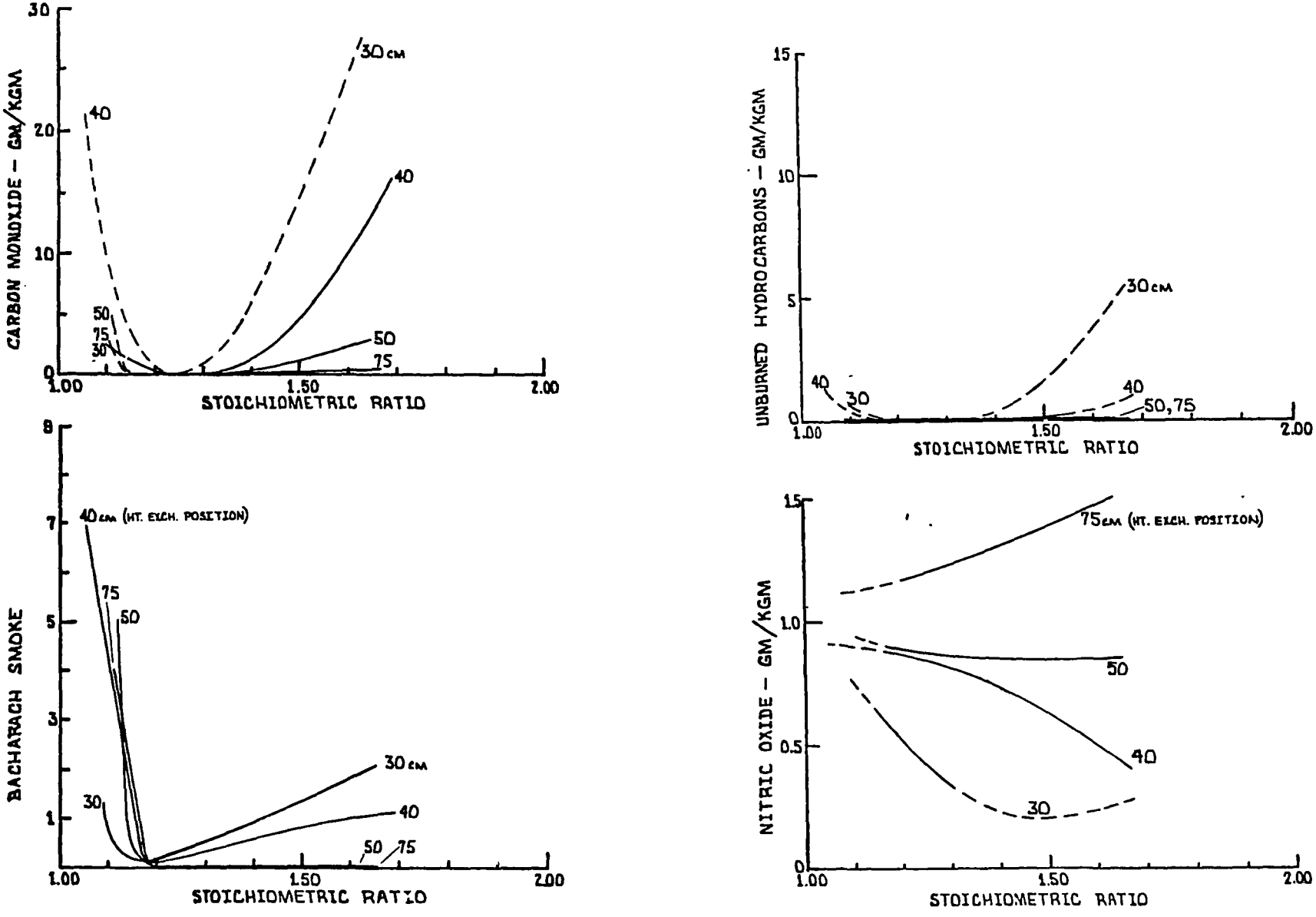

Figure 25. Cycle-Averaged Flue Gas Emissions, 1.0 ml/s Optimum Oil Burner in a 0.222 m Diameter, Insulated, Tunnel-Fired Combustor at Various Heat Exchanger Positions

Water-Cooled Combustion Chamber. The water-cooled combustor experiments involved adding a 0.53 m (20 inches) long water jacket to the outside of the 0.222 m (8.75 inches) diameter combustor. With the water-cooled, spiral-wound heat exchanger in place, the firebox region was enclosed completely in a water-cooled environment having inside wall temperatures on the order of 150 to 200 C (320 to 392 F). Cyclical tests were conducted by initiating the burner firing when the water in the jacket cooled down to 65 C (150 F) and maintaining burner-on for 10 minutes duration, which brought the water jacket temperature to about 90 to 95 C (194 to 203 F). Flue gas temperatures ranged between 195 to 245 C (380 to 480 F), a little lower than conditions obtained in the other types of chambers as a result of rejecting about 1/5 to 1/4 of the heat released to the water-cooled chamber walls.

In general, poor burner starting characteristics are associated with cold combustor walls; a starting puff of high CO, smoke, and UHC concentrations can raise the cycle-averaged emission values dramatically. Somewhat surprisingly, this problem was not encountered in the tunnel-fired, water-cooled combustor tests at conditions having less than 50-percent excess air.

Flue gas composition data for these water-cooled combustor tests are plotted in Fig. 26. The shortest chamber [0.30 m (12 inches)] was the only configuration which produced any significant amount of carbonaceous pollutant emissions; it also produced the lowest concentration of nitric oxide. The 0.40, 0.50, and 0.75 m (16, 20, and 30 inches) length combustors were very low in all carbonaceous pollutant emissions and operated at as low as 12-percent excess air with no apparent problems.

Side-Fired Orientation Results. The side-fired (perpendicular-port) burner orientation was evaluated in Runs 82 through 154 (Appendix E) with the 1 ml/s (gph) optimum burner fired in the same chambers and at much the same conditions that it was tunnel-fired, so that directly comparable data would be obtained with the two chamber types.

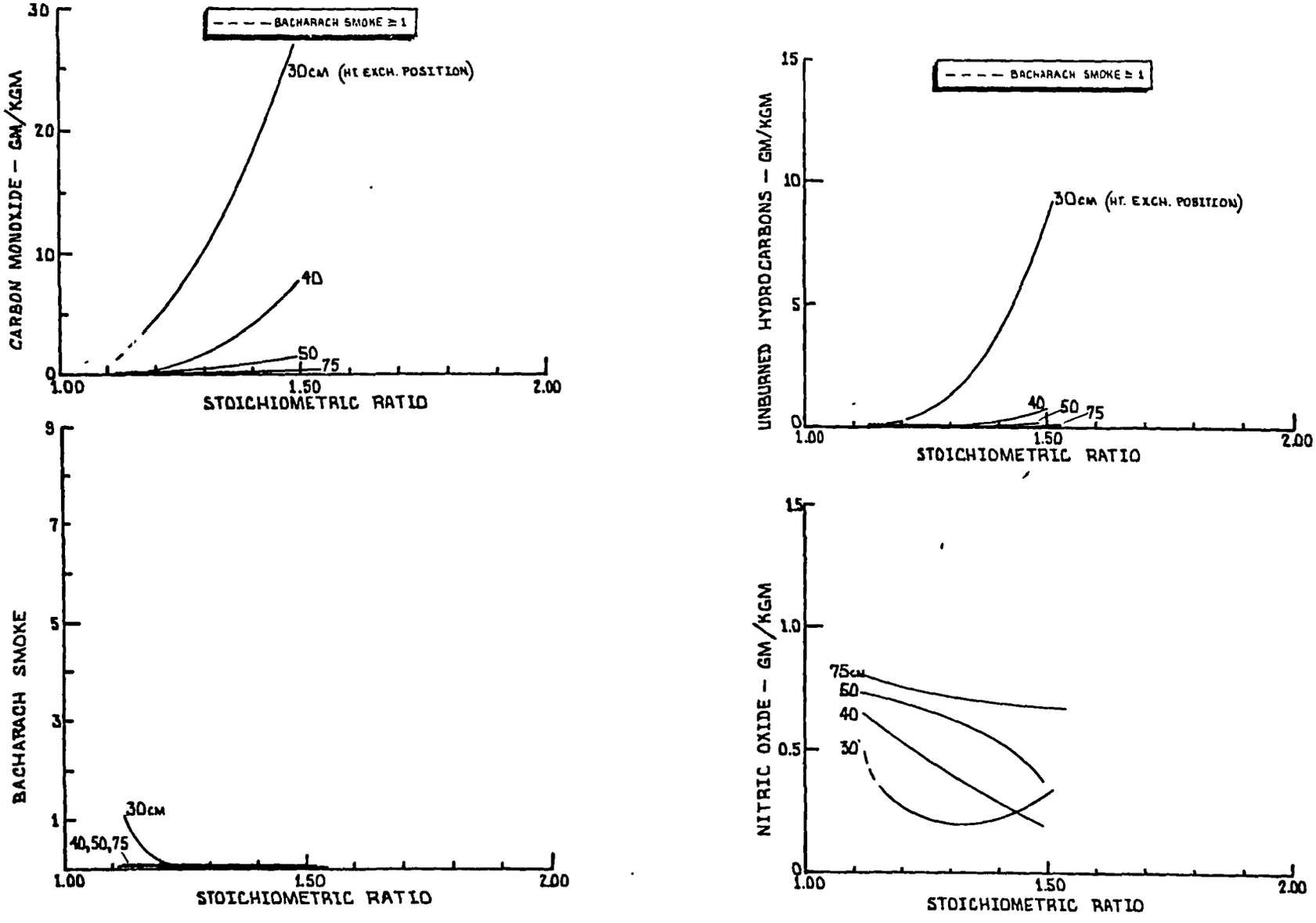

Figure 26. Cycle-Averaged Flue Gas Emissions, 1.0 ml/s (gph) Optimum Oil Burner in a 0.222 m (8.75 inches) Diameter, Water-Cooled, Tunnel-Fired Combustor at Various Heat Exchanger Positions

Air-Cooled Combustion Chambers. The 0.279 m (11 inches) ID, air-cooled (uninsulated) combustor was tested at heat exchanger positions of 0.30, 0.40, 0.50, and 0.75 m (12, 16, 20, and 30 inches). The cycle-averaged (10 minutes on, 20 minutes off) flue gas composition results are presented in Fig. 27. These data are "start-limited" on the right extremity of the stoichiometric ratio range, as were tunnel-fired, air-cooled chamber emissions data presented previously. A relatively higher excess-air ignition capability (SR $\approx$ 1.40) was demonstrated over the equivalent tunnel-fired configuration (SR $\approx$ 1.2). The higher upper-excess-air limit may be the result of an improvement in air/oil mixing effected by added turbulence generated by the crossflow entry of the side firing or to the supercharged combustion air fan. Evidence of improved mixing can be seen in the lower levels of both carbon monoxide and unburned hydrocarbon concentrations (i.e., more complete combustion). The smoke emission levels remained essentially unaffected by the change in burner/chamber orientation, probably because of the large chamber diameter that places the opposing wall at a relatively great distance of 0.279 m (11 inches) (approximately the length of the short chamber, L = 0.30 m (12 inches)). This distant opposing wall and the large air-cooled surface area of the 0.279 m (11 inches) ID chamber are probably responsible for the unexpected absence of an increase in nitric oxide emissions in the perpendicular port configuration.

The 0.222 m (8.75 inches) ID, air-cooled combustor was also fired, and the resulting flue gas composition data are shown in Fig. 28. Again, as in the 0.279 m (11 inches) ID chamber case, the side-fired configuration shows a higher excess-air ignition capability and more complete combustion (lower CO and UHC levels) than its tunnel-fired counterpart. Examination of smoke and nitric oxide emission levels reveals the more typical characteristics of side-fired chambers, i.e., more smoke and higher NO concentrations. The cycle-averaged Bacharach No. 1 smoke level appears to be at about 20 to 25-percent excess air as compared to about 8- to 10-percent excess air in the tunnel-fired chamber. The difference represents a 2- to 30-percent lower overall furnace thermal efficiency. The nitric oxide emission profiles in Fig. 28 show a nominal NO level of 0.8 g/kg which is nearly twice as high as was experienced in the air-cooled, tunnel-fired chamber. This factor of two times higher NO emissions from side-firing then from tunnel-firing is consistent with steady-state data obtained earlier with several different burners (Ref. 5).

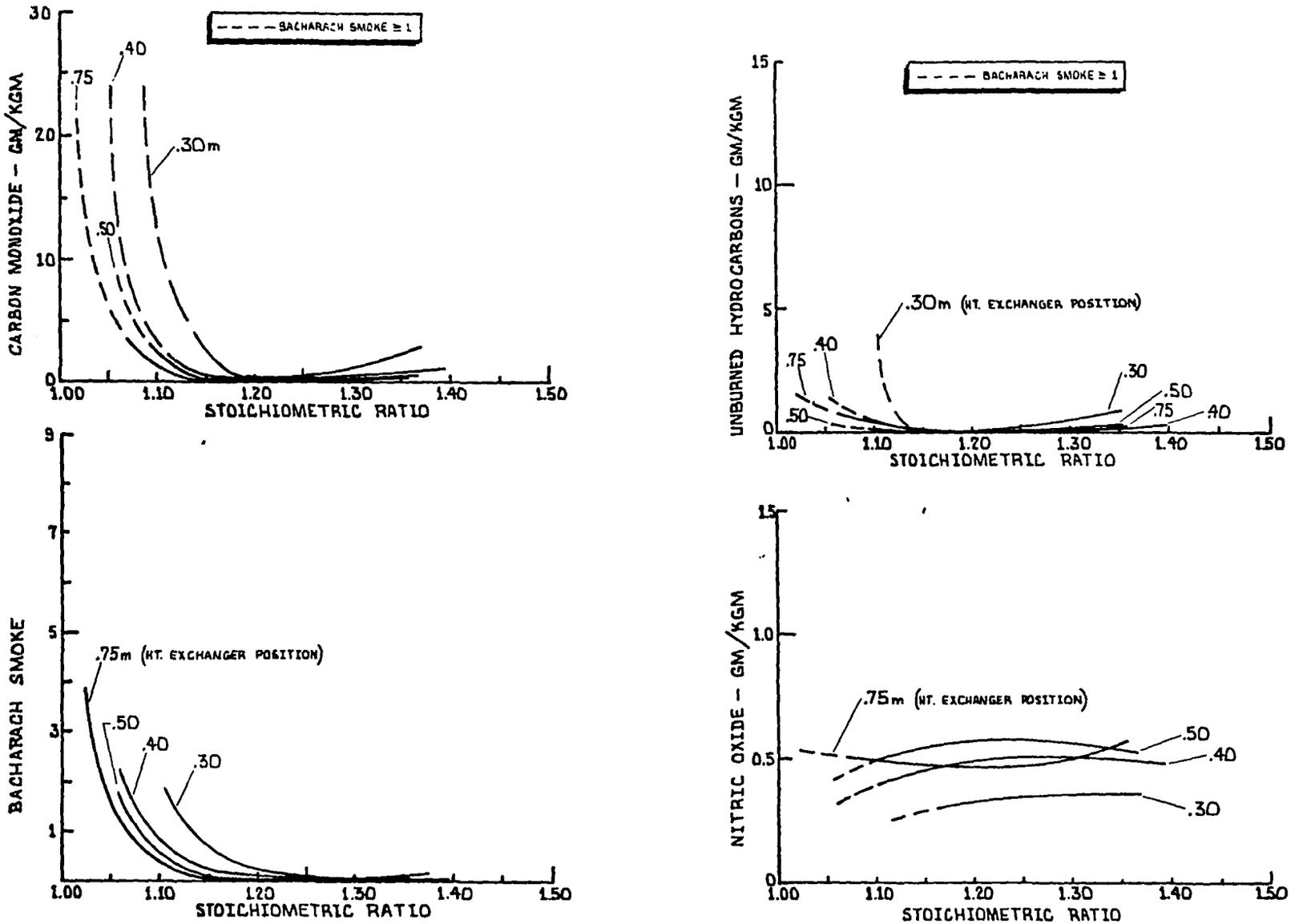

Figure 27. Cycle-Averaged Flue Gas Emissions, 1.0 ml/s (gph) Optimum Oil Burner in a 0.279 m (11 inches) Diameter, Air-Cooled, Side-Fired Combustor at Various Heat Exchanger Positions

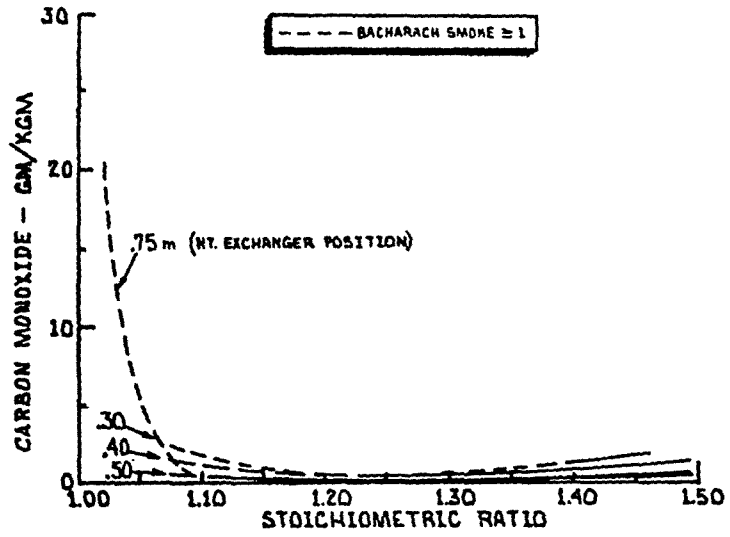

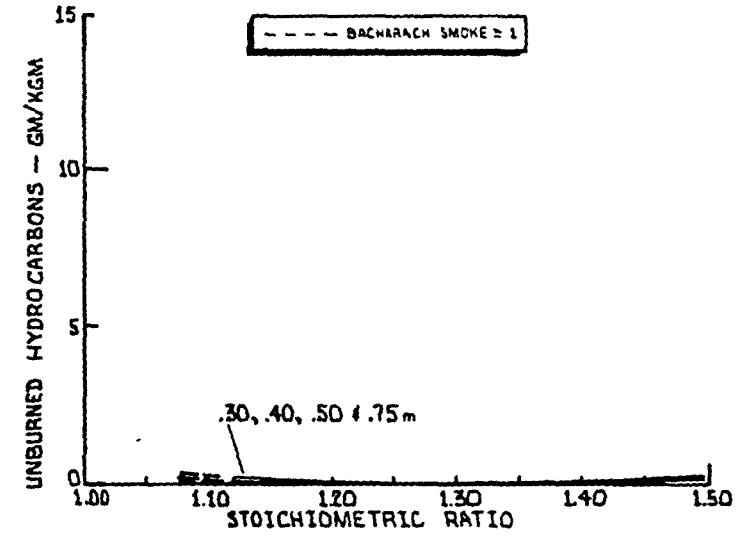

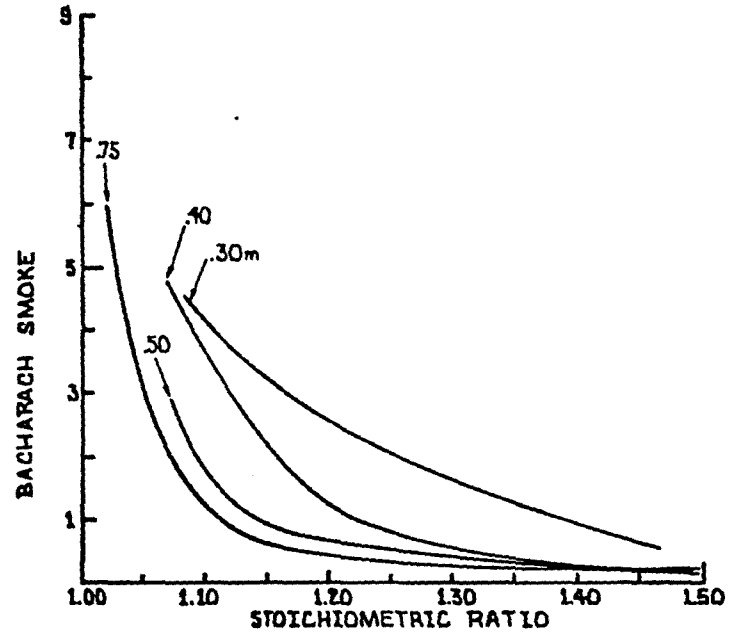

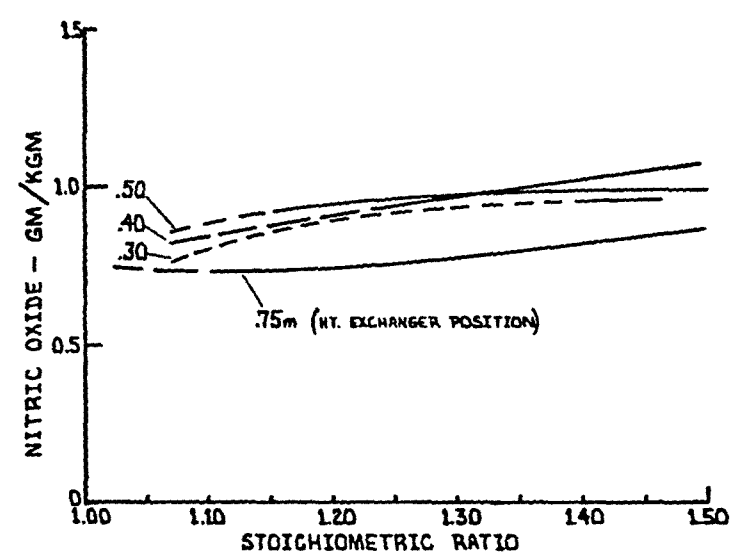

Figure 28. Cycle-Averaged Flue Gas Emissions, 1.0 ml/s (gph) Optimum Oil Burner in a 0.222 m (8.75 inches) Diameter, Air-Cooled, Side-Fired Combustor at Various Heat Exchanger Positions

The fractional, air-cooled, side-fired combustor test series was conducted as was its counterpart tunnel-fired combustor test series, in the 0.222 m (8.75 inches) ID combustor with the heat exchanger (i.e., chamber length) set at 0.40 m (16 inches) and using a 0.30 m (12 inches) length of external insulation. The cycle-averaged emissions data are presented in Fig. 29. The numerical label of each curve represents the fraction uninsulated, with the insulated section being moved away from the burner. The completely uninsulated curves are replots of the air-cooled chamber data from Fig. 29. Comparison of Fig. 29 with Fig. 23 reveals the same differences between the side- and tunnel-fired configurations as were previously noted for the air-cooled chambers (i.e., side-firing produces lower CO and UHC, higher smoke and NO, and, additionally, has better start capabilities). Further, partial insulation displayed about the same degree of apparent ineffectiveness in altering emission levels with the side-fired burner orientation as with tunnel-firing. This appearance is deceiving, however, because the emission data for the insulated chamber (zero fraction uninsulated) are not included on Fig. 23 and 29. Comparison of the NO data on Fig. 23 and 29 with those for the insulated 0.40 m (16 inches) chamber length in Fig. 24 and 30, respectively, shows that removing the insulation from the first quarter of the chamber did have a large beneficial effect even though little further benefit resulted from removing even more insulation.

Insulation Combustion Chambers. The 0.222 (8.75 inches) ID, insulated, side-fired combustor was tested at combustion chamber lengths (heat exchanger positions) of 0.30, 0.40, 0.50, and 0.75 m (12, 16, 20, and 30 inches). The cycle-averaged (10 minutes on, 20 minutes off) flue gas composition results are plotted in Fig. 30. An evaluation of the data reveals that unburned hydrocarbons (UHC) concentrations were very low for all cases, and the carbon monoxide (CO) concentrations were also very low, except for the 0.30 m (12 inches) configuration at low-excess-air levels. A comparison of UHC and CO concentrations from other configurations of the same diameter shows no differences in UHC emissions and some small differences in CO emission at SR <1.3 in the shorter chamber lengths [$\leq$0.4 m (16 inches)]. The smoke emission levels for the 0.50 and 0.75 m (20 and 30 inches) chamber lengths are comparable to the levels obtained in the tunnel-fired configuration, while the shorter 0.30 and 0.40 m (12 and 16 inches) side-fired chambers show greater than No. 1 smoke at SR $\leq$1.30. The cyclic nitric oxide emissions of this chamber were

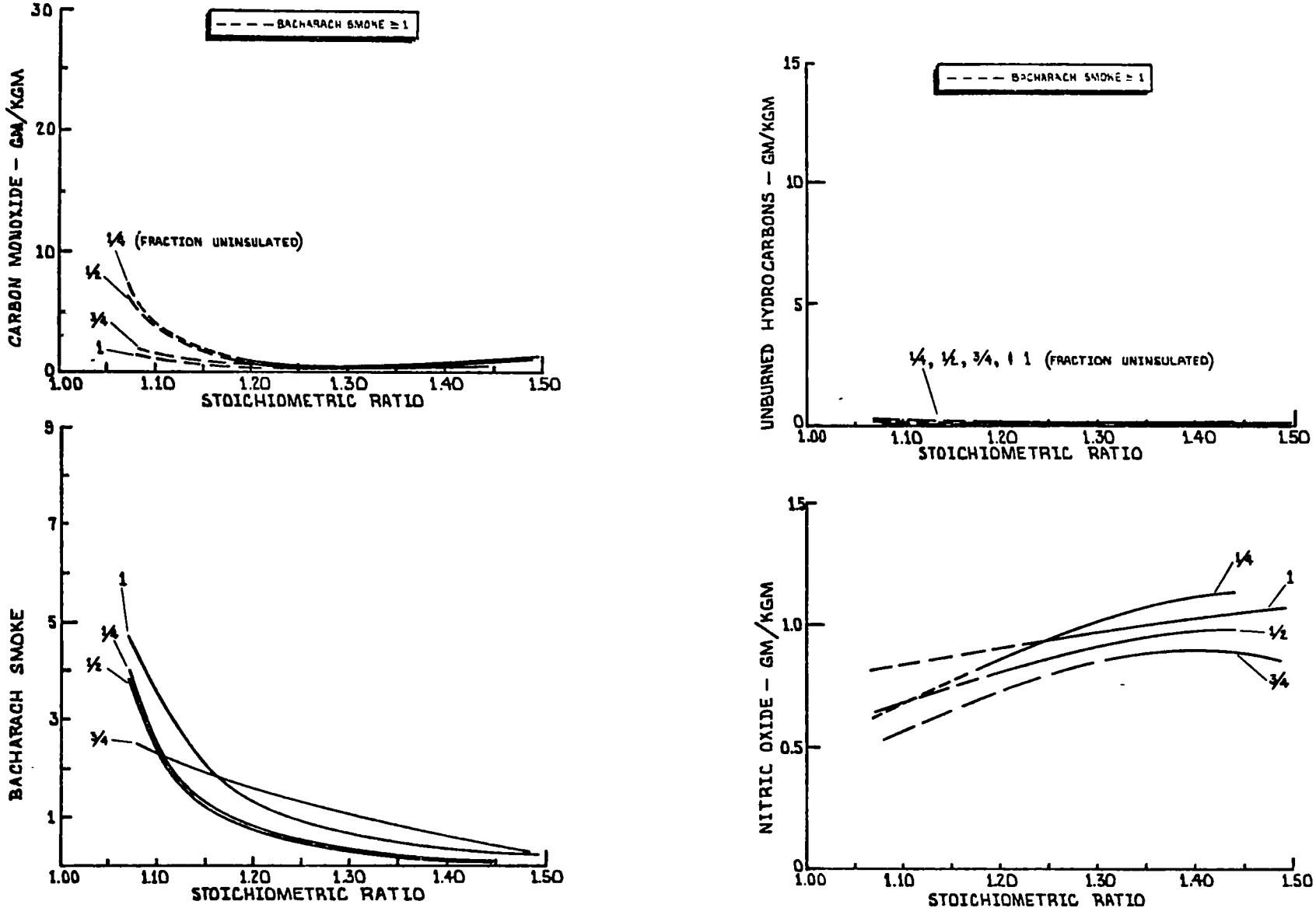

Figure 29. Cycle-Averaged Flue Gas Emissions, 1.0 ml/s Optimum Oil Burner in a 0.222 m (8.75 inches) Diameter, Partially Insulated, Side-Fired Combustor at a 0.40 m (16 inches) Heat Exchanger Position

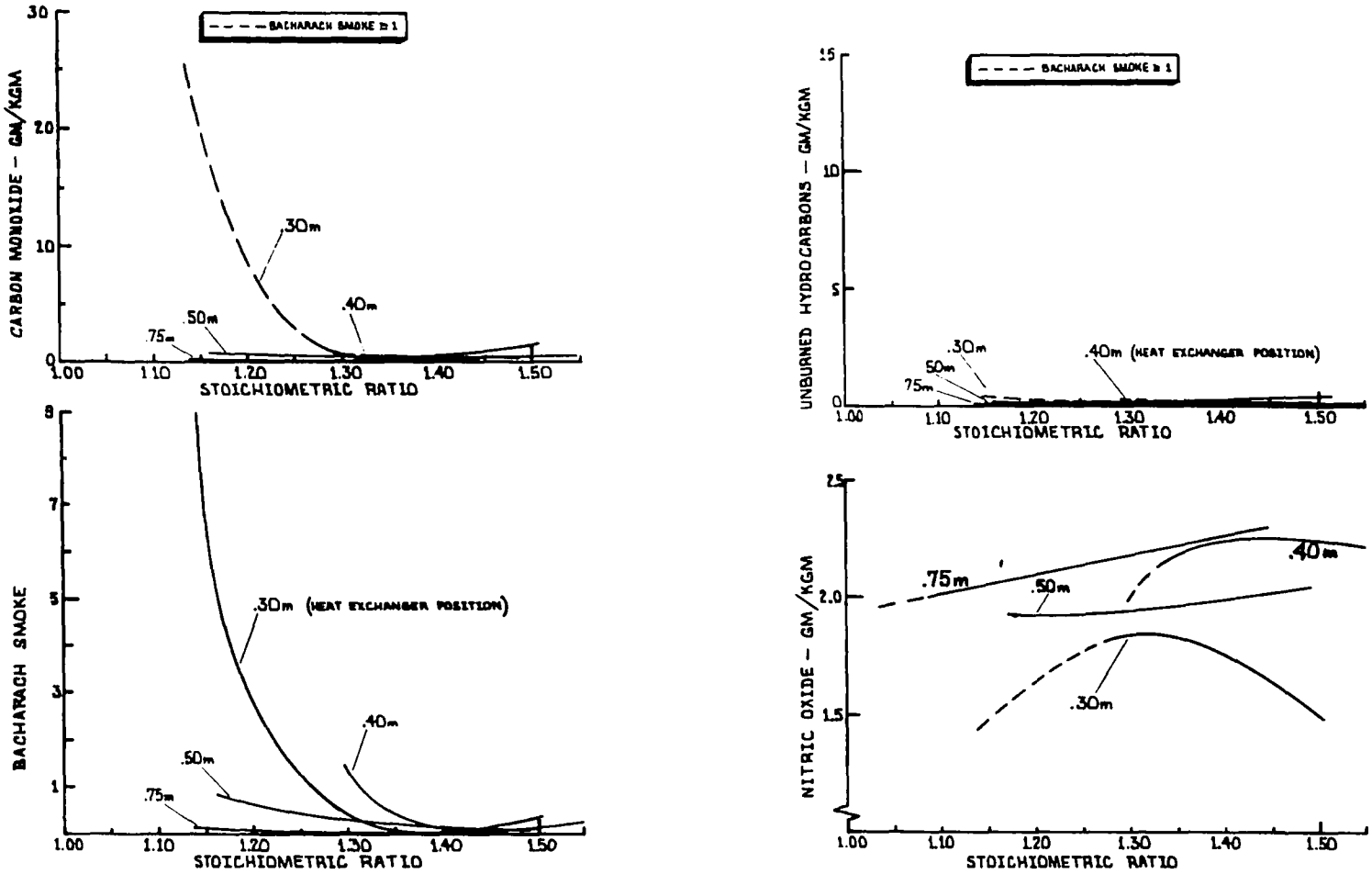

Figure 30. Cycle-Averaged Flue Gas Emissions, 1.0 ml/s Optimum Oil Burner in a 0.222m Diameter, Insulated, Side-Fired Combustor at Various Heat Exchanger Positions

a factor of two or more greater than any other configuration of the 0.222 m (8.7 inches) ID chamber, reconfirming the continuous-firing results reported in Ref. 5.

The 0.175 m (6.9 inches) ID insulated combustor was also tested at four chamber lengths, and the resulting flue gas composition data are presented in Appendix C, Runs 131 through 142. The UHC emission levels again do not appear to be of any concern for any of the four chamber lengths tested. The CO levels, however, show some noticeable concentrations ($\geq$1.0 g/kg) at chamber lengths $\leq$0.40 m (16 inches). The smoke concentrations were relatively high in this small chamber but, surprisingly, were comparable to those of the equivalent size tunnel-fired chamber. The smoke emissions showed a noticeable sensitivity to combustion chamber length, increasing with decreasing chamber length. The NO concentrations were again a factor of two higher than other comparable diameter configurations tested.

Water-Cooled Combustion Chamber. A 0.50 m (20 inches) long water jacket was added to the 0.222 m (8.7 inches) ID uninsulated combustor for the water-cooled combustor experiments. The cycle-averaged flue gas composition results are presented in Appendix C, Runs 143 through 154. The side-fired configuration showed some improvement in CO and UHC concentration at SR >1.20 over the tunnel-fired results, probably because of the better mixing in the combustion zone provided by the crossflow entry. The smoke emission levels were similar in the two chambers, with the exception of the short 0.30 m (12 inches) chamber that was unacceptably smoky in the side-fired configuration. The NO concentrations showed no sensitivity to orientation with water-cooled walls. The nominal NO level remained at about 0.6 to 0.7 g/kg of fuel burned.

Several months later, a brief series of tests was made with the 1 ml/s (gph) optimum burner side-fired in a water-cooled 0.279 m (11 inches) chamber. The larger-diameter chamber was tested to confirm the hypothesis, discussed in the following subsection, that using an unusually large combustion chamber diameter and a water-cooled firebox section would greatly reduce NO emissions. The data are listed in Appendix C, Runs 427 through 432. The cycle-averaged NO concentrations were very low indeed. The other pollutant emissions were acceptabley low, with the possible exception of CO, which indicated that the firebox might also have to be lengthened.

Discussion: Optimized Conventional Burner/Combustor Matching

The experimental data from firing the 1 ml/s (gph) optimum burner in the variety of chambers were evaluated to determine a preferred combustor configuration, the size and cooling method, and whether that preferred burner/chamber combination can meet the objectives listed in the Introduction.

Determining whether the objectives can be met necessitates defining acceptable emission levels for CO, UHC, and smoke. Values were selected in conformity with average values reported in the field survey of Ref. 4:

Emissions:	CO_2, percent	Smoke, Bacharach Number	g/kg Fuel		
			CO	UHC	NO
As Found:	~7.9	3.2	1.05	0.10	2.6
Tuned:	~8.1	1.2	0.65	0.06	2.7

These are quite lean conditions (8.0-percent CO_2 corresponds to 90-percent excess air and net thermal efficiencies of about 70 percent), which normally produce quite low values of carbonaceous emissions. In view of the other goal of increasing efficiency by 10 or more percent, partially achievable by reducing excess air, and the modest differences between "as found" and "tuned" CO and UHC, acceptable levels were selected to be: CO <1 g/kg; UHC <0.1 g/kg; smoke $\leq$Bacharach No. 1.

With those values used as limits, the data in Appendix C and Fig. 21 through 30 were studied to discern chamber design requirements. The results were synthesized into a tabular summary form amenable to extraction of trends and design criteria. This summary is given in Table 8 where the first three columns describe the combustion chamber and the next three columns list the chamber lengths and stoichiometric ratios for which the pollutant concentrations in the flue gas were acceptable. Few of the combustors' NO emissions were acceptably low so conditions that minimized NO production are listed under that pollutant. Further, the right-hand column of Table 8 lists approximate flue gas NO concentrations at 25-percent excess air (12-percent CO_2) for 0.50 m (20 inches) long chambers. It was seen that, with one or two exceptions, the combustion chamber designs tested generally failed to achieve the goal of NO <0.5 g/kg fuel.

TABLE 8. SUMMARY OF RESULTS FROM 1 ML/S (GPH) OPTIMUM BURNER/COMBUSTION CHAMBER MATCHING EXPERIMENTS

Chamber Design Attributes			Requirements For Acceptable (or Minimum) Emissions			NO, g/kg fuel @ L_c = 0.5 m & 1.25 S.R.
Configuration	Cooling Method	I.D., m	CO & UHC	Smoke (SN0.1)	NO	
Tunnel-Fired (Coaxial)	Air-Cooled	0.162	Rough-Burning Throughout Operating Range			-
	(Startable over a very narrow S.R. range)	0.222	$L_c \geq 0.5$m	S.R. ≥ 1.05	$L_c \approx 0.4$m	(0.6)*
		0.279	$L_c \approx 0.75$m	S.R. ≥ 1.1 or $L_c > 0.5$m	$L_c \approx 0.4$-0.5m	(0.4)
	Water-Cooled	0.222	$L_c > 0.5$m	S.R. > 1.15	Short L_c's Best	0.7
	Insulated	0.175	$L_c \geq 0.5$m	$L_c \geq 0.75$m or S.R. >1.3	Short L_c's Best	1.3
		0.22	$L_c \geq 0.5$m	$L_c \geq 0.5$m & S.R.>1.15	Short L_c's Best	0.9
Side-Fired (Perpendicular Port)	Air-Cooled	0.162	Rough-Burning Throughout Operating Range			-
		0.222	$L_c \geq 0.5$m	$L_c \geq 0.5$m S.R. ≥ 1.15	$L_c = 0.75$m slight favor	0.9
		0.279	$L_c \geq 0.4$m & S.R. ≥ 1.15	$L_c \geq 0.5$m & S.R. ≥ 1.08	Short L_c's Best	0.6
	(Forced Draft)**	0.250	$L_c \geq 0.5$m	$L_c \geq 0.5$m, S.R.>1.05	Short L_c's Best	0.6
	Water-Cooled	0.222	$L_c \geq 0.5$m	$L_c \geq 0.4$ & S.R. ≥ 1.2	Short L_c's Best	0.7
		0.279	$L_c \geq 0.5$m	$L_c \geq 0.5$ & S.R. ≥ 1.1	Short L_c's Best	0.4
	Insulated	0.175	$L_c \geq 0.4$m	$L_c \geq 0.5$ & S.R. ≥ 1.25	Short L_c's Best	2.0
		0.22	$L_c \geq 0.5$m	$L_c \geq 0.5$m & S.R. ≥ 1.15	Data Mixed	1.9

*Values enclosed in parentheses obtained by extrapolation outside the star table range
**Experiments described and discussed in Appendix F

Combustor design criteria that can be derived from Table 8 (and the larger body of data upon which it is based) are subdivided into categories of burner orientation, chamber size, and cooling medium in the following paragraphs.

Burner Orientation. Combustion chamber design requirements for ensuring acceptable levels of CO, UHC, and smoke emissions were found to be quite similar for both the side- and tunnel-fired burner orientations. That observation held for NO emissions from water-cooled combustors as well. However, NO production in refractory-lined and air-cooled chambers was about 1-1/2 to 2 times as high in the side-fired orientation as in the tunnel-fired. Ostensibly, this latter phenomenon resulted from substantially longer gas residence times at high temperatures in the stronger and more complicated eddies of a side-fired chamber.

Combustion Chamber Size. Chambers smaller than about 0.20 m (8 inches) ID must be refractory-lined to avoid operating with unacceptable combustion roughness. Operation of all designs was acceptable in this regard when their inside chamber diameter was 0.222 m (8.75 inches) or larger.

Larger-diameter chambers, with or without insulation, tend to require longer chamber lengths to achieve comparable levels of carbonaceous pollutants and, concurrently, to produce substantially lower levels of NO. Both phenomena are undoubtedly linked to the ingestion of recirculation combustion gases into the flame zone. For a given burner, larger and stronger recirculation eddies can be established in bigger chambers, thereby reducing the combustion intensity somewhat and lowering the rates of burnout of carbonaceous species. Also, larger-diameter chambers have greater wall areas for convective and radiant transmission of heat from the flame zone, which reduces peak flame temperatures somewhat. Increased average gas residence times should produce opposing trends for both NO production and carbon burnout, which could help account for some anomalies in the data. Further, the steady-state recirculation and radiation effects may be partially masked by starting transient effects, particularly with respect to smoke and UHC data.

Short combustion chambers generally were more faborable for low NO but, if they are too short, the fuel may not be completely burned before combustion reactions are quenched in the heat exchanger. A length of 0.5 m (20 inches) is a suitable compromise for most of the chamber designs tested. Slightly shorter chambers might be approproate if refractory linings were to be used.

Chamber Cooling Medium. Refractory-lined combustion chambers generally exhibited less combustion roughness and less sensitivity to starting conditions but also produced higher NO concentrations than did cooled-wall combustors. The air-cooled, side-fired configuration had better starting characteristics (but higher NO) than did the air-cooled, tunnel-fired chamber. Water-cooling appeared to be preferable to air-cooling, partially because of lower side-fired NO levels, but also because of smoother starting and more consistent CO and NO emission results. The water-cooled chambers in shorter lengths, however, were prone to produce excessive CO.

Tests with partially insulated, partially air-cooled chambers were not found to differ markedly from the fully air-cooled configuration.

COMBUSTION GAS RECIRCULATION (CGR) BURNER STUDY

CGR Burner

Circulation patterns are normally established within an operating combustion chamber. The main driving force is momentum exchange between the relatively high-velocity reactants emanating from burners and the lower-velocity gases in the chamber. Mixing of the ingested gases into the reactants as they burn lowers the reaction intensity and stretches the reaction zone. The impact of this internal combustion gas recirculation on NO formation covers a broad range, from negative to positive. In well-insulated, near-adiabatic combustors, the main effect of internal recirculation is to increase the average gas residence time; usually this results in higher NO concentrations via a closer approach to thermodynamic equilibrium. In cooled-wall combustors, recirculation eddies embedded within the flow downstream of a burner may similarly increase NO production, modulated only by radiant losses to the walls. Circulation currents that flow along the combustion chamber walls, however, are also convectively cooled. If sufficient heat is lost to the walls, these partially cooled recirculation gases drawn into the flame zone act as an inert diluent, reducing the combustion intensity and peak temperature, and inhibiting the formation of NO enough to more than offset the effects of increased average residence time.

Internal combustion gas recirculation patterns and their strengths are largely determined by the combination of firebox design, burner design, and burner placement. Some burners have been designed intentionally to promote this kind of recirculation (see Ref. 9), but they may be rather restricted in application to particular firebox designs and burner positions that do not inhibit the recirculation. Conceptually, such dependence can be reduced by forcing the recirculation of partially cooled combustion gases (e.g., by withdrawing gases from the combustor and recirculating them to and mixing them with the burner air supply). This recirculation is difficult to accomplish because the chamber gases are too hot for mechanical air blowers. Two viable approaches that have been tried are to

use the momentum of the combustion air of the burner to aspirate gases from the combustor (Ref. 10) and to dilute the hot gases with fresh combustion air before the mixture is supplied to the combustion air fan (Ref. 5). In both cases, a larger, more powerful fan is required in order to force the recirculation of the extra gases.

A burner embodying the latter approach, of diluting combustion gases withdrawn from the combustor with fresh combustion air, was studied in this program. The burner concept is shown schematically in Fig. 31 to have an air/combustion gas-mixing plenum surrounding the burner blast tube that was exhausted to the suction side of the combustion air fan of the burner. The CGR burner had the capability of drawing combustion gases from locations near its center (B), near the chamber wall (A), or from further downstream in the combustion zone (C). The burner was designed to fit in the air-cooled 0.22 m (8.75 inches) diameter combustor in either the tunnel-or side-fired orientations.

The burner head used the variable swirl vane assembly from the previous Rocketdyne burner studies (Ref. 5) and replaceable fixed-diameter choke plates so that these parameters could be optionized as appropriate with CGR variations.

Figure 32 is a photograph of the CGR burner assembly, showing the CGR manifold assembled around the variable swirl vane, versatile burner head assembly. The photograph does not show a 0.10 m (4 inches) diameter insulated ducting between the CGR manifold outlet and the blower inlet. The electric motor was remounted on 0.015 m (0.6 inches) insulating standoffs. The safety circuitry and spark transformer were removed from the CGR burner body to avoid anticipated "over-temp" problems. Also, the capacity of the combustion air fan was increased about 20 percent by adding a metal lip, inside the fan housing, to reduce the squirrel-cage impeller clearance to 0.002 m (1/8 inch). [The no-flow outlet pressure of the fan went from 310 N/m^2 (1.25 inches of water column) to 370 N/m^2 (1.50 inches of water column)].

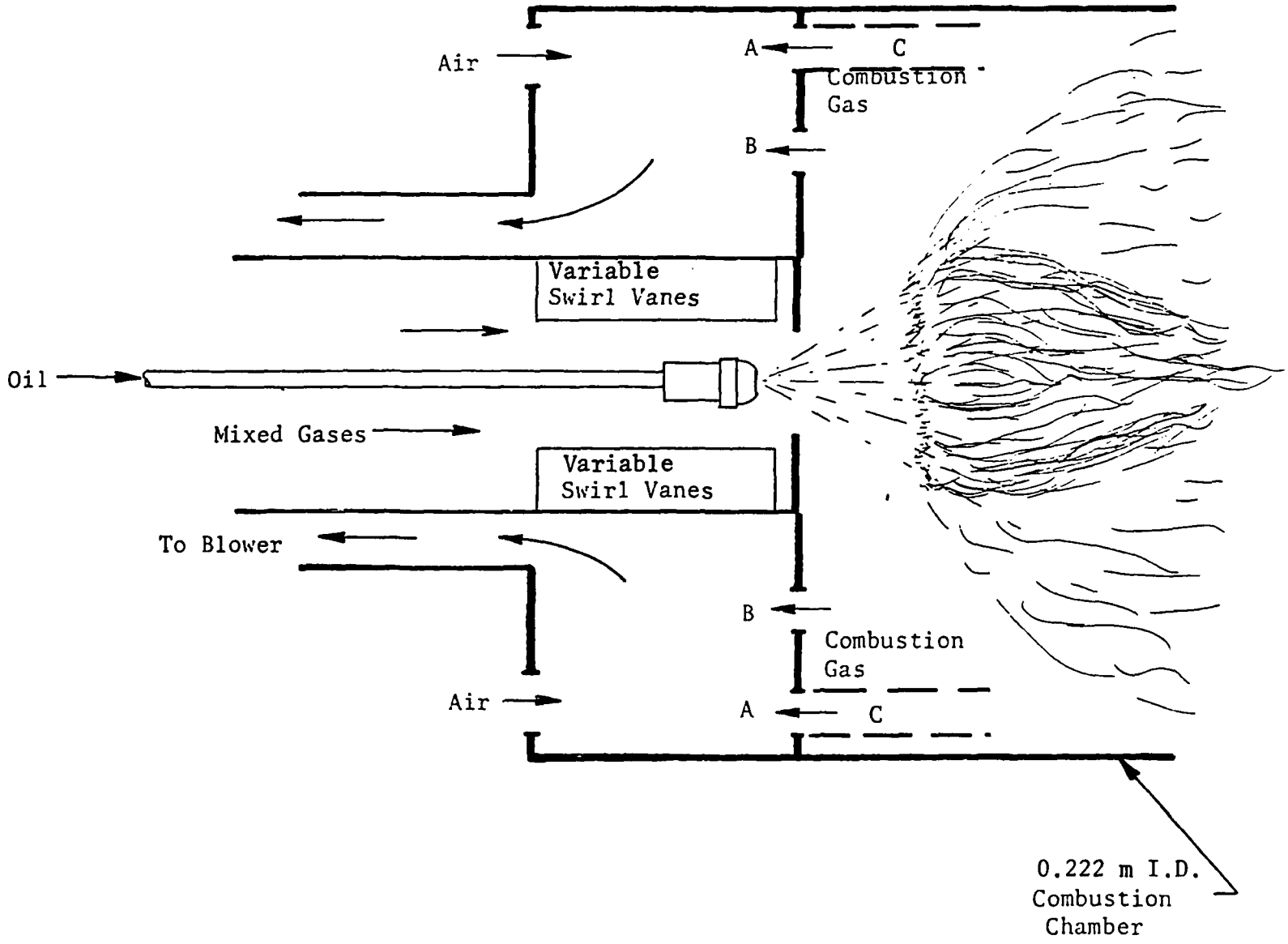

Figure 31. Burner/Chamber Configuration for Combustion Gas Recirculation (CGR) Tests

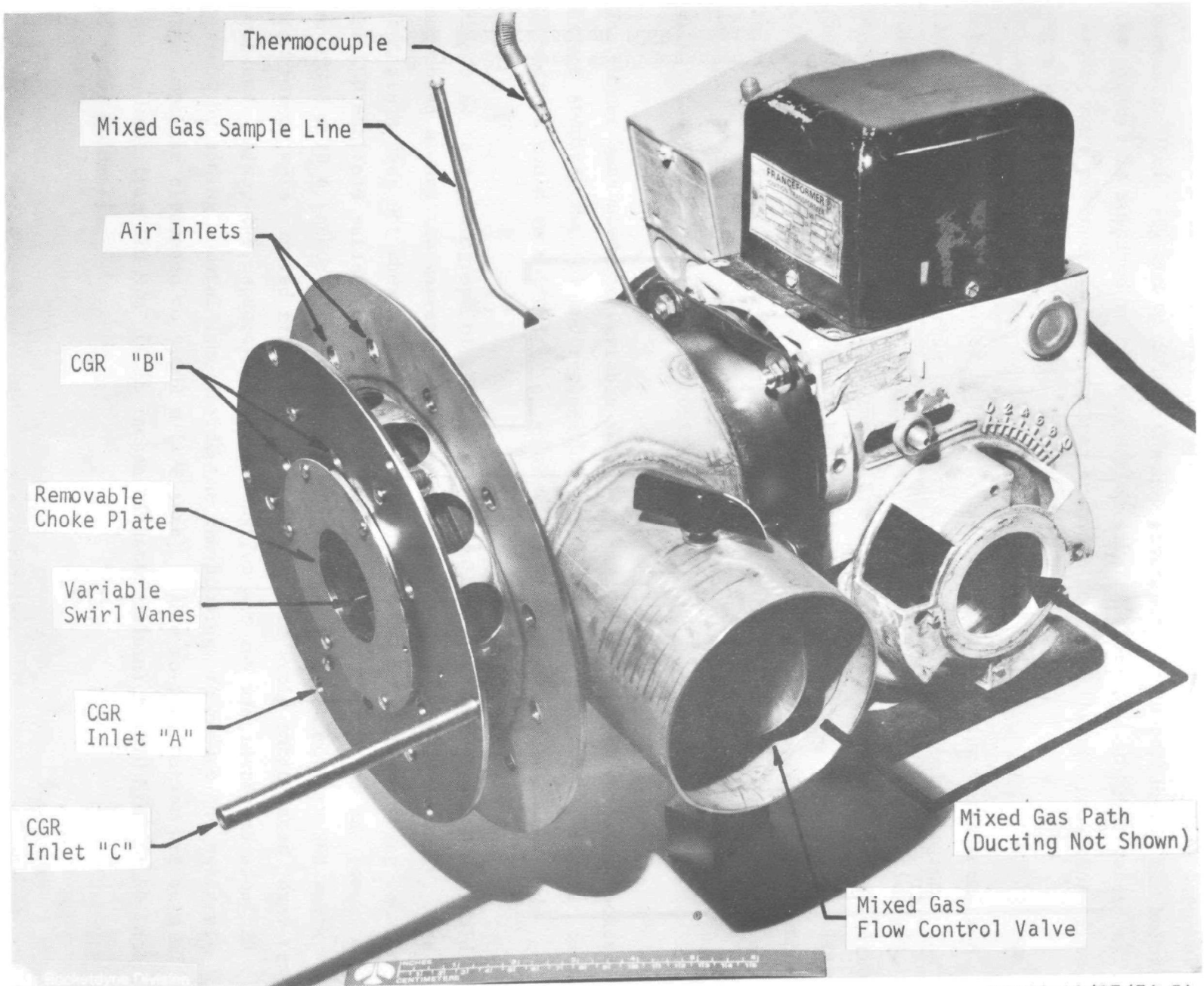

Figure 32. Photograph of Combustion Gas Recirculation Burner

Experimental Test Matrix

A matrix of tests was planned as tabulated in Table 9 for evaluating the emissions performance of the CGR burner in the tunnel-fired combustor orientation. Variations in the magnitude and source of CGR, excess air level, burner choke, and swirl were planned predominantly at steady-state conditions. Subsequently, with optimum values for those parameters, it was planned to vary the oil nozzle and supply pressure, and the chamber length and diameter during cylical testing.

Experimental Test Results

The CGR burner firings actually conducted, are summarized in Table 10. The flue gas and recirculated gas composition data are tabulated by run number in Appendix D.

After 17 firings (Runs 155 through 171) were conducted, it became apparent that the CO and UHC concentrations were significantly higher than those from conventional burners, and that the target values would not be obtained with the configurations and conditions specified by the Table 9 test matrix. Therefore, an exploratory firing series was initiated to investigate methods of improving the CO and UHC emissions. A baffle was added to the tunnel-fired chamber (Runs 172 through 183) 0.23 m (8.75 inches) from the burner head, hopefully to improve recirculation eddies and reflect radiant heat back into the combustion zone. The result was an improvement in the system operational characteristics, but no significant improvement in emissions. The side-fired burner orientation was tried both with a 1.0 60°-A nozzle and with a 0.75 60°-A nozzle (to increase the chamber volume/burner output ratio, i.e., a larger effective chamber diameter). The CO and UHC concentrations were not improved appreciably. Further experiments were conducted using the tunnel-fired chamber with various changes to burner, combustor, and run conditions. A 0.15 m (7.5 inches) length of Pyroflex insulation (added to retain heat in the combustion zone), higher excess air settings, a 0.02 m (1 inch) choke plate extension, and gas recirculation from 0.25 m (10 inches)

TABLE 9. COMBUSTION GAS RECIRCULATION BURNER TEST MATRIX

CGR, Percent	Excess Air, Percent	Choke Diameter, cm	Air Swirl Angle, Degrees	Chamber Diameter, m	Chamber Length, m	Oil Nozzle	Oil Pressure x10^5 N/M^2	Data Type	Chamber Wall
10	10	2.5	10,20,30,40	0.222	0.40	1.0-90A	6.89	Equilibrium	Air-Cooled
↓	↓	3.8	↓	↓	↓	↓	↓	↓	↓
20		5.1							
↓		2.5							
		3.8							
		5.1							
		6.4							
30		2.5							
↓		3.8							
		5.1							
		6.4							
Optimum	5	Optimum	Optimum						
↓	15	↓	↓						
	20								
	25								
	30								
	35								
	Optimum					0.6-90A	20.68	Transient	
	Optimum					0.6-90A	20.68	Equilibrium	
	10,20,40,80					1.1-90A	5.52	Equilibrium	
	Optimum					1.1-90A	5.52	Transient	
	↓				0.30	1.0-90A	6.89	↓	
					0.50	↓	↓		
					0.75				
				0.279	12				
				↓	16				
					20				
					30				
	5,10,20,30			Optimum	Optimum				
	Optimum								
↓		↓	↓			↓	↓	↓	↓

TABLE 10. SUMMARY OF COMBUSTION GAS RECIRCULATION BURNER, HOT FIRE EXPERIMENTS

Run No.	CGR Location	CGR Percent	Excess Air, Percent	Choke Diameter, m	Swirl Angle, Degrees	Oil Nozzle	Combustion Chamber		
							Dia., m	Length, m	Remarks
155-171	A	10-30	5-35	0.042	10-55	1.0-60-A	.22	.40	Air-Cooled (A/C) Tunnel-Fired
172-183	B	10-30	5-15	↓	10-40	1.0-60-A	↓	↓	A/C, Tunnel-Fired, Baffle at 0.23 m
184-186	A	15-40	15-40	↓	40	0.75-60-A	↓	↓	A/C, Side-Fired
187-190	A	15-25	1-20	0.042	↓	1.0-60-A	↓	↓	A/C, Side-Fired
191, 192	A	44, 40	55, 40	0.051	↓	↓	↓	↓	A/C, Tunnel-Fired, Baffle at 0.23 m
193-199	A	15-45	15-110	↓	↓	↓	↓	↓	A/C, Tunnel-Fired, Baffle at 0.23 m 0.15 m Insul.
200-212	A	10-35	15-70	↓	↓	↓	↓	↓	A/C, Tunnel-Fired, Baffle at 0.23 m
213-223	A	10-30	15-80	0.051 0.02m Ext.	40	↓	↓	↓	A/C, Tunnel-Fired, Baffle at 0.23 m
224-230	C 0.25 m shroud	15-45	15-50	0.051	0	↓	↓	↓	A/C, Tunnel-Fired Baffle at 0.40 m
231-238	C 0.25 m shroud	15-30	15-50	↓	40	↓	↓	↓	A/C, Tunnel-Fired, Baffle at 0.40 m
239-247	A	10-30	10-50	↓	↓	↓	↓	↓	Water-Cooled, Side-Fired
248, 249 Transient	A	20, 10	40, 25	0.051	40	1.0-60-A	.22	.40	Water-Cooled, Side-Fired

downstream (position C)* all resulted in CO and UHC emissions higher than the target values. A water-cooled, side-fired combustor produced very low NO emissions but showed no improvement in CO and UHC.

Only two cylical tests were conducted with the CGR burner. Minor ignition problems were encountered because of the high-excess air starts (because of the initial absence of combustion gas) but no start-to-blue-flame transition problems were noted.

It was found that the steady-state operation of the CGR burner gave acceptably low exhaust gas NO concentrations but generally had unacceptably high CO and UHC concentrations. A few conditions did have low enough CO, but the hydrocarbons remained high. Examination of the data strongly suggested that the UHC readings were probably erroneously high. Careful examination of the data revealed the following factors:

1. Among the various combustion gas sample analyses performed in the burner/furnace test laboratory, the UHC measurement system has the slowest response. During previous cyclical furnace tests in which appreciable UHC levels (~30 to 50 ppm) were measured, recovery to a precycle zero level took much of the 20-minute off-time of a 10-min on/20-min off cycle. With continued testing at these levels of UHC emission, precycle zeros frequently were not recovered, i.e., the system appeared to be retaining UHC which was desorbed quite slowly, resulting in apparent zero shifts.
2. In the CGR burner tests, samples were fed into the entire sample system alternately from the flue gases and from the mixture of CGR and combustion air within the burner. With several configurations and many

*Rather than using tubular extensions from position A holes, as illustrated in Fig. 31 and 32, position C experiments employed a 0.25 m (10 inches) long, 0.15 m (7.5 inches) ID stainless-steel shroud around the flame zone. This shroud was chosen to give a pseudo-simulation of the CGR burner reported by Cooper and Marek (Ref. 10).

operating conditions, the UHC levels in the recirculated combustion gases were extremely high so that the concentration in the mixed burner gases exceeded the meter range (>3300 ppm). Thus, particularly during steady-state testing, there were ample opportunities for the UHC sample system to absorb substantial quantities of UHC that would be slowly desorbed into subsequent samples, causing them to produce erroneously high UHC readings.

3. The probable magnitude of the error was estimated, from previous experience and from a few tests of the zero shift when an air purge was passed through the system, to be on the order of 20 to 30 ppm, corresponding to about 0.22 to 0.33 g/kg fuel. This is on the order of one-half the UHC levels recorded for those CGR burner conditions where the CO, NO, and smoke were acceptable; the indicated residual UHC concentrations are still higher than the target acceptable value of 0.1 g/kg.

It was decided that, in future testing, UHC zero shifts of this sort should be quantified by admitting air to the sample line after the analysis of each sample having high UHC. However, for these CGR burner experiments, even if the UHC readings were totally wrong and this pollutant had had acceptable concentrations in all of the tests, only some minimal design and operating conditions appeared where CO, smoke, NO and operability were all acceptable. Thus, it was decided to forego further testing of this concept, since it appeared to generate more problems than solutions.

FLUE GAS RECIRCULATION (FGR) BURNER STUDY

External recirculation of combustion gases is practical if they are obtained downstream of the furnace heat exchanger, i.e., from the exhaust flue. Mixed with the incoming combustion air, recirculated flue gases are a more effective diluent than an equal quantity of CGR because they are cooler. Peak flame zone temperatures are reduced by 300 to 400 C by 30 percent FGR, and NO emissions from burning distillate fuel oils have been lowered by as much as 85 percent. As

the level of FGR is increased, two phenomena are commonly observed: a diminishing effect occurs on NO level, and increasing difficulties develop in maintaining flame stability. The guiding principles for optimizing the level of FGR for given stoichiometric ratio and flue gas temperature conditions have been delineated in Ref. 11, but optimization of specific units currently depends more upon empirical testing than on theoretical analysis.

FGR Burner

The basic FGR burner is a modification of the 1-gph versatile burner (Ref. 5). The air inlet was modified to provide a mixture of FGR to the air on the suction side of the squirrel cage fan, and the variable choke plate was replaced by an interchangeable, fixed-diameter choke plate. The flue gas adapter was designed to be mated to a 0.1 m (4 inches) diameter galvanized steel flue gas return duct (Fig. 33).

Experimental Test Results

In view of the experiences with the CGR burner, a preconceived FGR burner test matrix was set aside and exploratory tests were conducted in various combustion chamber configurations to determine a suitable combustor to use for performing the FGR burner/chamber optimization. Flue gas composition data are tabulated in Appendix E.

Runs 250 to 321 are the preliminary steady-state chamber configuration experiments involving 0.222 m (8.75 inches) diameter chambers which were: (1) side-fired, water-cooled; (2) side-fired, insulated; and (3) tunnel-fired, insulated.

Tests of the water-cooled chamber (Runs 250 through 285) produced very low NO concentrations (0.2 through 0.4 g/kg), well below the 0.5 g/kg of fuel burned target value. However, the CO and UHC emission characteristics were very poor, and therefore, the side-fired, water-cooled combustion configuration was deemed as an unlikely candidate for FGR optimization.

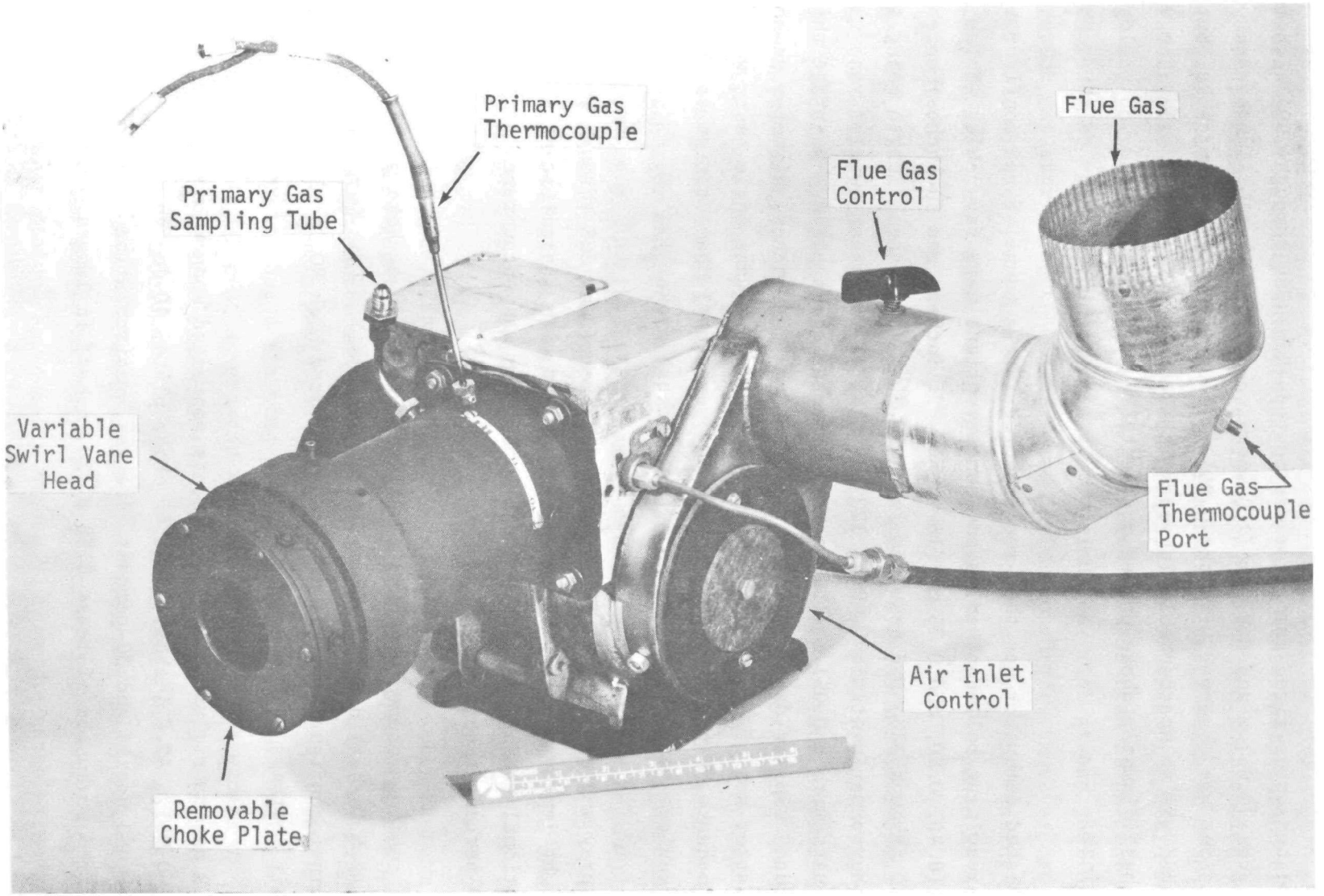

50P21-2/7/75-S1

Figure 33. Photograph of the Flue Gas Recirculation Research Burner

The insulated, side-fired combustor was tested (Runs 286 through 299) with two choke plates [0.051 m and 0.072 m (2.0 inches and 2.9 inches)]. Improvement in UHC emissions was observed with the 0.051 m (2.0 inches) diameter choke, but also experienced was an unacceptable increase in NO emissions (>0.5 g/kg). The 0.072 m (2.9 inches) diameter choke proved unacceptable in smoke, CO, and UHC at lower air settings.

The insulated combustor was then reconfigured into a tunnel-fired configuration, and the resulting pollutant emissions concentrations were favorable. Three chamber lengths [0.40, 0.50, and 0.75 m (16 inches, 20 inches, and 30 inches)] were tested (Runs 300 through 343) and resulted in the 0.50 m (20 inches) length being selected for further experimentation. Runs 322 through 343 represent swirler vane variation results with a 0.051 m (2.0 inches) diameter choke plate. Runs 344 through 357 produced similar data with a smaller 0.042 m (1.5 inches) diameter choke plate. In the latter set of experiments, the 10-degree swirl vane angle tests were eliminated because of the poor CO, smoke, and operational characteristics observed in the previous set with the 0.051 m (2.0 inches) choke.

An oil spray angle variation from 60 to 90 degrees (Runs 358 through 361) resulted in a slight improvement in NO concentration, but with a significant degradation of operational characteristics. Rough combustion was encountered at all settings below 20-percent excess air.

Hot-fire testing resumed with the 60-degree nozzle and a choke plate change to 0.064 m (2.5 inches) diameter (Runs 362 through 381). This large-diameter-choke-plate burner configuration was smoky and produced high NO levels at the lower excess air settings (~10 percent).

These FGR parametric variation experiments converged upon a burner configuration having a 0.051 m (2.0 inches) diameter choke plate, 40-degree swirl vane angle, 60-degree oil nozzle and 30-percent flue gas, recirculation in an insulated, tunnel-fired combustor at least 0.50 m (20 inches) in length. Runs 382 through

387 were made to recheck this preliminary, steady-state optimization of the FGR burner/chamber configuration before proceeding to the cyclical testing portion of the optimization testing. This brief series of tests began to display a characteristic that had to be corrected before the optimization could be completed: rough and noisy combustion prevented operation at less than 18-percent excess air. Since these tests were conducted on a very windy day with strong gusting, the poor operation was attributed to wind effects on firebox draft. However, it persisted on the following day, which was calm, and exploratory cyclical testing revealed no regions of acceptably quiet operation where data-taking runs could be made.

Inspection of the burner and combustion chamber revealed two conditions thought to be possible contributors to noisy operation; both were corrected. The first was that a piece of aluminum foil tape, used to thermally protect internal 110-VAC wiring in the burner, had come loose and was partially obstructing the flow around the squirrel-cage impeller of the fan. The second was that the Pyroflex liner of the chamber was partially separated into irregular and displaced layers near the heat exchanger end, presumably as a result of the many configuration changes that had been made. The insulation was removed and the chamber relined. However, rather than installing three layers of Pyroflex to form a 0.22 m (8.75 inches) ID, a single layer was initially used to form a 0.26 m (10.5 inches) ID chamber to test before completing the relining.

The 0.26 m (10.5 inches) diameter chamber was tested cyclically in both the tunnel- and side-fired configurations (Tests 388 through 382). Operation was quite satisfactory, with smooth starts and smooth, quiet burning to as low as 10-percent excess air. Carbonaceous pollutant levels were below the target levels at low-excess-air conditions, but a starting puff of smoke pushed the cycle-averaged UHC readings above 0.1 g/kg at greater than about 30-percent excess air. Cycle-averaged NO concentrations exceeded the 0.5 g/kg target value slightly; the increase over the previous steady-state levels was thought to result either from the 18-percent increase in chamber diameter or from the spark igniter having been left on for the entire burner-on time. Interestingly, the side-fired configuration did not produce appreciably higher NO than the tunnel-fired.

For tests 393 onward, the additional refractory lining was installed to reform the 0.22 m (8.75 inches) diameter chamber, which was then tunnel-fired. Tests 393 and 394 were made to provide a steady-state comparison of NO emissions with the spark igniter left on versus turning it off after ignition was achieved. There were no measurable changes in the flue gas composition.

The optimized FGR burner was then cyclically fired and the data (Runs 396 through 398) show some marginal emission level characteristics. The NO concentration was slightly higher than the targeted 0.50 g/kg, and the CO emission at less than 16-percent excess air began to show some unacceptable concentrations, mainly because of the "start spike" at ignition. Recirculating gas burners are characteristically poor starters as a result of the high excess air starts when cold air instead of combustion gas is available in the gas recirculation ducts. The FGR burner was start-limited at >35-percent excess air, but it displayed no ignition nor transition difficulties at the lower air settings.

Runs 399 through 403 represent a chamber length variation; the heat exchanger was moved to the 0.75 m (30 inches) position in the 0.22 m (8.75 inches) ID combustor. Comparison of these 0.75 m (30 inches) chamber length data with the 0.50 m (20 inches) data shows the 0.75m(30 inches) chamber to be slightly better in CO emissions, but also slightly worse in NO concentrations (from ~0.58 g/kg to ~0.61 g/kg at 30-percent FGR). Although the 0.50 m (20 inches) length chamber did show some increase in CO as stoichiometric ratio was lowered to about 15-percent excess air (mainly attributed to "spikes" in the FGR starts), its slightly lower NO levels makes it the preferred configuration over the 0.75 m (30 inches) chamber.

The nominal cycle-averaged NO emission level of 0.58 g/kg of fuel burned at 30-percent FGR is slightly higher than the 0.50 g/kg target value. If this target value is to be strictly adhered to, then the FGR system would require more recirculated gases (probably 40-to 45-percent FGR) with electrical or mechanical compensations (e.g., FGR control valve and programmed start cycle) to produce

"smoother" (no emission spikes) ignition characteristics. The oil burner/furnace industry would be opposed to any added "complexities" and, therefore, the commercial success of a residential-size FGR system would have to be supported by significant, saleable advantages and/or required to satisfy stringent pollutant emission standards.

So that the effect of changes in nominal oil spray dropsize may be studied, oil supply pressure variations were tested in Runs 404 through 408. Runs 404 and 405 were fired with a 1.25-gph, 60-degree A nozzle at 551 kN/m^2 (80 psig) oil supply pressure, and Runs 406 through 408 were fired with a 0.75 gph, 60-degree A nozzle at 2137 kN/m^2 (310 psig). The resulting pllutant emission data show no significant differences from the typical 1.00-gph, 60-degree A nozzle at 689 kN/m^2 (100 psig) oil supply pressure; however, slight operational differences were noted. The 551 kN/m^2 (i.e., larger dropsize) firings showed some combustion roughness (noisy), while the 2137 kN/m^2 firings appeared to light-off more smoothly. These results show no reason for the development of a different type of oil spray system.

The sensitivity of the optimum 1 ml/s (gph) FGR system configuration [0.051 m (2.0 inches) choke, 40-degree swirl burner head; 0.22 m (8.75 inches) ID x 0.50 m (20 inches) long, tunnel-fired insulated combustor] to changes in firing rate were intended to be investigated in Runs 409 through 412. However, Runs 409 through 420 were found to have been fired inadvertently at 551 kN/m^2 (80 psig) oil supply pressure. (Adjustments made to the pump system for a previous test series had not been reset.) Thus several data points were rerun later, so the 0.68 ml/s (gph) tests (Runs 409 and 410) should be compared with the later 1.21 ml/s (gph) tests (Runs 425 and 426). The lower 0.68 ml/s (gph) firing rate (as compared to the 0.98 ml/s (gph) optimized firing rate) resulted in increases in all carbonaceous pollutants. This result has been seen before with oversized burner choke configurations and is caused by lowering the firing rate with fixed burner geometry. Similarly, the 0.68 ml/s (gph) burner required more excess air for smoke-free operation. This additional air was probably needed to regain the exit air velocity (i.e., mixing energy) that was lost by the increase in effective choke diameter

brought about by the lower firing rate. The higher 1.21 ml/s (gph) firing rate (Runs 425 and 426) showed no significant effect upon the pollutant emission levels; however, it appeared to operate more noisily (combustion roughness) than the nominal 1 ml/s (gph) firing rate. The carbonaceous pollutant concentrations were all below the allowable "target" values, and the NO concentration, as expected from the reduced effective combustor size, increased slightly [from 0.58 g/kg at 0.98 ml/s (gph) to 0.64 g/kg at 1.21 ml/s (gph)]. The optimized FGR burner system appears to be no more sensitive to firing rate changes than are the conventional burner systems.

A pair of tests (Runs 413 and 414) was conducted to examine whether turning the spark igniter off after ignition would lower the cycle-averaged NO emission from the FGR burner. These two runs were also mistakenly fired at 551 kN/m^2 (80 psig); however, since no operational difficulties were noted, and the resulting emission levels were respectably low, the results were accepted as representative data. Run 413 is the "igniter-off" firing with the ignition spark turned off approximately 10 seconds after burner start, which is similar to an "interrupted spark" -type burner control.

Run 414 is the comparative "continuous spark" firing; there were no apparent differences in flue (and recirculated) gas compositions between the two runs. This lack of an effect on cycle-averaged NO emissions is consistent with that observed previously in steady-state igniter on/off firings. Although this evidence points in the direction of a "no effect from igniter" conclusion, experience gained in an earlier oil burner emissions study (Ref. 5) restrains the adoption of any "blanket" conclusion. It was seen in those earlier experiments that the igniter-off effect was significant with certain burners and insignificant with other burners. The FGR burner tested in the current experiments is of the mechanically pumped, forced-recirculation type, and it has shown no transition phase (ignition-to-steady-state) difficulties. The air-aspirated, induced-recirculation-type burners, which are dependent upon gas temperatures, densities, and resulting velocities may be greatly affected (both in operation and emissions) by an igniter-off condition during their difficult transition stage. Therefore, only a tentative conclusion can be made, restricting this "no effect from igniter" result to this specific (or specific type) FGR burner.

Oil furnace manufacturers expressed some concern about the quality of fuel oil that might be available during periods of petroleum supply crisis. Therefore, a short series of three FGR firings (Runs 415 through 417) was conducted with the quality of the No. 2 fuel oil degraded by a 20-percent volumetric (22-percent weight) contamination with No. 6 "residual" fuel oil. The chemical compositions of both No. 2 and No. 6 fuel oils are listed in Table 11, together with the calculated (linear averages) composition and properties of the 20/80 mixture (22/78 by weight) of the two oils.

With the oil mixture, significant increases in all of the flue gas pollutant concentrations were observed. The carbonaceous pollutant levels may have been influenced upward slightly by the inadvertently low 551 kN/m^2 oil pressure. However, the No. 2 fuel oil tests immediately preceding (Runs 413 through 414) were also fired at the lower oil pressure, and the carbonaceous pollutants were well within acceptable limits. The increase in fuel nitrogen, from No. 2 oil to the mixed oil, was a factor of about nine. The corresponding increase in flue gas NO was a factor of about four (0.53 g/kg to 2.21 g/kg at 10-percent excess air). From previous experimental studies of fuel nitrogen conversion to NO_x (see Ref. 3), it may be assumed that about 85 percent of low concentrations of fuel nitrogen will show up as flue gas NO. For No. 2 fuel oil, then, flue gas NO from fuel nitrogen was estimated to be about 0.16 g/kg fuel, leaving a balance of 0.37 g/kg thermal NO. Similar conversion of the mixed oils fuel nitrogen was estimated to produce about 1.46 g/kg fuel NO, leaving a balance of 0.75 g/kg NO attributable to thermal formation. This apparent doubling of thermal NO may have been caused by reduced radiation from the flame zone attending increased combustion gas capacity as indicated by increased smokiness.

Earlier experiments with a slightly larger 0.26 m (10.5 inches) ID, insulated, side-fired combustor rekindled some optimism for that configuration. Therefore, an experiment was made with a 0.15 m (6.0 inches) ID by 0.08 m (3 inches) long, side-port extension spool added to the 0.22 m (8.75 inches) ID, insulated combustor to increase the effective combustion chamber diameter. Runs 418 through

TABLE 11. COMPOSITION AND PROPERTIES OF FUEL OILS USED IN OIL BURNER EXPERIMENTS

	No. 6 Oil	No. 2 Oil	22% No. 6/ 78% No. 2*
Carbon, % (Weight %)	86.66	86.79	86.76
Hydrogen, %	11.85	13.16	12.87
Nitrogen, %	0.32	0.009	0.08
Sulfur, %	0.97	0.11	0.30
Ash, %	0.018	-	0.004
Carbon/Hydrogen	7.31	6.59	6.75
Gravity, API at 60 F	18.8	36.1	33.0
Specific Gravity	0.94	0.84	0.86
BTU/lb Gross	18,398	19,481	(19,240)
BTU/lb Net	17,548	18,372	18,190

*Calculated values for mixture using linear weight percent averaging.

424 were made with this extension; however, evaluation should be restricted to Runs 422 through 424 as the prior runs had oil supply pressure (Runs 418 through 420) and chamber warm-up (Run 421) qualification restrictions. The addition of the standoff spool did improve the smoke characteristics compared to the 0.22 m (8.75 inches) ID combustion chamber system, which had unacceptably high smoke emission with the spoolless configuration. However, it did not lower the NO emissions, and the nominal level remained approximately 15 to 20 percent (0.69 g/kg) higher than the tunnel-fired configuration at 10-percent excess air and 30-percent FGR.

SECTION VI

PROTOTYPE SYSTEM DESIGN INVESTIGATION

Results from the analytical and experimental studies reported in Sections IV and V, together with past experience and current contacts with furnace manufacturers, were synthesized to arrive at preliminary conceptual designs for a warm-air furnace and a hydronic boiler. The decision was made that the optimized conventional burner head would be used in a cooled combustion chamber for both designs.

Although the different cooling media of the furnace and the boiler cause substantial differences between the designs, a substantial commonality exists between them concerning basic objectives and approaches taken to meet the objectives. Therefore, the areas common to the two designs are subsequently discussed before specific descriptions for each design are presented.

Each prototype design concept was discussed with one or more representatives of a manufacturing company that makes and markets residential space heating equipment of the appropriate type. The format for this section first provides a description of each preliminary prototype design. Following which are given a summarization of manufacturer's comments, criticisms, and suggestions pertaining to each design. Appropriate responses to those manufacturer inputs, such as concept revision, design modification, and provisions for data-taking, are then discussed.

PRELIMINARY DESIGNS: AREAS OF COMMONALITY

Objectives

Design objectives were to conceptualize residential heating units with a nominal 1 ml/s (gph) firing rate that would satisfy the following requirements, listed in order of priority (with low emissions and high efficiency being of equal and primary concern):

1. Low pollutant emissions
    a. Nitric oxide (NO) $\leq$0.5 g/kg of fuel burned

b. Carbon monoxide (CO) $\leq$ 1.0 g/kg

c. Unburned hydrocarbons (UHC) $\leq$ 0.1 g/kg

d. Smoke $\leq$ Bacharach No. 1 scale

2. High efficiency (10 percent or more above conventional)

3. Compliance with safety codes and operational standards

4. Competitive costs, both initial retail price and subsequent operation and maintenance

5. Quiet

6. Compact, if possible.

Design options have been evaluated on the basis of a newly manufactured product line, with compromises involving retrofit versatility given a much lower priority. However, product saleability certainly is of concern and, therefore, unit costs and acceptability to manufacturers, service personnel, and customers have been considered in the design selection process.

Burner Unit

The oil burner unit used in both prototype furnace conceptual designs is a conventional burner (Beckett Model AF body) fitted with an optimized, nonretention, burner head and an air flow/draft loss control device (Fig. 34).

The optimized burner head is described in Section IV, and consists of six air swirl vanes canted 25 degrees from the blast tube centerline and a firing-rate-dependent choke diameter. The air swirl vanes are relatively large, approximately 0.05 m (2-inches) long, and extend from approximately 0.03 m (1.2-inch) diameter out to the diameter of the blast tube. The choke diameter size is dependent upon the specific installed firing rate according to:

$$D_{(m)} \quad 0.0254 \left[2.57 \dot{w}_{oil(ml/s)}\right]^{0.4}$$

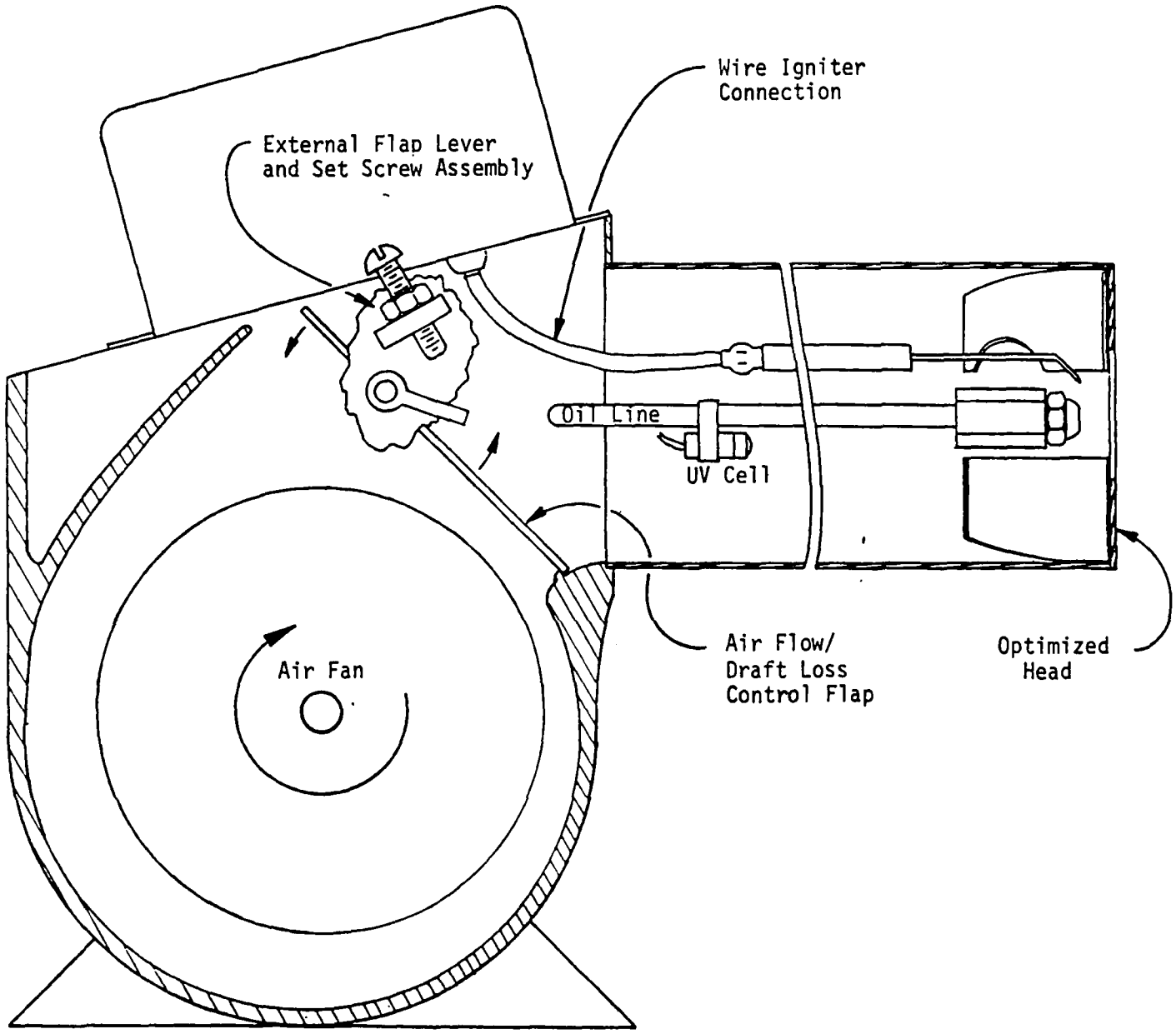

Figure 34. Schematic of the Residential-Size Optimized Burner With Positive-Pressure Air Flow/Draft Loss Control Device

or, equivalently,

$$D_{(inch)} = \left[2.7\ \dot{w}_{oil(gph)}\right]^{0.4}$$

The optimum choke diameter for the 1 ml/s (gph) burner is 0.042 m (1.65 inch). Both the choke diameter and the swirl angle requirements were determined experimentally, and the combination of these specifications result in minimum NO concentrations with very low carbonaceous pollutant levels at quite efficient operating conditions ($CO_2 \approx 13.5$ percent, SR≈1.10). The 1 ml/s (gph) optimized head configuration has been fitted to both a 0.076 m (3-inch) and a 0.102 m (4-inch) diameter blast tube with satisfactory results. The anticipated higher efficiency of the furnace system will stem primarily from the capability of the optimized burner head to operate reliably at 13.5 percent CO_2 (with low pollutant emissions).

Experiments have shown that a nonretention (conventional) type head is lower in NO_x emissions than the flame-retention type. The turbulent mixing (well-stirred reactor) within the retention cone promotes very rapid combustion with no heat being removed. At near-stoichiometric conditions (desirable for higher efficiency), this mixing produces quite high adiabatic peak flame temperatures and enhances production of high NO_x concentrations (Ref. 5). Therefore, the optimized burner head is of the nonretention, "plug-flow" type design.

The combustion air flow/draft loss control device (Fig. 34) is intended to provide improvements in both operating efficiency and combustion roughness. The device is a weighted flap that drops to a closed position when the burner unit (combustion air fan) is deactivated. Such closing of the combustion air flow passage eliminates the natural convection air flow through the furnace during the standby mode and thereby reduces standby thermal losses (~1 to 4 percent). Improvement in combustion roughness is expected to result from the air flow restriction device being located on the discharge side of the air fan. Such location allows an unrestricted air inlet and increases the static pressure within the fan chamber. The higher operating pressure should reduce the susceptibility of the air fan to

"stalling" (resulting in fan/flame coupled oscillations), and thereby improving the rough combustion characteristics. The air fan output pressure of the 1 ml/s (gph) optimized burner is approximately 310 N/m^2 (1.25 inch WC) at zero flowrate (dead-headed), typical of units capable of up to three times the firing rate.

The primary burner control unit will use a solid-state, interrupted-spark ignition (on-for-start) device with ultraviolet (UV) flame detection cell. Specification of solid state and interrupted spark reduce electrical power requirements by about 100 watts ($\sim$330 Btu/hr). However, considering the 35 percent efficiency of the electrical power generation loop, the net overall energy reduction is about 1000 Btu/hr or approximately 1 percent of the furnace output. An ultraviolet flame detection cell is specified because the optimized burner flames, under certain conditions, have had low luminosity (yellow spectrum), making applicability of CdS cells questionable. A potential problem arising from the sensitivity of the ultraviolet cell to emission from ignition sparks can be avoided by providing a shorter spark-on duration ($\sim$20 seconds) than safety control decision time (30 to 45 seconds). Such an early termination of the ignition spark will allow the ultraviolet cell to correctly evaluate and verify a "flame-on" condition.

Operational Efficiency Gains

Operational efficiency gains are expected to result from higher cycle-averaged heat recovery from the furnace flue gases and from reduction of typical energy losses.

Both conceptual prototype furnaces have burner/firebox designs optimized to operate much closer to stoichiometric conditions (SR$\approx$1.10 to 1.15) than either the average of the installed existing furnace population (SR$\approx$1.9) or the typical current commerical practice ($1.2 \leq SR \leq 1.6$). The effect of stoichiometric ratio on net cycle-averaged thermal efficiency of a common 1 ml/s (gph) residential furnace fired with several different burner heads has been illustrated in Fig. 9. Considering the midrange of the several operating lines in Fig. 9 to be representative of typical furnace behavior, net thermal efficiency may be estimated to

increase by approximately 4 percent to 13 percent if the stoichiometric ratio is decreased to 1.15 from 1.4 and 1.9, respectively. For the most part, these efficiency gains are achieved because the mass flowrate of flue gases is reduced as stoichiometric ratio is lowered, so that less sensible heat is convected up the flue. This would be the only reason for increased efficiency if the flue gas temperature were to remain invariant as stoichiometric ratio is changed. However, the reduced flue gas flowrate and altered flame combustion characteristics also alter the heat transfer conditions so that flue gas temperatures are not likely to stay constant. Normally, flue gas temperatures are somewhat lower at lower stoichiometric ratios, which contributes a portion of the actual efficiency gain. The range of operating line slopes experienced with different burner heads, Fig. 9, was probably caused by differing flame pattern influences on heat exchanger effectiveness. Further efficiency increases are being sought by designing the prototype units to minimize flue gas temperature within the firebox draft, condensation, and corrosion constraints discussed in Section IV.

Another substantial contributor to the convection of energy up the flue is the use of heated and humidified living space air for burner combustion air and for furnace barometric pressure control draft air (Fig. 35a). Energy deposited in room air used in these ways has been shown (Ref. 12) to be on the order of 10 percent of the residential heating load. These losses can be eliminated by supplying outdoor ambient air to the burner and to the barometric pressure control device. Such an air supply is known as a sealed air system; a typical installation is shown schematically in Fig. 35b.

Use of a sealed-air system to supply barometric control air should reduce the flue heat losses, on the average, by an amount equivalent to raising the furnace efficiency by about 8 percent. No operational problems are introduced, with the possible exception that very cold barometric control air might result in some temporary local condensation of combustion gas moisture in the flue system. Insulation of the sealed air system, up to and including the plenum around the barometric control device, will prevent convective heat transfer from the living space air and maximize the thermal benefits of using the sealed air system.

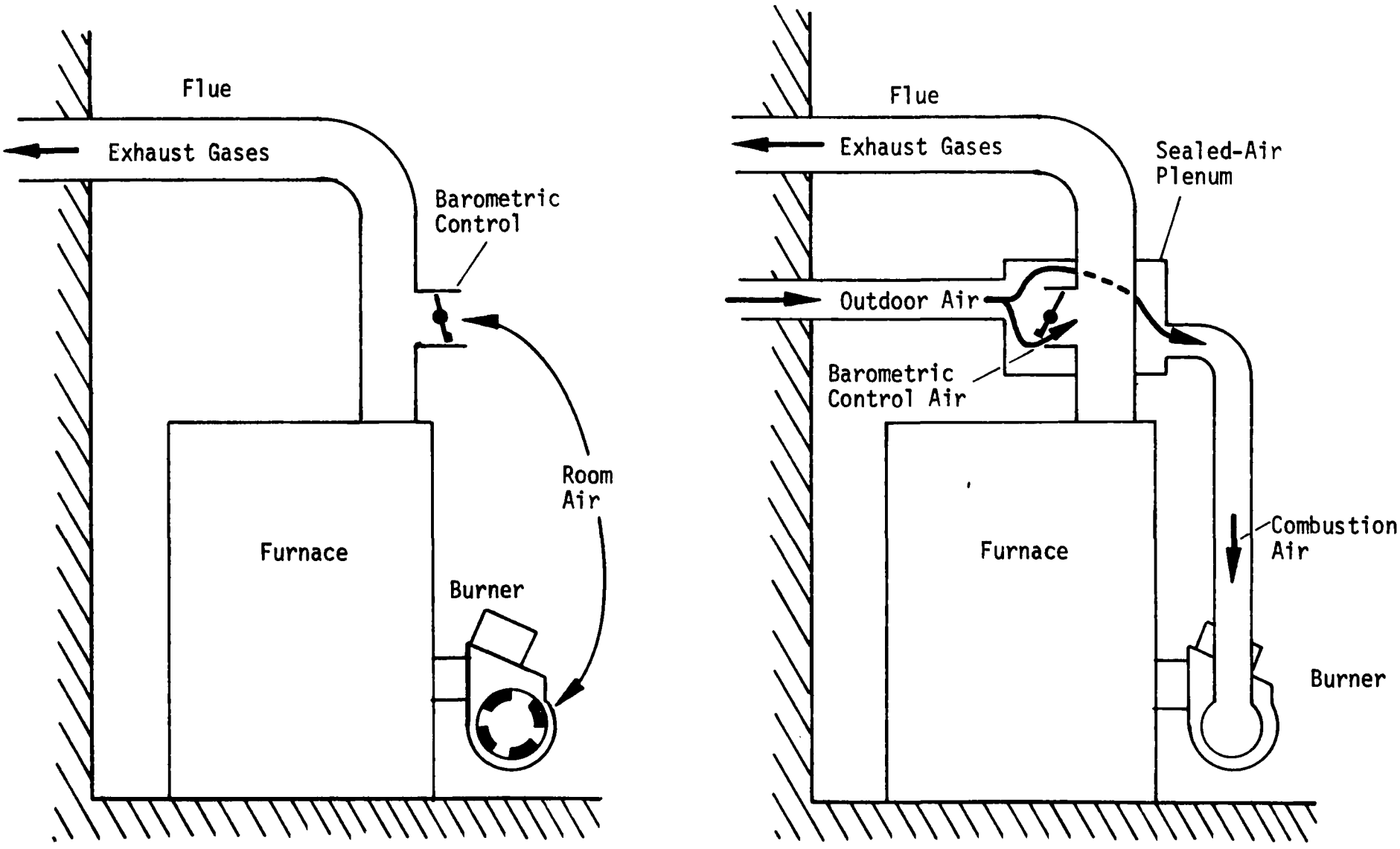

Figure 35. Conventional and Sealed-Air Furnace Installations

The impact on fuel utilization efficiency of using living space air for burner combustion air is less than 1/4 that of using such air for barometric control air. A lower average flowrate and the opportunity to recover the extra input heat in the heat exchanger contribute to lessening the impact. Nontheless, the 2-percent or so potential fuel saving is worth the little extra effort to include combustion air in the sealed air system, as less incentive exists for insulating the combustion air duct from being heated on its passage through the living space. In fact, in very cold weather, the outdoor air needs to be so tempered in order to avoid ignition problems and excessive start spikes of CO, UHC, and smoke. The combustion air will also be sealed and filtered to reduce effects of dust, lint, animal hair, etc., and maintain consistent combustion air-fan performance at the near-stoichiometric burner operating conditions. In addition to providing a modest heating system efficiency gain, an enclosed combustion air system also beneficially reduces odors, combustion noise, and combustion fan noise in the vicinity of the furnace.

Still another contributor to the convection of heat up the flue is the cooling of furnace components by a natural draft flow of air through the burner, firebox, etc., during the burner-off or standby period. Losses up to about 4 percent of the residential heat load may be caused by this phenomenon. In the conceptual prototype designs, the sealed combustion air systems should partially inhibit the natural draft flow through the system, but the draft loss control flap in the burner is intended to completely prevent it.

Combined, the foregoing reductions in flue heat losses sum to the order of 14- to 24-percent increase in cycle-averaged fuel utilization efficiency for the residential heating system. While the sealed air devices can affect substantial overall fuel economies, such devices do not contribute to increased thermal efficiency of the furance unit *per se*. Thus, reducing the stoichiometric ratio and stopping standby natural draft losses should raise the cycle-averaged furnace efficiency by between 6 and 16 percent, depending upon the magnitude of the stoichiometric ratio change.

Additional sources of heat losses which these conceptual prototype designs do not attempt to alleviate are:

1. The remaining sensible and latent heat in the flue gases (each on the order of 8 percent). Much larger heat exchangers, corrosion-resistant heat exchangers and flues, and the provision for condensate disposal and induced-draft, hot-gas fans would be required to achieve recovery of these losses. Such furnace attributes are considered not to be cost-competitive at this time.

2. Convention and radiation losses from the external cabinet of the furnaces (as much as 2 percent for warm air and 3-1/2 percent for hydronic units). Although such losses are from a furnace unit efficiency view-point, they commonly contribute to heating the living space and are not really residential heating system losses. The reduction of these losses is predominantly an insulation problem involving economic tradeoff of better furnace housing insulation and perhaps slightly better fuel economy against increased initial cost and attendant loss of competitiveness.

3. Transient start-up and shutdown losses, such as a starting puff of UHC, the dribble of oil from the spray nozzle after the burner is turned off, a flue gas temperature spike before the warm air fan is turned on. The aggregate of these losses is well below 1 percent; they are normally minimized because of emissions and good design standpoints rather than for the sake of efficiency.

Combustion Chambers

The combustion chamber is the primary component in the path of the combustion gases for controlling pollutant emissions. Therefore, extensive burner/combustor optimization experiments were conducted with the 1 ml/s (gph) optimized burner to provide information for favorable combustion chamber configurations that allow the burner to operate very near stoichiometric (SR$\approx$1.10, $CO_2\approx$13.5 percent) with minimum pollutant emissions and smooth combustion (Section IV).

A simplified summary of the results of cyclical (10 minutes on/20 minutes off) burner/chamber optimization experiments has been given in Table 8. From these data, it was concluded that:

1. Meeting the NO emission goal is more difficult than meeting the other emissions goals.
2. Cooled combustion chambers are required in order to begin to approach the NO goal of $\leq$0.5 g/kg fuel. (The combustion chamber is then the first, or primary, heat exchanger.)
3. Combustion chamber diameters of 0.25 m (10 inches) or larger are also required to reach the NO goal.
4. Combustor lengths in excess of 0.5 m (20 inches) are then required in order to ensure completion of combustion before reactions are quenched in the secondary heat exchanger.
5. Either the tunnel- or side-fired configurations can be used.

At this point, the different cooling media force different design approaches to be taken for the warm-air and hydronic units.

CONCEPTUAL DESIGN STUDY: WARM-AIR FURNACE

The warm-air-furnace design study commenced with evaluation of combustor cooling methods. A water-cooled combustor/warm-air heat exchanger combination was considered for the favorable heat transfer characteristics of the water coolant. However, the fabrication costs for a boiler-code-certified pressure vessel combined with a complicated combustion-gas-to-warm-air heat exchanger were considered to be prohibitive in the residential-size, warm-air-furnace market. Therefore, a finned, air-cooled combustor configuration that could more or less simulate the heating and cooling charcteristics of a water-cooled chamber was conceived. A preliminary layout drawing of such a combustor, combined with a commercial warm-air-furnace heat exchanger, is shown in Fig. 36, where the combustor is side-fired,

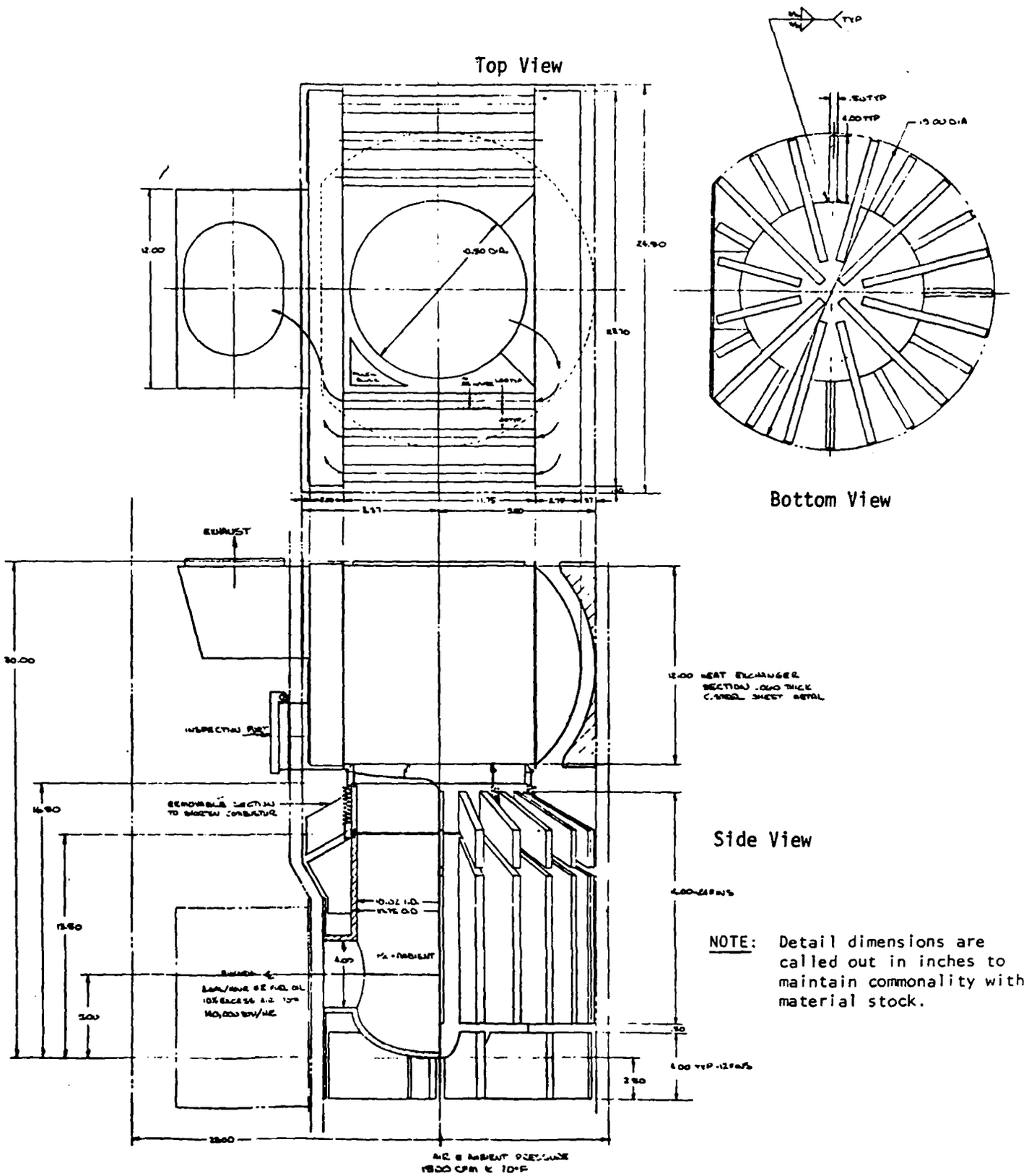

Figure 36. Preliminary Layout Drawing of the Air-Cooled-Combustor, Warm-Air Furnace

constructed from standard 0.25 m (10 inch) pipe with a standard pipe cap, and is rather heavily finned to provide both substantial convective cooling and a large heat sink.

Rather than this combustor design concept for the prototype warm air furnace being simply accepted, a finned research combustor was fabricated and tested to verify the pollutant emissions and performance expectations of a well-finned, air-cooled combustor. This additional experimental effort and its results are documented in Appendix F. The results are seen to be very promising, with the carbonaceous pollutants well under control [L = 0.75 m (30inches)] at design operating conditions (10- to 15-percent excess air), and the NO emissions ($\sim$ 0.6 g/kg) approaching the target value of 0.5 g/kg. The total heat extracted from the finned section [8200 J/sec (28,000 Btu/hr)] was more than the 7300 J/sec (25,000 Btu/hr) limit established by the earlier water-cooled experiments wherein no emissions or stability problems were encountered. The differences in heat transfer profiles between the cooling methods were probably responsible for both the differences in heat extraction and in NO emission between the two types of cooled chambers.

A heat transfer analysis of the combustor/heat exchanger combination shown in Fig. 36, was conducted to verify design estimates; the results are presented in Table 12. The analysis estimated a heat extraction rate from the combustor of 6260 J/sec (21,400 Btu/hr) at 0.707 m^3/s (1500 cfm) coolant flow with the 0.076 m (3 inch) fin extension section. The experimental finned combustor, without the extended fins, removed 8200 J/sec (28,000 But/hr) at 1.18 m^3/s (2500 cfm) air flowrate. Use of the Dittus-Boelter equation to account for the differences in surface areas and coolant flow enables a calculated experimental heat extraction value for the lower air flowrate (0.707 m^3/s)of 6500 J/sec (22,200 Btu/hr) to be derived, which is in good agreement with both the design estimate and the heat transfer analysis ($\sim$3.5 percent).

Although the total heat removal was well within design expectations, some rearrangement of the fins and/or a larger combustor diameter was believed to be appropriate for the prototype, so as to ensure meeting the 0.5 g/kg NO requirement.

TABLE 12. SUMMARY OF FINNED COMBUSTOR/HEAT EXCHANGER OPERATING CONDITIONS HEAT TRANSFER ANALYSIS

Finned Combustor Section	
T_{air} in/out, ^{o}C (^{o}F)	21/28 (70/83)
T_{gas} in/out, ^{o}C (^{o}F)	1871/1578 (3400/2872)
q, J/sec (Btu/sec, Btu/hr)	6260 (5.93/21,400)
h_g, W/m^2-K (Btu/$in.^2$-sec-R)	12.9 (0.440×10^{-5})
h_c, W/m^2-K (Btu/$in.^2$-sec-R	24.9 (0.847×10^{-5})
$\bar{T}_{WG}$, ^{o}C (^{o}F)	135 (275)
A_{sg}, m^2 ($in.^2$)	.309 (480.1)
A_{sc}, m^2 ($in.^2$)	2.311 (3583)
Oil Flow, ml/sec (gph)	1.05 (1.0)
$\dot{W}_{gas}$, kg/sec (lb/sec)	0.015 (0.035)
$\dot{W}_{air}$, kg/sec (lb/sec)	0.852 (1.88)
A_g, m^2 ($in.^2$)	0.050 (78.4)
A_c, m^2 ($in.^2$)	0.092 (143.3)
ΔP_a, Pa (psi)	81.3 (0.0118)
ΔP_g, Pa (psi)	0.50 (7.21×10^{-5})
Heat Exchanger Section	
T_{air} in/out, ^{o}C (^{o}F)	28/62 (83/144)
T_{gas} in/out, ^{o}C (^{o}F)	1578/224 (2872/435)
q, J/sec (Btu/sec, Btu/hr)	28,900 (27.4/98,650)
h_g, W/m^2-K (Btu/$in.^2$-sec-R)	28.8 (0.978×10^{-5})
h_c, W/m^2-K (Btu/$in.^2$-sec-R)	71.5 (2.43×10^{-5})
T_{WG}, ^{o}C(^{o}F)	232 (450)
A_{sg}, m^2 ($in.^2$)	1.713 (2656)
A_{sc}, m^2 ($in.^2$)	1.713 (2656)
A_g, m^2 ($in.^2$)	0.040 (63.4)
A_c, m^2 ($in.^2$)	0.112 (174.4)
ΔP_a, Pa (psi)	95.8 (0.0139)
ΔP_g, Pa (psi)	0.50 (7.31×10^{-5})

Preliminary Warm-Air-Furnace Design

The preliminary conceptual warm-air furnace design is illustrated in Fig. 37. This design is based on modifying an existing, commercially purchased warm-air furnace* to incorporate the larger-diameter, forced-convection, air-cooled combustion chamber matched to the 1 ml/s (gph) optimum burner and sealed air system.

The combustion chamber for the prototype warm-air furnace is a carefully optimized, side-fired, cool-wall configuration. Based on the optimization experiments, the combustor section is provided with 24 radial fins, increasing the combustor outside surface area approximately 6-1/2 times, to remove approximately 20 to 25 percent of the total furnace heat output. The primary purpose of cooling the combustion chamber is to reduce the peak flame temperatures and thus minimize formation of NO. However, it has been determined experimentally that removal of more than 25 percent of the heat from the combustion zone leads to premature quenching of the chemical reactions, and incomplete combustion products (CO, UHC, and smoke) in the flue gases.

The combustion chamber inside wall temperature is expected to average about 230 to 260 C (450 to 500 F) even though an inner, hot-wall retort will not be used. This lower-than-usual metal wall temperature results from using a relatively large 0.30 m (12 inch) firebox inside diameter (ID), which should be less susceptible to direct flame impingement on the wall, and from using a quite massive firebox construction. For the prototype design, the combustion chamber wall consists of a standard 12-inch pipe cap welded to an eccentric 12-inch to 10-inch pipe reducer, the small end of which is mated to the existing secondary heat exchanger of the furnace. The eccentric reducer configuration is expected to be beneficial in several ways. The rear-biased eccentricity allows a packaging advantage by allowing the burner to sit closer to the unit centerline. The

*A Lennox Model 011-140 furnace is the unit selected.

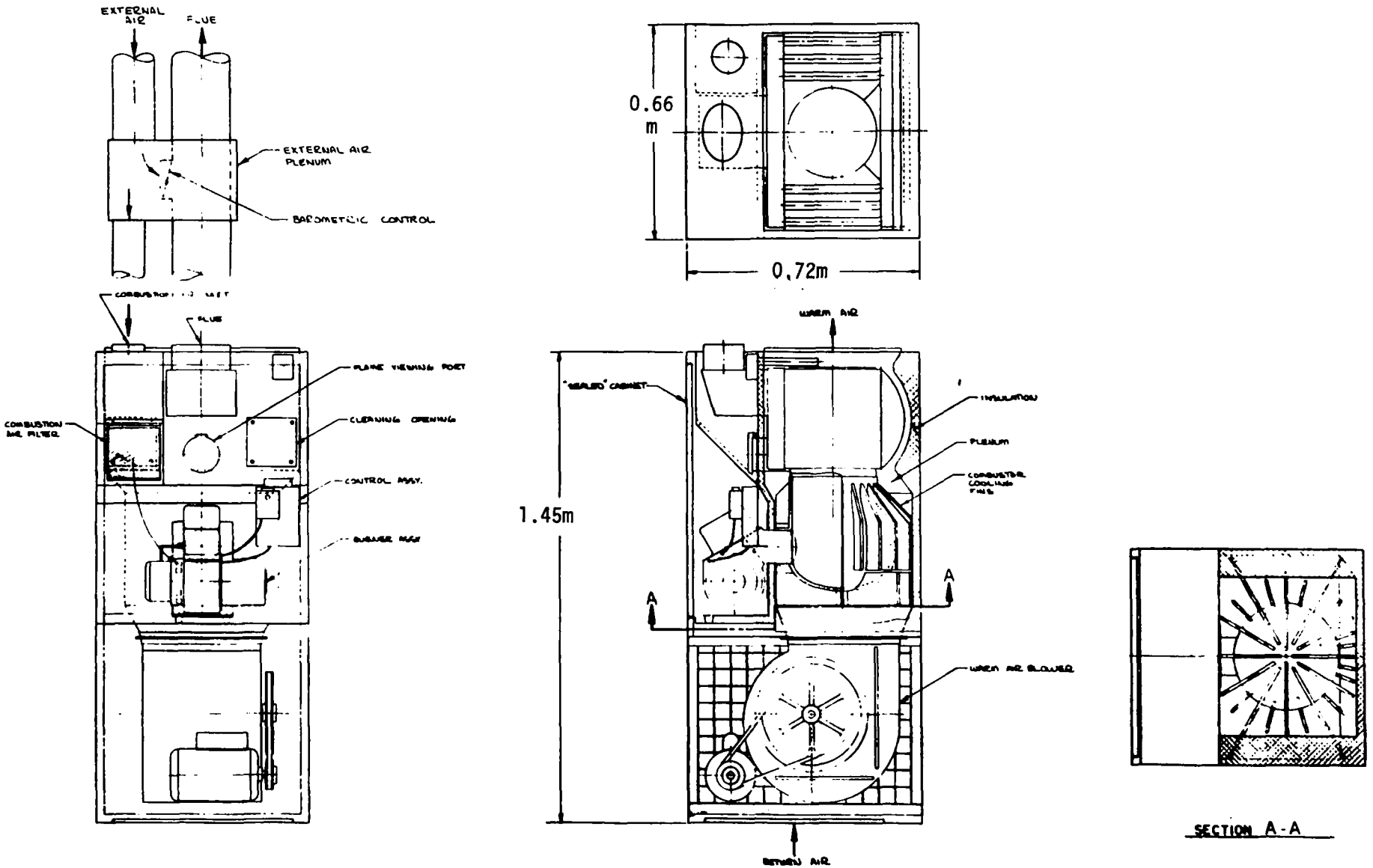

Figure 37. Layout Drawing of the Finned-Combustion, Prototype Warm-Air-Furnace Unit With a Sealed Air System

forward-biased combustor exit induces combustion gases back along the cooled walls to the burner area enhancing a combustion gas recirculation (CGR) effect to help ensure lower peak-flame temperatures (i.e., lower NO_x). Also, the reduction in flow area caused by the reduction from 12 to 10 inches accelerates the combustion gas flow and promotes mixing of any remaining fuel species. The reduction in warm-air passage area on the side opposite could be a problem, because the air coolant flowrate is reduced there; additional fins have been added in that area that is likely to have the highest local wall temperature.

With the external fins welded to those firebox components, the combustion chamber assembly is expected to weigh on the order of 90 kg (200 pounds). This rather massive construction was intentionally adopted to accomplish two objectives other than to simply reject heat from the combustion zone. Both are related to the heat sink aspects of a massive chamber. First, a massive heat sink chamber can more readily approach uniform inside surface temperatures than can a lightweight, unlined metal chamber. This fact is important for avoiding excessive NO formation and wall erosion (or possibly burnout) at "hot-spots", and for avoiding smoke and UHC formation at "cold-spots".

The second objective is for the combustion chamber to retain most of its stored heat during burner-off times so that the firebox is considerably warmer at burner startup than is the usual warm-air-furnace practice. This objective arose from the observation that start-transient spike emissions of CO, smoke, and UHC were considerably lower with water-cooled than with uninsulated air-cooled combustors. In a very real sense, the massive, finned combustion chamber design represents a way to achieve beneficial effects found experimentally with water-cooled chambers.

The side-port orientation was chosen principally for its conventional packaging in "Hi-Boy" or "Low-Boy" flexibility. The opposing wall in the side-fire orientation, like the bias in the eccentric reducer, also helps to induce recirculation of some partially cooled combustion gases back into the air/oil mixing and combustion zone, aiding in maintaining flame zone temperature uniformity and combustion stability.

The prototype warm-air furnace will retain a conventional secondary heat exchanger for several reasons. The lowering of pollutant emissions is accomplished by the burner and combustion chamber, and modifications to the heat exchanger have very little effect on the composition of the flue gas. While increased thermal efficiency will be accomplished primarily by the ability of the optimized burner head to operate near stoichiometric conditions, the addition of the cooled combustion chamber supplements that gain by increasing the heat exchanger capacity by about 25 percent. Thus, the heat exchanger could be made smaller. However, since the heat exchanger accounts for only 20 to 30 percent of the total furnace volume, a significant reduction in heat exchanger size (with associated increase in cost) could result in only a nominal reduction in furnace unit size. Therefore, the Lennox heat exchanger section supplied with the stock furnace unit will be used in the construction of the prototype furnace.

Manufacturer Review. The layout drawing and an explanatory memorandum for the preliminary, conceptual, warm-air-furnace design were sent to engineering personnel at Lennox Industries for review and comment. The Lennox comments and recommendations were transmitted verbally to the authors during a June 10, 1975 visit to Lennox's main plant in Marshalltown, Iowa. The substance of discussions held that day are documented in this subsection.

Firebox. The massive, finned-steel firebox was viewed as being a technically viable approach, whose experimental test results should prove to be interesting. Reservations were expressed in two specific areas: metal temperature and weight. Some doubt was expressed as to whether the heat sink capacity of the firebox would be high enough to keep its average inside wall temperature anywhere near the 230 to 260 C (450 to 500 F) estimated by heat transfer calculations, and that a substantially higher-than-average temperature hot-spot opposite the side-fired burner port may be experienced.

An estimated firebox weight had not been included in the explanatory memorandum. Upon learning that it would be well in excess of 50 kg (110 pounds), Lennox personnel recommended that its weight be minimized, within the constraint of ensuring

acceptable pollutant emissions. Three areas of concern were indicated: shipping weight, supporting the extra weight within the cabinet, and extra bearing loads on floors of frame residences. The most serious of the three is the increased shipping weight; it would tend to reduce a manufacturer's competitiveness with increasing distance from his factory. Two illustrations were given. First, Lennox has converted from firebrick firebox linings to refractory fiber linings, largely to reduce shipping weights by approximately 11 to 14 kg (25 to 30 pounds). Second, Twentieth Century's warm-air furnace, featuring cast-iron fireboxes and cast-iron heat exchangers, weighs on the order of 180 kg (400 pounds) more than competing warm-air furnaces and, as a direct result, is essentially limited to a one-city market.

Burner. Having studied Ref. 5, which details the development and performance of the optimized burner, Lennox personnel apparently feel comfortable with the potential applicability of the technology supporting this burner. However, they did make comments and suggestions concerning several aspects of its application in the preliminary conceptual design.

The gravity-actuated flap within the burner to eliminate draft air flow during standby was the item of most concern. The group generally agreed that the flap would substantially change the uniformity of air flow distribution within the blast tube, possibly degrading the ability of the burner to operate at low stoichiometric ratios with acceptably low smoke and UHC emissions. Reliability of flap operation was questioned. In fact, it was stated that such an alteration of the burner may abrogate its UL listing, and that recommending the use of unlisted equipment entails substantial legal liabilities for manufacturers. Gaining a UL listing is not very likely unless a positive flap actuator, such as a solenoid, and an electrical sensor, to confirm the actuator is open, are provided. A preferred way of eliminating draft air, particularly with the sealed combustion air supply, is to place a low-cost solenoid-actuated, butterfly valve in the combustion air supply line to the burner.

Some burner problems may develop as a result of eliminating the standby draft air flow. Oil spray nozzles are commonly coated with a varnish-like residue if they are heated above about 95 C (200 F). In conventional equipment, nozzles may be heated convectively by backflow of combustion gases into a furnace room with negative ambient pressure [room drafts as low as -25 N/m^2 (-0.1 inch WC) are not uncommon], radiantly by "viewing" high temperature firebox refractory surfaces, or both. If a backflow is not present, an inflow of draft air normally provides enough convective cooling to offset the radiant heating. Positive cut-off of the burner air supply duct would eliminate the backflow problem but accentuate the radiant heating problem. The low-temperature steel firebox should reduce the magnitude of this latter problem, which needs to be estimated and checked experimentally. A related problem is the possibility of overheating the flame detector cell and the high-voltage ignition components, none of which should be allowed to reach temperatures above 52 C (125 F). Radiant heat transfer from the firebox to these components is not expected to be much of a problem because they have a rather limited exposure to the combustion chamber through the burner choke plate. However, if the objective of maintaining a warm firebox during standby is achieved, heat conduction to these temperature-sensitive components may be a significant problem. Monitoring of burner component temperatures during prototype furnace testing was recommended.

Another potential overheating problem arises from use of the burner vestibule as a plenum for the sealed combustion air supply. The vestibule cover, a part of the external furnace cabinet, is louvered at both the bottom and the top. Normally, considerably more furnace-room air circulates by natural draft through the vestibule than is drawn into the burner as combustion air; this flow cools the vestibule. It was doubted if the combustion air alone would provide sufficient vestibule cooling. Three problem areas should be anticipated: overheating burner components, overheating electrical controls mounted in the vestibule, and overheating painted cabinet panels. Warm-air-furnace codes and standards specify maximum temperature for electrical wiring of 60 C (140 F). While higher temperature wiring could be used, at some additional expense, it is unlikely that

anything but 60 C (140 F) wiring would be used for field installation, so this temperature limit should be maintained. It was recommended that vestibule temperatures be measured during prototype furnace testing and, if they are too high, that vestibule louvers having a separate sealed air duct to the burner again be used.

Ultraviolet flame detector cells are suitable, although more expensive than CdS cells, largely because the ultraviolet cells are not produced in large quantities. Concerning the criticality of timing the cut-off of the spark igniter and the flame-on decision point, it was noted that Honeywell has anultraviolet flame detector system whose circuit is integrated with the ignition system such that the circuit evaluates the flame intermittently (60 Hz), between sparks..

Several miscellaneous comments regarding burners may be helpful. Rocketdyne personnel were reminded that in selecting combustion air fan characteristics, ambient air density varies with altitude. For example, at the same furnace firing rate and excess air condition, approximately 10-percent greater volumetric flowrate of air is required in Denver than in Des Moines. Another cautionary note: the closer a burner is operated to stoichiometric conditions (high CO_2), the more sensitive it is to unintentional in-leakage of air. That is, maintaining seals, closing peep-holes, etc., becomes more critical.

Furnace Evaluation Test Procedures. An appropriate experimental warm-air-furnace performance evaluation set-up, minimum instrumentation requirements, and test procedures are delineated in ANSI Z91.1; safety codes are given in UL 727 for warm-air furnaces and UL 296 for oil burners. There is also a new standard in preparation, ANSI Z91.2, for oil burners smaller than 6.7 ml/s (7 gph).

Lennox is currently performing extensive experimental laboratory characterization of several stock furances. The company is using a set-up similar to that specified in ANSI Z91.1, but is making substantially more than the minimum measurements. As an example, ambient air is supplied to the burner, for both combustion and draft air, through a forced-draft metering section that has a draft-balancing system for ensuring zero-draft at the burner inlet. Thus draft-air

thermal losses can be determined as functions of other variables, such as cycle frequency, fractional burner-on-time, and firing rate. The first furnace tested, fired at 1 ml/s (gph), was found to have about 1-1/2-percent draft-air loss during 8 minutes on/4 minutes off cycles; this condition increased to about 2-1/2 percent during 4 minutes on/8 minutes off cycles. Rocketdyne personnel were privileged to examine the Lennox test setup. (Several of their ideas are reflected in the prototype furnace test assembly to be used in Phase II of this program.)

Compact Heat Exchangers and Achieving Higher Efficiencies. Since the prototype furance design is basically a set of modifications to a Lennox 011 furnace, which entails essentially no impact on the secondary heat exchanger, Lennox remarks on this component were confined to explanations of potential hot spots and a breif discussion of effective ways of mating the heavy-walled, combustion-chamber section to the thin-walled, 17-gage heat exchanger. Essentially, it was agreed that a simple nonwelded mechanical connection could be used in a prototype unit, even though this might be unacceptable in production runs because of high cycle-fatigue or long-term leakage potentials.

Although the parallel-plate, clam-shell, secondary heat exchanger used in the Lennox 011 furnaces is relatively compact, Lennox is considering using a modified annular type secondary heat exchanger surrounding the combustion chamber in the Lennox new furnace series. Mainly, this design change reduces the sheet metal welding cost and results in a less-expensive furnace. Lennox periodically examines more-compact, higher-effectivity heat exchanger concepts, but commonly finds that such concepts either do not meet their proponents' claims, simply cannot compete economically, or both. Lennox expects an industry response to limited supplies and higher costs of fuels will be to abandon industry's reliance on conventional chimney-type flues. Exhausting the flue gases through a short, small-diameter, corrosion-resistant vent through the outside wall of the residence would require the use of a pressurized combustor but would permit extraction of most of the sensible heat of the exhaust gas, would obviate the need for barometric control air, and would virtually eliminate draft-air losses. A conventional heat

exchanger for such a unit would need at least two to three times the area of present heat exchangers, so that higher fabrication and shipping weight costs might then support the use of compact heat exchanger designs.

Prototype Design Modifications. In response to the manufacturer's comments and suggestions, some aspects of the preliminary prototype design were reassessed and modifications made.

Firebox. Cyclical furnace performance analyses were undertaken with the WAFURN warm-air-furnace thermal analysis computer program to assess the thermal effects of reducing combustion-chamber and cooling-fin thicknesses. It was determined that, from a zero-dimensional, heat-sink standpoint, a considerably lighter assembly could provide the desired average thermal behavior. It was also decided that both the firebox wall and fin thicknesses could be reduced to 0.0063 m (1/4 inch), whereupon the assembly weight would be about 49 kg (108 pounds).* It was thought that even thinner fins would exhibit significant temperature gradients and force the firebox to deviate substantially from an ideal heat sink. This may prove to be no problem, in which case even greater weight reductions can be considered for the final design.

Burner. A decision was made to eliminate the draft-air control flap from inside the burner. The intended function of the flap will be performed by a solenoid-actuated butterfly valve in the sealed combustion air supply duct.

Concerning the possible overheating of burner components, it was decided to provide insulation between the burner and the firebox to limit conductive heating. Excessive radiant heating of the spray nozzle, flame detector, and ignition

*This weight is substantially below the originally projected 90 kg (200 pounds). However, it is based upon using Schedule (Sch) 20 pipe components. Attempts to locate Sch 20 caps and eccentric reducers have so far been fruitless. If none is found, the prototype furnace will be built with standard Sch 40 components, and the finned firebox will weigh about 57 kg (126 pounds).

system will be watched for during prototype furnace evaluation testing. Similarly, possible problems from too high temperatures in the vestibule will be monitored. One change will be made in the design to better cool the electrical controls and burner motor: the combustion air inlet to the vestibule will be removed from the left to the right side, where the controls are located.

CONCEPTUAL DESIGN STUDY: HYDRONIC BOILER

Preliminary Hydronic Unit Design

The preliminary conceptual hydronic furnace design is illustrated in Fig. 38. This design is based on substantially all new construction, principally because no commercially available unit was identified as being readily adaptable to the larger-diameter, water-cooled combustion chamber for the optimum burner.

Based on the burner/firebox matching experimental results, a horizontal, tunnel-fired, water-cooled, combustion-chamber configuration was selected. The tunnel-fired configuration offers structural, packaging, and pollutant emissions advantages over the side-fired arrangement. The straight-through, tunnel-fired chamber can be welded directly to the front and rear boiler tube sheets, contributing to the pressure vessel strength. Analysis of a side-fired arrangement indicated such an arrangement would increase installation volume by nearly 50 percent because it needed an additional 0.2 m (8 inches) of width for burner placement as well as a further additional 0.15 to 0.2 m (6 to 8 inches) to allow room for servicing the burner. By contrast, the tunnel-fired arrangement employs the space below the flue manifold for the burner and provides all required access for servicing, and combustor and heat exchanger cleaning from the front of the unit.

The firebox is designed to remove between 20 and 25 percent of the total heat output from the combustion gases before they enter an internally finned fire-tube, secondary, heat exchanger section. It has been determined experimentally that

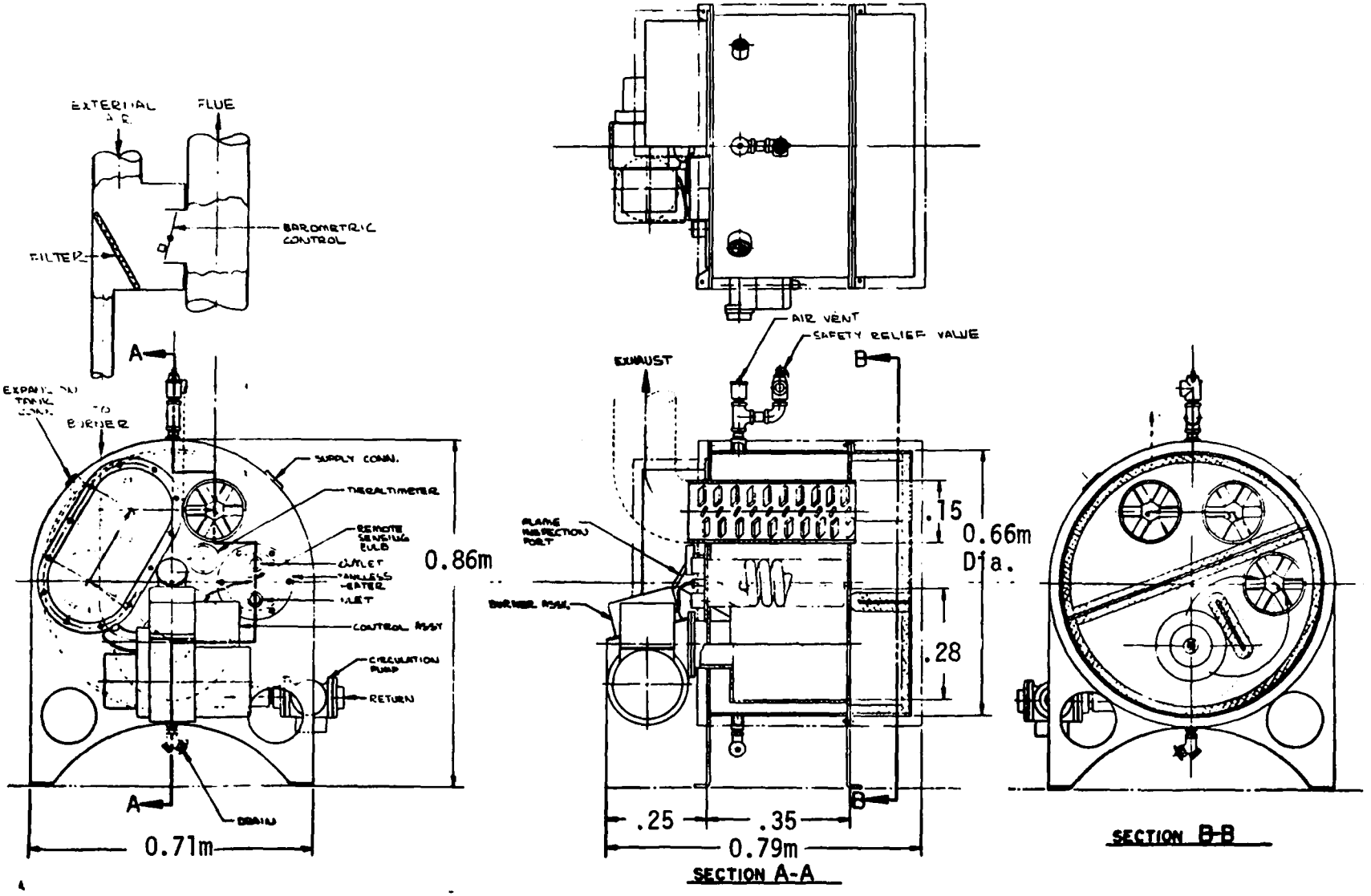

Figure 38. Layout Drawing of the Horizontal-Pass, Prototype Hydronic-Furnace With a Sealed Air System

removal of more than 25 percent of the heat from the combustion zone leads to premature quenching of the combustion reactions and produces high concentrations of CO, UHC, and smoke. That fraction of the heat can be extracted in about 0.3 m, (12 inches), so the water-cooled combustion chamber is only 0.28 m (11 inches) long. Combustion reactions are not expected to be complete by then; the flow-reversing firebox-to-secondary-heat-exchanger manifold is considered to be part of the primary combustion volume. It is partially insulated to lower the heat extraction rate and avoid further quenching of the combustion process.

Close confinement of the burner flame can also lead to premature quenching of part of the combustibles (fuel contacting the cooled walls). Additionally, flame-front instabilities (combustion roughness) can be caused by too-high bulk gas velocities in small-diameter chambers. Therefore, and in conformance with the experimental burner/firebox matching results, a relatively large 0.28 m (11 inch) ID, tunnel-fired, combustion chamber is proposed for the optimum hydronic unit. The combination of the optimized burner, the large-diameter combustion chamber, the controlled heat extraction, and a combustion-chamber, discharge, choke plate is expected to prevent the occurrence of combustion roughness commonly experienced with nonretention head burners in wet-base combustors.

The chamber discharge choke plate is shown in Fig. 38 simply as a 0.178 m (7 inch) hole in the rear tube sheet. The purpose of the plate is to promote recirculation of the combustion gases back along the cooled walls to the burner insertion region. Ingestion of these partially cooled gases into the initial flame region aids in stabilizing the flame and, adding a mild diluent slightly reduces peak flame temperatures, thereby aiding in the reduction of NO_x emission concentrations. The choke ring also will accelerate the gases leaving the chamber, promoting better mixing and consumption of residual unburned fuel species.

The secondary heat exchanger is a multiple-pass, horizontal, firetube configuration (see Fig. 38). Three series-connected firetubes are internally finned, 0.15 m (6 inch) diameter pipes* with inner (combustion-gas-side) surface area

*These pipes are manufactured commercially by the Bock Corporation, Madison, Wisoncin, and are known by the trade name "Turboflue".

3-1/2 times greater than the outer (water-side) surface area for improved gas-side heat transfer. Successive passes are arranged in an ascending direction to aid internal combustion gas draft and provide more favorable conditions for natural circulation of the water during burner-on. The water temperatures will be hotter on the left side (Fig. 38, front view) and induce a clockwise circulation pattern. The input of return water through the circulation pump is also biased in a clockwise direction to further assist this circulation pattern.

The tankless coil will carry a 3-1/2 gpm (2.2×10^{-5} m^3/s) rating. The water temperature gradients within the tank are not expected to be significant during the burner-off standby mode. The central height location of the coil is, therefore, not foreseen to be a disadvantage as compared to being located at the top of the boiler. During the burner-on mode, the clockwise circulation of the heated water places the tankless coil immediately downstream of the last heat exchanger element, providing very hot water to the coil. The location of the coil also provides some simplification of the firetube cross-manifolding. The water temperature sensing element is mounted on the tankless coil flange; this location was chosen because it is felt important to monitor closely the temperature of the water that the inhabitants of the dwelling may contact directly.

The baffling within the rear cover is intended to direct the combustion gas flow so that the full volume of the reduced heat transfer zone is used to complete combustion before the gases are cooled rapidly in the firetubes. The rear cover is designed to be removed with only 2 inches of rear clearance required and with all fasteners accessible from the front. The bolt pattern of the rear cover can be indexed to prevent misaligned assembly during manufacturing or servicing. Rear-cover removal is required only if repair of the pyroflex lining is necessary. All other internal servicing can be done through the front of the furnace.

All water ports are located at their respective preferred locations. The inlet port enters tangentially at the bottom to assist the clockwise water circulation. The air vent is located at the very top of the tank for optimum air collection, and the residential heating water outlet is located immediately downstream of the last heat exchanger element.

Manufacturer Review. The layout drawing and explanatory memorandum for the preliminary conceptual hydronic furnace design were sent to the director of engineering of the Burnham Corporation for review and comment. Rocketdyne personnel then visited Burnham on June 9, 1975, to discuss their evaluation of the conceptual design.

Basically, the preliminary design was assessed as representing a buildable, workable hydronic unit. In fact, in 1973 Burnham investigated a hydronic boiler having many of the same general features. Rocketdyne personnel were given prints of layout drawings showing to be very similar: vertical front and rear tube sheets; front-mounted burner, tunnel-fired into a water-cooled horizontal combustion chamber; insulated 180-degree return manifold to a secondary heat exchanger section embodying horizontal fire-tubes; and combustor, heat exchanger, and tankless coil orientations to promote tangential water circulation in the boiler. The design was not developed further because it was found to offer no significant cost advantage over Burnham's existing dry-base, vertical-fire-tube, production steel boiler design. The ways in which the Rocketdyne conceptual design differs from the Burnham preliminary design constituted the main points of discussion. The most significant difference is the use of series-connected Turboflue sections for the secondary heat exchanger. Although not familar with Turboflue *per se*, Burnham has evaluated many candidate extended-surface heat exchangers and has invariably found them not to be cost-competitive with simple cylindrical boiler tubes, particularly when the latter are fitted with replaceable internal turbulators. With installed 0.075 m (3 inch) diameter boiler tube costing $1 per linear foot, an increased heat transfer area can be obtained at much less expense by adding one or more boiler tubes than by using extended surface configurations. That this is a valid comment is borne out by Rocketdyne's estimate that the installed Turboflue heat exchanger would cost between 2 and 3 times that amount.

Concern was expressed that the Turboflue heat exchanger would have higher pressure drops than turbulated boiler tubes. Citing Bock Corporation estimates of vertical Turboflue draft losses was insufficient argument to dissuade Burnham from viewing

this as a probable problem. Further, the series connection involves three 180-degree flow reversals, which are also high-pressure-loss devices. Combining these, it was estimated that the firebox would probably be slightly pressurized and that a larger-size burner (costing an additional 10 to 15 dollars) would be needed to ensure delivery of adequate combustion air. (Subsequently, these expectations have been more or less confirmed by draft-loss calculations summarized in the following subsection.)

Another potential Turboflue problem is the avoiding of buildup of hard carbonaceous scales in the heat exchanger sections. Burnham experience calls for direct line-of-slight access for rodding-out (cleaning) such deposits; it is doubtful that the Turboflue sections could be effectively cleaned by either spiral brushing or water-mist washing suggested by the Turboflue manufacturer. For this reason, Burnham uses removable, disposable, boiler-tube turbulators.

The refractory linings in the aft flow-reversing manifolds are likely to be damaged during periodic rodding-out. The fact that the hot combustion gas flow is being turned against the surfaces most likely to be damaged, increases the chances of burning through the manifold housing, which would constitute a serious residential fire hazard. Provisions should be made for ready replacement of damaged linings.

It was also noted that, for the same reason, the flow-reversing manifolds must be positively sealed to prevent leakage. One method for achieving such a seal was suggested: construct a refractory fiber liner such that it has a peripheral compressed flange serving as a gasket between two bolted metal flanges.

For the foregoing reasons, the aft reversing manifolds might better be built as separate units than combined in a single metal housing as shown in Fig. 38.

Some comments concerned construction methods. Shearing steel plates rather than cutting or burning them is less expensive; therefore, square or rectangular tube sheets are preferable to circular or circular-derivative sheets such as those

shown in the preliminary conceptual design. Uncooled protuberances into the high temperature combustion gases will sooner or later be burned off. Thus, forming a combustor discharge choke plate as an uncooled section of the aft tube sheet would be highly unsatisfactory. A bolt-on refractory metal or ceramic choke plate is preferable. Extended, uncooled ends of firetubes must be kept to the minimum length needed for welding them to the tube sheets.

Finally, it was noted that building the firebox as sketched in Fig. 38 with a water-cooled, small-diameter, burner insertion tube, is more costly and both more difficult to weld and to repair than would be a single cylinder through both tube sheets. However, the more complicated design provides cooling for the burner end of the chamber, providing an important contribution to flame-zone cooling and minimum NO formation.

Prototype Design Modifications. The manufacturer's assessments of the warm-air and hydronic, preliminary, conceptual designs were discussed with the EPA Project Officer immediately following their communication to Rocketdyne personnel. In consideration of those assessments, the estimated relative difficulty in effecting recommended (and accepted) modifications, the relative population of warm-air and hydronic units, their production rates, etc., a decision was made to build and test a prototype warm-air furnace rather than a hydronic prototype. As a result, modification of the preliminary hydronic conceptual design to a producible prototype design became an academic exercise that did not extend beyond the decision stage.

In response to Burnham's concern about combustion-gas pressure drop or draft losses, a complete draft loss analysis was performed. Component pressure drops were calculated for operation at 1 ml/s (gph) firing rate with 15-percent excess air by means of formulae given in Ref. 13. A limited amount of draft loss data for a 0.15 m (6-inch) diameter Turboflue were obtained from the Bock Corporation

and used to back-calculate friction factors.* The total draft loss from the firebox to the barometric control was estimated to be 7.84 N/m^2 (0.0315 inch WC) distributed as follows:

Portion of Flow Path	Percent of Draft Loss
Choke Plate	11.9
3 180-degree Returns	25.7
3 Turboflue Entrances	13.8
2 Turboflue Exits	9.2
Turboflue Passes	32.8
Flue Connection	6.6

By contrast, comparable calculations for a design with seven, parallel 0.076 m (3-inch) diameter boiler tubes in a single pass following a single 180-degree return and no combustor discharge choke plate predict only a 1.25 N/m^2 (0.005 in WC) draft loss. This loss confirms the essential validity of the Burnham expectation of high draft loss for the preliminary hydronic design. Also, the foregoing distribution table shows that the biggest contributors to the draft loss, in order of decreasing importance, are the series arrangement with multiple return bends, inlets, and exits; the Turboflue heat exchanger tubes; and the combustor exhaust choke plate.

The calculated stack effect between the combustion chamber and the barometric control is only 1.5 N/m^2 (0.006 in WC). Thus, if a firebox draft of 2.5 N/m^2 (0.01 in WC) is desired, the barometric control device should control to 8.8 N/m^2 (0.036 in WC) draft. The chimneys on many residences cannot reliably provide that high a draft at the barometric control; therefore, this condition tends to confirm the fact that the preliminary design layout would have (or approach) a pressurized combustion chamber.

*Friction factors calculated were f = 0.24 and 0.51 at Reynolds numbers of approximately 5200 and 6500, respectively. These values are approximately an order of magnitude larger than those for relatively smooth pipe.

The draft loss could be approximately halved by changing the hydronic unit design to (1) eliminate the combustor exhaust choke plate, (2) use only one 180-flow return, and (3) use either parallel single-pass Turboflues or one long one. While such a design would approach giving acceptably low-combustion-gas pressure drops, the undoubtedly higher fabrication costs and questionable ability to clean deposits from the Turboflue interior combine to make inadvisable the pursuit of the application of this device without definitive testing first being performed.

SECTION VII

REFERENCES

1. Hall, R. E., J. H. Wasser, and E. E. Berkau, "NAPCA Combustion Research Programs to Control Pollutant Emissions from Domestic and Commerical Heating Systems," New and Improved Oil Burner Equipment Workshop, NOFI Tech. Publ. 108 ED, National Oil Fuel Institute, Inc., New York, N.Y., September 1970, pp. 83-93.

2. Hall, R. E., H. H. Wasser and E. E. Berkau, "A Study of Air Pollutant Emissions from Residential Heating Systems," EPA-650/2-74-003, Environmental Protection Agency, Research Triangle Park, N. C., January 1974.

3. Martin, G. B., and E. E. Berkau, "Evaluation of Various Combustion Modification Techniques for Control of Thermal and Fuel-Related Nitrogen Oxide Emissions," presented at the Fourteenth Symposium (International) on Combustion, Pennsylvania State University, August 1972.

4. Barrett, R. E., S. E. Miller, and D. W. Locklin, "Field Investigation of Emissions from Combustion Equipment for Space Heating," EPA R2-73-084a (API Publ. 4180), Environmental Protection Agency, Research Triangle Park, N. C., June 1973.

5. Dickerson, R. A., and A. S. Okuda, "Design of an Optimum Distillate Oil Burner for Control of Pollutant Emissions," EPA-650/2-74-047, Environmental Protection Agency, Research Triangle Park, N. C., June 1974.

6. Hagel, J. A., "Una-Spray Integrated Furnace," New and Improved Oil Burner Equipment Workshop, Tech. Publ. 108 ED, National Oil Fuel Institute, New York, N.Y., September 1970.

7. Howekamp, D. P., and M. H. Hooper, "Effect of Combustion Improving Devices on Air Pollutant Emissions from Residential Oil-Fired Furances," Paper No. APCA 70-45, Annual Meeting of the Air Pollution Control Association, St. Louis, Mo., June 1970.

8. Turner D. W., et al., "Efficiency Factors for Domestic Oil Heating Units," Addendum to the Proceedings of the Conference on Improving Efficiency in HVAC Equipment and Components for Residential and Small Commercial Buildings, Purdue University, Lafayette, Indiana, October 1975.

9. Bailey, F. W., "Blue Flame Burner Development at the Blue Flame Laboratory," New and Improved Oil Burner Equipment Workshop, Tech. Publ. 108 ED, National Oil Fuel Institute, New York, N. Y., September 1970.

10. Cooper, P. W., and C. J. Marek, "Design of Blue-Flame Oil Burner Utilizing Vortex Flow or Attached-Jet Entrainment," API Publ. 1723-A, American Petroleum Institute, New York, N. Y., January 1965.

11. Locklin, D. W., et al., "Design Trends and Operating Problems in Combustion Modification of Industrial Boilers," EPA-650/2-74-032, U. S. Environmental Protection Agency, Washington, D. C., April 1974.

12. Peoples, G., "Sealed Oil Furnace Combustion System Reduces Fuel Consumption," Addendum to the Proceedings, Conference on Improving Efficiency in HVAC Equipment and Components for Residential and Small Commercial Buildings, Purdue University, Lafayette, Indiana, October 1974.

13. Steam/Its Generation and Use, Chapters 3 and 14, 38th Edition, Babcock and Wilcox Co., New York, N. Y., 1972.

APPENDIX A

WARM AIR OIL FURNACE COMPUTER MODEL

An analytical model of the thermal behavior of a warm air residential oil furnace during cyclical operation has been formulated and programmed for solution on a Honeywell 440 Timeshare computer. This appendix contains: a summarization of the model formulation, including assumptions, limitations and capabilities; a listing of the computer program; and examples of the program's computer printout.

The computer program is entitled WAFURN (warm air furnace). Given a furnace's design data, input fuel oil and combustion air flowrates and conditions data, warm air flowrate, ambient temperature conditions, cycle timing, etc, it marches in time through two or more furnace operational cycles and computes the unit's thermal behavior. Principal output data are temperatures of various components and flow streams as functions of time and values of net heat input,* heat transferred, and heat stored or lost during one of a series of nearly-identical cycles. Program input data and all computations are in the modernized metric (SI) system of units; to facilitate interpretation of computed results, a portion of the printout is also given in English engineering units.

FURNACE SYSTEM MODELLED

A schematic illustration of the furnace components and flows modelled by the WAFURN computer program is given in Fig. A-1. The furnace consists of a housing surrounding a combustion firebox and a heat exchanger, an oil burner, a combustion gas flue system, and a warm air supply and removal system.

* Net heat input is based on the fuel's lower (net) heating value.

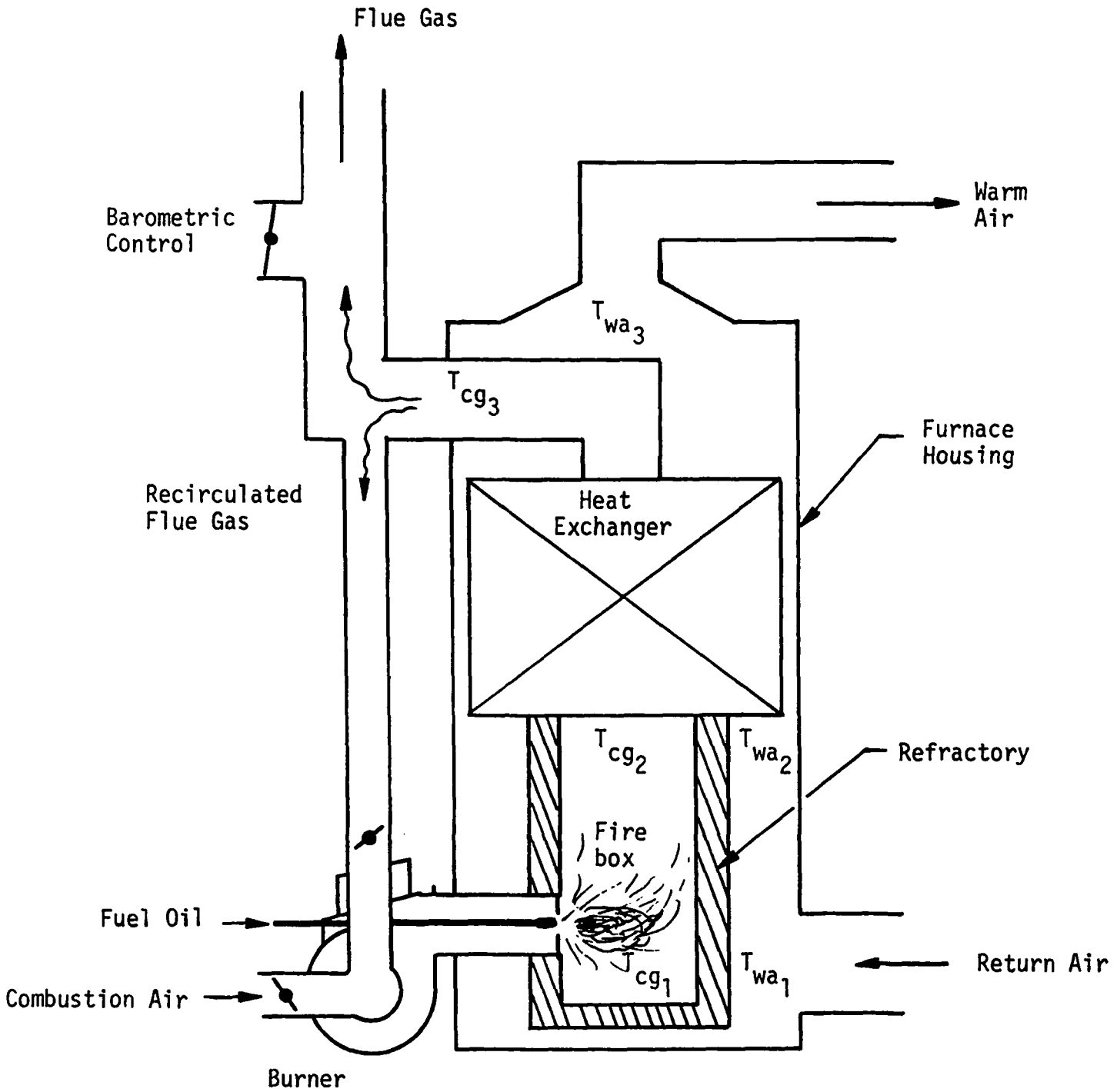

Figure A-1. Schematic of Furnace Modelled by WAFURN Computer Program

The warm air is the furnace cooling medium; it flows within the housing, over the external surfaces of the firebox, heat exchanger, and perhaps part of the exhaust flue and removes heat from them; it is circulated through the residential living spaces and returned as not-so-warm air to the furnace. Two important warm-air components not shown in Fig. A-1 are a filter to remove airborne household dust and a blower to drive the flow of warm air. The filter does not enter into the WAFURN calculations and the blower is considered only in the cycle timing control sense of when the specified volumetric flowrate of warm air is started and stopped.

The oil burner is assumed to be supplied with a specified volumetric flowrate of a No. 2 distillate fuel oil and with the correct flowrate of combustion air to support combustion at a prescribed stoichiometric ratio. It is further assumed to be an efficient burner which causes the input reactant streams to be mixed thoroughly and reacted completely to thermodynamic equilibrium combustion products soon after their entry into the firebox. A typical No. 2 oil having a net (lower) heating value of 4.273×10^7 J/kg (18,387 Btu/lb) is built into the program. It may be supplied as a water emulsion (by specifying a nonzero mass fraction of water in the fuel) and its supply temperature may take on any reasonable value. Similarly, the combustion air supply temperature and percentage humidity are independent input parameters. As sketched in Fig. A-1, the combustion air may be mixed with a quantity of externally-recirculated flue gas by simply specifying the fraction of FGR. Because the flue gas temperature is a time-varying parameter, the heat content of the mixed combustion air/FGR reactant stream is time-varying and, as a result, so is the adiabatic flame temperature. Condensation in the FGR circuit is assumed not to occur, so the combustion gas composition is maintained at thermodynamic equilibrium for the dry combustion air/dry oil stoichiometric ratio whether or not there are humidity in the air, water in the oil and/or FGR; if one or more of these are present, they are treated as simple diluents which act to reduce the flame temperature.

RM 608-B-13 REV. 10-73

The firebox is assumed to have a right circular cylindrical configuration and to consist of a steel shell with or without a refractory lining for its interior surface. One end of the cylinder is closed, the other communicates with the heat exchanger. Configurational details such as tunnel- or side-fired mounting of the burner and vertical or horizontal orientation of the firebox are not dealt with explicitly; if they are influential, they must be accounted for in the expressions for convective film coefficients. Thus the firebox design information employed are rather limited in scope; they include inside and outside diameters, total weights of refractory and steel shell, interior and exterior surface areas for heat transfer, and interior and exterior cross-sectional areas available for gas and air flows.

Consideration of the heat exchanger is similarly rather vaguely nondescriptive concerning design details. As will be seen, the convective exchange coefficients included in the heat transfer model assume that the heat exchanger is one or more firetubes with external air crossflow. The user is given the responsibility for translating his actual heat exchanger into a consistent set of design parameters for that heat transfer model, or for changing to a more appropriate model.

The flue system is assumed to be fitted with a weighted-damper barometric control device for automatic regulation of firebox draft. Draft considerations enter the model calculations only when the burner is turned off. Then, a natural draft flow of air is drawn in through the burner, firebox, etc., and passes out the flue. Draft air flowrate is determined by the draft pressure in the firebox and by the effective open area of the combustion air supply louvers in the burner's blower shroud. This effective area is given as a specified constant at unity stoichiometric ratio and is thereafter treated as a variable proportional to actual stoichiometric ratio. The firebox draft is calculated using conventional stack effect formulae, but is divided into two pieces--a firebox-to-heat-exchanger stack effect and a heat-exchanger-to-barometric-control stack effect.

RM 608-B-13 REV. 10-73

THERMAL ANALYSIS

The thermal analysis approach taken in the WAFURN computer model is essentially an input, output and storage accounting method. Input reactants provide a known flowrate of a combustion gas stream having known composition, temperature, heat content, specific heat, etc. to the firebox. While flowing through the firebox and, subsequently, the heat exchanger, heat is transferred from that gas stream to these components. Any residual heat content left in the gases as they are exhausted up the flue constitutes a thermal loss. Meanwhile, a more-or-less simultaneous flow of warm air is passed over the outside of the firebox and heat exchanger; heat is transferred from the components to the airflow. Heat taken up by this airstream represents the useful portion of the heat supplied.

If the heat transferred to a particular furnace component differs in magnitude from that being transferred from it, that component's heat content and, therefore, its temperature change. Such changes constitute heat storage. Depending upon its ultimate disposition, storage may become part of the useful heat or part of the lost heat. To minimize the impact of time-varying storage terms on the overall accounting of cyclical heat disposition, WAFURN is structured to analyze sequential cycles until the total heat storage during a cycle is less than one percent of that cycle's input heat.

The only thermal losses presently accounted for in WAFURN are the flue gas and draft air losses. While there are certainly natural and forced convective heat transfer from the warm air to the furnace housing as well as radiant transfer from the firebox and heat exchanger to the housing, conventional practice is to insulate the inside of the housing sufficiently well that these losses are limited to less than one percent during steady-state operation. Although continued losses after burner cutoff will magnify that value by perhaps as much as three times, the total furnace setting losses were believed to be small enough and well enough understood that their omission would not impair the utility of the WAFURN solutions.

Heat Transfer Models

As indicated earlier, heat transfer analyses in WAFURN are based on a rather generalized approach that does not get very involved in specifics of component design. The heat transfer models incorporated as subroutines in the program were adopted from Chapters 4 and 14 of Ref. A-1.

The rate of heat transferred from the combustion gases to the inside surface of an unlined firebox or of a metal heat exchanger was calculated by means of the following expressions appropriate for heat transfer inside cylindrical tubes. The heat given up by the combustion gases at a given instant is:

$$\dot{Q} = \dot{w}_{cg}\, \bar{c}_{p_{cg}} \left[\left(T_{in} \right)_{cg} - \left(T_{out} \right)_{cg} \right], \text{ (J/s)} \qquad \text{(A-1)}$$

Simultaneously, the same quantity of heat is accepted by the inside surface of the furnace component

$$\dot{Q} = U\, A_{surf}\, \Delta\bar{T}_{cg\text{-}steel} \qquad \text{(A-2)}$$

where

$$U = U_c + U_r, \text{ (J/s-m}^2\text{-K)} \qquad \text{(A-3)}$$

$$\Delta\bar{T}_{surf} = \left[2\bar{T}_{steel} + \left(T_{in} \right)_{cg} + \left(T_{out} \right)_{cg} \right] / 4, \text{ (K)} \qquad \text{(A-4)}$$

$$U_c = 30.385\, F_{pp}\, F_T\, \dot{G}_{cg}^{0.8} / D_{inside}^{0.2} \qquad \text{(A-5)}$$

$$F_{pp} = \left[1 + 0.58 \left(X_{H_2O} \right)_{cg} \right] \left(0.195 + 2.79 \times 10^{-5}\, \Delta\bar{T}_{surf} + 7500 / \Delta\bar{T}_{surf}^{\,2} \right) \qquad \text{(A-6)}$$

FORM 608-B-13 REV. 10-73

$$F_T = \left[\left[\left(T_{in}\right)_{cg} + \left(T_{out}\right)_{cg}\right] \Big/ \left(2\ \Delta\overline{T}_{surf}\right)\right]^{0.8} \tag{A-7}$$

$$\dot{G}_{cg} = \dot{w}_{cg} / (A_{cs})_{inside}\ ,\ (kg/m^2\text{-}s) \tag{A-8}$$

$$U_r = K_r\ (0.0572\ \ \Delta T_{lm} + 0.096\ \overline{T}_{steel} - 47.3) \tag{A-9}$$

$$\Delta T_{lm} = \left[\left(T_{in}\right)_{cg} - \left(T_{out}\right)_{cg}\right] \Big/ \ln\ \left[\left[\left(T_{in}\right)_{cg} - \overline{T}_{steel}\right] \Big/ \left[\left(T_{out}\right)_{cg} - \overline{T}_{steel}\right]\right],(K) \tag{A-10}$$

$$K_r = \left[0.574\ D_{inside}\ (p_{H_2O})_{cg} \Big/ P\right]^{1/2} \tag{A-11}$$

This system of equations is solved in subroutine HEXHT by an iterative process for the heat transfer rate, $\dot{Q}$, and the combustion gas exit temperature, $(T_{out})_{cg}$. Note that the gas stream and metal component temperatures are treated as bulk mean averages, with no accounting for axial or radial gradients. The same subroutine is used also for unlined firebox and heat exchanger cooling by draft air.

For the refractory-lined firebox, essentially the same system of equations is used but the temperature at the refractory's inside surface is also included as a variable to be solved for in the iterative solution procedure in subroutine RFBHT. Simplifying assumptions have been made in order to approximate transient heat conduction through and heat storage by the refractory. When the burner is turned on, the inside surface temperature is assumed to reach very quickly a value corresponding to that it will have later during steady-state operation. It is this pseudo-steady-state temperature that is solved for in subroutine RFHBT. Heat transferred from the

combustion gases to the refractory is conducted radially outward as a thermal wave. It is assumed to be stored in the refractory such as to establish a radial thermal gradient consistent with the eventual steady-state distribution

$$\frac{T(r) - T_{steel}}{T_{surf} - T_{steel}} \qquad \frac{\ln (r/r_{steel})}{\ln (r_{surf}/r_{steel})} \tag{A-12}$$

In other words, until that temperature profile is established in the refractory, no heat is transferred to the firebox's steel shell. Thereafter, steady-state conduction is assumed, with the conduction rate maintaining consistency with both the inside refractory and outside steel temperatures.

When the burner is turned off, the hot refractory is cooled from the inside by convection to the draft air. Then, a cooling wave propagates into the refractory, penetrating more deeply as time progresses. It is assumed that the same form of radial temperature profile (but with reversed slope) is established from the inside to the penetration radius, and that the temperature at that penetration point corresponds to that of the earlier steady-state conduction when the burner was on. Meanwhile heat continues to be conducted down that same earlier gradient to the steel shell. This somewhat simplified solution to a rather complicated problem is accomplished by subroutine RFBHT in conjunction with subroutine REFKUL to define the penetration point. During this process, radiation from the refractory to the air is neglected, since the only constituents of air which will absorb radiation are the low concentrations of CO_2 and H_2O.

For the external cooling of the firebox steel shell and the heat exchanger, convective heat transfer coefficients for crossflow of a gas outside a bank of cylindrical tubes is used. A single tube was assumed to represent the firebox and, in consideration of the flow pattern through the Lennox OF7 heat exchanger, it was assumed to correspond to four tubes. The system of

ORM 608-B-13 REV. 10-73

equations is very similar to that for heat transfer inside the metal heat exchanger, except that

$$U = U_c = 86.14\ F_{pp}\ F_a\ \dot{G}_{air}^{0.61} / D_{outside}^{0.39} \qquad \text{(A-13)}$$

$$F_{pp} = 0.0695 + 8.19 \times 10^{-5}\ \Delta\bar{T}_{surf} - 395/\Delta\bar{T}_{surf}^2 \qquad \text{(A-14)}$$

$$F_a \quad 0.587 \left[\frac{\dot{G}_{air}\ D_{outside}}{\mu_{air}} \right]^{0.167} \qquad \text{(A-15)}$$

and all other parameters are defined for air and conditions outside the tubes. This problem is solved iteratively for the rate of heat transfer to the warm air stream and for the output temperature of the warm air by subroutine AIRHT.

The foregoing heat transfer calculations are carried out by subroutines RFBHT, HEXHT, and AIRHT at each time step under the assumption that the firebox metal and heat exchanger metal temperatures are known. Following their completion, the difference between the heat transfer to and heat transfer from each component is used to calculate a new component metal temperature for the next time step. Temperature gradients in the metal are not considered.

Cycle Thermal Efficiency

As the thermal analysis proceeds in time, a number of heating terms are integrated and, after the cycle time is reached, are used to calculate thermal efficiency and the distribution of losses. Cycle thermal efficiency is defined as the sum of heat accepted by the warm air divided by the net heat input to the furnace. As noted earlier, losses accounted for are the heat transported out of the furnace by the incompletely-cooled combustion gases and by the draft air flows.

PROGRAM LISTING AND SAMPLE PRINTOUTS

Table A-1 is a listing of the WAFURN main programs and all of the nonlibrary subroutines and function subprograms which it calls. It is included in this report simply as a matter of record. Although it obviously has not been documented well enough for formal delivery, the design and operational data on the first two pages are easily understood, so the program certainly could be used by others.

Following the program listing is Table A-2, a reduced-size reproduction of a portion of the computer printout for the 4 minute firing, 12 minute cycle of the Lennox OF7 furnace at 1.0 ml/sec dry oil.

REFERENCES

A-1. Steam, Its Generation and Use, 38th Edition, The Babcock and Wilcox Co., New York, N. Y., 1974.

NOMENCLATURE

A	= area, m^2
c_p	= heat capacity at constant pressure, J/kg-K
D	= diameter, m
F_a, F_{pp}, F_T	= empirical coefficients in convective heat transfer equations
$\dot{G}$	= mass flux, kg/s-m^2
K_r	= empirical radiant heat transfer coefficient
P	= combustor static pressure, N/m^2
P_{H_2O}	= partial pressure of water, N/m^2
$\dot{Q}$	= heat transfer rate, J/s
r	= radius, m
T	= temperature, K
ΔT	- temperature difference, K

BRM 608-B-13 REV. 10-73

U = heat transfer coefficient, $J/s\text{-}m^2\text{-}K$

$\dot{w}$ = flowrate, kg/s

X_{H_2O} = mass fraction water vapor

μ = viscosity, kg/m-s (centipose$*10^{-3}$)

[-] = mean value of parameter

Subscripts

air	pertains to warm air
c	pertains to convective heat transfer
cg	pertains to combustion gas
in, out	pertain to inlet, outlet conditions
inside, outside	pertain to surfaces of components through which heat is being transferred
lm	pertains to logarithmic mean temperature difference
r	pertains to radiant heat transfer
steel	pertains to metal shell of firebox or heat exchanger
surf	pertains to surface of firebox or heat exchanger material

TABLE A-1. LISTING OF WAFURN COMPUTER PROGRAM

WAFURN

```
100C     OIL-FIRED WARM AIR FURNACE THERMAL ANALYSIS PROGRAM
120C
140C        L. P. COMBS  D/522-198  EXT 5014  6 JAN 1975
160C
170C    (INPUT PARAMETERS CORRESPOND TO LENNOX OF7 FURNACE.)
180C
200 DIMENSION  DATE(3), TSAT(10),WRSAT(10), TTSR(8),TTEQ(8)
220C
240 DATA TSAT/400, 460, 490, 500, 510, 520, 525, 530, 535, 540/
260 DATA WRSAT/0.0, .0023, .0034, .0051, .0077, .011, .0131,
280&             .0157, .0187, .0224/
300C
320  DATA TTSR/1.0, 1.2, 1.4, 1.6, 1.8, 2.0, 2.2, 2.4/
340 DATA TTEQ/2280., 2105., 1914., 1754., 1630., 1512.,
360&           1425., 1340./
380C
400 CALL DATIME(IT,TOD,DATE)
420C
440C TIME-LINE PARAMETERS
460      TON = 0.0
480      TFAN1 = 1.0
500      TOFF = 4.0
510      HITIME = 12.0
515C  (IF TOFF IS LESS THAN TCYC, SET HITIME EQUAL TO TCYC.)
520      TCYC = 12.0
540      DELT = 0.1
560C
580C INPUT CONDITIONS FOR OIL & AIR
600      FVOL = 1.0E-06
620      FTEMP = 273.2
640      FRHO = 845.
660      CPOIL = 1860.
680      HVN = 4.273E+07
700      CPWL = 4190.
720      FXH20 = 0.0
740C
760      SRI = 1.20
780      CATMP = 273.2
800      CAHUM = 0.6
820C
840      WAVOL = 0.5
860      WAT1 = 293.2
880      WAHUM = 0.3
900      WATOFF = 320.
920C
940C FRACTION OF FLUE GAS RECIRCULATED
960      RECIRC = 0.0
980C
1000C DESIGN PARAMETERS FOR BURNER & FURNACE
1020      CAREA = 0.0013
```


WAFURN CONTINUED

```
1040      HFBHE = 0.50
1060      HHEBC = 1.5
1080      DIFB = 0.2635
1100      AIFB = 0.3068
1120      TIIFB = 450.
1140     WRFB = 1.88
1160     CSIFB = 0.0545
1180     QCR = 0.065
1200      CPR = 837.
1220C
1240     DSFB = 0.3048
1260     ASFB = 0.365
1280     TISFB = 375.
1300     WSFB = 4.54
1320     CSOFB = 0.143
1340      CPSFB = 500.
1360C
1380     DIHE = 0.14
1400     AIHE = 2.25
1420     TIHE = 300.
1440     WSHE = 21.0
1460     CSIHE = 0.025
1480     CSOHE = 0.088
1500     CPSHE = 500.
1520C
1540C ADDITIONAL DATA REQUIRED
1560     TAMB = 273.2
1580     DSR = 0.3
1600     NSR = 4
1620     IPRD = 0
1640C
1660C DERIVED PARAMETERS
1680     SR = SRI
1700     FWD = FVOL*FRHO
1720     FWDW = FWD*FXH20
1740     FWDO = FWD*(1. - FXH20)
1760     CAWRW = XTRP(1.8*CATMP,TSAT,WRSAT)*CAHUM
1780     CALL CPAIR(CAWRW,CACA,CACB,CACC)
1800     WAWRW = XTRP(1.8*WAT1,TSAT,WRSAT)*WAHUM
1820     CALL CPAIR(WAWRW,WACA,WACB,WACC)
1840     WAXW = WAWRW/(1. + WAWRW)
1860     WARHO = 6364.9/(WAT1*(16.02 + 10.94*WAXW))
1880     WAWD = WAVOL*WARHO
1900     WAGFB = WAWD/CSOFB
1920     WAGHE = WAWD/CSOHE
1940     IR = 0
1960     IF(WRFB.LE.0.)   GO TO 5
1980     IR = 1
2000     RRFB = DSFB*ALOG(DSFB/DIFB)/(2.*QCR)
2020     TFUNC = (DIFB*(1.-ALOG(DIFB/DSFB))-DSFB)/
```

TABLE A-1. (Continued)

WAFURN CONTINUED

```
2040&           (ALOG(DIFB/DSFB)*(DSFB-DIFB))
2060    5 CONTINUE
2080C
2100 DO 500 K=1,NSR
2110      IF(K.GE.2)  CALL HIFIRE(2,HITIME,TCYC,FWD,FWDW,FWD0,CAWD,CAWDW,
2111&                 CGWDW,CGWD,CGGFB,CGGHE,QREF,QINPUT)
2120      TMIFB = TIIFB
2140      TMSFB = TISFB
2160      TMHE = TIHE
2180      CAWD = (1. + CAWRW)*14.49*SR*FWD0
2200      CAXW = CAWRW/(1. + CAWRW)
2220      CAWDW = CAWD*CAXW
2240      CAVOL = 1.570E-04*CAWD*CATMP*(18.02 + 10.94*CAXW)
2260      CGWRW = 0.14604 - 0.09205*SR + 0.01934*SR**2
2280      CGWDW = FWDW + CAWDW + CGWRW*(FWD0 + CAWD*(1.-CAXW))
2300      CGWD = (FWD + CAWD)/(1. - RECIRC)
2320      CGXW = CGWDW/(FWD + CAWD)
2340      CGGFB = CGWD/CSIFB
2360      CGGHE = CGWD/CSIHE
2380      CGTEQ = XTRP(SR,TTSR,TTEQ)
2400      QREF = (FWD0*CPOIL + FWDW*CPWL)*(FTEMP - 298.2)
2420&           + CAWD*CPMEAN(CATMP,298.2,CACA,CACB,CACC)*
2440&             (CATMP - 298.2) - 2.44E+06*FWDW
2460      CGXXW = (FWDW + CAWDW)/(FWD + CAWD)
2480      CALL CPCG(SR,0.0,CGCA,CGCB,CGCC)
2500      QINPUT = (FWD + CAWD)*(1. - CGXXW)*(CGTEQ - 298.2)*6C.*
2520&              (TOFF - TON)*CPMEAN(CGTEQ,298.2,CGCA,CGCB,CGCC)
2540      CALL CPCG(SR,CGXXW,CGCA,CGCB,CGCC)
2560      CGTX = CGTEQ - 30.
2580 DO 10  N=1,5
2600      CGTX = CGTEQ + (QREF - (FWDW*CAWDW)*(CGTX-298.2)*
2620&           CPMEAN(CGTX,298.2,0.4052,1.3654E-04,0.0))/((FWD +
2640&           CAWD)*CPMEAN(CGTEQ,CGTX,CGCA,CGCB,CGCC)) ,
2660C  10 CONTINUE
2670      CALL HIFIRE(1,HITIME,TCYC,FWD,FWDW,FWD0,CAWD,CAWDW,
2671&                 CGWDW,CGWD,CGGFB,CGGHE,QREF,QINPUT)
2680      IF(SR.NE.SR1)   GO TO 100
2700C
2720C PRINT INPUT DATA
2740      PRINT 15,
2760      PRINT 20, DATE
2780   15 FORMAT(///)
2800   20 FORMAT(4X,"W A R M  A I R  O I L-F U R N A C E  ",
2820&           "C Y C L E  A N A L Y S I S"//23X,
2840&           "ANALYSIS DATE: ",3A6/)
2860      PRINT 25,
2880   25 FORMAT(2X,"FURNACE DESIGN DATA:        FIREBOX",9X,
2900&           "FIREBOX",10X,"HEAT"/28X,"REFRACTORY",8X,
2920&           "STEEL",9X,"EXCHANGER")
2940      IF(IR.LE.0)   GO TO 35
```


WAFURN CONTINUED

```
2960      PRINT 30, DIFB,DSFB,DIHE,WRFB,WSFB,WSHE,AIFB,ASFB,AIHE,
2980&             CSIFB,CSIHE,CSOFB,CSOHE,TMIFB,TMSFB,TMHE
3000   30 FORMAT(10X,"DIAMETER,M :",1P3E15.4/14X,"MASS,KG:",
3020&           3E15.4/9X,"H.T. AREA,M2:",3E15.4/9X,"INT. C.S.,M2:",
3040&           E15.4,16X,E15.4/9X,"EXT. C.S.,M2:",16X,2E15.4/
3060&           7X,"INIT. TEMP.,K :",0PF13.2,2F16.2/)
3080      GO TO 45
3100   35 PRINT 40, DSFB,DIHE,WSFB,WSHE,ASFB,AIHE,CSIFB,CSIHE,
3120&             CSOFB,CSOHE,TMSFB,TMHE
3140   40 FORMAT(10X,"DIAMETER,M :",15X,1P2E15.4/14X,"MASS,KG:",
3160&           15X,2E15.4/9X,"H.T. AREA,M2:",15X,2E15.4/9X,
3180&           "INT. C.S.,M2:",15X,2E15.4/9X,"EXT. C.S.,M2:",
3200&           15X,2E15.4/7X,"INIT. TEMP.,K :",13X,0P2F16.2/)
3220   45 PRINT 50, HFBHE,HHEBC,CAREA,WAVOL,WAT1,WAWD
3240   50 FORMAT(5X,"FB-HE HT. =",0PF5.2," M,  HE-SC HT. =",F5.2,
3260&        " M,  C.A. AREA =",F6.5," M2"//2X,"WARM AIR FLOWRATE,",
3280&           "M3/S:",E12.4,4X,"INLET TEMP.,K:",0PF8.2/20X,
3300&           "KG/S:",1PE12.4/)
3320      PRINT 55, FVOL,CAVOL,FWD,FWD0,CAWD,FWDW,CAWDW,FTEMP,
3340&             FTEMP,CATMP,RECIRC,TAMB
3360   55 FORMAT(2X,"INPUT FUEL & COMBUSTION AIR(@ SR=1.2):",
3380&           /29X,"EMULSION",6X,"DRY OIL",8X,"COMB. AIR"/
3400&           8X,"FLOWRATE,M3/S:",1PE15.4,16X,E15.4/17X,"KG/S:",
3420&           3E15.4/8X,"MOISTURE,KG/S:",E15.4,16X,E15.4/6X,
3440&           "INIT. TEMP.,K:",0PF13.2,2F16.2//2X,"RECIRCULATED FLUE",
3460&           " GAS,%:",2PF9.2//2X,"OUTDOOR AMBIENT TEMP.,K:",0PF9.2/)
3480      PRINT 60, TON, TON, TFAN, TCYC, TOFF, WATOFF, DELT
3500   60 FORMAT(2X,"CYCLE TIMING (MINUTES):      CYCLE",10X,"BURNER",
3520&           9X,"W.A. FAN"/18X,"ON :",0PF13.2,2F16.2/16X,"OFF:",
3540&           F13.2,F16.2,7X,"@",F6.1," K"//6X,
3560&           "MARCHING INTERVAL,MIN:",F6.3)
3580C
3600 100 CONTINUE
3620      JCYC = TCYC/DELT
3640      SQFBR = 0.0
3660      IF(IR.EQ.1)    SQFBR = WRFB*CPR*(TMSFB - CATMP + TFUNC*
3680&                              (TMIFB - TMSFB))
3700      SQHES = WSHE*CPSHE*TMHE
3720      SQFBS = WSFB*CPSFB*TMSFB
3740      FBSMIN = WSFB*CPSFB*CATMP
3760      WAT2 = WAT1
3780      WAT3 = WAT1
3800      QDFBA = 0.0
3820      NCYC = 0
3840      ITER = 0
3860 105 ITER = ITER + 1
3870      IF(ITER.GT.1)    CALL HIFIRE(3,HITIME,TCYC,FWD,FWDW,FWD0,CAWD,CAWDW
3871&                                  CGWDW,CGWD,CGGFB,CGGHE,QREF,QINPUT)
3880      SQWA = 0.0
3900      SQDL = 0.0
```

TABLE A-1. (Continued)


```
WAFURN CONTINUED

3920     SQFL = -60.*QREF*(TQFF - TQN)
3940     QFBRI = SQFBR
3960     QFBSI = SQFBS
3980     QHESI = SQHES
4000     CGT1 = CGTX
4020     CGT2 = CGTX - 100.
4040     CGT3 = 400.
4060     TFAN2 = TQFF + 5.
4080     T = DELT
4100      IPR = 20
4120     JPR1 = 0
4140     IRC = 0
4150     NHI = 4
4160C
4180C PERFORM TRANSIENT HEAT TRANSFER ANALYSIS(1ST: F.B., 2ND: H.E.)
4200     DO 400   J=1,JCYC
4220     IF(T.LE.TFAN2)   GO TO 108
4240     IPR = 10
4260     IF(T.LE.(TFAN2 + 2.*DELT))   JPR1 = J/IPR
4280 106 DELT = 60.*DELT
4300     HESMIN = WSHE*CPSHE*WAT2
4320     IF(T.GT.TFAN2.OR.CGT2.LT.WAT2)   HESMIN = WSHE*CPSHE*CGT2
4340     QDFBS = 0.0
4360     QDFBG = 0.0
4380     IF(T.GT.TQFF)   CGT1 = CATMP
4385     IF(T.LE.HITIME.OR.NHI.GT.4)   GO TO 109
4390     CALL  HIFIRE(NHI,HITIME,TCYC,FWD,FWDW,FWDO,CAWD,CAWDW,
43914                  CGWDW,CGWD,CGGFB,CGGHE,QREF,QINPUT)
4395 109 CONTINUE
4400     IF(T.LE.TQN.OR.T.GT.TQFF)   GO TO 120
4420     CGT1 = ((FWD*CAWD)*CPMEAN(298.2,CGTX,CGCA,CGCB,CGCC)*
44404            (CGTX-298.2) + RECIRC*CGWD*(CGT3-298.2)*
44604            CPMEAN(298.2,CGT3,CGCA,CGCB,CGCC))/(CGWD*
44804            CPMEAN(298.2,CGT1,CGCA,CGCB,CGCC)) + 298.2
4500C BURNER ON, UNLINED FIREBOX
4520     IF(IR.NE.0)   GO TO 110
4540     CALL HEXHT(SR,CGT1,CGGFB,TMSFB,AIFB,DIFB,CGWD,CGXW,CGCA,
45604                CGCB,CGCC,CGT2,QDFBS,IPRD)
4580     SQFBS = SQFBS + DELT*QDFBS
4600     GO TO 140
4620C BURNER ON, REFRACTORY-LINED FIREBOX
4640 110 CALL RFBHT(SR,CGT1,CGGFB,TMIFB,TMSFB,AIFB,ASFB,DIFB,DSFB,
46604                RRFB,CGWD,CGXW,CGCA,CGCB,CGCC,CGT2,QDFBG,IPRD)
4680     QSTORQ = WRFB*CPR*(TMSFB - CATMP + TFUNC*(TMIFB - TMSFB))
4700     IF((SQFBR+QDFBG*DELT).GE.QSTORQ)   QDFBS = QDFBG
4720     SQFBR = SQFBR + DELT*(QDFBG - QDFBS)
4740     SQFBS = SQFBS + DELT*QDFBS
4760     GO TO 140
4780 120 CALL DRAFT(SR,CAREA,HFBHE,HHEBC,CGT1,CGT2,CGT3,
48004                CATMP,CAXW,DAWD)
```



```
WAFURN CONTINUED

4820     DAGFB = DAWD/CSIFB
4840     DAGHE = DAWD/CSIHE
4860     IF(IR.NE.0)   GO TO 130
4880C BURNER OFF, UNLINED FIREBOX
4900     CALL HEXHT(-1,CATMP,DAGFB,TMSFB,AIFB,DIFB,DAWD,CAXW,CACA,
49204                CACB,CACC,CGT2,QDFBS,IPRD)
4940     IF(QDFBS.GT.0..OR.(SQFBS+DELT*QDFBS).GT.FBSMIN)   GO TO 125
4960     CPDA = CPMEAN(CATMP,CGT2,CACA,CACB,CACC)
4980     CGT2 = CGT2 + (SQFBS+DELT*QDFBS-FBSMIN)/(DELT*DAWD*CPDA)
5000     QDFBS = (SQFBS - FBSMIN)/DELT
5020 125 SQFBS = SQFBS + DELT*QDFBS
5040     GO TO 140
5060C BURNER OFF, REFRACTORY-LINED FIREBOX
5080 130 IRC = IRC + 1
5100     IF(IRC.GT.1)   GO TO 135
5120     TMP = TMSFB + (SQFBR/(WRFB*CPR)+WAT1-TMSFB)/TFUNC
5140     RRP = RRFB
5160     CQEFF = WRFB*CPR
5180 135 CALL REFKUL(IRC,TMSFB,DSFB,TMIFB,DIFB,AIFB,SQFBR,CQEFF,
52004                TMP,DP,AP,RRP)
5220     CALL RFBHT(-1,CATMP,DAGFB,TMIFB,TMP,AIFB,AP,DIFB,DP,RRP,
52404                DAWD,CAXW,CACA,CACB,CACC,CGT2,QDFBG,IPRD)
5260     QDFBS = (TMP-TMSFB)*ASFB/RRFB
5280     SQFBR = SQFBR + DELT*(QDFBG-QDFBS)
5300     SQFBS = SQFBS + DELT*QDFBS
5320 140 CONTINUE
5340C FIREBOX HEATING OF WARM AIR
5360     IF(T.LE.TFAN1.OR.T.GT.TFAN2)   GO TO 180
5380     CALL AIRHT(WAT1,WAGFB,TMSFB,ASFB,DSFB,WAWD,WACA,WACB,WACC,
54004                WAT2,QDFBA,IPRD)
5420     SQFBS = SQFBS - DELT*QDFBA
5440 180 CONTINUE
5460C (CALL F.B. REGION RAD'N LOSS SUBR.)
5480     IF(T.LE.TQN.OR.T.GT.TQFF)   GO TO 200
5500C BURNER ON, HEAT EXCHANGER COOLING COMBUSTION GASES
5520     CALL HEXHT(SR,CGT2,CGGHE,TMHE,AIHE,DIHE,CGWD,CGXW,CGCA,CGCB,
55404                CGCC,CGT3,QDHES,IPRD)
5560     SQHES = SQHES + DELT*QDHES
5580     GO TO 220
5600C BURNER OFF, HEAT EXCHANGER HEATING DRAFT AIR
5620 200 CALL HEXHT(-1,CGT2,DAGHE,TMHE,AIHE,DIHE,DAWD,CAXW,CACA,CACB
56404                CACC,CGT3,QDHES,IPRD)
5660     IF(QDHES.GE.0..OR.(SQHES+DELT*QDHES).GT.HESMIN)   GO TO 210
5680     CPDA = CPMEAN(CGT2,CGT3,CACA,CACB,CACC)
5700     CGT3 = CGT3 + (SQHES + DELT*QDHES - HESMIN)/(DELT*DAWD*CPDA)
5720     QDHES = (SQHES - HESMIN)/DELT
5740 210 SQHES = SQHES + DELT*QDHES
5760C HEAT EXCHANGER HEATING OF WARM AIR
5780 220 IF(T.LE.TFAN1.OR.T.GT.TFAN2)   GO TO 260
5800     CALL AIRHT(WAT2,WAGHE,TMHE,AIHE,DIHE,WAWD,WACA,WACB,WACC,
```

TABLE A-1. (Continued)

- 7 -

```
WAFURN CONTINUED

5820&              WAT3,QDHEA,IPRD)
5840     IF(QDHEA.LE.0..OR.(SQHES-DELT*QDHEA).GT.HESMIN)   GO TO 240
5860     CPWA = CPMEAN(WAT2,WAT3,WACA,WACB,WACC)
5880     WAT3 = WAT3 + (SQHEA-DELT*QDHEA-HESMIN)/(DELT*WAWD*CPWA)
5900     QDHEA = (SQHES - HESMIN)/DELT
5920 240 SQHES = SQHES - DELT*QDHEA
5940 260 CONTINUE
5960C (CALL H.E. REGION RAD'N LOSS SUBR.)
5960     TMHE = SQHES/(WSHE*CPSHE)
6000     TMSFB = SQFBS/(WSFB*CPSFB)
6020     ITPR1 = 1.8*CGTX - 459.7
6040     ITPR2 = 1.8*TMIFB - 459.7
6060     ITPR3 = 1.8*TMSFB - 459.7
6080     ITPR4 = 1.8*TMHE - 459.7
6100     ITPR5 = 1.8*CGT1 - 459.7
6120     ITPR6 = 1.8*CGT2 - 459.7
6140     ITPR7 = 1.8*CGT3 - 459.7
6160     ITPR8 = 1.8*WAT3 - 459.7
6180     IF(NCYC.EQ.0)   GO TO 320
6200     IF(J.EQ.1)   PRINT 280,  SR,CGTX,ITPR1
6220 280 FORMAT(////2X,"STOICH. RATIO =",OPF5.2,",  ADIAB. FLAME ",
6240&           "TEMP. =",F7.1," K"/44X,I6,"   F"/14X,
6260&           "CURRENT   AVERAGE   TEMPERATURES,   DEGREES   K   ",
6280&           "(F)"/4X,"TIME,  FIREBOX  FIREBOX    HEAT    FLAME   ",
6300&           "FIREBOX    FLUE    WARM"/5X,"MIN.  REFRACT.  STEEL  ",
6320&           " EXCHANG.   ZONE     EXIT      GAS      AIR")
6340     JPR2 = J/IPR
6360     IF(J.LE.2)   GO TO 290
6380     IF(JPR2.LE.JPR1)   GO TO 320
6400     JPR1 = JPR2
6420 290 IF(IR.EQ.0)   GO TO 310
6440     PRINT 300,  T,TMIFE,TMSFB,TMHE,CGT1,CGT2,CGT3,WAT3,
6460&                ITPR2,ITPR3,ITPR4,ITPR5,ITPR6,ITPR7,ITPR8
6480 300 FORMAT(OPF8.2,F8.1,6F9.1/9X,7I9)
6500     GO TO 320
6520 310 PRINT 315,  T,TMSFB,TMHE,CGT1,CGT2,CGT3,WAT3,
6540&                 ITPR3,ITPR4,ITPR5,ITPR6,ITPR7,ITPR8
6560 315 FORMAT(OPF8.2,8X,6F9.1/16X,6I9)
6580 320 CONTINUE
6600     IF(T.GT.TFAN1.AND.T.LE.TFAN2)   SQWA = SQWA + DELT*WAWD*
6620&          CPMEAN(WAT1,WAT3,WACA,WACB,WACC)*(WAT3 - WAT1)
6640     IF(T.GT.TON.AND.T.LE.TOFF)   SQFL = SQFL + DELT*(FWD+CAWD)*
6660&                CPMEAN(CGT3,298.2,CGCA,CGCB,CGCC)*(CGT3-298.2)
6680     IF(T.LE.TON.OR.T.GT.TOFF)   SQDL = SQDL + DELT*DAWD*
6700&                CPMEAN(CGT3,CATMP,CACA,CACB,CACC)*(CGT3-CATMP)
6720     IF(T.GT.TOFF.AND.TFAN2.GT.T.AND.WAT3.LE.WATOFF)   TFAN2=T
6740     DELT = DELT/60.
6760     T = T + DELT
6780 400 CONTINUE
6800C
```

- 8 -

```
WAFURN CONTINUED

6820     QSTFBR = SQFBR - QFBRI
6840     QSTFBS = SQFBS - QFBSI
6860     QSTHES = SQHES - QHESI
6880     QSTTOT = QSTFBR + QSTFBS + QSTHES
6900     QSUM = QSTTOT + SQWA + SQDL + SQFL
6920     QFRST = QSTTOT/QINPUT
6940     IF(NCYC.GT.0)   GO TO 410
6960     IF(QFRST.LE.0.01.OR.ITER.EQ.3)   NCYC = ITER + 1
6980     GO TO 105
7000C
7020C CALCULATE & PRINT THERMAL EFFICIENCY DATA
7040 410 ETATH = 100.*SQWA/QINPUT
7060     ETADL = 100.*SQDL/QINPUT
7080     ETAFL = 100.*SQFL/QINPUT
7100     QINBTU = QINPUT/1055.056
7120     WABTU = SQWA/1055.056
7140     PRINT 415,   NCYC      '
7160 415 FORMAT(/10X,"PRINTOUT IS FOR CYCLE NO.",I2)
7180     PRINT 420,   QINPUT,QINBTU,SQWA,ETATH,WABTU,QSTTOT,
7200&                 QFRST,SQFL,ETAFL,SQDL,ETADL
7220 420 FORMAT(/"    CYCLE THERMAL RESULTS:    HEAT, J      ",
7240&           " EFFICIENCY,"/31X,"(BTU)",10X,"PERCENT"/8X,"NET ",
7260&           "HEAT INPUT:"5X,1PE10.4/30X,"(",OPF7.0,")"/6X,
7280&           "WARM AIR GAIN :",5X,1PE10.4,OPF13.2/30X,"(",F7.0,
7300&           ")"/8X,"STORED OR LOST:"/12X,"COMPONENTS",6X,1P
7320&           E10.4,2PF13.2/12X,"FLUE GASES",6X,1PE10.4,OPF13.2/
7340&           12X,"DRAFT  AIR",6X,1PE10.4,OPF13.2)
7360     SR = SR + DSR
7380 500 CONTINUE
7400     END
7420
7440
7460
8000 FUNCTION XTRP(TX,T,Q)
8020C
8040C PERFORMS LINEAR INTERPOLATION
8060C
8080 DIMENSION T(1),Q(1)
8100 QX=Q(1)
8120 IF(TX.LE.T(1))  GO TO 200
8140 DO 100 I=2,20
8160 I1=I-1
8180 I2=I
8200 IF(TX.GE.T(I1).AND.TX.LE.T(I))  GO TO 150
8220 100 CONTINUE
8240 150 QX=Q(I1)+(Q(I2)-Q(I1))*(TX-T(I1))/(T(I2)-T(I1))
8260 200 XTRP=QX
8280 RETURN
8300 END
8320
```

TABLE A-1. (Continued)

WAFURN CONTINUED

```
8340
8360
8500 FUNCTION CPMEAN(T1,T2,A,B,C)
8520C
8540C CALCULATES MEAN GAS SPECIFIC HEAT (J/KG-K) BETWEEN
8560C       TEMPERATURES T1 AND T2 (K)
8580C
8600 CPMEAN = 4186.8*(A + B*(T2 + T1)/2. + C/(T1*T2))
8620 RETURN
8640 END
8660
8680
8700
9000 SUBROUTINE CPAIR(WRH,CA,CB,CC)
9020C
9040C CALCULATES COEFFICIENTS A, B, C FOR MOIST AIR SPECIFIC HEAT
9060C       CPM(CAL/G-K) = A + B*T + C/T**2   AT  TEMPERATURE T(K)
9080C
9100 FAC = 1./(1. + WRH)
9120 CA = FAC*(0.2219 + 0.4052*WRH)
9140 CB = FAC*1.0E-05*(2.602 + 13.654*WRH)
9160 CC = FAC*(-324.)
9180 RETURN
9200 END
9220
9240
9260
9500 SUBROUTINE CPCG(SR,SXW,CA,CB,CC)
9520C
9540C CALCULATES COEFFICIENTS A, B, C FOR EQUILIBRIUM DRY OIL/
9560C       DRY AIR COMBUSTION PRODUCTS WITH ADDED MOISTURE
9580C       CPM(CAL/G-K) = A + B*T + C/T**2  AT TEMPERATURE T(K)
9600C
9620 DIMENSION  TSR(8), TA(8), TB(8), TC(8)
9640 DATA  TSR/1.0, 1.2, 1.4, 1.6, 1.8, 2.0, 2.2, 2.4/
9660 DATA  TA/ .2538, .2491, .2454, .2425, .2403, .2385, .237, .2358/
9680 DATA  TB/ 4.23, 4.02, 3.83, 3.69, 3.57, 3.47, 3.39, 3.33/
9700 DATA  TC/-1158,-1102,-1006,-926,-862,-809,-765,-730/
9720C
9740 FAC = 1. - SXW
9760 CA = FAC*XTRP(SR,TSR,TA) + 0.4052*SXW
9780 CB = FAC*1.0E-05*XTRP(SR,TSR,TB) + 1.3654E-04*SXW
9800 CC = FAC*XTRP(SR,TSR,TC)
9820 RETURN
9840 END
9860
9880
9900
10000 SUBROUTINE HEXHT(SR,TIN,GG,TM,A,D,W,XW,CA,CB,CC,TOUT,QDOT,IPR)
10010       DIMENSION  TG(25),DTG(25),TSR(8),TPR(8)
```


WAFURN CONTINUED

```
10020C
10030C SOLVES HEAT TRANSFER INSIDE METAL HEAT EXCHANGER
10040C
10050    DATA TSR/1.0, 1.2, 1.4, 1.6, 1.8, 2.0, 2.2, 2.4/
10060    DATA TPR/.2361, .2136, .1868, .1649, .149, .1331, .1224,
10070&           .1116/
10080C
10090 CK = 0.0
10100 IF(SR.GE.1.)    CK = SQRT(0.574*D*XTRP(SR,TSR,TPR))
10110 10 DELG = 10.
10120 TG(1) = TOUT
10130 IF(SR.GE.1..AND.TOUT.LE.TM)    TG(1) = TM + 1.
10140C
10150 DO 50  J=1,24
10160 TAV = (TIN + TG(J))/2.
10170 TF = (TM+TAV)/2.
10180 FT = (TAV/TF)**0.8
10190 FPP = (1. + 0.58*XW)*(0.195 + 1.55E-05*1.8*TF -
10200&          24300./(1.8*TF)**2)
10210 UG = 20.257*FPP*FT*GG**0.8/D**0.2
10220    UG = 1.5*UG
10230 IF (SR.LE.0.)    GO TO 15
10240 TRATIO = (TIN - TM)/(TG(J) - TM)
10250 IF(TRATIO.GT.0.0)    DTLM = (TIN-TG(J))/ALOG(TRATIO)
10260 UR = CK*(0.0572*DTLM + 0.096*TM - 47.3)
10270 USUM = UG + UR
10280 IF(UR.GT.0.)    UG = USUM
10290 15 CPM = CPMEAN(TIN,TG(J),CA,CB,CC)
10300 TDUM = (TIN*(W*CPM-UG*A/2.)+UG*A*TM)/(W*CPM+UG*A/2.)
10310 QDUM = W*CPM*(TIN - TDUM)
10320 QMAX = W*CPM*(TIN - TM)
10330 IF(ABS(QDUM).LE.ABS(QMAX))    GO TO 20
10340 QDUM = QMAX
10350 TDUM = TIN - QDUM/(W*CPM)
10360 20 CONTINUE
10370 IF(IPR.LE.0)    GO TO 40
10380 IF(J.EQ.1)  PRINT 22,
10390 22 FORMAT(" SUBROUTINE HEXHT"/"   J     TG(J)       TDUM",
10400&          "          CPM          QDUM")
10410 PRINT 32,  J,TG(J),TDUM,CPM,QDUM
10420 32 FORMAT(I4,1P4E10.3)
10430 40 CONTINUE
10440 DTG(J) = TG(J) - TDUM
10450 IF(ABS(DTG(J)).LE.2.)    GO TO 100
10460 CALL TADJ(J,2,DTG,TG,DELG,X1,Y1,X2,Y2,S1,S2,0S,IF)
10470 50 CONTINUE
10480 100 QDOT = QDUM
10490 TOUT = TDUM
10500 RETURN
10510 END
```

TABLE A-1. (Continued)

WAFURN CONTINUED

```
10520
10530
10540
11000 SUBROUTINE RFBHT(SR,TIN,GG,TMI,TMS,AI,AS,DI,DS,RR,W,XW,
11010&      CA,CB,CC,TBUT,QDBT,IPR)
11020C
11030C SOLVES HEAT TRANSFER INSIDE REFRACTORY-LINED FIREBOX
11040C
11050      DIMENSION TG(25),TI(25),DTG(25),DTI(25),TSR(8),TPR(8)
11060C
11070  DATA TSR/1.0, 1.2, 1.4, 1.6, 1.8, 2.0, 2.2, 2.4/
11080  DATA TPR/.2361, .2136, .1868, .1649, .149, .1331,
11090&          .1224, .1116/
11100C
11110 CK = 0.0
11120 IF(SR.GE.1.)   CK = SQRT(0.574*DI*XTRP(SR,TSR,TPR))
11130 D1 = -150.
11140 D3 = -150.
11150 10 TG(1) = TBUT
11160 IF(SR.GE.1..AND.TBUT.LE.TMI)   TG(1) = TMI + 1.
11170 TI(1) = TMI
11180 IIG = 0
11190 III = 0
11200C
11210 DO 50   J=1,24
11220 JLI = J + 1
11230 JLG = J + 1
11240 TAV = (TIN +TG(J))/2.
11250 TF = (TI(J) + TAV)/2.
11260 FT = (TAV/TF)**0.8
11270 FPP = (1. + 0.58*XW)*(0.195 + 1.8*1.55E-05*TF -
11280&          24300./(1.8*TF)**2)
11290 UG = 20.257*FPP*FT*GG**0.8/DI**0.2
11300   UG = 1.5*UG
11310 IF(SR.LT.1.)   GO TO 15
11320 TRATIO = (TIN -TMI)/(TG(J) - TMI)
11330 IF(TRATIO.GT.0.0)   DTLM = (TIN-TG(J))/ALOG(TRATIO)
11340 UR = CK*(0.0572*DTLM + 0.096*TMI -47.3)
11350 USUM = UG + UR
11360 IF(UR.GT.0.)   UG = USUM
11370 15 CPM = CPMEAN(TIN,TG(J),CA,CB,CC)
11380 TDUM = (TIN*(W*CPM-UG*AI/2.)+UG*AI*TI(J))/(W*CPM+UG*AI/2.)
11390 QDUMI = W*CPM*(TIN-TDUM)
11400 QMAX = W*CPM*(TIN - TMI)
11410 IF(ABS(QDUMI).LE.ABS(QMAX))   GO TO 20
11420 QDUMI = QMAX
11430 TDUM = TIN - QDUMI/(W*CPM)
11440 20 CONTINUE
11450 TDUMI = TMS + QDUMI*RR/AS
11460 IF(IPR.LE.0)   GO TO 40
```


WAFURN CONTINUED

```
11470 IF (J.EQ.1)   PRINT 32,
11480 32 FORMAT(" SUBROUTINE RFBHT"/"   J     TG(J)       TDUM",
11490&          "        CPM        QDUMI       TI(J)       TDUMI")
11500 PRINT 42,   J,TG(J),TDUM,CPM,QDUMI,TI(J),TDUMI
11510 42 FORMAT(I4,1P6E10.4)
11520 40 CONTINUE
11530 DTG(J) = TG(J) - TDUM
11540 DTI(J) = TI(J) - TDUMI
11550 IF(J.GT.2.AND.ABS(DTG(J)).LT.1.)   IIG = 1
11560 IF(IIG.NE.0)   JLI = J - 1
11570 IF(J.GT.2.AND.ABS(DTI(J)).LT.1.)   III = 1
11580 IF(III.NE.0)   JLG = J - 1
11590 IF(IIG.EQ.0) CALL TADJ(J,JLG,DTG,TG,D1,X1,Y1,X2,Y2,S1,S2,B2,N2)
11600 IF(IPR.GT.0)   PRINT 52,
11610&          J,N2,S1,S2,B2,X1,Y1,X2,Y2,TG(J),TG(J+1)
11620 52 FORMAT(2I4,0P3F4.0/0P6E11.4)
11630 IF(IIG.EQ.1)   TG(J+1) = TG(J)
11640 IF(III.EQ.0) CALL TADJ(J,JLI,DTI,TI,D3,X3,Y3,X4,Y4,S3,S4,B4,N4)
11650 IF(IPR.GT.0)   PRINT 52,
11660&          J,N4,S3,S4,B4,X3,Y3,X4,Y4,TI(J),TI(J+1)
11670 IF(III.EQ.1)   TI(J+1) = TI(J)
11680 IF(IIG.EQ.1.AND.III.EQ.1)   GO TO 100
11690 50 CONTINUE
11700 100 QDBT = QDUMI
11710     TBUT = TDUM
11720     TMI = TDUMI
11730 RETURN
11740 END
11750
11760
11770
12000 SUBROUTINE AIRHT(TIN,GA,TM,A,D,W,CA,CB,CC,TBUT,QDBT,IPR)
12020   DIMENSION  TA(25),DTA(25)
12040C
12060C SOLVES HEAT TRANSFER OUTSIDE FIREBOX OR HEAT EXCHANGER
12080C
12100 AMU = 1.86E-05
12120 FA = 0.587*(GA*D/AMU)**0.1667
12140 FD = 1.00
12160 DELA = 25.
12180 TA(1) = TBUT
12200C
12220 DO 50  J=1,24
12240 TF = (TM + (TIN + TA(J))/2.)/2.
12260 FPP = 0.0695 + 1.8*4.55E-05*TF - 1279./(1.8*TF)**2
12280 UA = 57.429*FPP*FD*FA*(GA**0.61/D**0.39)
12300   UA = 1.5*UA
12320 CPM = CPMEAN(TIN,TA(J),CA,CB,CC)
12340 TDUM = (TIN*(W*CPM-UA*A/2.)+UA*A*TM)/(W*CPM+UA*A/2.)
12360 QDUM = W*CPM*(TDUM - TIN)
```

TABLE A-1. (Continued)


```
WAFURN CONTINUED

12380 QMAX = W*CPM*(TM - TIN)
12400 IF(ABS(QDUM).LE.ABS(QMAX))   GO TO 20
12420 QDUM = QMAX
12440 TDUM = TIN + QDUM/(W*CPM)
12460 20 IF(IPR.LE.0)   GO TO 40
12480 IF(J.EQ.1)   PRINT 22,
12500 22 FORMAT(" SUBROUTINE AIRHT"/"   J     TA(J)       TDUM",
12520&           "          CPM        QDUM")
12540 PRINT 32,  J,TA(J),TDUM,CPM,QDUM
12560 32 FORMAT(I4,1P4E10.3)
12580 40 CONTINUE
12600 DTA(J) = TA(J) - TDUM
12620 IF(ABS(DTA(J)).LE.1.)   GO TO 100
12640 CALL TADJ(J,2,DTA,TA,DELA,X1,Y1,X2,Y2,S1,S2,0S,IF)
12660 50 CONTINUE
12680 100  QDOT = QDUM
12700      TOUT = TDUM
12720 RETURN
12740 END
12760
12780
12800
13000 SUBROUTINE TADJ(I,IL,DE,T,DT,X1,Y1,X2,Y2,S1,S2,0S,IFP)
13020C
13040C   METHOD OF FALSE POSITION FOR ITERATION CONVERGENCE
13060C
13080    DIMENSION   DE(25),T(25)
13100C
13120    IF(I.GT.1)   GO TO 20
13140    S1 = 1.
13160    IF(DE(1).LT.0.)   S1 = -1.
13180    0S = -S1
13200    T(2) = T(1) + S1*DT
13220    X1 = T(1)
13240    Y1 = DE(1)
13260    IFP = 0
13280    GO TO 100
13300 20 S2 = 1.
13320    IF(DE(I).LT.0.)   S2 = -1.
13340    IF(S1.NE.S2)   IFP = 1
13360    IF(I.GT.IL.AND.IFP.EQ.1)   GO TO 40
13380    X2 = T(I)
13400    Y2 = DE(I)
13420    GO TO 50
13440 40 IF(S2.NE.0S)   GO TO 60
13460    X1 = T(I)
13480    Y1 = DE(I)
13500    GO TO 50
13520 60 X2 = T(I)
13540    Y2 = DE(I)
```



```
WAFURN CONTINUED

13560 50 B = (Y2*X1 - Y1*X2)/(X1 - X2)
13580    SM = (Y1 - B)/X1
13600    T(I+1) = -B/SM
13620    IF(ABS(DE(I)).GT.10.)   T(I+1) = (T(I+1) + T(I))/2.
13640 100 RETURN
13660    END
13680
13700
13720
14000  SUBROUTINE  REFKUL(IRC,TS,DS,TI,DI,AI,SQ,C,TP,DP,AP,RR)
14020C
14040C  CALCULATES REFRACTORY COOLING PARAMETERS
14060C
14080 DD = (DS - DI)/100.
14100 JLIM = 100
14120 IF(IRC.GT.1)   GO TO 40
14140 SURF = TP
14160 SHELL = TS
14180 HEAT = SQ
14200 FRR = RR
14220 DP = DI + DD
14240 JLOW = 1
14260 JLIM = 10
14280C
14300 40 DELTAQ = HEAT - SQ
14320 DO 60   J=JLOW,JLIM
14340 IF(J.GT.JLOW)   DP = DP + DD
14360 JLOW = J
14380 CR = C*(DP**2 - DI**2)/(DS**2 - DI**2)
14400 T = SHELL + (SURF - SHELL)*ALOG(DP/DS)/ALOG(DI/DS)
14420 DQ = CR*(SURF-SHELL)*((DP*(ALOG(DP/DS)-1.)-DI*(ALOG(DI/DS)-1.)
14440&     ((DP-DI)*ALOG(DI/DS))) + CR*(SHELL - (T+TI)/2.)
14460 IF(IRC.GT.1.AND.DQ.GE.DELTAQ)   GO TO 60
14480 60 CONTINUE
14500 80 TP = T
14520 AP = AI*DP**2/DI**2
14540 RR = FRR*DP*ALOG(DP/DI)/(DS*ALOG(DS/DI))
14560C
14580 100 RETURN
14600 END
14620
14640
14660
15000 SUBROUTINE DRAFT(SR,A,H1,H2,T1,T2,T3,TA,XW,WD)
15020C
15040C    CALCULATES DRAFT AIR FLOWRATE INTO FIREBOX
15060C
15080    M = 1./((1. - XW)/28.96 + XW/18.02)
15100    TB1 = (T1 + 2.*T2 + T3)/4.
15120    TB2 = (T2 + T3 + 2.*TA)/4.
```

TABLE A-1. (Continued)

WAFURN CONTINUED

```
15140     RH01 = 12.193*M/TB1
15160     RH02 = 12.193*M/TB2
15180     RH0A = 12.193*M/TA
15200     DP1 = 9.805*H1*RH01*(T1-T3)/(T1+2.*T2+T3)
15220     DP2 = 9.805*H2*RH02*(T2+T3-2.*TA)/(T2+T3+2.*TA)
15240     WD = 0.0
15260     IF((DP1+DP2).GT.0.0)    WD = .6*A*SR*SQRT(2.*RH0A*(DP1+DP2))
15280 RETURN
15300 END
15320
15340
15360
16000     SUBROUTINE HIFIRE(N,TH,TC,F1,F2,F3,C1,C2,C3,C4,C5,C6,Q1,Q2)
16020C
16040     C = 1.0
16060     IF(N.GT.1)    GO TO 40
16080     FD1 = F1
16100     FD2 = F2
16120     FD3 = F3
16140     CD1 = C1
16160     CD2 = C2
16180     CD3 = C3
16200     CD4 = C4
16220     CD5 = C5
16240     CD6 = C6
16260     Q1 = Q1*(TH + 1.5*( TC - TH))/TC
16280     Q2 = Q2*(TH + 1.5*(TC -TH))/TC
16300     GO TO 100
16320 40  IF(N.GT.2)    GO TO 60
16340     F1 = FD1
16360     F2 = FD2
16380     F3 = FD3
16400     GO TO 100
16420 60  IF(N.EQ.3)    GO TO 90
16440     C = 1.5
16460     N = 5
16480 90  F1 = C*FD1
16500     F2 = C*FD2
16520     F3 = C*FD3
16540     C1 = C*CD1
16560     C2 = C*CD2
16580     C3 = C*CD3
16600     C4 = C*CD4
16620     C5 = C*CD5
16640     C6 = C*CD6
16660 100 RETURN
16680     END
```

TABLE A-2. SAMPLE TABULATION FROM THE WAFURN COMPUTER PROGRAM FOR A 12-MINUTE FIRING CYCLE IN A LENNOX MODEL OF7 FURNACE CONFIGURATION

W A R M A I R O I L-F U P N A C E C Y C L E A N A L Y S I S

ANALYSIS DATE: DEC 05, 1974

FURNACE DESIGN DATA:	FIREBOX REFRACTORY	FIREBOX STEEL	HEAT EXCHANGER
DIAMETER,M :	2.6350E-01	3.0480E-01	1.4000E-01
MASS,KG:	1.8600E+00	4.5400E+00	2.1000E+01
H.T. AREA,M2:	3.0680E-01	3.6500E-01	2.2500E+00
INT. C.S.,M2:	5.4500E-02		2.5000E-02
EXT. C.S.,M2:		1.4300E-01	9.9000E-02
INIT. TEMP.,K :	450.00	375.00	300.00

FB-HE HT. = 0.50 M, HE-BC HT. = 1.50 M, C.A. AREA = 0.00130 M2

WARM AIR FLOWRATE,M3/S: 0.5000E+00 INLET TEMP.,K: 293.20
KG/S: 6.0076E-01

INPUT FUEL & COMBUSTION AIR(@ SR=1.2):

	EMULSION	DRY OIL	COMB. AIR
FLOWRATE,M3/S:	1.0000E-06		1.1396E-02
KG/S:	8.4500E-04	8.4500E-04	1.4725E-02
MOISTURE,KG/S:	0.0000E+00		3.2611E-03
INIT. TEMP.,K:	273.20	273.20	273.20

RECIRCULATED FLUE GAS,%: 00.00

OUTDOOR AMBIENT TEMP.,K: 273.20

CYCLE TIMING (MINUTES):	CYCLE	BURNER	W.A. FAN
ON :	0.00	0.00	1.00
OFF:	12.00	4.00	@ 320.0 K

MARCHING INTERVAL,MIN: 0.100

STOICH. RATIO = 1.20, ADIAB. FLAME TEMP. = 2080.8 K
3285 F

	CURRENT	AVERAGE	TEMPERATURES, DEGREES K (F)				
TIME, MIN.	FIREBOX REFFACT.	FIREBOX STEEL	HEAT EXCHANG.	FLAME ZONE	FIREBOX EXIT	FLUE GAS	WARM AIR
0.10	1777.8	465.9	345.7	2080.8	1995.9	570.0	319.2
	2740	378	162	3285	3133	566	114
0.20	1823.4	465.9	361.5	2080.8	1993.0	579.4	319.2
	2822	378	191	3285	3127	583	114
0.50	1823.3	465.9	408.4	2080.8	1993.0	608.2	319.2
	2822	378	275	3285	3127	635	114
1.00	1823.3	465.9	484.6	2080.8	1993.0	656.1	319.2
	2822	378	412	3285	3127	721	114
1.50	1812.9	389.3	416.4	2080.8	1989.5	628.0	373.1
	2803	240	289	3285	3121	670	211
2.00	1804.9	347.7	392.6	2080.8	1986.9	610.0	353.9
	2789	166	247	3285	3116	638	177
2.50	1800.5	324.5	383.6	2080.8	1985.5	602.9	346.6
	2781	124	230	3285	3114	625	164
3.00	1798.3	311.3	379.8	2080.8	1984.7	600.4	343.5
	2777	100	223	3285	3112	621	158
3.50	1796.9	303.7	378.1	2080.8	1984.2	599.3	342.1
	2774	86	220	3285	3111	619	156
4.00	1796.1	299.3	377.3	2080.8	1984.0	598.8	341.4
	2773	79	219	3285	3111	618	154
5.00	1269.1	334.7	330.7	273.2	316.9	326.0	319.3
	1824	142	135	32	110	127	115
6.00	1122.2	366.2	330.7	273.2	312.7	324.5	319.3
	1560	199	135	32	103	124	115
7.00	1035.9	392.4	330.5	273.2	309.9	323.4	319.3
	1404	246	135	32	98	122	115
8.00	950.7	414.6	330.4	273.2	307.0	322.3	319.3
	1251	286	135	32	92	120	115
9.00	894.6	433.7	330.3	273.2	304.9	321.5	319.3
	1150	320	134	32	89	119	115
10.00	852.9	450.3	330.2	273.2	303.3	320.9	319.3
	1075	350	134	32	86	117	115
11.00	811.5	464.7	330.0	273.2	301.7	320.2	319.3
	1000	376	134	32	83	116	115
12.00	784.1	477.4	329.9	273.2	300.6	319.7	319.3
	951	399	134	32	81	115	115

PRINTOUT IS FOR CYCLE NO. 4

CYCLE THERMAL RESULTS:	HEAT, J (BTU)	EFFICIENCY, PERCENT
NET HEAT INPUT:	8.3401E+06 (7905.)	
WARM AIR GAIN :	6.8601E+06 (6502.)	82.25
STORED OR LOST:		
COMPONENTS	6.8034E+04	0.82
FLUE GASES	1.3762E+06	16.50
DRAFT AIR	3.4779E+04	0.42

STOICH. RATIO = 1.50, ADIAB. FLAME TEMP. = 1809.6 K
2797 F

	CURRENT	AVERAGE	TEMPERATURES, DEGREES K (F)				
TIME, MIN.	FIREBOX REFFACT.	FIREBOX STEEL	HEAT EXCHANG.	FLAME ZONE	FIREBOX EXIT	FLUE GAS	WARM AIR
0.10	1517.7	436.8	342.6	1809.6	1749.3	603.4	317.8
	2272	326	156	2797	2689	635	112
0.20	1557.3	436.8	357.6	1809.6	1747.1	617.8	317.8
	2343	326	183	2797	2685	652	112
0.50	1557.6	436.8	401.8	1809.6	1747.1	646.4	317.8
	2344	326	263	2797	2685	703	112
1.00	1557.6	436.8	473.3	1809.6	1747.1	693.1	317.8
	2344	326	392	2797	2685	787	112
1.50	1547.8	373.6	408.7	1809.6	1744.6	665.3	367.5
	2326	212	275	2797	2680	737	201
2.00	1540.5	339.0	386.5	1809.6	1742.9	647.6	349.8
	2313	150	236	2797	2677	706	170
2.50	1536.2	319.5	378.3	1809.6	1741.9	640.9	343.2
	2305	115	221	2797	2675	693	158
3.00	1533.8	308.4	375.0	1809.6	1741.3	638.5	340.5
	2301	95	215	2797	2674	689	153
3.50	1532.4	302.0	373.5	1809.6	1741.0	637.4	339.3
	2298	83	212	2797	2674	687	150
4.00	1531.6	298.3	372.8	1809.6	1740.8	636.9	338.7
	2297	77	211	2797	2673	686	149
5.00	1097.8	327.6	328.7	273.2	310.3	322.0	317.8
	1516	129	131	32	98	119	112
6.00	976.1	353.6	328.5	273.2	306.5	320.5	317.8
	1297	176	131	32	91	117	112
7.00	892.9	375.2	328.4	273.2	303.6	319.3	317.8
	1147	215	131	32	86	115	112
8.00	834.3	393.5	328.2	273.2	301.4	318.4	317.8
	1042	248	131	32	82	113	112
9.00	788.0	409.3	328.1	273.2	299.6	317.6	317.8
	958	277	130	32	79	112	112
10.00	753.7	422.9	327.9	273.2	298.2	317.0	317.8
	896	301	130	32	77	110	112
11.00	719.6	434.8	327.7	273.2	296.8	316.4	317.8
	835	322	130	32	74	109	112
12.00	697.0	445.2	327.6	273.2	295.8	315.9	317.8
	794	341	129	32	72	108	112

PRINTOUT IS FOR CYCLE NO. 4

CYCLE THERMAL RESULTS:	HEAT, J (BTU)	EFFICIENCY, PERCENT
NET HEAT INPUT:	8.3684E+06 (7932.)	
WARM AIR GAIN :	6.4201E+06 (6085.)	76.72
STORED OR LOST:		
COMPONENTS	4.9988E+04	0.60
FLUE GASES	1.8610E+06	22.24
DRAFT AIR	3.7972E+04	0.45

TABLE A-2. (Continued)

STOICH. RATIO = 1.80, ADIAB. FLAME TEMP. = 1605.4 K
2430 F

TIME, MIN.	CUPRENT FIPEBOX REFPACT.	AVEPAGE FIPEBOX STEEL	HEAT EXCHANG.	FLAME ZONE	TEMPERATUPES, DEGREES K (F) FIPEBOX EXIT	FLUE GAS	WARM AIR
0.10	1326.8	415.2	339.7	1605.4	1560.7	623.8	316.4
	1928	287	151	2430	2349	663	109
0.20	1359.1	415.2	353.8	1605.4	1559.1	632.9	316.4
	1986	287	177	2430	2346	679	109
0.50	1360.1	415.2	395.6	1605.4	1559.1	660.6	316.4
	1988	287	252	2430	2346	729	109
1.00	1360.1	415.2	462.6	1605.4	1559.1	705.3	316.4
	1988	287	372	2430	2346	809	109
1.50	1351.1	361.9	401.6	1605.4	1557.3	678.4	362.5
	1972	191	263	2430	2343	761	192
2.00	1343.9	332.5	380.9	1605.4	1556.0	661.5	346.1
	1959	138	225	2430	2341	730	163
2.50	1339.8	315.8	373.4	1605.4	1555.3	655.2	340.1
	1951	108	212	2430	2339	719	152
3.00	1337.4	306.3	370.4	1605.4	1554.9	652.9	337.7
	1947	91	206	2430	2339	715	148
3.50	1336.1	300.8	369.1	1605.4	1554.7	651.9	336.6
	1945	81	204	2430	2338	713	146
4.00	1335.3	297.6	368.5	1605.4	1554.5	651.4	336.1
	1943	76	203	2430	2338	712	145
5.00	971.1	322.3	326.7	273.2	305.2	318.5	316.4
	1288	120	128	32	89	113	109
6.00	868.1	344.2	326.5	273.2	301.7	317.0	316.4
	1102	159	128	32	83	110	109
7.00	797.8	362.4	326.4	273.2	299.1	315.9	316.4
	976	192	127	32	78	108	109
8.00	748.4	377.9	326.2	273.2	297.2	315.1	316.4
	887	220	127	32	75	107	109
9.00	709.4	391.2	326.0	273.2	295.6	314.3	316.4
	817	244	127	32	72	106	109
10.00	680.5	402.7	325.8	273.2	294.4	313.8	316.4
	765	265	126	32	70	105	109
11.00	651.7	412.6	325.6	273.2	293.1	313.2	316.4
	713	283	126	32	67	103	109
12.00	632.7	421.4	325.4	273.2	292.3	312.7	316.4
	679	298	125	32	66	103	109

PRINTOUT IS FOR CYCLE NO. 4

CYCLE THERMAL RESULTS:	HEAT, J (BTU)	EFFICIENCY, PERCENT
NET HEAT INPUT:	8.3588E+06 (7923.)	
WARM AIR GAIN :	6.0153E+06 (5701.)	71.96
STOPED OR LOST:		
COMPONENTS	3.6435E+04	0.44
FLUE GASES	2.2677E+06	27.13
DRAFT AIR	4.0126E+04	0.48

STOICH. RATIO = 2.10, ADIAB. FLAME TEMP. = 1443.8 K
2139 F

TIME, MIN.	CUPRENT FIPEBOX REFPACT.	AVEPAGE FIPEBOX STEEL	HEAT EXCHANG.	FLAME ZONE	TEMPERATURES, DEGREES K (F) FIPEBOX EXIT	FLUE GAS	WARM AIR
0.10	1176.9	391.6	343.2	1443.8	1409.5	629.9	319.9
	1658	245	158	2139	2077	674	116
0.20	1204.1	391.6	356.6	1443.8	1408.3	638.6	319.9
	1707	245	182	2139	2075	689	116
0.50	1205.1	391.6	395.8	1443.8	1408.2	664.8	319.9
	1709	245	252	2139	2075	737	116
1.00	1205.1	391.6	458.3	1443.8	1408.2	706.8	319.9
	1709	245	365	2139	2075	812	116
1.50	1197.7	349.0	396.5	1443.8	1407.0	678.6	358.9
	1696	168	254	2139	2072	761	186
2.00	1190.8	325.2	376.1	1443.8	1406.1	661.7	343.0
	1683	125	217	2139	2071	731	157
2.50	1187.2	311.7	368.8	1443.8	1405.6	655.7	337.3
	1677	101	204	2139	2070	720	147
3.00	1185.1	303.9	366.0	1443.8	1405.3	653.5	335.1
	1673	87	199	2139	2069	716	143
3.50	1183.9	299.4	364.9	1443.8	1405.2	652.6	334.1
	1671	79	197	2139	2069	714	141
4.00	1183.2	296.8	364.4	1443.8	1405.1	652.2	333.7
	1669	74	196	2139	2069	714	140
5.00	849.8	318.1	331.7	273.2	300.1	319.3	319.9
	1069	112	137	32	80	115	116
6.00	764.9	336.2	331.5	273.2	297.1	317.9	319.9
	917	145	136	32	75	112	116
7.00	706.9	351.1	331.2	273.2	294.8	316.8	319.9
	812	172	136	32	70	110	116
8.00	666.3	363.8	330.9	273.2	293.1	316.0	319.9
	739	195	135	32	67	109	116
9.00	634.3	374.6	330.7	273.2	291.7	315.3	319.9
	682	214	135	32	65	107	116
10.00	610.5	384.1	330.4	273.2	290.7	314.7	319.9
	639	231	134	32	63	106	116
11.00	586.9	392.2	330.1	273.2	289.6	314.1	319.9
	596	246	134	32	61	105	116
12.00	563.5	399.4	329.8	273.2	288.5	313.5	319.9
	554	259	133	32	59	104	116

PRINTOUT IS FOR CYCLE NO. 3

CYCLE THERMAL RESULTS:	HEAT, J (BTU)	EFFICIENCY, PERCENT
NET HEAT INPUT:	8.3152E+06 (7881.)	
WARM AIR GAIN :	5.6117E+06 (5319.)	67.49
STOPED OR LOST:		
COMPONENTS	4.5752E+04	0.55
FLUE GASES	2.6127E+06	31.42
DRAFT AIR	4.5862E+04	0.55

APPENDIX B

FLUE GAS COMPOSITIONAL ANALYSIS

The sample flow train used for analyzing flue gas composition is illustrated in Fig. B-1. A 0.006 m (1/4 in) diameter stainless steel tubing sample probe was inserted near the combustor centerline, downstream of the heat exchanger. Flue gas aspirated into the sample probe flowed through a line to an air-cooled condensibles trap where particulates and heavy oils were separated out. Next, the gas passed into an ice-cooled, stainless-steel condensibles trap where most of the water and any condensible, low-volatility hydrocarbons were removed. After the condenser, the gas passed into a pyrex wool-filled glass cylinder which served as a final separator for heavy oils and particulates, and provided a visual indication of the cleanliness of the gas being admitted to the analysis instruments. Table B-1 gives a summary of the gas analysis instruments used. The gas leaving the glass wool filter was split into three parallel paths. One path led directly to the total hydrocarbon analyzer. A second path led through a Drierite bed where water was removed, and then into the series-plumbed carbon monoxide, carbon dioxide, and oxygen analyzers. The third path passed through a combined Drierite and 3 Å molecular sieve bed for total water removal, and then into the nitric oxide analyzer. The gas was pumped through the system by three diaphragm pumps located downstream of the nitric oxide analyzer, total hydrocarbon, and carbon monoxide + carbon dioxide analyzers. The system also has the capability for dilution of gas passing through the carbon monoxide, carbon dioxide, and oxygen path. The

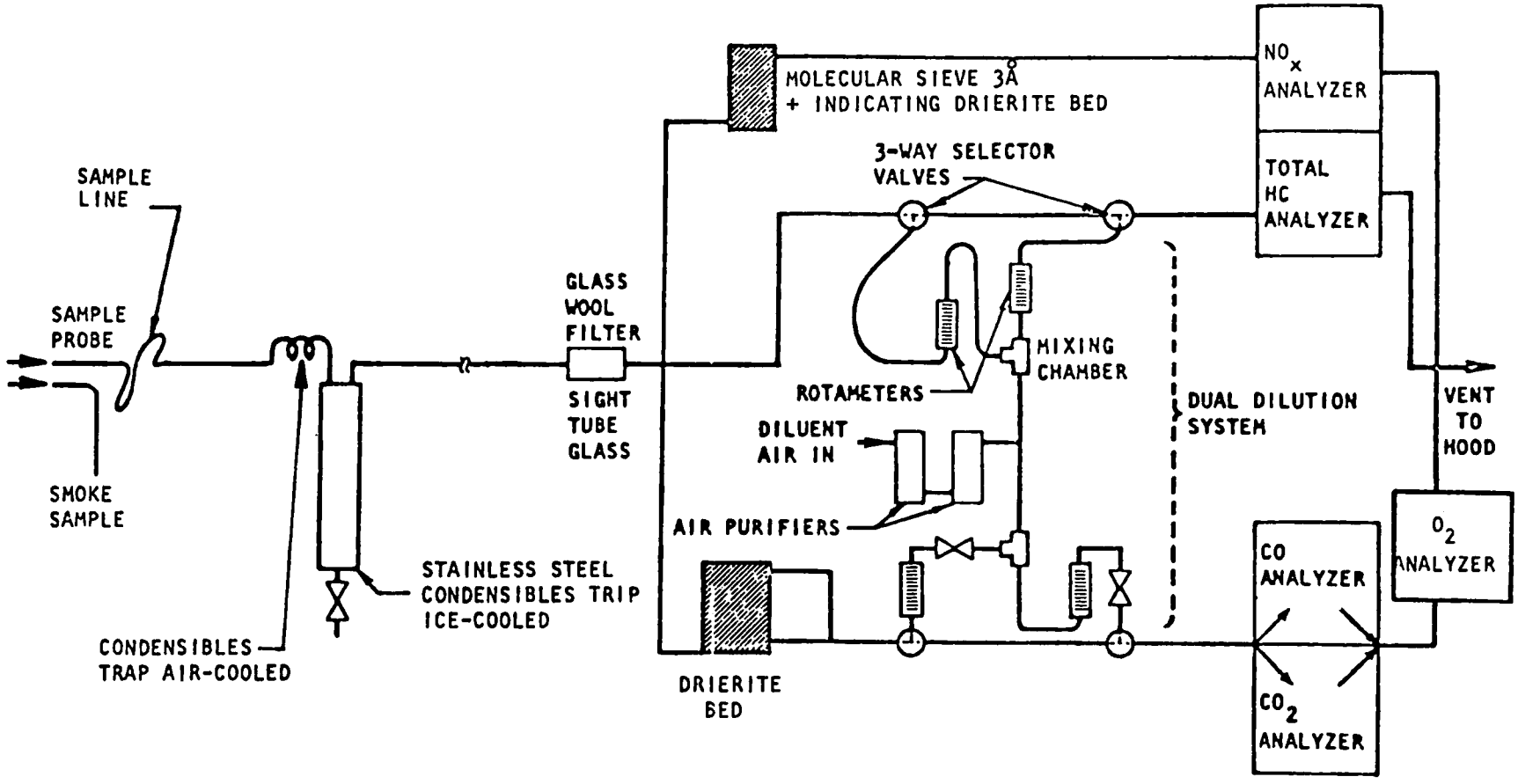

Figure B-1 Analytical system for fuel oil burner emissions analysis

Table B-1. EXHAUST ANALYSIS INSTRUMENTS

	CO	CO_2	NO	Total HC	Oxygen	Smoke
Type	MSA Nondispersive IR LIRA Model 300	MSA Nondispersive IR LIRA Model 300	MSA Nondispersive IR LIRA Model 200	MSA H_2 flame ionization detector	Beckman polarographic	Bacharach (manual)
Range	0 to 1500 ppm (mole)	0 to 20 mole %	0 to 500 ppm (mole)	0.2 to 800 ppm total HC by volume as CH_4	0 to 100%	0 to 9
Sensitivity	30 ppm minimum detectable	0.25% minimum detectable	10 ppm minimum detectable	10 ppm minimum detectable	~0.1%	1
Calibration	1000 ppm CO in N_2 standard gas	14% CO_2 in N_2 standard gas	0.82% C_2H_4 in N_2 used as simulant for 410-ppm NO standard	3% CH_4 in helium used as a standard	Air - 21% N_2 = 0%	Ten spots of monotonically varying darkness

dilution allowed use of those analytical instruments on gas samples more concentrated than the highest range of the instruments. It was achieved by admission of air metered through parallel rotameters.

When the analytical system shown in Fig. B-1 is used to analyze gases which may have been quenched before combustion was completed, there are two factors that must be considered in reducing the data: (1) only burned or partly pyrolyzed fuel is included in the analysis, since minute quantities of liquid or vapor fuel may be removed by the cold trap, and (2) water formed from hydrogen and oxygen during the combustion process is also removed from the analyzed sample by the cold trap.

Values calculated from the measured flue gas compositional data included: the overall stoichiometric ratio, the weight of nitric oxide per unit weight of burned fuel, and the weight of carbon monoxide per unit weight of burned fuel. The method of calculation to obtain these values is described below.

The calculations were based on air having the following nominal composition:

Component	Mole Percent	Wt. Percent
N_2	78.08	75.63
O_2	20.95	23.19
Noble gases (Ar,He & Ne)	0.94	1.13
CO_2	0.03	0.05
	100.00	100.00

The composition of the fuel was assumed to be characterized by the formula CH_x where, for the No. 2 fuel oil burned in this program, x = 1.814. The following symbols were used in the calculations:

AIR = moles of air to produce 100 moles of dry flue gas

FUEL = moles of fuel to produce 100 moles of dry flue gas

CO = moles of carbon monoxide in 100 moles of dry flue gas

CO_2 = moles of carbon dioxide in 100 moles of dry flue gas

NO = moles of nitric oxide in 100 moles of dry flue gas

O_2 = moles of oxygen in 100 moles of dry flue gas

HC = moles of hydrocarbon, as CH_4, in 100 moles of dry flue gas

The values of CO, CO_2, NO, O_2, and HC were obtained directly from the analysis instruments. In the following, it is assumed that all hydrogen is oxidized to water and condensed out of the system at the cold trap, prior to analysis.

An oxygen balance yields:

$$0.2095\ AIR = CO_2 - 0.0003\ AIR + 0.5\ CO + 0.25x\ (CO_2 + CO - 0.0003\ AIR) + 0.5\ NO + O_2 \qquad (B\text{-}1)$$

The left hand side of the above equation represents the total free oxygen contributed by the air. The first two items on the right side represent moles of oxygen tied up in CO_2, less the amount of CO_2 originally present in the air. The third term represents moles of oxygen tied up as carbon monoxide. The fourth term represents oxygen consumed to oxidize hydrogen, yielding the water condensed out in the cold trap. The fifth term is the oxygen tied up in nitric oxide. The sixth term is free oxygen remaining

in the sample reaching the analysis treatments. Eq. (B-1) can be arranged to yield:

$$AIR = \frac{(1 + \frac{x}{4})\ CO_2 + (1/2 + \frac{x}{4})\ CO + 1/2\ NO + O_2}{0.2095 + 0.0003 + 0.0003\ x/4} \qquad (B\text{-}2)$$

A carbon balance can be used to calculate the moles of burned fuel per 100 moles of dry flue gas:

$$FUEL = CO_2 - 0.0003\ AIR + CO \qquad (B\text{-}3)$$

The moles of air available per mole of burned fuel in the sample gas can be obtained by taking the ratio of the values from Eq. (B-2) and (B-3). AIR must be calculated first, before calculation of FUEL. If the combustion were in stoichiometric proportions, the moles of air would be, by an oxygen demand calculation:

$$AIR_{stoich} = \frac{(1 + x/4)\ FUEL}{0.2095} \qquad (B\text{-}4)$$

The stoichiometric ratio of the locally sampled burned gases is a parameter frequently used in this report. It is defined as the ratio of AIR to AIR_{stoich}:

$$SR = \frac{AIR}{AIR_{stoich}} \qquad (B\text{-}5)$$

Combination of Eq. (B-2) through (B-5) yields a direct calculation of the burned gas stoichiometric ratio in terms of the measured parameters:

$$SR = \frac{\dfrac{(1 + \frac{x}{4})\ CO_2 + (1/2 + \frac{x}{4})\ CO + 1/2\ NO + O_2}{0.2095 + 0.0003 + 0.0003x/4}}{\dfrac{(1 + \frac{x}{4})}{0.2095}\left[CO_2 + CO - 0.0003\ \dfrac{(1 + \frac{x}{4})\ CO_2 + (1/2 \times \frac{x}{4})\ CO + 1/2\ NO + O_2}{0.2095 + 0.0003 + 0.0003x/4}\right]} \qquad (B\text{-}6)$$

According the the above definition, when the sample contains just a sufficient amount of air to oxidize all of the fuel in the sample to CO_2 plus condensed-out water, then SR = 1. As a second example, if there is twice the required amount of air for complete oxidation of the fuel, then SR = 2. Note that the stoichiometric ratio, as calculated from Eq. (B-6) does not require that the products in the flue gas be in chemical equilibrium.

Note that the accuracy of the stoichiometric ratio calculation would be affected very little if all terms in Eq. (B-6) containing the factors 0.0003 and NO were ignored. These factors represent the carbon dioxide originally present in free air, and the oxygen tied up in nitric oxide, respectively.

One partially questionable assumption made in the formulation of Eq. (B-6) was that all hydrogen originally present in the fuel becomes oxidized to water and is removed in the cold trap. This was a necessary assumption, since there was no instrument available to measure the actual hydrogen content of the sample gas. The assumption is very good under the combined conditions of air-rich stoichiometric ratios (SR > 1) and chemical equilibrium. To test this assumption, a Rocketdyne thermochemical computer code was used to calculate the species concentrations under conditions of chemical equilibrium for stoichiometric ratios from 0.8 to 2.8. These calculations included the equilibrium presence of free H_2. The actual stoichiometric ratios of these combustion gases, compared to those calculated by Eq. (B-6) (which does not recognize the presence of H_2) are given in Table B-2, where it can be seen that Eq. (B-6) is quite accurate except for SR < 1. Calculated equilibrium conditions are tabulated in Tables B-3 and B-4.

TABLE B-2. VALIDITY OF STOICHIOMETRIC RATIO CONDITIONS

Actual Stoichiometric Ratio	Stoichiometric Ratio Calculated from Eq. (B-6)
0.800	0.844
1.000	1.003
1.200	1.197
1.400	1.400
1.600	1.600
2.000	2.002
2.400	2.404
2.800	2.804

The primary cause of the inaccuracy at SR < 1 is the unaccounted for presence of H_2. In nonequilibrium gases, there is likely to be H_2 present even where none would be indicated from equilibrium calculations and, at fuel-rich conditions, there could be more or less than indicated from equilibrium calculations. Because of this likelihood of nonequilibrium, no attempt was made to correct the calculations of Eq. (B-6) by means of equilibrium calculations.

The concentration of CO_2 (dry basis) in the flue gas is the parameter most often used in the space heating industry as an indication of combustion conditions. To illustrate the relationship of $\%CO_2$ to the stoichiometric ratio, equilibrium data from Table B-4 were used to calculate the curve shown in Fig. B-2; a calculated $\%O_2$ curve is also shown. A number of values of measured CO_2 concentrations in actual furnace flue gases are also plotted on Fig. B-2. The measured data are seen to be very well correlated by the calculated equilibrium curve at SR $\gtrsim$ 1.1 (the calculated maximum

TABLE B-3. EQUILIBRIUM COMBUSTION GAS PROPERTIES FOR NO. 2 DISTILLATE FUEL OIL BURNED WITH AIR

($CH_{1.814}$, 18,443 Btu/lb Net Heat of Combustion with Air at 14.67 psia)

Stoich. Ratio*	Oil + Air Inlet Temp., F	Flame Temperature, F	C_p Frozen, Btu/lb-R	γ Frozen	Viscosity, centipoise	Thermal Conductivity, Btu/hr-ft-F	Prandtl Number	Molecular Weight
0.8	0	3429	0.346	1.261	0.0666	0.0702	0.7946	27.73
1.0		3614	0.341	1.254	0.0687	0.0711	0.7984	28.80
1.2		3290	0.333	1.260	0.0653	0.0661	0.7954	29.00
1.4		2940	0.324	1.267	0.0615	0.0610	0.7915	29.03
1.6 Air		2649	0.318	1.275	0.0581	0.0567	0.7880	29.03
2.0 Rich		2209	0.307	1.288	0.0527	0.0500	0.7820	29.02
2.4		1897	0.298	1.298	0.0487	0.0452	0.7771	29.01
2.8		1663	0.291	1.308	0.0456	0.0415	0.7730	29.00
0.8	70	3778	0.347	1.261	0.0671	0.0709	0.7948	27.72
1.0		3649	0.341	1.254	0.0691	0.0715	0.7984	28.77
1.2		3336	0.333	1.259	0.0658	0.0667	0.7956	29.00
1.4		2991	0.325	1.267	0.0621	0.0617	0.7918	29.03
1.6		2703	0.318	1.274	0.0589	0.0574	0.7884	29.03
2.0		2765	0.308	1.286	0.0535	0.0509	0.7825	29.02
2.4		1955	0.299	1.297	0.0495	0.0461	0.7778	29.01
2.8		1722	0.193	1.306	0.0464	0.0425	0.7738	29.00
0.8	200	3867	0.347	1.260	0.0681	0.0720	0.7951	27.71
1.0		3709	0.342	1.257	0.0698	0.0725	0.7983	28.73
1.2		3418	0.334	1.259	0.0668	0.0678	0.7958	28.98
1.4		3085	0.326	1.266	0.0632	0.0629	0.7923	29.02
1.6		2802	0.320	1.273	0.0600	0.0588	0.7890	29.02
2.0		2369	0.309	1.284	0.0548	0.0524	0.7834	29.02
2.4		2061	0.301	1.294	0.0509	0.0477	0.7790	29.01
2.8		1831	0.295	1.303	0.0479	0.0441	0.7751	29.00

*Stoichiometric ratio is unity at 14.49 masses of air per mass of fuel, and proportionately greater than unity for increasing relative mass of air.

TABLE B-4. CALCULATED EQUILIBRIUM COMBUSTION GAS COMPOSITION, VOLUME OR MOLE PERCENT

Stoich. Ratio	Oil + Air Inlet Temp., F	H	O	Ar	OH	H_2	H_2O	CO	CO_2	NO	N_2	O_2
0.8	0	0.0630	0.0000	0.821	0.0499	2.016	12.263	7.243	8.687	0.000	68.837	0.000
1.0		0.0397	0.0313	0.866	0.2816	0.250	11.690	1.393	12.052	0.253	72.522	0.619
1.2		0.000	0.0217	0.882	0.1862	0.030	10.141	0.161	11.247	0.390	73.784	3.160
1.4		0.000	0.0000	0.890	0.0757	0.000	8.832	0.0203	9.841	0.2955	74.465	5.566
1.6		0.000	0.0000	0.895	0.0790	0.000	7.799	0.000	8.679	0.2080	74.947	7.444
2.0		0.000	0.0000	0.902	0.000	0.000	6.297	0.000	7.000	0.0829	75.603	10.107
2.4		0.000	0.0000	0.907	0.000	0.000	5.276	0.000	5.864	0.0339	76.028	11.888
2.8		0.000	0.0000	0.910	0.000	0.000	4.541	0.000	5.046	0.000	76.326	13.161
0.8	70	0.0737	0.0000	0.821	0.0613	1.996	12.271	7.268	8.659	0.017	68.901	0.000
1.0		0.0455	0.0362	0.866	0.3072	0.269	11.647	1.501	11.934	0.272	72.456	0.666
1.2		0.0000	0.0261	0.882	0.2082	0.036	10.121	0.195	11.210	0.404	73.751	3.159
1.4		0.0000	0.0000	0.890	0.0885	0.000	8.824	0.026	9.835	0.322	74.447	5.553
1.6		0.0000	0.0000	0.895	0.0351	0.000	7.795	0.000	8.678	0.223	74.933	7.432
2.0		0.0000	0.0000	0.902	0.000	0.000	6.297	0.000	7.000	0.096	75.596	10.100
2.4		0.0000	0.0000	0.907	0.000	0.000	5.276	0.000	5.863	0.041	76.023	11.884
2.8		0.0000	0.0000	0.910	0.000	0.000	4.541	0.000	5.046	0.018	76.323	13.159
0.8	200	0.0964	0.0000	0.821	0.0878	1.964	12.273	7.318	8.604	0.027	68.796	0.000
1.0		0.0577	0.0468	0.864	0.3579	0.304	11.562	1.710	11.705	0.310	73.328	0.754
1.2		0.0000	0.0356	0.882	0.2533	0.048	10.078	0.270	11.127	0.451	73.683	3.162
1.4		0.0000	0.0000	0.890	0.1157	0.000	8.806	0.042	9.816	0.373	74.405	5.526
1.6		0.0000	0.0000	0.895	0.0493	0.000	7.787	0.000	8.672	0.268	74.905	7.406
2.0		0.0000	0.0000	0.902	0.0000	0.000	6.295	0.000	7.000	0.125	75.582	10.085
2.4		0.0000	0.0000	0.907	0.0000	0.000	5.276	0.000	5.863	0.059	76.015	11.876
2.8		0.0000	0.0000	0.910	0.0000	0.000	4.541	0.000	5.046	0.028	76.319	13.154

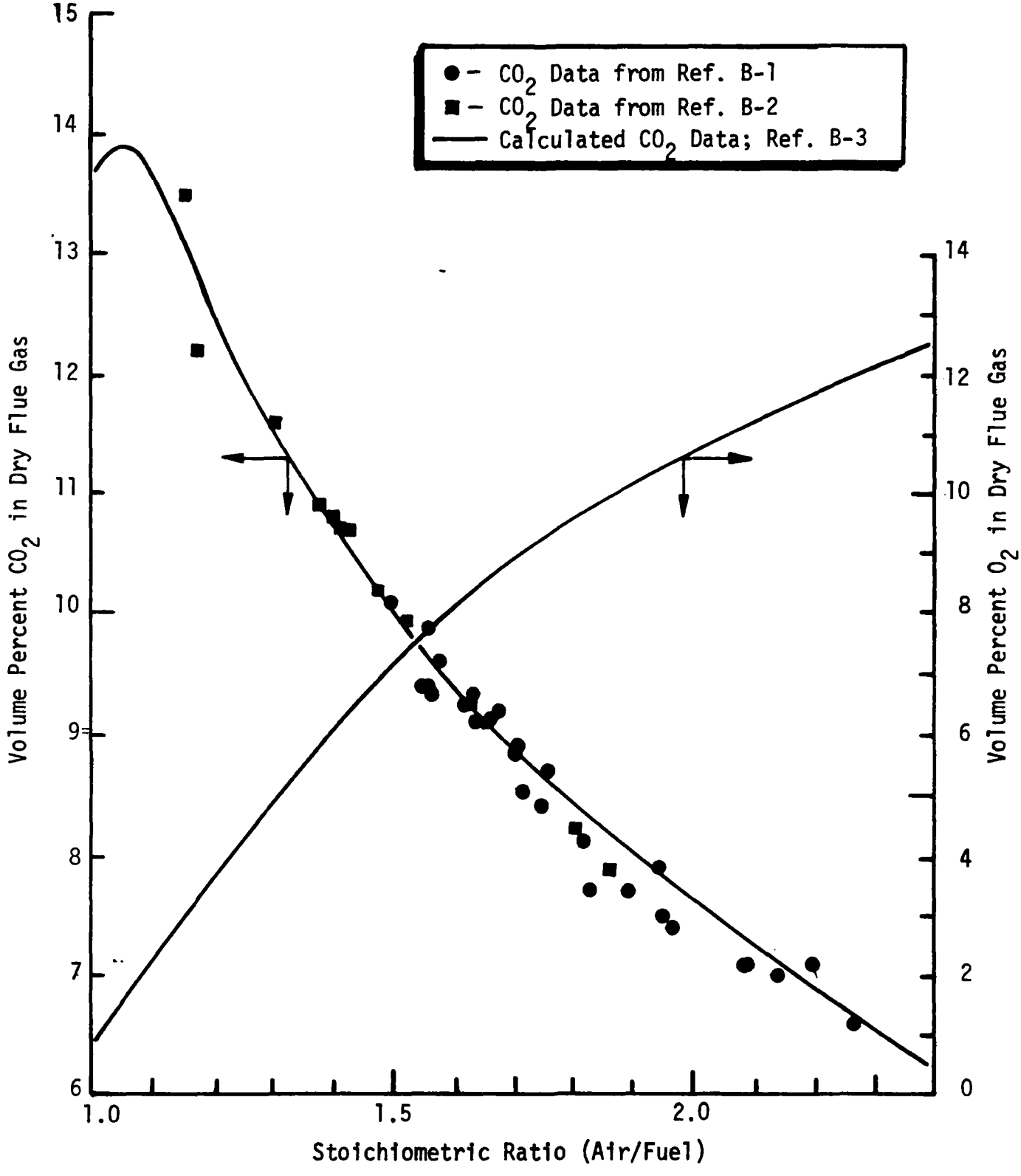

Figure B-2. Flue Gas CO_2 and O_2 Concentrations for No. 2 Fuel Oil Burned in Ambient Air at 1 ATM

CO_2 concentration as the stoichiometric condition is approached by reducing excess air is not normally observed in furnace testing).

Other parameters of interest for the flue gases are the mass ratio of nitric oxide to burned fuel, the mass ratio of carbon monoxide to burned fuel, and the mass ratio of unburned hydrocarbons (as CH_4) to burned fuel. These ratios are generally expressed herein as grams of nitric oxide per kilogram of burned fuel (g NO/kg fuel), grams of methane per kilogram of fuel (g CH_4/kg fuel), and grams of carbon monoxide per kilogram of burned fuel (g CO/kg fuel). These parameters are calculated by aid of Eq. (B-2) and (D-3) from the following relationships:

$$\frac{\text{g NO}}{\text{kg fuel}} = \frac{(1000)\ (\text{NO})\ (MW_{NO})}{(CO_2 - 0.0003\ \text{AIR} + \text{CO})\ (MW_F)} \qquad \text{(B-7)}$$

$$\frac{\text{g CO}}{\text{kg fuel}} = \frac{(1000)\ (\text{CO})\ MW_{CO}}{(CO_2 - 0.0003\ \text{AIR} + \text{CO})\ (MW_F)} \qquad \text{(B-8)}$$

$$\frac{\text{g HC}}{\text{kg fuel}} = \frac{(1000)\ (\text{HC})\ (MW_{CH_4})}{(CO_2 - 0.0003\ \text{AIR} + \text{CO})\ (MW_F)} \qquad \text{(B-9)}$$

where

MW_{NO} = molecular weight of NO = 30.01

MW_F = molecular weight of fuel

= 12.01 + 1.01 x = 13.84

MW_{CO} = molecular weight of CO = 28.01

MW_{CH_4} = molecular weight of methane = 16.04

For calculation of the above quantities, the term 0.0003 AIR can be neglected without introducing more than about 0.1-percent error in the calculations,

or AIR can be computed from Eq. B-3 and included in the calculation. The numbers given in this report include the effect of the term. The experimental data were reduced, according to the above equation, by means of a remote terminal timeshare computer program.

In addition to the gaseous pollutants described above, the smoke content of the mixed gases was also measured. The instrument utilized for this purpose was a Bacharach smoke meter. (It is manufactured by the Bacharach Instrument Company, Pittsburgh, Pennsylvania.) This is a hand-held device which, when pumped, sucks flue gases from a 1/4-inch-OD, uncooled sample probe through a piece of white filter paper; 10 strokes of the pump, over a period of about 15 seconds, causes the passage of 57.2 m^3 of flue gas per m^2 of filter paper (2250 in^3/in^2). The smoke particles deposit out on the filter paper. A reading is taken by comparing the darkness of the smoke deposition spot to a scale of 10 such calibrated spots provided with the instrument. The readings vary from 0 to 9. A reading of zero corresponds to no visually detectable deposit on the filter paper, while a reading of 9 corresponds to a dark black deposit. Intermediate readings are varying shades of black and gray, increasing in darkness with increasing reading numbers. A reading of 1 is generally accepted by the industry as a very acceptable degree of smoke. At the opposite extreme, a reading of 9, which is totally unacceptable, still does not correspond to sufficient smoke to be easily visible from observation of the exhaust stack outlet. In some instances reported herein, when the reading was obviously greater than 9, the number of strokes was halved and smoke spot reading doubled, thus extending the smoke scale to a maximum of 18.

REFERENCES

B-1. Barrett, R. E., S. E. Miller and D. W. Locklin, "Field Investigation of Emissions from Combustion Equipment for Space Heating," EPA R2-73-084a (API Publ. 4180), Environmental Protection Agency, Research Triangle Park, N. C., June 1973.

B-2. Hall, R. E., J. H. Wasser, and E. E. Berkau, "A Study of Air Pollutant Emissions from Residential Heating Systems," EPA-650/2-74-003, Environmental Protection Agency, Research Triangle Park, N. C., January 1974.

B-3. Dickerson, R. A., and A. S. Okuda, "Design of an Optimum Distillate Oil Burner for Control of Pollutant Emissions," EPA-650/2-74-047, Environmental Protection Agency, Research Triangle Park, N. C., June 1974.

APPENDIX C

DATA TABULATION: OPTIMUM BURNER EXPERIMENTS

Combustion chamber design parameters, burner operating conditions and flue gas composition data are tabulated for the optimum burner experiments described and discussed in Section V. Except where specifically called out as being different, the nominal burner firing rates were 1.0 ml/s (gph) and experiments were 10 min on/20 min off cyclical tests. All flue gas composition data, including smoke, are cycle-averaged values.

LEN. m	RUN NO.	STOIC. RATIO	CO2 %	O2 %	CO PPM	NO PPM	UHC PPM	CO GM/KGM	NO GM/KGM	UHC GM/KGM	BACH. SMOKE	TFG C
- - - - - 0.22m I.D., Air-Cooled, Tunnel-Fired - - - - -												
.75		1.11	13.9	2.3	83	46	7	1.24	0.734	0.059	0.0	260
.75	2	1.25	12.6	4.5	57	40	24	0.96	0.715	0.227	0.0	250
.75	3	1.16	13.3	3.0	53	17	21	0.83	0.294	0.183	0.0	235
.30	4	1.10	13.9	1.9	464	33	70	6.72	0.513	0.579	0.1	260
.30	5	1.12	13.8	2.4	505	18	206	7.47	0.292	1.741	1.0	280
.30	6	1.02	14.3	0.6	≥1600	49	1395	≥21.72	0.725	10.819	4.0	270
.40	7	1.07	14.1	1.6	1124	26	127	15.99	0.405	1.031	0.3	315
.40	8	1.15	13.4	3.0	776	18	493	11.83	0.309	4.290	0.3	310
.40	9	1.18	13.6	3.6	447	22	328	7.00	0.369	2.929	0.3	310
.50	10C	1.12	13.6	0.0	133	30	61	1.97	0.484	0.515	0.3	295
.50	11	1.12	13.6	0.0	118	33	78	1.76	0.532	0.660	0.0	310
.50	12	1.08	14.1	0.0	335	38	36	4.80	0.588	0.294	0.0	310
.50	13	1.05	14.5	0.0	≥1600	44	96	≥22.20	0.664	0.761	1.5	310
- - - - - - 0.28m I.D., Air-Cooled, Tunnel-Fired - - - - - -												
.30	14	1.04	14.2	0.9	≥1600	30	510	≥22.03	0.447	4.012	1.5	157
.30	15	1.14	13.3	2.8	≥1600	30	1804	≥24.12	0.486	15.539	2.0	217
.30	16	1.04	14.2	0.9	≥1600	35	538	≥22.06	0.517	4.239	2.5	203
.40	17	1.13	13.6	2.7	671	20	222	10.07	0.334	1.903	0.5	174
.40	18	1.10	13.8	2.1	≥1600	13	117	≥23.27	0.207	0.972	1.2	179
.40	19	1.16	13.0	3.1	≥1600	8	161	≥24.52	0.140	1.410	1.7	176
.50	20	1.06	13.8	1.3	≥1600	12	187	≥22.43	0.184	1.498	2.0	186
.50	21	1.22	12.6	4.1	1442	22	1751	23.28	0.381	16.153	0.2	188
.50	22	1.11	13.9	2.2	1192	19	315	17.42	0.313	2.629	1.0	183

LEN m	RUN NO.	STOIC. RATIO	CO2 %	O2 %	CO PPM	NO PPM	UHC PPM	CO GM/KGM	NO GM/KGM	UHC GM/KGM	BACH. SMOKE	TFG C
- - - - - - 0.27m I.D., Air-Cooled, Tunnel-Fired - - - - - -												
.75	23	1.03	14.7	0.7	175	38	2	2.40	0.570	0.016	0.3	181
.75	24	1.14	13.6	2.7	81	25	46	1.23	0.404	0.395	0.4	185
.75	25	1.18	13.0	3.4	228	11	198	3.57	0.187	1.766	0.2	186
- - - - - - 0.22m I.D., Fractional Insulation, Tunnel-Fired - - - - - -												
.40 3/4	26	1.12	13.8	2.5	1304	22	179	19.33	0.358	1.516	0.2	169
.40 1/2	27	1.11	13.9	2.2	1064	23	126	15.55	0.361	1.052	0.2	174
.40 1/4	28	1.11	13.9	2.3	1160	20	157	17.04	0.323	1.317	0.2	171
.40 1/4	29	1.17	13.2	3.3	253	24	184	3.92	0.400	1.630	0.5	171
.40 1/2	30	1.19	13.0	3.7	210	24	204	3.32	0.416	1.844	0.5	174
.40 3/4	31	1.20	12.9	3.8	234	26	192	3.73	0.445	1.746	0.5	178
.40 3/4	32	1.04	14.6	1.0	≥1600	40	326	≥22.08	0.600	2.571	2.0	188
.40 1/2	33	1.05	14.5	1.2	≥1600	38	393	≥22.28	0.574	3.128	2.5	186
.40 1/4	34	1.06	14.3	1.4	≥1600	35	322	≥22.50	0.542	2.587	2.0	186
- - - - - - 0.22m I.D., Insulated, Tunnel-Fired - - - - - -												
.30	35C	1.05	14.6	1.2	1483	87	3	20.67	1.302	0.024	3.0	192
.30	36	1.14	13.5	2.8	96	40	13	1.47	0.661	0.111	0.1	185
.30	37	1.09	14.4	1.8	192	47	7	2.76	0.738	0.055	1.5	192
.30	38	1.12	14.2	2.5	95	40	9	1.42	0.641	0.073	0.5	189
.40	39	1.21	13.1	3.9	35	49	3	0.57	0.845	0.024	0.1	189
.40	40	1.21	12.9	4.0	41	46	4	0.68	0.802	0.039	0.0	192
.40	41	1.05	14.1	1.1	≥1600	61	170	≥22.21	0.918	1.349	7.0	175
.50	42	1.11	13.7	2.3	422	59	2	6.22	0.939	0.015	5.0	192
.50	43	1.22	12.6	4.0	37	50	3	0.61	0.871	0.032	0.1	189
.50	44	1.14	13.4	2.8	43	54	5	0.67	0.890	0.048	0.5	194

LEN m	RUN NO.	STOIC. RATIO	CO2 %	O2 %	CO PPM	NO PPM	UHC PPM	CO GM/KGM	NO GM/KGM	UHC GM/KGM	BACH. SMOKE	TFG C
	- - - - - - 0.22m I.D., Insulated, Tunnel-Fired - - - - - -											
.75	45	1.33	11.7	5.6	11	54	6	0.21	1.041	0.059	0.0	226
.75	46	1.20	13.0	3.7	12	66	3	0.21	1.123	0.024	0.0	213
.75	47	1.10	13.9	2.1	184	72	1	2.70	1.136	0.008	4.0	209
.75	48C	1.41	11.1	6.5	17	59	5	0.34	1.194	0.050	0.0	247
.75	49C	1.07	14.1	1.5	15	73	0	0.23	1.118	0.000	0.0	230
	- - - - - - 0.17m I.D., Insulated, Tunnel-Fired - - - - - -											
.50	50	1.73	9.0	9.5	103	46	40	2.42	1.162	0.538	0.3	217
.50	51	1.36	11.4	5.9	45	68	7	0.81	1.322	0.072	0.7	213
.50	52	1.23	12.6	4.2	155	77	3	2.54	1.349	0.033	4.0	213
.40	53	1.11	13.9	2.2	401	81	5	5.89	1.273	0.042	6.0	202
.40	54	1.50	10.2	7.5	155	42	9	3.12	0.911	0.099	0.5	207
.40	55	1.77	8.7	9.8	406	16	57	9.71	0.433	0.784	0.2	200
.75	56	1.60	9.9	8.6	12	64	13	0.28	1.491	0.159	0.0	247
.75	57	1.32	12.0	5.5	15	75	1	0.28	1.409	0.010	0.0	234
.75	58	1.17	13.7	3.4	21	89	1	0.34	1.482	0.009	0.3	224
.30	59	1.60	9.8	8.6	1153	10	156	24.67	0.244	1.906	4.1	215
.30	60	1.23	12.6	4.2	313	54	5	5.10	0.951	0.051	4.0	187
.30	61	1.10	12.7	2.0	>1600	72	152	>23.33	1.135	1.266	9.0	202

LEN m	RUN NO.	STOIC. RATIO	CO2 %	O2 %	CO PPM	NO PPM	UHC PPM	CO GM/KGM	NO GM/KGM	UHC GM/KGM	BACH. SMOKE	TFG C
	- - - - - - 0.22m I.D., Insulated, Tunnel-Fired - - - - - -											
.30	62	1.67	9.2	9.2	>1600	10	409	>35.88	0.256	5.242	2.1	226
.40	63	1.69	9.1	9.2	683	6	88	15.50	0.169	1.141	1.0	224
.40	64	1.43	11.0	6.8	76	35	2	1.47	0.734	0.022	0.8	228
.30	65	1.38	11.3	6.3	275	11	28	5.07	0.220	0.290	1.5	221
.50	66	1.42	10.8	6.6	28	54	1	0.55	1.116	0.011	0.0	273
.50	67	1.66	9.1	8.7	130	28	9	2.89	0.681	0.112	0.1	273
.75	68	1.44	11.1	7.1	12	67	10	0.25	1.397	0.108	0.0	288
.75	69	1.67	9.5	9.2	22	63	23	0.52	1.535	0.294	0.0	298
	- - - - - - 0.22m I.D., Water-Cooled, Tunnel-Fired - - - - - -											
.75	70	1.54	9.8	7.7	28	30	10	0.60	0.676	0.118	0.0	170
.75	71	1.12	13.7	2.4	17	50		0.27	0.806	0.008	0.0	168
.75	72	1.26	12.0	4.6	13	40	1	0.23	0.734	0.010	0.0	168
.30	73	1.28	12.1	5.0	519	10	110	8.84	0.194	1.069	0.0	211
.30	74	1.11	13.9	2.3	110	31		1.62	0.490	0.013	1.1	210
.30	75	1.51	10.1	7.6	>1600	15	820	>32.20	0.342	9.431	0.1	200
.40	76	1.28	12.1	4.9	71	24	10	1.22	0.438	0.097	0.0	200
.40	77	1.12	13.8	2.4	33	41	5	0.50	0.656	0.042	0.0	187
.40	78	1.49	10.5	7.5	387	9	65	7.72	0.205	0.744	0.0	202
.50	79	1.49	10.4	7.4	75	18	13	1.49	0.393	0.149	0.0	204
.50	80	1.36	11.4	6.0	28	30	3	0.53	0.594	0.027	0.0	204
.50	81	1.13	13.7	2.5	25	46	7	0.37	0.735	0.060	0.0	196

LEN m	RUN NO.	STOIC. RATIO	CO2 %	O2 %	CO PPM	NO PPM	UHC PPM	CO GM/KGM	NO GM/KGM	UHC GM/KGM	BACH. SMOKE	TFG C
	- - - - - - 0.17m I.D., Air-Cooled, Side-Fired - - - - - -											
.75	82	1.20	13.4	4.0	295	41	59	4.71	0.702	0.538	0.3	172
.75	83	1.27	12.6	4.9	314	38	14	5.29	0.701	0.131	0.3	187
.75	84	1.61	9.1	8.2	>1600	19	1630	>34.47	0.462	20.068	8.5	128
	- - - - - - 0.28m I.D., Air-Cooled, Side-Fired - - - - - -											
.75	85	1.28	12.0	4.9	30	21	4	0.51	0.383	0.039	0.0	196
.75	86	1.17	13.3	3.2	25	30	3	0.39	0.506	0.026	0.0	243
.75	87	1.02	15.0	0.0	>1600	36	181	>21.69	0.537	1.402	3.9	230
.75	88	1.35	11.7	5.9	35	31	15	0.63	0.597	0.151	0.0	243
.50	89	1.36	11.5	6.0	55	29	16	0.99	0.564	0.163	0.1	230
.50	90	1.07	14.1	1.4	598	27	24	8.44	0.409	0.190	1.6	209
.50	91	1.17	13.1	3.3	26	35	2	0.42	0.583	0.022	0.0	217
.40	92	1.18	13.1	3.4	33	29	4	0.53	0.486	0.035	0.0	224
.40	93	1.39	11.1	6.3	78	25	16	1.46	0.497	0.168	0.1	234
.40	94	1.06	14.1	1.4	>1600	21	146	>22.51	0.317	1.174	2.1	226
.30	95	1.13	13.4	2.6	>1600	15	470	>23.86	0.254	4.005	2.2	221
.30	96	1.37	11.5	6.2	170	17	72	3.11	0.350	0.747	0.1	245
.30	97	1.12	14.0	2.4	363	15	27	5.38	0.243	0.229	0.5	243

LEN m	RUN NO.	STOIC. RATIO	CO2 %	O2 %	CO PPM	NO PPM	UHC PPM	CO GM/KGM	NO GM/KGM	UHC GM/KGM	BACH. SMOKE	TFG C
	- - - - - - 0.22m I.D., Air-Cooled, Side-Fired - - - - - -											
.75	98	1.35	11.7	5.9	11	41		0.22	0.794	0.010	0.4	192
.75	99	1.02	14.9	0.6	1532	51	60	20.78	0.745	0.465	6.0	202
.75	100	1.62	9.5	8.6	25	40	39	0.54	0.953	0.485	0.1	230
.50	101	1.07	14.4	1.5	50	56	1	0.71	0.862	0.012	2.9	230
.50	102	1.52	10.2	7.7	31	45	8	0.65	0.996	0.093	0.1	234
.50	103	1.26	12.0	4.5	28	54	5	0.48	0.966	0.048	0.5	221
.40	104	1.25	12.2	4.5	35	52	6	0.58	0.938	0.057	0.8	226
.40	105	1.07	14.3	1.4	127	54	4	1.81	0.831	0.036	4.8	241
.40	106	1.49	10.4	7.4	65	51	19	1.31	1.092	0.216	0.2	251
.30	107	1.46	10.7	7.1	101	46	23	1.98	0.970	0.256	0.5	256
.30	108	1.07	14.2	1.5	184	50	6	2.62	0.764	0.047	4.5	258
.30	109	1.22	12.5	4.0	45	52	6	0.73	0.912	0.055	2.8	243
	- - - - - - 0.22m I.D., Fractional Insulation, Side-Fired - - - - - -											
.40 3/4	110	1.08	14.4	1.7	139	34	5	2.00	0.529	0.045	2.5	189
.40 3/4	111	1.32	11.9	5.5	25	46	1	0.46	0.874	0.015	0.9	198
.40 3/4	112	1.49	10.5	7.5	60	39	10	1.99	0.853	0.110	0.2	213
.40 1/2	113	1.07	14.5	1.5	456	42	13	6.46	0.641	0.108	3.8	189
.40 1/2	114	1.24	12.7	4.5	21	47	1	0.36	0.847	0.014	0.5	198
.40 1/2	115	1.44	11.1	7.1	40	47	2	0.77	0.980	0.024	0.1	219
.40 1/4	116	1.44	11.0	7.0	39	54	2	0.63	1.131	0.022	0.1	224
.40 1/4	117	1.25	12.5	4.6	22	52	1	0.38	0.938	0.010	0.9	196
.40 1/4	118	1.07	14.5	1.4	545	40	38	7.69	0.617	0.309	4.0	196

LEN m	RUN NO.	STOIC. RATIO	CO2 %	O2 %	CO PPM	NO PPM	UHC PPM	CO GM/KGM	NO GM/KGM	UHC GM/KGM	BACH. SMOKE	TFG C
	- - - - - - 0.22m I.D., Insulated, Side-Fired - - - - - -											
.30	119	1.33	13.3	6.3	23	97	6	0.49	1.833	0.056	0.1	200
.30	120	1.14	13.7	2.8	≥1600	89	45	≥24.03	1.436	0.386	9.0	170
.30	121	1.51	10.5	7.8	85	68	31	1.72	1.480	0.356	0.2	208
.40	122	1.38	11.3	6.2	25	119	12	0.46	2.208	0.126	0.1	183
.40	123	1.31	11.9	5.4	15	108	6	0.26	2.032	0.060	1.0	166
.40	124	1.57	9.9	8.1	10	97	10	0.21	2.181	0.120	0.3	204
.50	125	1.17	13.3	3.3	20	116	1	0.33	1.926	0.009	0.8	172
.50	126	1.35	11.5	5.9	11	101		0.22	1.953	0.015	0.3	181
.50	127	1.48	10.7	7.4	12	97	5	0.26	2.052	0.056	0.1	189
.75	128	1.19	13.1	3.6	15	110		0.25	1.864	0.009	0.1	275
.75	129	1.44	11.0	7.0	15	110	3	0.29	2.275	0.030	0.0	296
.75	130	1.14	13.7	2.8	18	136		0.29	2.206	0.013	0.1	279
	- - - - - 0.17m I.D., Insulated, Side-Fired - - - - - -											
.30	131	1.21	13.1	3.9	134	95	2	2.15	1.627	0.016	7.0	185
.30	132	1.35	11.7	6.0	65	88	2	1.17	1.699	0.021	1.2	192
.30	133	1.49	10.6	7.6	125	73	27	2.51	1.572	0.308	0.2	198
.40	134	1.65	9.5	9.0	57	68	24	1.29	1.625	0.311	0.1	226
.40	135	1.44	10.8	6.9	32	96	3	0.63	1.984	0.038	0.1	215
.40	136	1.16	13.4	3.2	60	107	2	0.92	1.775	0.015	6.0	192
.50	137	1.18	13.3	3.4	45	112		0.70	1.875	0.013	2.5	213
.50	138	1.59	9.7	8.3	35	81	14	0.75	1.852	0.175	0.1	241
.50	139	1.35	11.3	5.8	50	106	2	0.90	2.059	0.026	0.1	232

LEN m	RUN NO.	STOIC. RATIO	CO2 %	O2 %	CO PPM	NO PPM	UHC PPM	CO GM/KGM	NO GM/KGM	UHC GM/KGM	BACH. SMOKE	TFG C
	- - - - - - 0.17m I.D., Insulated, Side-Fired - - - - - -											
.75	140	1.24	13.2	4.6	15	129		0.25	2.274	0.009	0.1	239
.75	141	1.72	9.1	9.5	20	75	4	0.46	1.881	0.049	0.2	268
.75	142	1.54	10.4	8.2	15	108		0.31	2.403	0.018	0.0	264
	- - - - - - 0.22m I.D., Water-Cooled, Side-Fired - - - - - -											
.40	143	1.47	10.6	7.2	142	21	16	2.80	0.441	0.179	0.1	179
.40	144	1.05	14.2	1.2	1307	40	49	18.24	0.603	0.389	5.2	170
.40	145	1.24	12.6	4.4	60	34	14	0.99	0.599	0.134	0.7	172
.30	146	1.23	12.7	4.3	117	26	16	1.93	0.456	0.146	2.8	177
.30	147	1.58	9.9	8.3	365	8	111	7.71	0.193	1.343	0.3	183
.30	148	1.06	14.5	1.4	1532	30	49	21.52	0.453	0.396	5.0	189
.50	149	1.11	14.4	2.4	131	45	2	1.94	0.713	0.013	2.7	172
.50	150	1.42	11.2	6.8	80	28	7	1.53	0.569	0.073	0.1	183
.50	151	1.25	13.0	4.7	46	38	2	0.78	0.682	0.019	0.5	175
.75	152	1.24	13.2	4.6	30	42	2	0.51	0.745	0.019	0.5	194
.75	153	1.11	14.6	2.1	45	46		0.66	0.724	0.008	1.0	189
.75	154	1.54	10.4	8.2	191	12	38	3.94	0.282	0.447	0.0	209

- - - - 0.28m I.D., Water-cooled, Side-fired - - - -

	RUN NO.	STOIC. RATIO	CO2 %	O2 %	CO PPM	NO PPM	UHC PPM	CO GM/KGM	NO GM/KGM	UHC GM/KGM	BACH. SMOKE	TFG C
L = 0.50m	427	1.04	14.7	0.9	1083	16	113	14.90	0.249	0.888	0.4	257
	428	1.24	12.4	4.4	503	10	124	8.30	0.188	1.167	0.2	259
	429	1.14	13.5	2.7	298	10	44	4.48	0.172	0.382	0.2	249
	430	1.40	11.0	6.4	951	4	155	17.74	0.086	1.652	0.1	269
L = 0.75m	431	1.13	13.5	2.5	85	4	4	1.28	0.072	0.034	0.2	274
	432	1.27	12.1	4.7	150	3	29	2.52	0.068	0.283	0.2	288

APPENDIX D

DATA TABULATION: CGR BURNER EXPERIMENTS

Combustion chamber design parameters, burner operating conditions, and flue gas and recirculated combustion gas composition data are tabulated for the CGR (combustion gas recirculation) burner experiments discussed in Section V. Except where specifically called out as being different, nominal burner firing rates were 1.0 ml/s (gph). All experiments were steady-state runs except Runs No. 248 and 249, which were 10 min on/20 min off cyclical tests.

Two rows of data are given for each test. Composition data in the first row pertain to the exhaust flue gas while those in the second row pertain to the mixture of recirculated gas and fresh air supplied to the burner. The parameter listed as "RR" is a calculated recirculation ratio (recirculated burned gas mass divided by fresh reactant mass) expressed as a percentage. It is calculated by

$$RR = (100.)\ (14.49 + 1.0)/(14.49\ (SRM-1.0))$$

where SRM is the stoichiometric ratio for the gas mixture supplied to the burner. (Values of SRM are not tabulated but can be derived from the mixed gas composition data using the methods of Appendix B.)

BURNER: CGR-A (.042 M DIA)
NOZZLE: 1.0-60-A

COMBUSTOR: .22 M DIA., TUNNEL-FIRED, .40 M LENGTH, Air-cooled

RUN NO.	STOIC. RATIO	CO2 %	O2 %	CO PPM	NO PPM	UHC PPM	CO GM/KGM	NO GM/KGM	UHC GM/KGM	PATH. SMOKE	TEG C	Swirl Angle
155	1.09	14.3	1.9	148	20	67	2.14	0.317	0.552	1.0	239	40°
RR = 26%		2.6	17.0	≥1600	20	1500					143	
156	1.08	14.1	1.7	910	10	375	13.01	0.163	3.061	1.0	241	30°
RR = 24%		2.4	17.2	≥1600	21	1800					138	
157	1.04	14.5	1.0	≥1600	26	400	≥22.09	0.386	3.156	1.5	199	30°
RR = 31%		2.8	16.3	≥1600	35	≥3299					154	
158	1.23	12.4	4.2	187	16	900	3.07	0.296	1.868	1.0	254	30°
RR = 12%		1.1	19.9	179	2	900					127	
159	1.07	12.7	1.3	≥1600	38	3000	≥22.54	0.587	24.152	6.5	214	30°
RR = 11%		0.5	19.0	≥1600	21	1750					77	
160	1.11	12.3	2.0	≥1600	41	≥3299	≥23.40	0.655	≥27.581	8.0	193	40°
RR = 12%		0.5	18.9	≥1600	15	1500					71	
161	1.06	14.5	1.2	278	31	970	3.89	0.465	2.156	1.0	224	40°
RR = 26%		1.9	17.0	≥1600	21	1550					135	
162	1.19	13.4	2.3	397	10	300	5.87	0.169	2.531	0.5	257	20°
RR = 11%		0.7	19.0	472	9	750					82	
163	1.07	12.6	1.3	≥1600	49	≥3299	≥22.56	0.746	≥26.590	0.5	213	20°
RR = 23%		1.4	17.3	≥1600	40	≥3299					99	

BURNER: CGR-A (.042 M DIA)
NOZZLE: 1.0-60-A

COMBUSTOR: .22 M DIA., TUNNEL-FIRED, .40 M LENGTH, Air-cooled

RUN NO.	STOIC. RATIO	CO2 %	O2 %	CO PPM	NO PPM	UHC PPM	CO GM/KGM	NO GM/KGM	UHC GM/KGM	PATH. SMOKE	TEG C	Swirl Angle
164	1.10	No Go										20°
RR = 30%												
165	1.14	10.1	2.1	≥1600	68	≥3299	≥24.04	1.101	≥28.338	2.0	160	55°
RR = 31%		1.4	16.4	≥1600	72	≥3299					113	
166	1.10	13.9	2.0	711	35	480	10.32	0.559	3.977	4.0	222	55°
RR = 12%		0.7	18.9	749	5	370					93	
167	1.34	9.7	5.0	≥1600	32	≥3299	≥28.60	0.614	≥33.713	6.0	138	55°
RR = 20%		0.7	17.7	≥1600	28	2400					88	
168	1.14	11.0	2.3	≥1600	26	1500	≥24.07	0.490	12.894	2.5	168	55°
RR = 19%		1.5	17.9	≥1600	21	1500					88	
169	1.05	14.5	1.2	≥1600	36	1500	≥22.29	0.559	11.939	1.5	238	10°
RR = 14%		1.2	18.6	≥1600	21	1250					66	
170	1.16	11.0	2.6	≥1600	72	≥3299	≥24.47	1.191	≥28.844	2.0	182	10°
RR = 19%		1.4	17.9	≥1600	40	3000					74	
171	1.10	No Go										10°
RR = 30%												

PURNER: CGR-B (.042 M DIA)
NOZZLE: 1.0-60-A

COMBUSTOR: .22 M DIA., TUNNEL-FIRED, .40 M LENGTH, Air-cooled, Baffle at .23m

RUN NO.	STOIC. RATIO	CO2 %	O2 %	CO PPM	NO PPM	UHC PPM	CO GM/KGM	NO GM/KGM	UHC GM/KGM	SMOKE	TFG C	Swirl Angle
172	1.12	12.9	2.4	≥1600	40	2000	≥23.75	0.649	16.961	1.0	198	10°
RR = 29%		2.9	16.6	≥1600	10	750					218	
173	1.08	13.4	1.6	≥1600	35	1300	≥22.79	0.549	10.580	3.0	174	20°
RR = 31%		2.8	16.4	≥1600	26	2500					216	
174	1.16	12.9	3.0	≥1600	32	1950	≥24.61	0.529	10.989	3.0	174	30°
RR = 31%		2.8	16.4	≥1600	18	2150					218	
175	1.12	13.1	2.4	≥1600	36	750	≥23.71	0.587	6.351	3.0	174	30°
RR = 27%		2.6	16.8	≥1600	10	900					218	
176	1.14	13.6	2.8	110	43	220	1.66	0.699	1.898	5.0	204	40°
RR = 11%		1.1	19.1	≥1600	8	340					135	
177	1.17	13.3	3.2	50	41	200	0.77	0.691	1.764	1.0	135	20°
RR = 10%		0.9	19.3	383	5	180					199	
178	1.07	14.3	1.5	397	40	200	5.63	0.620	1.619	3.0	199	10°
RR = 11%		1.1	19.0	≥1600	7	630					143	
179	1.08	13.6	1.7	730	36	210	10.47	0.568	1.720	5.5	216	10°
RR = 15%		1.9	18.5	≥1600	9	850					154	
180	1.06	13.3	1.3	≥1600	32	1800	≥22.49	0.483	14.457	2.0	199	20°
RR = 26%		1.9	17.0	≥1600	20	2150					191	
181	1.10	12.7	1.9	≥1600	31	600	≥23.21	0.483	4.974	4.0	185	20°
RR = 26%		2.2	17.0	≥1600	10	1250					193	
182	1.04	14.1	1.0	≥1600	40	390	≥22.11	0.598	3.080	2.0	189	30°
RR = 26%		2.5	17.0	≥1600	8	540					207	
183	1.11	12.9	2.0	≥1600	31	2700	≥23.42	0.487	22.581	4.0		40°
RR = 26%		2.6	17.0	≥1600	5	710					216	

PURNER: CGF-A (.042 M DIA)
NOZZLE: .75 -60-A (184-186)
1.0-60-A (187-190)

COMPUSTOR: .22 M DIA., SIDE-FIRED, .40 M LENGTH, Air-cooled

RUN NO.	STOIC. RATIO	CO2 %	O2 %	CO PPM	NO PPM	UHC PPM	CO GM/KGM	NO GM/KGM	UHC GM/KGM	SMOKE	TFG C	Swirl Angle
184	1.14	12.6	2.6	≥1600	31	1650	≥24.05	0.501	14.172	3.0	132	40°
RR = 14%		2.4	18.6	≥1600	5	430					110	
185	1.16	12.1	3.0	≥1600	21	1550	≥24.64	0.347	13.640	0.5	121	
RR = 38%		3.6	15.6	≥1600	5	450					210	
186	1.41	8.6	5.3	≥1600	68	≥3299	≥30.10	1.378	≥35.479		104	
RR = 23%		1.6	17.4	≥1600	21	1750					152	
187	1.15	13.7	3.0	55	21	150	0.84	0.351	1.305	0.0	221	
RR = 13%		1.9	18.7	10	5	100					202	
188	1.01	15.1	0.4	≥1600	26	850	≥21.51	0.376	6.529	0.0	221	
RR = 23%		2.6	17.3	315	6	160					224	
189	1.02	15.0	0.6	≥1600	28	900	≥21.69	0.415	6.973	0.1	207	
RR = 24%		3.1	17.2	503	8	340					224	
190	1.19	13.1	3.6	35	27	130	0.55	0.457	1.170	0.1	227	40°
RR = 13%		1.6	18.8	137	5	150					179	

PURNER: CGR-A (.051 M DIA)
NØZZLE: 1.0-60-A

COMPUSTØR: .22 M DIA., TUNNEL-FIRED, .40 M LENGTH, Air-cooled, Baffle at .23 m

RUN NØ.	STØIC. RATIØ	CØ2 %	Ø2 %	CØ PPM	NØ PPM	UHC PPM	CØ GM/KGM	NØ GM/KGM	UHC GM/KGM	RACH. SMØKE	TFG C	Swirl Angle
191	1.55	10.0	8.1	1099	23	280	22.82	0.594	3.321	0.5		40°
RR = 24%		4.6	15.0	≥1600	11	50					299	
192	1.42	10.2	6.4	≥1600	33	1400	≥30.27	0.690	15.134	0.1	191	
RR = 40%		3.8	15.4	≥1600	31	1900					216	
193	1.94	7.5	10.5	≥1600	21	110	≥42.06	0.592	1.652	0.0		
RR = 34%		2.8	16.0	≥1600	32	2350					210	
194	2.09	7.1	11.2	20	32	73	0.57	0.975	1.183	0.0	154	
RR = 15%		1.7	18.4	629	8	120					168	
195	1.51	10.2	7.5	20	33	64	0.42	0.723	0.736	0.0	138	
RR = 21%		2.4	17.6	≥1600	9	260					188	
196	1.51	9.1	7.0	≥1600	18	570	≥39.37	0.400	6.589	0.0	127	
RR = 45%		3.6	14.9	≥1600	31	2350						
197	1.54	8.0	6.5	≥1600	26	≥3299	≥32.99	0.576	≥38.883	0.0	93	
RR = 32%		2.6	16.2	≥1600	50	≥3299					218	
198	1.16	12.6	3.1	≥1600	31	380	≥24.63	0.521	3.343	0.0	160	
RR = 27%		2.1	16.8	≥1600	26	2050					177	
199	1.27	9.2	3.8	≥1600	35	≥3299	≥27.03	0.652	≥31.854	3.0	141	40°
RR = 17%		1.1	18.2	≥1600	63	≥3299					132	

0.15m Pyroflex Insulation

PURNER: CGR-A (.051 M DIA)
NØZZLE: 1.0-60-A

COMPUSTØR: .22 M DIA., TUNNEL-FIRED, .40 M LENGTH, Air-cooled, Baffle at .23 m

RUN NØ.	STØIC. RATIØ	CØ2 %	Ø2 %	CØ PPM	NØ PPM	UHC PPM	CØ GM/KGM	NØ GM/KGM	UHC GM/KGM	RACH. SMØKE	TFG C	Swirl Angle
200	1.18	13.3	3.4	157	30	120	2.46	0.502	1.067	0.0	154	40°
RR = 12%		1.1	18.9	≥1600	5	420					96	
201	1.69	9.4	9.4	30	22	105	0.68	0.536	1.361	0.0	185	
RR = 16%		2.2	18.3	10	8	85					138	
202	1.15	13.5	3.0	70	30	90	1.07	0.492	0.784	0.0	191	
RR = 14%		1.6	18.6	≥1600	8	480					132	
203	1.42	10.6	6.4	40	22	90	0.75	0.446	0.971	0.0	168	
RR = 29%		3.2	16.6	≥1600	8	400					163	
204	1.32	11.3	0.0	41	18	68	0.74	0.346	0.680	0.1	149	
RR = 31%		3.0	16.4	≥1600	11	670					168	
205	1.48	10.4	7.4	1580	21	110	31.17	0.444	1.240	0.0	143	
RR = 36%		3.2	15.8	≥1600	19	1350					185	
206	1.56	8.4	7.0	≥1600	21	1100	≥33.36	0.470	13.108		121	
RR = 30%		2.2	16.5	≥1600	27	2250					163	
207	1.64	7.8	7.5	≥1600	28	≥3299	≥35.22	0.674	≥41.505	2.5	135	
RR = 15%		1.1	18.4	1580	31	2430					113	
208	1.58	7.7	6.6	≥1600	40	≥3299	≥33.78	0.924	≥39.808	2.5		40°
RR = 23%		1.4	17.4	≥1600	41	≥3299					116	

BURNER: CGP-A (.051 M DIA)
NOZZLE: 1.0-60-A

COMBUSTOR: .22 M DIA., TUNNEL-FIRED, .40 M LENGTH, Air-cooled Baffle at .23m

RUN NO.	STOIC. RATIO	CO2 %	O2 %	CO PPM	NO PPM	UHC PPM	CO GM/KGM	NO GM/KGM	UHC GM/KGM	PATCH. SMOKE	TFG C	Swirl Angle
209	1.49	10.4	7.4	61	21	150	1.23	0.448	1.705	0.0	146	40°
RR = 34%		3.4	16.0	1051	10	160					199	
210	1.32	11.7	5.5	808	22	120	14.18	0.414	1.203	0.0	179	
RR = 26%		2.6	17.0	10	8	100					196	
211	1.70	9.0	9.1	15	21	110	0.34	0.515	1.437	0.1	163	
RR = 25%		2.4	17.1	10	5	100					193	
212	1.46	10.4	6.9	17	21	95	0.35	0.448	1.055	0.0	157	40°
RR = 21%		1.8	17.6	≥1600	6	440					166	

BURNER: CGR-A (.051 M DIA) 3/4" Choke Ext.
Nozzle: 1.0-60-A

COMBUSTOR: .22 M DIA., TUNNEL-FIRED, M LENGTH, Air-cooled, Baffle at .23m

RUN NO.	STOIC. RATIO	CO2 %	O2 %	CO PPM	NO PPM	UHC PPM	CO GM/KGM	NO GM/KGM	UHC GM/KGM	PATCH. SMOKE	TFG C	Swirl Angle
213	1.57	10.1	8.3	25	15	23	0.53	0.357	0.276	0.0	154	40°
RR = 31%		3.5	16.3	153	5	30					185	
214	1.52	8.8	6.8	≥1600	18	1850	≥32.50	0.402	21.471	0.1	132	
RR = 31%		2.4	16.3	≥1600	41	≥3299					127	
215	1.29	10.2	4.4	≥1600	22	3200	≥27.32	0.403	31.225	0.0	135	
RR = 33%		2.2	16.1	≥1600	40	≥3299					129	
216	1.48	8.2	5.9	≥1600	38	≥3299	≥31.61	0.824	37.260	3.0	116	
RR = 22%		1.2	17.5	≥1600	45	≥3299					91	
217	1.19	11.0	3.1	≥1600	31	2350	≥25.15	0.523	21.105	6.0	160	
RR = 13%		0.9	18.7	≥1600	10	1000					71	
218	1.37	10.8	6.0	≥1600	27	350	≥29.24	0.531	3.655	3.0	171	
RR = 19%		1.2	17.9	≥1600	12	1250					102	
219	1.51	10.1	7.4	20	26	130	0.42	0.563	1.497	0.0	199	
RR = 17%		1.4	18.1	10	5	110						
220	1.76	8.3	9.1	20	15	120	0.47	0.402	1.621	0.0	171	
RR = 16%		1.8	18.3	10	5	110					163	
221	1.32	11.7	5.5	40	26	120	0.70	0.492	1.207	0.2	185	
RR = 13%		0.9	18.7	≥1600	5	350					110	
222	1.17	11.3	2.9	≥1600	26	2600	≥24.76	0.432	22.988	0.5	160	
RR = 24%		1.4	17.2	≥1600	18	1850					113	
223	1.78	8.3	9.4	50	25	110	1.20	0.644	1.507	0.0	210	40°
RR = 12%		0.9	18.9	10	5	105					118	

BURNER: CGR-C* (.051 M DIA) .15m D x .25m L Shroud
Nozzle: 1.0-60-A

COMBUSTOR: .22 M DIA., TUNNEL-FIRED .40 M LENGTH, Air-cooled

FUN NO.	STOIC. RATIO	CO2 %	O2 %	CO PPM	NO PPM	UHC PPM	CO GM/KGM	NO GM/KGM	UHC GM/KGM	BACH. SMOKE	TFG C	Swirl Angle
224	1.51	9.9	7.4	693	15	130	13.99	0.343	1.499	1.0	213	0°
RR = 14%		1.4	18.6	21	12	68					99	
225	1.53	9.5	7.5	≥1600	30	80	≥32.73	0.659	0.935	0.1	168	
RR = 25%		1.8	17.1	≥1600	9	280					129	
226	1.29	8.9	3.6	≥1600	26	1800	≥27.40	0.479	17.614	6.0	129	
RR = 15%		0.9	18.4	≥1600	11	720					88	
227	1.45	10.6	6.9	355	25	60	6.86	0.518	0.662	0.0	159	
PR = 45%		3.8	14.9	≥1600	11	200					154	
228	1.21	12.9	3.9	90	21	48	1.44	0.360	0.439	0.1	202	
RR = 25%		2.8	17.1	41	10	100					146	
229	1.07	14.5	1.4	182	26	51	2.58	0.394	0.411	0.1	202	
PR = 31%		3.2	16.4	≥1600	9	135					174	
230	1.15	13.6	3.0	60	21	56	0.91	0.343	0.488	0.0	196	0°
RR = 32%		3.4	16.2	41	9	95					191	

BURNER: CGR-C* (.051 M DIA) .15m D x .25m L Shroud
Nozzle: 1.0-60-A

COMBUSTOR: .22 M DIA., TUNNEL-FIRED, .40 M LENGTH, Air-cooled

RUN NO.	STOIC. RATIO	CO2 %	O2 %	CO PPM	NO PPM	UHC PPM	CO GM/KGM	NO GM/KGM	UHC GM/KGM	BACH. SMOKE	TFG C	Swirl Angle
231	1.28	12.0	4.9	20	30	53	0.34	0.548	0.515	0.0	191	40°
RR = 24%		2.6	17.2	10	9	49					185	
232	1.36	11.5	6.0	31	31	53	0.58	0.602	0.548	0.0	177	
RR = 24%		2.6	17.2	503	9	70					168	
233	1.13	13.8	2.6	30	31	52	0.45	0.506	0.444	0.0	182	
RR = 26%		2.6	17.0	355	9	69					160	
234	1.24	12.6	4.3	17	31	55	0.29	0.546	0.515	0.0	185	
RR = 31%		3.0	16.4	30	10	53					210	
235	1.41	9.7	6.0	≥1600	21	1100	≥30.16	0.424	11.849	2.0	157	
RR = 33%		2.5	16.1	≥1600	10	820					168	
236	1.18	13.1	3.5	20	31	53	0.31	0.522	0.475	0.0	174	
RR = 32%		3.1	16.2	57	11	55					199	
237	1.52	10.1	7.6	15	35	46	0.31	0.785	0.535	0.0	188	
RR = 14%		1.4	18.6	10	9	43					163	
238	1.18	13.1	3.5	20	50	48	0.31	0.845	0.430	0.0	185	40°
PR = 15%		1.2	18.5	139	9	61					141	

BURNER: CGR-A (.051 M DIA)
NOZZLE: 1.0-60-A

COMBUSTOR: .22 M DIA., SIDE-FIRED,
.40 M LENGTH, Water-cooled

RUN NO.	STOIC. RATIO	CO2 %	O2 %	CO PPM	NO PPM	UHC PPM	CO GM/KGM	NO GM/KGM	UHC GM/KGM	PATCH. SMOKE	TFG C	Swirl Angle
239	1.29	11.9	5.0	838	11	27	14.32	0.205	0.263	0.1	174	40°
RR = 31%		2.8	16.3	412	5	210					163	
240	1.10	14.5	2.2	>1600	21	1150	>23.27	0.327	9.557	0.1	177	
RR = 31%		3.0	16.3	404	5	200					149	
241	1.17	11.9	3.0	177	40	47	2.76	0.680	0.417	7.0	202	
RR = 11%		0.5	19.0	30	2	50					77	
242	1.89	7.3	9.7	>1600	14	800	>40.93	0.407	11.693	0.1	291	
RR = 12%		0.4	18.9	220	2	140					74	
243	1.39	10.8	6.1	130	21	80	2.41	0.417	0.846	0.0	241	
RR = 11%		0.9	19.0	10	2	46					59	
244	1.16	14.5	3.4	80	20	34	1.93	0.338	0.299	2.0	202	
RR = 22%		0.7	17.5	77	2	39					107	
245	1.49	9.7	6.9	665	8	130	13.21	0.170	1.474	0.0	204	
RR = 21%		0.5	17.6	214	2	100					124	
246	1.41	9.0	5.4	157	6	48	2.98	0.130	0.517	1.0	163	
RR = 22%		1.4	17.5	57	2	36					113	
247	1.39	10.4	6.0	441	9	110	8.20	0.191	1.167	0.5	196	40°
RR = 29%		1.1	16.6	231	2	90					152	

BURNER: CGR-A (.051 M DIA)
NOZZLE: 1.0-60-A

COMBUSTOR: .22 M DIA., SIDE-FIRED,
.40 M LENGTH, Water-cooled

RUN NO.	STOIC. RATIO	CO2 %	O2 %	CO PPM	NO PPM	UHC PPM	CO GM/KGM	NO GM/KGM	UHC GM/KGM	PATCH. SMOKE	TFG C	Swirl Angle
248	1.38	11.0	6.1	753	10	228	13.83	0.210	2.391	0.1	174	40°
RR = 19%		2.2	17.9	369	4	216					114	
249	1.26	12.1	4.6	65	27	9	1.09	0.486	0.086	2.2	157	40°
RR = 12%		1.1	18.9	20	2	1					79	

APPENDIX E

DATA TABULATION: FGR BURNER EXPERIMENTS

Combustion chamber design parameters, burner operating conditions and flue gas composition data are tabulated for the FGR (flue gas recirculation) burner experiments discussed in Section V. Steady-state data are given in Tables E-1 through E-3. Cycle-averaged data are given in Tables E-4 and E-5. Cyclical tests were all 10 min on/20 min off experiments.

Two rows of data are given for each test. Composition data in the first row pertain to the exhaust flue gas while those in the second row pertain to the mixture of recirculated gas and fresh air supplied to the burner. The parameter listed as "RR" is a calculated recirculation ratio (recirculated burned gas mass divided by fresh reactant mass) expressed as a percentage. It is calculated by

$$RR = (100.)\ (14.49 + 1.0)/(14.49\ (SRM - 1.0))$$

where SRM is the stoichiometric ratio for the gas mixture supplied to the burner. (Values of SRM are not tabulated but can be derived from the mixed gas composition data using the methods of Appendix B.

TABLE E-1. STEADY-STATE FLUE GAS RECIRCULATION DATA FROM A 0.22 M I.D., WATER-COOLED SIDE-FIRED COMBUSTOR WITH THE 1.0-60°-A NOZZLE FGR BURNER

0.051m Choke L = 0.40m

RUN NO.	STOIC. RATIO	CO2 %	O2 %	CO PPM	NO PPM	UHC PPM	CO GM/KGM	NO GM/KGM	UHC GM/KGM	SMOKE NUMBER	TEG °C	Swirl
250	1.33	11.3	5.5	>1600	25	1500	>25.19	0.472	15.101	2.0	207	40°
RR = 29%		3.9	16.6	799	10	600					49	
251	1.13	13.3	2.7	>1600	33	>2000	>24.01	0.531	17.148	2.0	239	
RR = 35%		3.8	15.9	495	10	630					54	
252	1.44	10.2	6.7	>1600	30	2100	>30.71	0.619	23.034	2.0	235	
RR = 22%		2.2	17.5	569	10	615					52	
253	1.58	9.3	8.0	>1600	20	1150	>33.77	0.464	13.872	0.5	232	
RR = 11%		0.9	19.0	202	5	300					35	
254	1.09	13.8	1.9	769	15	420	11.11	0.246	3.447	0.0	201	
RR = 30%		2.8	16.5	157	5	220					46	
255	1.12	13.3	2.4	303	10	230	4.50	0.170	1.953	2.0	202	
RR = 21%		1.8	17.6	70	5	130					38	
256	1.29	11.5	4.7	278	11	140	4.73	0.204	1.359	1.0	207	
RR = 13%		0.9	18.9	45	4	80					29	
257	1.20	12.2	3.6	511	11	260	8.13	0.191	2.343	0.5	201	40°
RR = 22%		1.8	17.5	70	7	110					46	

0.042m Choke L = 0.75m

RUN NO.	STOIC. RATIO	CO2 %	O2 %	CO PPM	NO PPM	UHC PPM	CO GM/KGM	NO GM/KGM	UHC GM/KGM	SMOKE NUMBER	TEG °C	Swirl
266	1.14	13.4	2.7	193	13	105	2.91	0.222	0.903	0.0	196	40°
RR = 28%		3.3	16.7	50	7	55					46	
267	1.19	14.3	4.0	30	45	37	0.47	0.772	0.334			
RR = 1%		0.0	20.9	0	0	0					18	
268	1.15	13.4	3.0	997	15	240	15.17	0.259	2.435	0.1	241	
RR = 29%		3.1	16.6	328	10	210					52	
269	1.37	11.1	6.0	209	10	70	3.81	0.208	0.729	0.0	191	
RR = 11%		1.1	19.0	30	5	45					29	
270	1.25	12.0	4.4	383	10	110	6.36	0.199	1.042	0.0	227	
RR = 21%		2.2	17.6	80	5	50					44	
271	1.09	14.2	0.5	>1600	31	1900	>21.62	0.450	14.672	0.1	193	
RR = 26%		1.9	17.0	1179	5	170					41	
272	1.06	14.3	1.3	220	8	110	3.09	0.129	0.893	0.0	207	
RR = 21%		1.9	17.6	40	8	55					41	
273	1.18	12.9	3.5	1099	20	600	17.21	0.344	5.366	0.1	232	
RR = 27%		2.6	16.8	231	10	160					49	
274	1.42	10.6	6.5	503	14	110	9.53	0.201	1.189	0.0	179	
RR = 11%		0.7	19.0	50	5	55					29	
275	1.26	12.0	4.5	70	15	50	1.17	0.284	0.477	0.0	164	
RR = 11%		0.7	19.0	10	5	40					27	
276	1.25	12.0	4.5	1403	19	500	23.29	0.355	7.583	0.1	227	40°
RR = 30%		2.6	16.5	383	10	160					54	

TABLE E-1. (Concluded)

0.051m Choke L = 0.75m

RUN NO.	STOIC. RATIO	CO2 %	O2 %	CO PPM	NO PPM	UHC PPM	CO GM/KGM	NO GM/KGM	UHC GM/KGM	EFFIC. SMOKE	TEG C	Swirl
258	1.12	13.6	2.5	148	21	35	2.21	0.335	0.297	0.1	229	40°
RR = 29%		3.6	16.6	50	7	24					47	
259	1.48	10.6	7.4	456	10	110	12.94	0.225	1.239	0.1	259	
RR = 11%		1.6	19.1	70	4	40					29	
260	1.36	11.1	6.0	>1600	20	800	>28.95	0.398	9.280	0.1		
RR = 28%		3.5	16.7	544	8	200					54	
261	1.41	10.8	6.6	1297	15	350	26.19	0.320	3.765	0.1	246	
RR = 19%		2.6	17.9	254	6	110					46	
262	1.18	13.1	3.5	315	13	110	4.95	0.293	0.984	0.0	224	
RR = 30%		3.6	16.5	90	5	75					52	
263	1.24	12.4	4.4	177	10	70	2.93	0.188	0.688	0.0	233	
RR = 21%		2.8	17.6	40	5	53					43	
264	1.29	11.9	5.0	75	23	54	1.28	0.432	0.529	0.1	213	
RR = 12%		1.6	18.9	20	5	44					39	
265	1.13	13.8	2.6	70	21	59	1.05	0.336	0.444	0.1	204	40°
RR = 21%		2.4	17.6	20	5	44					39	

0.051m Choke L = 0.75m

RUN NO.	STOIC. RATIO	CO2 %	O2 %	CO PPM	NO PPM	UHC PPM	CO GM/KGM	NO GM/KGM	UHC GM/KGM	EFFIC. SMOKE	TEG C	Swirl
277	1.36	11.5	6.0	388	8	72	6.82	0.165	0.762	0.0	207	0°
RR = 11%		1.4	19.0	41	2	15					29	
278	1.24	12.4	4.5	>1600	24	1500	>24.27	0.461	14.124	0.1	249	
RR = 31%		3.4	16.4	711	9	40					69	
279	1.28	12.0	4.9	1083	10	230	19.22	0.193	3.675	0.0	246	
RR = 22%		2.6	17.5	177	2	100					59	
280	1.25	12.6	4.4	>1600	18	1000	>27.72	0.446	13.470	0.1	254	
RR = 11%		1.2	19.0	274	4	140					41	
281	1.49	10.1	7.3	>1600	14	800	>31.79	0.328	9.083	0.1	252	
RR = 22%		1.9	17.5	472	4	220					58	
282	1.40	10.8	6.4	>1600	21	1450	>29.80	0.490	15.434	0.1	254	
RR = 29%		2.8	16.4	711	5	290					63	
283	1.10	13.7	2.0	>1600	18	410	>23.18	0.284	5.049	0.5	199	
RR = 23%		2.2	17.4	1088	4	200					49	
284	1.39	11.1	6.2	954	10	120	6.69	0.211	1.965	0.1	213	
RR = 17%		1.0	18.8	37	2	100					39	
285	1.28	11.8	4.9	>1600	19	1150	>27.11	0.363	11.133	0.1	252	0°
RR = 30%		2.8	16.5	485	4	240					60	

TABLE E-2. STEADY STATE FLUE GAS RECIRCULATION DATA FROM A 0.22 M I.D., INSULATED COMBUSTOR WITH THE 1.0-60°-A NOZZLE FGR BURNER

Side-Fired

0.051m Choke L = 0.40m

RUN NO.	STOIC. RATIO	CO2 %	O2 %	CO PPM	NO PPM	UHC PPM	CO GM/KGM	NO GM/KGM	UHC GM/KGM	BACH. SMOKE	TFG C	Swirl
286	1.71	8.8	9.0	18	47	1	0.44	1.190	0.013	0.0	279	40°
RR = 11%		1.4	19.0	10	8	2					29	
287	1.63	9.3	8.5	17	30		0.39	0.704	0.019	0.0	293	
RR = 30%		3.4	16.5	10	9	2					44	
288	1.67	9.4	9.2	17	31	1	0.40	0.761	0.019	0.0	291	
RR = 21%		2.4	17.6	10	8	2					38	
289	1.55	9.7	7.7	40	23	2	0.83	0.593	0.024	0.0	288	
RR = 30%		3.4	16.5	10	10	2					49	
290	1.38	11.1	6.2	849	23	13	15.95	0.463	0.136	0.0	271	
RR = 30%		3.4	16.5	254	6	80					44	
291	1.31	11.5	5.1	130	41	6	2.95	0.777	0.059	0.5	268	
RR = 22%		2.4	17.5	80	5	14					39	
292	1.46	10.1	6.7	30	52	9	0.58	1.095	0.100	0.0	271	
RR = 14%		1.6	18.6	10	6	17					29	
293	1.82	8.2	10.0	>1600	45	2500	>39.99	1.198	35.016	0.1	279	40°
RR = 75%		6.5	12.5	>1600	26	2000						

Tunnel-Fired

0.051m Choke L = 0.75m

RUN NO.	STOIC. RATIO	CO2 %	O2 %	CO PPM	NO PPM	UHC PPM	CO GM/KGM	NO GM/KGM	UHC GM/KGM	BACH. SMOKE	TFG C	Swirl
300	1.26	12.4	4.6	20	22	3	0.33	0.393	0.029	0.0	327	40°
RR = 30%		3.6	16.5	10	8	4						
301	1.30	12.0	5.2	20	26	2	0.34	0.462	0.020	0.0	338	
RR = 22%		2.7	17.5	10	5	3					63	
302	1.47	11.0	7.5	20	36	0	0.39	0.809	0.000	0.0	341	
RR = 11%		1.2	19.0	10	5	1					35	
303	1.01	14.6	0.2	>1600	21	6	>21.33	0.300	0.061	0.0	302	
RR = 69%		6.1	12.9	>1600	5	4					85	
304	1.13	13.8	2.5	25	21	2	0.37	0.335	0.017	0.0	316	
RR = 30%		3.5	16.5	15	5	1						
305	1.15	13.5	2.9	20	28	1	0.30	0.465	0.009	0.0	313	
RR = 22%		2.6	17.5	10	2	1					52	
306	1.20	12.9	3.8	20	35	1	0.32	0.614	0.009	0.0	313	
RR = 12%		1.8	16.9	10	2	1					35	
307	1.19	13.1	3.4	20	15	1	0.31	0.266	0.009	0.0	313	
RR = 31%		3.8	16.4	10	2	1					64	
308	1.44	10.8	6.9	20	15	0	0.38	0.327	0.000	0.0	335	
RR = 30%		3.6	16.5	10	4	1					82	
309	1.53	10.2	7.6	20	21	0	0.41	0.459	0.000	0.0	341	
RR = 22%		2.9	17.5	10	4	1					68	
310	1.67	9.5	9.2	17	27	0	0.40	0.650	0.000	0.0	346	
RR = 11%		1.6	19.0	10	2	0					38	
311	1.38	11.8	6.5	20	15	0	0.37	0.313	0.000	0.0	332	
RR = 42%		4.8	15.2	10	3	1					96	
312	1.21	12.7	3.9	20	10	1	0.32	0.163	0.009	0.0	329	40°
RR = 61%		5.9	13.6	10	5	2					102	

TABLE E-2. (Concluded)

Side Fired

0.072m Choke L = 0.40m

RUN NO.	STOIC. RATIO	CO2 %	O2 %	CO PPM	NO PPM	UHC PPM	CO GM/KGM	NO GM/KGM	UHC GM/KGM	BACH. SMOKE	TFG C	Swirl
294	1.19	13.1	3.5	187	31	28	2.94	0.530	0.251	8.0	288	40°
RR = 31%		4.0	16.4	55	10	220					57	
295	1.31	11.9	5.4	120	47	24	2.09	0.895	0.239	9.0	277	
RR = 21%		2.8	17.4	30	10	22					49	
296	1.28	12.2	5.0	110	63	22	1.87	1.146	0.214	9.0	280	
RR = 11%		1.6	19.0	17	6	19					34	
297	1.66	9.1	9.0	1419	14	280	31.79	0.255	3.574	0.1	307	
RR = 21%		2.6	17.4	328	9	100					64	
298	1.62	9.3	8.6	>1600	22	800	>34.76	0.525	9.920	0.1	307	
RR = 29%		3.2	16.6	749	10	250					95	
299	1.84	8.2	10.1	315	10	68	7.56	0.294	0.967	0.0	288	40°
RR = 11%		1.2	19.0	50	5	50					35	

Tunnel-Fired

0.051m Choke L = 0.40m

RUN NO.	STOIC. RATIO	CO2 %	O2 %	CO PPM	NO PPM	UHC PPM	CO GM/KGM	NO GM/KGM	UHC GM/KGM	BACH. SMOKE	TFG C	Swirl
313	1.50	10.4	7.6	309	9	29	6.21	0.206	0.332	0.0	299	40°
RR = 21%		2.8	17.6	90	5	9					60	
314	1.24	12.7	4.4	148	10	21	2.43	0.187	0.197	0.0	285	
RR = 31%		4.0	16.3	41	4	7					66	
315	1.32	11.9	5.5	110	5	13	1.93	0.101	0.130	0.0	285	
RR = 22%		2.8	17.5	30	2	2					54	
316	1.40	11.1	6.5	50	27	1	0.93	0.542	0.011	0.0	285	
RR = 11%		1.5	19.0	10	2	1					37	
317	1.12	13.9	2.5	50	13	1	0.74	0.211	0.006	0.0	282	
RR = 32%		3.9	16.2	20	2	0						
318	1.02	15.1	0.5	1367	11	12	15.74	0.169	0.093	0.0	285	
RR = 48%		5.0	14.6	1179	2	14						
319	1.32	11.9	5.5	60	21	3	1.05	0.395	0.030	0.0	282	
RR = 15%		1.8	18.5	11	2	2					38	
320	1.12	14.1	2.4	100	9	12	1.48	0.152	0.101	0.0	291	
RR = 45%		4.8	14.9	40	2	3					74	
321	1.26	12.2	4.9	80	11	5	1.34	0.212	0.048	0.0	274	40°
RR = 21%		2.6	17.4	20	2	4					52	

TABLE E-3. STEADY-STATE FLUE GAS RECIRCULATION DATA FROM A 0.22 M I.D., INSULATED, TUNNEL-FIRED COMBUSTOR WITH THE 1.0-60°-A NOZZLE FGR BURNER

0.051m Choke L = 0.50m

RUN NO.	STOIC. RATIO	CO2 %	O2 %	CO PPM	NO PPM	UHC PPM	CO GM/KGM	NO GM/KGM	UHC GM/KGM	BACH. SMOKE	TFG C	Swirl
322	1.12	13.8	2.5	153	26	2	2.26	0.416	0.017	4.0	299	10°
RR = 11%		1.8	19.0	40	5	0					29	
323	1.03	14.8	0.7	≥1600	10	16	≥21.79	0.156	0.125	0.0	288	
RR = 32%		3.9	16.2	805	2	5					49	
324	1.21	12.8	3.9	177	6	24	2.84	0.110	0.220	0.5	310	
RR = 22%		2.8	17.5	40	2	4					43	
325	1.16	13.4	3.2	110	8	9	1.69	0.132	0.079	0.5	299	
RR = 22%		2.8	17.5	20	2	1					43	
326	1.09	14.1	1.9	148	10	6	2.14	0.165	0.050	0.0	307	
RR = 30%		3.6	16.5	50	2	1					46	
327	1.10	14.0	2.1	105	13	3	1.53	0.207	0.028	1.0	299	10°
RR = 22%		2.8	17.5	20	2	0					41	
328	1.09	14.2	1.8	90	22	0	1.29	0.339	0.000	0.1	293	20°
RR = 28%		3.0	16.7	30	5	0						
329	1.20	12.7	3.7	40	23	0	0.64	0.401	0.000	0.5	282	
RR = 22%		2.4	17.5	5	2	0					41	
330	1.07	14.3	1.5	290	21	0	4.12	0.327	0.000	4.0	293	
RR = 23%		2.6	17.4	90	2	0					41	
331	1.22	12.6	4.0	40	31	0	0.65	0.547	0.000	2.0	291	
RR = 13%		1.5	18.7	5	4	0					32	
332	1.13	13.5	2.6	45	35	0	0.67	0.578	0.000	5.0	286	20°
RR = 16%		0.2	18.3	7	2	0					32	
333	1.25	12.4	4.5	50	11	1	0.83	0.208	0.009	0.0	313	30°
RR = 31%		3.0	14.3	11	2	1					57	
334	1.19	12.7	3.6	27	25	0	0.44	0.425	0.000	0.0	299	
RR = 29%		3.4	16.6	10	5	1					58	
335	1.27	12.9	4.7	30	23	0	0.50	0.424	0.000	0.0	302	
RR = 23%		2.9	17.4	10	4	1					41	
336	1.36	11.3	5.9	20	39	0	0.36	0.621	0.000	0.0	296	30°
RR = 14%		1.6	18.6	5	2	1					29	
337	1.33	11.9	5.6	17	40	0	0.32	0.771	0.000	0.0	304	40°
RR = 11%		1.6	19.0	5	5	0					35	
338	1.15	13.6	2.9	17	31	0	0.27	0.505	0.000	0.0	293	
RR = 21%		3.1	17.6	7	4	0					38	
339	1.10	14.1	2.1	30	21	0	0.44	0.328	0.000	0.0	302	
RR = 30%		4.4	16.5	11	5	0					47	
340	1.26	12.4	4.7	20	35	0	0.33	0.589	0.000	0.0	293	
RR = 12%		2.2	18.9	10	2	0					35	
341	1.21	12.9	3.9	21	29	0	0.35	0.488	0.000	0.0	294	
RR = 12%		2.2	18.9	10	2	0					29	
342	1.26	12.4	4.7	31	24	0	0.54	0.448	0.000	0.0	299	
RR = 30%		4.0	16.5	15	10	0					40	
343	1.32	12.0	5.5	27	31	0	0.49	0.582	0.000	0.0	307	40°
RR = 23%		3.2	17.4	10	4	0					54	

TABLE E-3. (Continued)

0.042m Choke L = 0.50

RUN NO.	STOIC. RATIO	CO2 %	O2 %	CO PPM	NO PPM	UHC PPM	CO GM/KGM	NO GM/KGM	UHC GM/KGM	EACH. SMOKE	TEG C	Swirl
344	1.12	13.9	2.5	90	27	0	1.34	0.432	0.000	0.0	257	40°
RR = 28%		3.4	16.7	45	2	0					41	
345	1.37	11.1	6.0	20	30	0	0.37	0.588	0.000	0.0	213	
RR = 22%		2.9	17.5	10	4	0					41	
346	1.40	11.1	6.4	20	35	0	0.37	0.719	0.000	0.0	232	40°
RR = 13%		1.2	18.8	10	2	0					27	
347	1.07	14.6	1.4	187	23-	0	2.65	0.356	0.000	1.0	291	30°
RR = 29%		3.4	16.6	60	4	0					46	
348	1.07	14.5	1.4	61	21	0	0.87	0.318	0.000	0.0	302	
RR = 31%		3.9	16.3	30	2	0					54	
349	1.13	13.8	2.6	30	21	0	0.45	0.336	0.000	0.0	302	
RR = 28%		3.5	16.7	10	2	1					52	
350	1.21	13.0	3.9	21	23	0	0.35	0.403	0.000	0.0	299	
RR = 22%		2.9	17.5	10	2	1						
351	1.18	13.1	3.5	27	28	0	0.44	0.480	0.001	0.5	258	
RR = 22%		2.6	17.5	10	3	1					41	
352	1.12	13.4	2.4	120	31	1	1.78	0.494	0.005	0.5	268	
RR = 23%		2.7	17.4	25	2	1					43	
353	1.49	10.4	7.4	20	35	1	0.40	0.768	0.009	0.5	227	30°
RR = 11%		0.9	19.1	10	2	1					35	
354	1.09	14.1	1.8	130	29	3	1.97	0.449	0.025	0.0	269	20°
RR = 28%		3.6	16.7	81	5	6					46	
355	2.39	1.3	2.6	47	21	0	1.56	0.732	0.000	0.0	293	
RR = 23%		3.1	17.4	15	5	0					46	
356	1.22	12.7	4.0	40	21	0	0.64	0.363	0.000	1.0	277	
RR = 15%		2.1	18.5	7	2	0					32	
357	1.45	10.6	7.0	469	26	0	16.80	0.540	0.000	4.0	207	20°
RR = 12%		1.5	18.9	40	2	0					29	

1.0-90°-A Oil Nozzle

0.051m Choke L = 0.50m

RUN NO.	STOIC. RATIO	CO2 %	O2 %	CO PPM	NO PPM	UHC PPM	CO GM/KGM	NO GM/KGM	UHC GM/KGM	EACH. SMOKE	TEG C	Swirl
358	1.24	12.4	4.4	30	22	0	0.50	0.390	0.000	0.0	299	40°
RR = 31%		4.0	16.4	11	6	1					66	
359	1.27	12.2	4.7	35	21	0	0.59	0.378	0.000	0.0	296	
RR = 32%		3.9	16.2	20	6	0						
360	1.22	12.7	4.0	27	22	0	0.45	0.380	0.000	0.0		
RR = 31%		3.7	16.4	13	5	1					63	
361	1.39	11.1	6.3	40	16	0	0.74	0.335	0.000	0.0	313	40°
RR = 31%		4.0	16.3	20	5	0					85	

TABLE E-3. (Continued)

0.064m Choke L = 0.50m

RUN NO.	STOIC. RATIO	CO2 %	O2 %	CO PPM	NO PPM	UHC PPM	CO GM/KGM	NO GM/KGM	UHC GM/KGM	EACH. SMOKE	TEG C	Swirl
362	1.28	12.0	5.0	535	10	120	9.13	0.195	1.266	2.0	302	20°
RR = 31%		3.8	16.4	130	4	25						
363	1.13	13.4	2.6	90	15	11	1.35	0.255	0.094	1.0	293	
RR = 30%		3.7	16.5	25	5	1					49	
364	1.19	12.9	3.5	80	21	8	1.24	0.354	0.072	3.0	282	20°
RR = 22%		2.6	17.5	15	2	2					35	
365	1.31	11.5	5.1	45	21	0	0.78	0.391	0.002	1.0	307	30°
RR = 31%		3.2	16.4	20	6	0					57	
366	1.15	13.0	2.9	25	30	0	0.38	0.500	0.000	0.5	289	
RR = 30%		3.4	16.5	10	6	0					41	
367	1.20	12.5	3.7	20	39	0	0.32	0.682	0.000	1.0	285	
RR = 21%		2.4	17.6	7	5	0					35	
368	1.12	13.4	2.3	30	45	0	0.44	0.722	0.000	5.0	280	
RR = 23%		2.8	17.4	10	4	0					32	
369	1.19	12.7	3.5	20	50	0	0.31	0.849	0.000	4.0	277	
RR = 14%		1.4	18.6	10	5	0					29	
370	1.76	8.6	9.5	70	26	1	1.66	0.663	0.015	0.0	321	
RR = 12%		1.4	18.9	10	6	0					29	
371	1.47	10.2	7.0	165	10	16	3.95	0.224	0.179	0.0	318	30°
RR = 31%		3.2	16.4	50	6	4					66	
372	1.55	9.9	7.9	139	10	9	2.99	0.237	0.098	0.0	318	40°
RR = 22%		2.8	17.5	40	7	2					57	
373	1.41	11.0	6.5	41	21	2	0.79	0.423	0.024	0.0	321	
RR = 28%		3.4	16.7	20	5	2					66	
374	1.38	11.1	6.1	17	36	0	0.33	0.726	0.000	0.0	310	
RR = 22%		2.7	17.5	7	6	0					49	
375	1.16	13.1	3.1	20	31	0	0.31	0.513	0.000	0.0	296	
RR = 30%		3.6	16.5	7	9	0					49	
376	1.36	11.4	5.9	20	35	0	0.38	0.696	0.000	0.0	324	
RR = 31%		3.6	16.3	10	14	0					74	
377	1.17	13.3	3.3	20	50	0	0.31	0.836	0.000	0.0	304	
RR = 23%		3.0	17.4	10	10	1					52	
378	1.10	13.9	2.0	25	54	0	0.36	0.855	0.000	3.0	293	
RR = 22%		2.5	17.5	10	10	1					39	
379	1.40	11.5	6.6	18	74	0	0.35	1.491	0.000	0.5	304	
RR = 13%		1.5	18.8	5	9	1					29	
380	1.07	14.5	1.4	60	40	0	0.85	0.617	0.000	5.0	285	
RR = 30%		3.4	16.5	25	10	1						
381	1.11	13.8	2.1	30	40	0	0.44	0.639	0.000	0.5	285	40°
RR = 31%		3.4	16.3	10	10	1					52	

TABLE E-3. (Concluded)

0.051m Choke L = 0.50m

RUN NO.	STOIC. RATIO	CO2 %	O2 %	CO PPM	NO PPM	UHC PPM	CO GM/KGM	NO GM/KGM	UHC GM/KGM	SMOKE NUMBER	TEMP C	Swirl
382	1.20	12.9	3.8	21	26	0	0.35	0.445	0.000	0.0	296	40°
RR = 31%		3.8	16.4	10	10	1					60	
383	1.40	11.1	6.4	35	19	0	0.65	0.398	0.000	0.0	284	
RR = 29%		3.6	16.6	10	5	1					71	
384	1.37	11.3	6.0	20	25	0	0.36	0.488	0.000	0.0	301	
RR = 29%		3.6	16.6	10	5	1					66	
385	1.29	12.0	5.0	20	26	0	0.34	0.477	0.000	0.0	304	
RR = 29%		3.7	16.6	10	5	1					66	
386	1.25	12.4	4.5	20	26	0	0.33	0.463	0.000	0.0	302	
RR = 31%		3.9	16.4	10	5	1					66	
387	1.18	13.3	3.4	20	22	0	0.21	0.369	0.000	0.0	296	40°
RR = 31%		4.0	16.4	7	5	1					60	

TABLE E-4. FLUE GAS RECIRCULATION DATA OBTAINED IN INSULATED, TUNNEL-FIRED, 0.50 M LENGTH COMBUSTION CHAMBERS WITH THE 0.051 M CHOKE, 40° SWIRL ANGLE FGR BURNER

		RUN NO.	STOIC. RATIO	CO2 %	O2 %	CO PPM	NO PPM	UHC PPM	CO GM/KGM	NO GM/KGM	UHC GM/KGM	BACH. SMOKE	TFG C
0.26m I.D. Combustor	Cycle-Averaged Data	388	1.13	13.8	2.5	25	37	8	0.37	0.597	0.065	0.0	266
		RR = 33%		4.2	16.1	10	11	0					77
		389	1.36	11.4	6.0	49	26	16	0.90	0.507	0.162	0.0	316
		RR = 29%		3.4	16.6	10	10	2					62
	Side-Fired	390	1.13	13.7	2.5	18	36	6	0.28	0.613	0.048	0.0	307
		RR = 31%		3.6	16.4	7	10	0					66
		391	1.35	11.5	5.8	44	32	30	0.80	0.616	0.311	0.0	316
		RR = 30%		3.4	16.5	10	10	0					77
		392	1.21	12.6	3.9	23	35	10	0.36	0.620	0.096	0.0	313
		RR = 31%		3.5	16.3	5	10	0					71
0.22m Diameter Combustor	Steady-State Ign. On	393	1.28	12.1	5.0	20	28	0	0.34	0.522	0.000	0.0	
		RR = 33%		3.9	16.1	10	9	0					66
	Ign. Off	394	1.29	12.0	5.0	20	28	0	0.34	0.523	0.000	0.0	286
		RR = 33%		3.9	16.1	10	9	0					66
	Cycle-Averaged Data	395	1.10	13.6	1.9	1043	33	1	15.11	0.513	0.012	0.2	249
		RR = 37%		4.4	15.7	187	6	0					54
		396	1.16	13.1	3.1	33	35	1	0.52	0.578	0.009	0.1	232
		RR = 31%		3.7	16.4	10	8	0					49
		397	1.32	11.0	5.4	25	30	6	0.44	0.573	0.065	0.1	304
		RR = 31%		3.9	16.4	15	10	0					65
		398	1.15	13.3	2.9	187	35	2	2.86	0.587	0.017	0.0	241
		RR = 31%		3.9	16.4	60	10	0					60

TABLE E-5. CYCLE-AVERAGED, FLUE GAS RECIRCULATION DATA WITH THE 40° SWIRL, 0.051 M CHOKE FGR BURNER IN THE 0.22 M I.D. INSULATED COMBUSTOR

		RUN NØ.	STOIC. RATIO	CO2 %	O2 %	CØ PPM	NØ PPM	UHC PPM	CØ GM/KGM	NØ GM/KGM	UHC GM/KGM	BACH. SMØKE	TFC C
Tunnel-Fired L = 0.75m	1.0-60°-A at 689 kN/m² 0.98 m/s	399	1.40	11.1	6.4	40	40	12	0.75	0.808	0.129	0.0	349
		RR - 23%		3.0	17.3	10	9	0					79
		400	1.33	11.6	5.5	51	32	14	0.92	0.622	0.146	0.0	343
		RR 32%		3.8	16.2	15	10	0					88
		401	1.09	14.1	1.9	23	38	2	0.35	0.595	0.018	0.0	332
		RR = 33%		4.4	16.1	10	10	0					79
		402	1.22	12.7	4.0	20	35	8	0.34	0.613	0.073	0.0	327
		RR = 31%		3.8	16.4	10	9	0					82
		403	1.01	14.8	0.4	-1600	42	1	-21.51	0.616	0.008	2.3	313
		RR = 32%		3.8	16.2	1499	5	0					66
Tunnel-Fired L = 0.50m	1.25-60°-A @ 551 kN/m² 1.13 m/s	404	1.04	14.6	0.9	85	35	2	1.19	0.533	0.016	1.2	301
		RR - 30%		3.5	16.5	41	7	0					49
		405	1.15	13.3	2.8	28	31	8	0.44	0.514	0.067	0.3	277
		RR - 33%		3.6	16.1	10	5	0					57
	0.75-60°-A @ 2137 kN/m² 1.03 m/s	406	1.12	13.8	2.3	23	40	1	0.35	0.638	0.008	0.0	261
		RR = 32%		4.0	16.2	10	11	2					57
		407	1.20	12.5	3.6	48	34	10	0.78	0.583	0.091	0.6	263
		RR - 31%		3.7	16.3	7	10	0					52
		408	1.02	14.4	0.6	-1600	44	1	-21.71	0.649	0.012	1.2	227
		RR = 33%		3.4	16.1	-1600	11	2					35

TABLE E-5. (Continued)

551 kN/m^2 Oil Supply Pressure

1.0-60°-A — 20% No.6/80% No.2 Oil Mixture

- Ign. Off
- Ign. On

1.25-60°-A — 1.14 ml/s

0.75-60°-A — 0.68 ml/s

RUN NO.	STOIC. RATIO	CO2 %	O2 %	CO PPM	NO PPM	UHC PPM	CO GM/KGM	NO GM/KGM	UHC GM/KGM	BACH. SMOKE	TFG C
409	1.27	12.1	4.8	30	29	11	0.52	0.540	0.106	0.0	248
RR - 32%		3.4	16.2	5	9	0					38
410	1.16	13.0	3.2	-1600	11	60	-24.64	0.184	0.532	7.4	227
RR = 29%		3.4	16.6	535	5	20					35
411	1.08	14.7	1.7	112	44	8	1.61	0.683	0.062	0.3	248
RR = 29%		3.2	16.6	90	10	0					38
412	1.13	13.7	2.5	43	36	14	0.66	0.582	0.117	0.1	262
RR - 30%		3.2	16.5	10	6	0					46
413	1.10	14.0	2.1	28	34	8	0.42	0.532	0.064	0.0	256
RR - 32%		4.2	16.2	10	10	0					46
414	1.10	14.1	2.1	27	34	8	0.41	0.532	0.064	0.0	253
RR = 34%		4.4	16.0	10	11	0					46
415	1.09	14.0	1.9	73	146	6	1.07	2.268	0.048	3.9	278
RR = 31%		4.0	16.4	5	44	0					46
416	1.38	11.1	6.2	354	95	187	6.53	1.877	1.968	2.6	292
RR - 28%		3.6	16.7	10	26	0					57
417	1.13	13.2	2.5	80	134	18	1.21	2.156	0.158	2.8	282
RR = 37%		4.2	15.7	10	43	0					57

TABLE E-5. (Concluded)

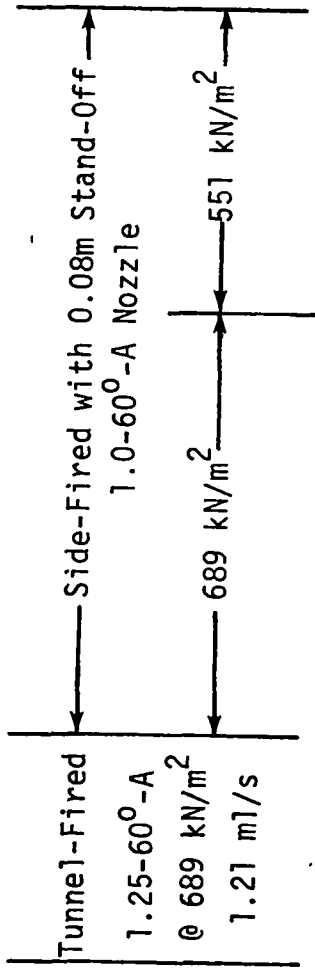

RUN NØ.	STØIC. RATIO	CØ2 %	Ø2 %	CØ PPM	NØ PPM	UHC PPM	CØ GM/KGM	NØ GM/KGM	UHC GM/KGM	BACH. SMOKE	TFG C
418	1.16	13.3	3.1	95	40	5	1.47	0.672	0.044	0.4	244
RR = 33%		4.2	16.1	20	15	0					52
419	1.35	11.3	5.8	83	11	8	1.51	0.226	0.087	0.1	276
RR	31%	3.7	16.4	10	4	0					57
420	1.27	12.1	4.8	43	24	8	0.74	0.445	0.079	0.0	252
RR	33%	3.9	16.1	7	8	0					49
421	1.19	12.7	3.6	67	23	21	1.08	0.399	0.190	0.0	243
RR = 33%		3.8	16.1	20	6	0					57
422	1.15	13.2	2.9	30	42	2	0.47	0.698	0.018	0.0	237
RR	29%	3.6	16.6	10	8	0					41
423	1.10	13.8	1.9	27	43	1	0.41	0.679	0.011	0.2	227
RR	31%	3.6	16.4	10	7	0					46
424	1.48	10.3	7.2	162	26	26	3.22	0.563	0.299	0.1	255
RR	30%	3.2	16.5	20	10	5					74
425	1.01	14.8	0.2	-1600	44	1	-21.33	0.638	0.011	0.0	263
RR = 31%		3.2	16.4	-1600	10	0					49
426	1.10	13.7	2.0	50	40	4	0.73	0.637	0.030	0.0	278
RR	31%	3.3	16.3	10	10	0					54

APPENDIX F

PRE-PROTOTYPE AIR-COOLED FINNED COMBUSTOR TESTS

In order to ascertain that a heavily air-cooled firebox could indeed duplicate the emission behavior of the water-cooled fireboxes discussed in Section IV, before committing the prototype conceptual warm air furnace design to such a combustor, one was built and tested. Figure F-1 is a layout drawing and Figure F-2 is a photograph of the combustor, showing the side-fire burner orientation and twenty-four heavy cooling fins spaced around the combustion chamber perimeter. The finned section was wrapped with a sheet metal shroud for containment of the forced air coolant flow. Although air-cooled side-fire chambers were fired earlier in this task, the chambers used were simple cylindrical surfaces with only free convection air-cooling resulting in an inside wall temperature of ~815 C (1500 F). This side-fired, finned combustor was designed to stay considerably cooler (by about 500-600 C) during the burner-on time but also to stay quite warm (~60-100 C) during the burner-off time.

Hot firings in the finned research combustor were conducted with the same 1.0 ml/s optimum burner described in Section IV. The results are presented in Table F-1. The parameters that were varied during these tests were: (1) cycle time, (2) chamber length, and (3) firing rate. Runs 433 to 446 were made with a 0.75m chamber length and with varying cycle times (33%-on constant). The 10 minutes-on/20 minutes-off cycles were typical of earlier data taken, while the 4 minutes-on/8 minutes-off

NOTE: Detail dimensions are called out in inches to maintain commonality with material stock.

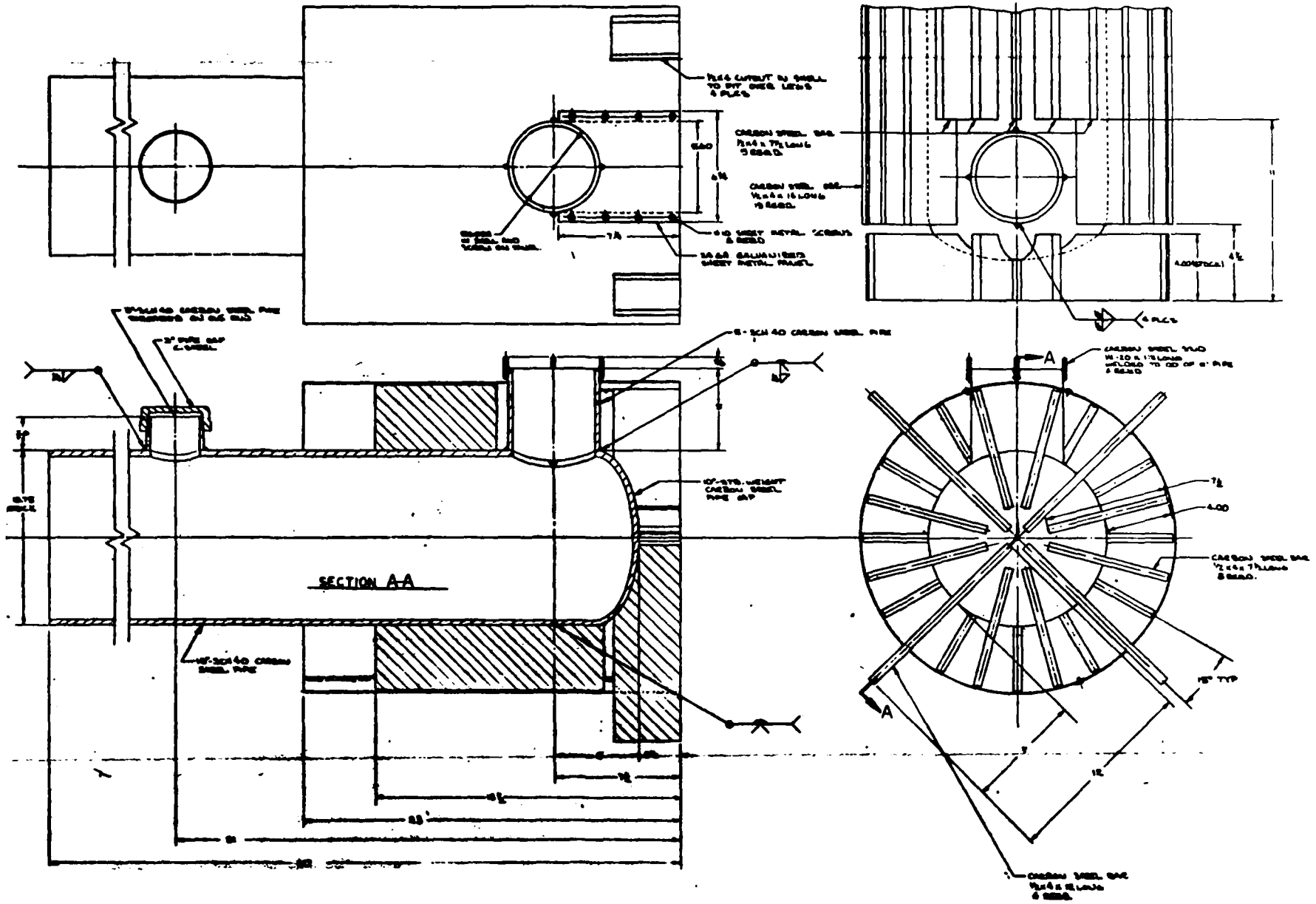

Figure F-1. Layout Drawing of the Finned Air-Cooled Research Combustor

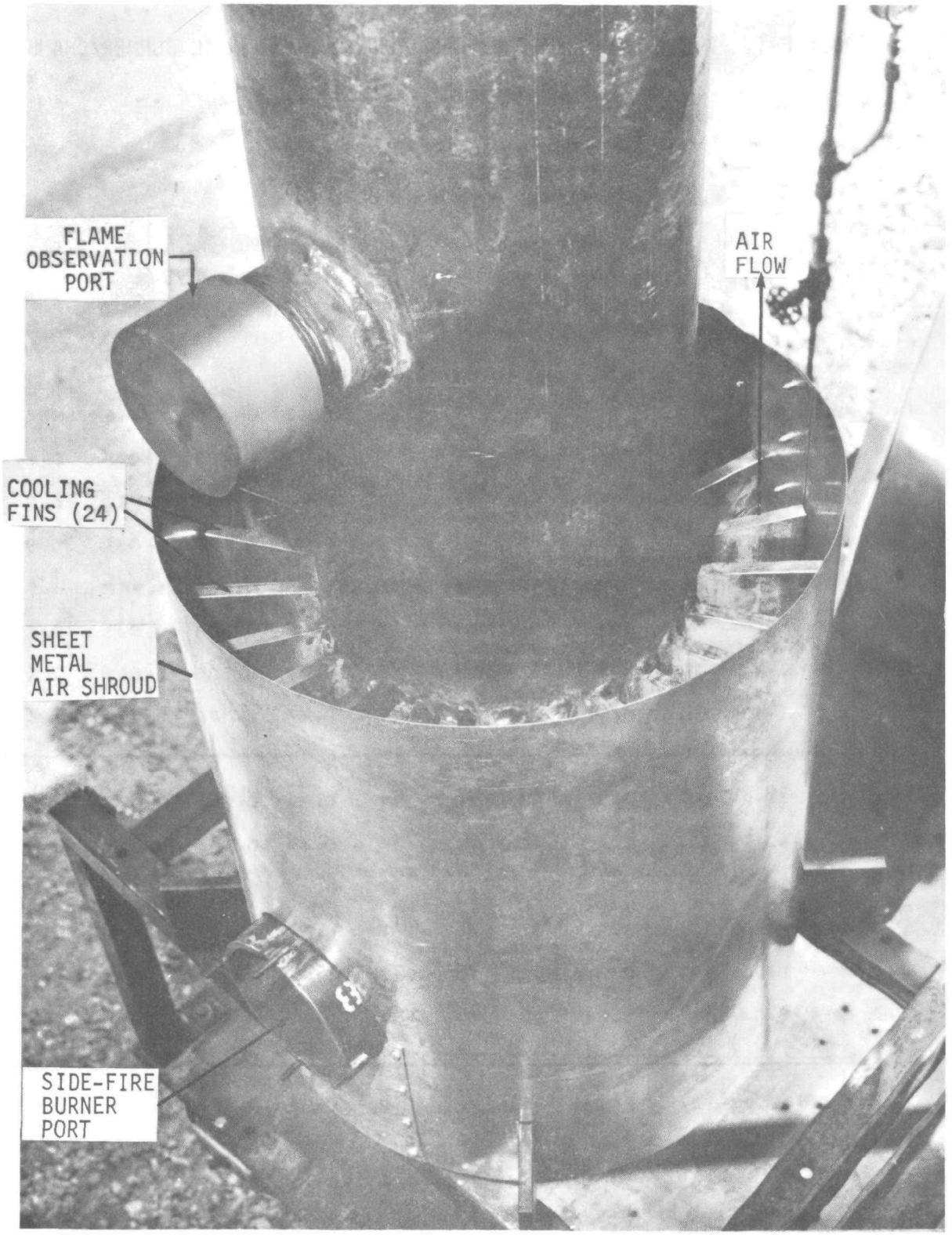

Figure F-2. Photograph of the Finned Air-Cooled Research Combustor (Shown Without the Lower Air Coolant Inlet Duct)

TABLE F-1. CYCLE-AVERAGED FLUE GAS ANALYSIS DATA, OIL BURNER/CHAMBER MATCHING EXPERIMENTS

Burner: 1.0 ml/s Optimum
Nozzle: 1.0-60-A

ØIL FLØWRATE = 1.000 ML/S

ANALYSIS: MAY 02, 1975

COMBUSTOR:
0.25m x 0.75 mL
FINNED, SIDE-FIRED

	RUN NØ.	STØIC. RATIØ	CØ2 %	Ø2 %	CØ PPM	NØ PPM	UHC PPM	CØ GM/KGM	NØ GM/KGM	UHC GM/KGM	BACH. SMØKE	TFG C
10 ON/20 OFF (MINUTES)	433	1.14	13.5	2.6	17	26	5	0.27	0.423	0.043	0.6	209
	434	1.28	12.1	4.9	50	24	29	0.87	0.439	0.282	0.0	226
	435	1.23	12.5	4.1	30	35	3	0.49	0.627	0.031	0.0	157
	436	1.01	14.8	0.2	≥1600	42	260	≥21.35	0.605	1.988	4.2	177
	437	1.08	14.1	1.6	26	39	5	0.39	0.603	0.041	[illegible]	[illegible]
	438	1.11	13.9	2.2	27	34	7	0.41	0.535	0.063	[illegible]	
	439	1.13	13.6	2.5	32	23	7	0.49	0.376	0.060	0.0	
4 ON/8 OFF	440	1.12	13.7	2.3	20	40	11	0.29	0.645	0.093	[illegible]	[illegible]
	441	1.12	13.7	2.4	30	41	16	0.44	0.664	0.135	[illegible]	
	442	1.17	13.1	3.2	31	41	22	0.49	0.693	[illegible]	[illegible]	
	443	1.20	12.6	3.7	37	45	27	0.61	0.779	[illegible]	[illegible]	
	444	1.00	14.5	0.2	≥1600	43	912	≥21.31	0.617	[illegible]	[illegible]	
	445	1.04	14.4	0.9	65	41	9	0.91	0.611	[illegible]	[illegible]	
15 ON 30 OFF	446	1.09	13.9	1.8	25	42	2	0.36	0.652	0.016	0.2	[illegible]

TABLE F-1. (Concluded)

Burner: 1.0 ml/s Optimum
Nozzle: 1.0-60-A, 1.25-60-A, 0.75-60-A

OIL FLOWRATE - 1.000 ML/S

ANALYSIS: MAY 02, 1975

COMBUSTOR:
0.25m I.D. x 0.50 mL
FINNED, SIDE-FIRED

	RUN NO.	STOIC. RATIO	CO2 %	O2 %	CO PPM	NO PPM	UHC PPM	CO GM/KGM	NO GM/KGM	UHC GM/KGM	PATH. SMOKE	TEG C
1.0-60°-A NOZZLE 10 ON/20 OFF	447	1.08	14.0	1.7	43	35	4	0.63	0.553	0.035	1.1	260
	448	1.13	13.6	2.5	27	36	6	0.42	0.590	0.053	1.1	260
	449	1.16	13.2	3.1	26	38	8	0.41	0.641	0.074	0.1	266
	450	1.22	12.5	4.0	30	34	11	0.50	0.599	0.102	0.0	271
	451	1.26	12.1	4.5	35	35	11	0.58	0.634	0.105	0.0	275
1.0-60°-A NOZZLE 4 ON/8 OFF	452	1.25	12.1	4.4	45		46	0.76		0.437	0.0	
	453	1.04	14.4	0.9	418	37	18	5.68	0.561	0.146	3.9	
	454	1.14	13.3	2.6	45	35	20	0.68	0.572	0.172	0.9	
	455	1.22	12.5	3.9	45	35	26	0.74	0.606	0.240	0.0	
		--- Chamber Length ---										
10 ON/20 OFF 1.25-60°-A NOZZLE	456	1.17	13.2	3.2	35	52	23	0.56	0.871	0.207	1.0	
	457	1.11	13.8	2.1	25	52	9	0.37	0.884	0.075	2.4	271
	458	1.18	13.1	3.3	63	47	30	1.00	0.800	0.267	0.7	
10 ON/20 OFF 0.75-60°-A NOZZLE	459	1.16	13.3	3.1	120	21	10	1.84	0.354	0.086	0.9	204
	460	1.35	11.4	5.9	869	11	143	15.55	0.214	1.462	0.7	204
	461	1.08	14.1	1.7	132	30	6	1.90	0.473	0.050	3.7	
	462	1.59	9.4	8.3	>1600	15	720	>34.14	0.363	8.778	0.9	209

cycles were more representative of current practice. Examination of the results revealed that the burner/combustor operated well (low carbonaceous pollutant concentrations) at very low stoichiometric ratio conditions, but the NO emissions ranged between 0.4 and 0.6 g/kg, and averaged slightly above the target value of 0.5 g/kg. The heat extracted from the combustion chamber section was on the order of 8205 J/sec (28,000 Btu/hr), which is nominally equivalent to the heat extracted from the water-cooled combustor that resulted in <0.5 g/kg of NO. The difference in the NO concentrations was probably due to higher temperature gradients (hot spots), that are often encountered in air-cooled systems, resulting in slightly higher local peaks in flame temperature. The finned combustor was of heavy wall design to reduce hot spotting by increasing heat conduction, however the temperature gradients were probably still greater than in a water-cooled system.

The effect of cycle time variation was most noticeable in the carbonaceous pollutant concentrations, primarily due to the averaging of the start "spikes" over varying time spans. As can be seen in Table F-1, the shorter 4-on/8-off cycle is generally higher in the carbonaceous pollutant concentrations, due to the shorter time-span averaging.

Runs 447 to 455 were tests with the shorter 0.50m length chamber. As anticipated, they showed a slight increase in carbonaceous pollutants and a corresponding decrease (5-8%) in nitric oxide emissions. The shifting of the levels of carbonaceous pollutants resulted in

unfavorable combinations (exceeding target specifications) of emission levels, suggesting that longer (>.50m) chambers should be used.

Variations of firing rate were made to investigate the versatility of this combustor/burner combination. Runs 456 to 458 were made with a 1.25-60°-A (~1.3 ml/s) oil nozzle and the results showed a corresponding rise in all pollutant concentrations. The smoke emissions showed the greatest increase, probably due to oil droplets contacting the cooled wall at this higher flowrate. Runs 459 to 462 were fired with a lower flowrate, 0.75-60°-A nozzle (~0.8 ml/s). This reduction in firing rate did result in a significant reduction in nitric oxide emissions. However, the carbonaceous pollutant levels increased, but that was probably due to the off-optimum choke plate rather than to the finned combustor. It has been noted before that underfiring an optimized burner head results in sensitivity to production of carbonaceous emissions, especially smoke. The lower nitric oxide levels were interpreted to mean that a slightly larger diameter combustor would be more suitable for the 1.0 ml/s firing rate. Examination of the combustor after the 30 test series showed no sooting on the cooled combustor walls.

TECHNICAL REPORT DATA
(Please read Instructions on the reverse before completing)

1. REPORT NO.	2.	3. RECIPIENT'S ACCESSION NO.
EPA-600/2-76-038		

4. TITLE AND SUBTITLE	5. REPORT DATE
Residential Oil Furnace System Optimization--Phase I	February 1976
	6. PERFORMING ORGANIZATION CODE

7. AUTHOR(S)	8. PERFORMING ORGANIZATION REPORT NO.
L. P. Combs and A. S. Okuda	R-9815

9. PERFORMING ORGANIZATION NAME AND ADDRESS	10. PROGRAM ELEMENT NO.
Rocketdyne Division Rockwell International 6633 Canoga Avenue Canoga Park, CA 91304	1AB014; ROAP 21BCC-27
	11. CONTRACT/GRANT NO.
	68-02-1819

12. SPONSORING AGENCY NAME AND ADDRESS	13. TYPE OF REPORT AND PERIOD COVERED
EPA, Office of Research and Development Industrial Environmental Research Laboratory Research Triangle Park, NC 27711	Final; 6/74-8/75
	14. SPONSORING AGENCY CODE
	EPA-ORD

15. SUPPLEMENTARY NOTES

EPA project officer for this report is B. Martin, 919/549-8411, Ext 2235.

16. ABSTRACT The report gives results of an analytical and experimental investigation of technology for improving pollutant emission characteristics and thermal efficiency of residential oil furnaces. A digital computer model was programmed for cyclical (transient) thermal analyses of typical warm air oil furnaces; design features and operating conditions were varied parametrically to discern influences on thermal efficiency. Heat in the exhaust flue gases, found to be the major source of inefficiency, can best be reduced by burning the fuel with minimum excess air and by reducing the flue gas temperature, both within the practical constraints of emission production and cost. Furnace operability and pollutant emissions were studied experimentally by testing three burner types in several combustor sizes, configurations, and wall constructions (cooling methods). Tests showed that the optimized conventional burner in a larger-than-usual cooled combustor has the best potential for minimizing emissions and maximizing efficiency. Test results were incorporated into two conceptual designs for prototype low-emission units capable of satisfying program goals. One design, a warm air unit, was selected to be built and tested in Phase II.

17. KEY WORDS AND DOCUMENT ANALYSIS

a. DESCRIPTORS		b. IDENTIFIERS/OPEN ENDED TERMS	c. COSATI Field/Group
Air Pollution	Design	Air Pollution Control	13B
Furnaces	Hot Water Heating	Stationary Sources	13A
Fuel Oil	Warm Air Heating	Emission Control	21D
Residential Buildings		Recirculation	13M
Optimization			12A
Thermal Efficiency			20M

18. DISTRIBUTION STATEMENT	19. SECURITY CLASS *(This Report)*	21. NO. OF PAGES
Unlimited	Unclassified	223
	20. SECURITY CLASS *(This page)*	22. PRICE
	Unclassified	

EPA Form 2220-1 (9-73)